FEASIBILITY OF USING RECYCLED CONCRETE AGGREGATE IN DENSE-GRADED AND GAP-GRADED HOT MIX ASPHALTS

MOHAMMAD SAEED POURTAHMASB

FACULTY OF ENGINEERING

UNIVERSITY OF MALAYA

KUALA LUMPUR

2016

UNIVESRITY OF MALAYA

ORIGINAL LITERARY WORK DECLARATION

Name of Candidate: **Mohammad Saeed Pourtahmasb**

Registration/Matric No: **KHA 090037**

Name of Degree: **Doctor of Philosophy**

Title of Project Paper/Research Report/Dissertation/Thesis:

Feasibility of Using Recycled Concrete Aggregate in Dense-Graded and Gap-Graded Hot Mix Asphalts

Field of Study: **Highway and Transportation Engineering**

I do solemnly and sincerely declare that:

(1) I am the sole author/writer of this Work;
(2) This Work is original;
(3) Any use of any work in which copyright exists was done by way of fair dealing and for permitted purposes and any excerpt or extract from, or reference to or reproduction of any copyright work has been disclosed expressly and sufficiently and the title of the Work and its authorship have been acknowledged in this Work;
(4) I do not have any actual knowledge nor do I ought reasonably to know that the making of this work constitutes an infringement of any copyright work;
(5) I hereby assign all and every rights in the copyright to this Work to the University of Malaya ("UM"), who henceforth shall be owner of the copyright in this Work and that any reproduction or use in any form or by any means whatsoever is prohibited without the written consent of UM having been first had and obtained;
(6) I am fully aware that if in the course of making this Work I have infringed any copyright whether intentionally or otherwise, I may be subject to legal action or any other action as may be determined by UM.

Candidate's Signature Date:

Subscribed and solemnly declared before,

Witness's Signature Date:

Name:

Designation:

ABSTRACT

In recent years, several studies have been carried out on the utilization of Construction and Demolition (C&D) wastes in developed countries, particularly the reuse of waste materials in new construction sectors. Both scientists and policy-makers have sought to explore the environmental and economic advantages of waste material recycling. Recycled Concrete Aggregate (RCA), produced from the demolition of concrete structures such as buildings, bridges and dams, is one of the largest wastes in the world in terms of volume. RCAs have different physical, chemical and mechanical properties to natural aggregates. In particular, the porous structure of the concrete and cement paste often attached to the surface of the recycled aggregates can lead to lower abrasion resistance, lower density and higher absorption than virgin aggregates. At the same time, there have been some recent studies showing the successful use of RCA materials in new concrete constructions. Several studies have also been carried out on the possibility of using RCA in base and sub-base either as unbound materials or bitumen-treated or cement-treated granular materials.

The present study presents experimental research on the feasibility of utilizing RCAs in stone mastic asphalt (SMA) and hot mix asphalt (HMA) mixtures for pavements. The RCA materials under study were divided into three categories: Fine RCA (F-RCA) containing aggregate particle sizes of 2.36 mm and smaller; Coarse RCA (C-RCA) containing aggregate particle sizes larger than 2.36 mm; and mixtures of F-RCA and C-RCA, called M-RCA. The Marshall mix design method was used to produce HMA and SMA specimens containing various percentages (0%, 20%, 40%, 60% and 80% by the weight of total mix) and sizes (coarse, fine and mix) of RCA. The volumetric and mechanical properties of these various HMA and SMA specimens were then subjected to a series of tests: Marshall Stability (MS), Flow, Density, Voids in Total Mix (VTM), Voids Filled with Asphalt (VFA), Voids in Mineral Aggregates (VMA), Resilient Modulus, Loaded Wheel Tracking (Rutting), Indirect Tensile (IDT) Strength, Moisture Susceptibility and finally Flexural Beam Fatigue tests. The outcomes were statistically analyzed using an analysis of variances (ANOVA).

The test results indicated that, regardless of the size of the RCA particles, using RCA to replace virgin aggregates increases the binder content needed in both HMA and SMA mixtures. However, they also showed that, despite the significant impact of the RCA content on the volumetric and mechanical properties of the asphalt mixtures, utilizing up to 40% coarse, 80% fine and 40% mixed RCA in SMA, and up to 60% coarse, 50% fine and 60% mixed RCA in HMA, can comfortably satisfy the standard requirements, for pavements in terms of project and traffic volumes. At the same time, as SMA mixtures are highly influenced by their aggregate characteristics, particular care needs to be taken with regard to the properties of SMA mixtures containing RCA to ensure these meet the desired performance criteria.

ABSTRAK

Kebelakangan ini, beberapa kajian telah dijalankan ke atas penggunaan terhadap Perobohan Pembinaan (C&D) bahan buangan di negara-negara maju. Kemungkinannya adalah, untuk menggunakan semula bahan-bahan buangan dalam sektor pembinaan baru. Adalah menjadi tanggugjawab ahli-ahli sains dan penyelidik, serta orang-orang yang berkuasa, untuk meneroka sisa kitar semula bahan untuk kebaikan alam sekitar dan ekonomi. Agregat Konkrit (RCA) yang dikitar semula dianggap sebagai salah satu daripada bahan-bahan buangan yang terbesar di seluruh dunia yang dihasilkan dengan merobohkan struktur konkrit seperti bangunan, jambatan dan empangan. RCAs mempunyai sifat fizikal, kimia dan sifat-sifat mekanik yang berbeza berbanding agregat semulajadi. Struktur berliang konkrit dan pes simen yang melekat pada permukaan agregat yang dikitar semula menyebabkan rintangan lelasan yang lebih rendah, ketumpatan yang lebih rendah dan penyerapan yang lebih tinggi berbanding dengan agregat virgin. Kajian baru-baru ini menunjukkan bahawa, bahan RCA telah berjaya digunakan dalam pembinaan konkrit baru. Tambahan pula, beberapa kajian telah dijalankan mengenai kemungkinan menggunakan RCA dalam asas dan sub-asas sama ada bahan-bahan yang tak terbatas atau bitumen dirawat atau bahan berbutir simen dirawat. Kajian semasa membentangkan satu kajian eksperimen mengenai kemungkinan menggunakan agregat konkrit kitar semula (RCA) di batu asfalt warna kuning muda (SMA) dan campuran asfalt panas (HMA). Bahan-bahan RCA telah dibahagikan kepada tiga kategori; RCA Halus (F-RCA) yang mengandungi saiz zarah agregat 2.36 mm dan lebih kecil, RCA Kasar (C-RCA) yang mengandungi saiz zarah agregat lebih besar daripada 2.36 mm dan campuran F-RCA dan C-RCA bernama M-RCA. Kaedah rekabentuk campuran Marshall digunakan untuk fabrikasi HMA dan SMA spesimen dan isipadu dan sifat-sifat mekanik spesimen yang mengandungi pelbagai peratusan (0%, 20%, 40%, 60% dan 80%) dan saiz (kasar, halus dan campuran) RCA telah dinilai.

Hasil telah dianalisis menggunakan analisis varians (ANOVA). Hasil ujian menunjukkan bahawa, tanpa mengira saiz tertentu RCA, menggunakan RCA untuk menggantikan agregat virgin meningkat kandungan pengikat yang diperlukan dalam kedua-dua HMA dan campuran SMA. Namun begitu, keputusan ujian menunjukkan bahawa walaupun kandungan RCA member impak yang ketara ke atas sifat-sifat volumetric dan mekanikal campuran asphalt, penggunnan sehingga 40% kasar, 80% halus dan 40% campuran RCA dalam SMA, dan penggunaan sehingga 60% kasar, 50% halus dan 60% campuran RCA dalam HMA, depat memenuhi keperluan standard dengan selesa, bagi pavements dari segi projek dan jumlah trafik. Tambahan lagi, kerana campuran SMA adalah sangat dipengaruhi oleh ciri-ciri agregat, untuk mencapai prestasi wajar, lebih berhati-hati perlu dibuat ke atas hartanah campuran SMA mengandungi RCA.

ACKNOWLEDGMENTS

In the name of GOD, the compassionate, the merciful. This thesis becomes a reality with the kind support and help of many individuals. I would like to extend my sincere thanks to all those who helped me with their kindness and support during my research to accomplish my PhD thesis.

Foremost, I want to offer this endeavor to our almighty God for the wisdom he bestowed upon me, the strength, peace of my mind and good health in order to finish this research.

I would like to express my gratitude towards my supervisor, Prof. Dr. Mohamed Rehan Bin Karim for giving me the opportunity to work under his supervision which increased my knowledge of pavement engineering considerably and without his advices and supports this study would not have been possible. His friendship and good advices have been invaluable to me during the hard times. His patience, flexibility, genuine caring, concern and faith in me during the research process enabled me to attend to life while also doing my research. He has been motivating, encouraging, and enlightening.

I would also like to acknowledge the center of research grant management, institute of research management and monitoring of University of Malaya (UM) for providing grant and financial support of this research.

Last but not least, I would like to express my gratitude to Neda Naderali, my wife, for her support, encouragement, quiet patience and unwavering love. I appreciate my family, which I owe a big debt of gratitude to them for their endless love, encouragement and supporting me in all my pursuits**.**

TABLE OF CONTENTS

List of Figures

List of Tables

List of Symbols and Abbreviations

A	Mass of Dry Specimen
AAPA	Australian Asphalt Pavement Association
AASHTO	American Association of State Highway and Transportation Officials
ACV	Aggregate Crushing Value
AI	Asphalt Institute
AIV	Aggregate Impact Value
AN	Angularity Number
ANOVA	Analysis of Variance
APA	Asphalt Pavement Analyzer
ASTM	American Society for Testing and Materials
b	Average Specimen Width
BS	British Standard
C	Mean Control Sample Skid Value
C&D	Construction and Demolition
CA	Coarse Aggregate
Cal-trans	California Department of Transportation
CBR	California Bearing Ratio
CEI	Construction Energy Index
CKC	California Kneading Compactor
COC	Cleveland Open Cup
C-RCA	Coarse Recycled Concrete Aggregate
CTGM	Cement-Treated Granular Material
d	Bulk density

D	Dissipated Energy
DGA	Dense Graded Asphalt
D_i	Dissipated Energy for the i^{th} Load Cycle
DW	Demolished Waste
e	Natural Logarithm
E^*	Dynamic Modulus
ESAL	Equivalent Single Axle Load
F	Fahrenheit
f	Load Frequency
FA	Fine Aggregate
FHWA	Federal Highway Administration
F-RCA	Fine Recycled Concrete Aggregate
G_{mb}	Bulk Specific Gravity of Mix
G_{sb}	Bulk Specific Gravity of Aggregates
G_b	Specific Gravity of Asphalt Cement
G_{se}	Effective Specific Gravity of Mix
G_{mm}	Maximum Theoretical Specific Gravity
G_A	Specific Gravity of Aggregate
GGA	Gap Graded Asphalt
GLWT	Georgia Loaded Wheel Tester
H	Total Recoverable Horizontal Deformation
h	Average Specimen Height
HL	Hydrated Lime
HMA	Hot Mix Asphalt
HWTD	Hamburg Wheel Tracking Device

Hz	Hertz
IDT	Indirect Tensile Strength
in	Inch
JKR	Jabatan Kerja Raya
KN	Kilo Newton
kPa	Kilo Pascal
l	Interior Length of Mold
LA	Los Angeles Abrasion
lb	Pound
LCPC	French Wheel Tracker
LVDT	Linear Variable Displacement Transducer
LWT	Loaded Wheel Tracking
M	Mass of slab
MATTA	Material Testing Apparatus
MF	Mineral Filler
mm	Millimeter
MPa	Mega Pascal
M_R	Resilient modulus
M-RCA	Mixed Recycled Concrete Aggregate
MS	Marshall Stability
n	Load Cycles
NAPA	National Asphalt Pavement Association
OAC	Optimum Asphalt Content
OGA	Open Graded Asphalt
OGFC	Open-Graded Friction Courses
P	Maximum Vertical Load

P_b	Asphalt Content
PCCP	Portland Cement Concrete Pavements
PCRCA	Pre-Coated RCA
PG	Performance Graded
PSV	Polished Stone Value
R&B	Ring and Ball
RAP	Recycled Asphalt Pavements
RBM	Reclaimed Building Materials
RCA	Recycled Concrete Aggregate
RCP	Recycled Concrete Pavements
RFA	Recycled Fine Aggregate
r_n	Depth measurement at n^{th} reading
S	Flexure Stiffness
s	Time Lag between P_{max} and δ_{max}
SGS	Superpave Gyratory Compactor
SHRP	Strategic Highway Research Program
SLTA	Singapore Land Transport Authority
SMA	Stone Mastic Asphalt
SSD	Saturated Surface Dry
t	Thickness of Specimen
TMD	Theoretical Maximum Density
T_R	Tracking Rate
T_{RM}	Mean Value of T_R
TSR	Tensile Strength Ratio
USCOE	U.S. Army Corps of Engineers
v	Air voids

VA	Virgin Aggregate
VFA	Void Filled with Asphalt
VMA	Void in Mineral Aggregate
W	Weight of Aggregates in Cylinder.
W_D	Mass of Specimen in Air
W_{SSD}	Saturated Surface Dry Mass
W_{SUB}	Mass of Specimen in Water
WAPA	Washington Asphalt Pavement Association
WES	Waterways Experiment Station
W_{TR}	Wheel Tracking Rate
α	Significance Level
δ	Maximum Deflection at Center of Beam
ϕ	Phase Angle
ε_t	Maximum Tensile Strain
σ_t	Maximum Tensile Stress
ρ_w	Density of water
μ	Poisson's ratio
ω	Width of wheel's contact area

List of Appendices

CHAPTER I

1 INTRODUCTION

1.1 Background

The major role of pavements (road surfaces) is to support a wheel load on the pavement surface and to transfer and spread that load to the sub-grade without exceeding either the strength of the sub-grade or the internal strength of the pavement itself. Aggregate constitutes the main structural skeleton of asphalt mixtures, designed to absorb and control different stresses on the pavement. It is essential to design an asphalt mixture carefully in laboratory conditions to ensure optimal performance during its service life. In the laboratory phase, it is important to select the most suitable materials for the asphalt mixture. In order to prevent any failure in the pavement, one of the key design elements are the aggregate and binder qualities, which provide the mix with cohesion and also with the necessary tensile and shear strength to resist traffic loading and environmental damage (Bardesi, 2010).

Aggregates used in asphalt mixtures may be either crushed stone or crushed gravel. In both cases, the material must be thoroughly crushed, and the resulting particles should be cubical in shape rather than flat or elongated. Aggregates also need to be free of dust, dirt, clay and other deleterious materials. In addition, because aggregate particles carry most of the load in hot mix asphalt pavements, aggregates need to be tough and abrasion resistant (Topal and Sengoz, 2008).

In recent years, many studies have been carried out on the use of construction and demolition (C&D) wastes in new civil construction sectors. A number of scientists, researchers, and policy-makers have endeavored to explore the potential environmental and economic advantages of recycling waste materials, and specifically the possibility of re-using solid waste in pavement (i.e. road) construction (Xue *et al*., 2009). Waste materials used in pavement construction can come from different sources, such as the demolition of civil engineering structures or industrial wastes. Some studies indicate that, utilizing industrial wastes such as marble dust, granite dust and fly ash as filler can improve the performance of asphalt mixtures in terms of moisture susceptibility, rutting and fatigue (Satish and Rajan, 2013).

Industrial waste materials are generally classified according to their sources: for example, industrial by-products (steel slag and coal fly ash), demolition by-products (concrete, tiles and bricks) and road by-products such as Recycled Asphalt Pavements (RAP) or Recycled Concrete Pavements (RCP) (Pihl and Milvang-Jensen, 2001; Tapkin, 2008).

Concrete, one of the most basic and common construction materials around the world, essentially consists of aggregates (sand, crushed stone or gravel), cement and water. When a concrete structure is demolished, repaired or renewed, it is increasingly common to try to recycle and re-use the resulting concrete rubble. This is unsurprising, since waste material from demolished concrete structures is one of the largest sources of waste in the entire world, and has therefore become a global concern that requires a sustainable solution (CSIR, 2000).

Europe alone produces around 180 million tons of concrete waste, or 480 kg per capita, per year (Aggregates Advisory Service, 1999) – ranging from over 700 kg per person in Germany and the Netherlands, to 500 kg in the UK, to just under 200 kg in Greece, Sweden and Ireland. Meanwhile, according to the US Federal Highway Administration (FHWA), approximately 2 billion tons of natural aggregate are produced each year in the US; a figure that is expected to increase to over 2.5 billion tons per year by 2020. This huge demand for aggregate has raised concerns about whether sufficient natural aggregate will be available in the future (FHWA, 2004). This is where Recycled Concrete Aggregate (RCA) from concrete structures such as buildings, bridges, dams or Recycled Concrete Pavements (RCP) may have a role to play. RCAs were initially used as filler materials and, according to previous research, could be used as road sub-base materials or for non-structural concrete applications such as kerbs, canal linings, driveways and footpaths (Arm, 2001; Huang *et al*., 2002; McGrath, 2001; Mroueh and Wahlstram, 2002).

Recent studies on RCAs have shown that they have the potential to produce strong and durable materials for HMA pavements. However, the amount of fine RCA must not exceed more than 30% of the fine aggregate portion of the pavement mixture. This is because, as the ratio of fine RCA increases, the density of the mixture decreases due to the higher mortar content in the fines, which causes higher water absorption (Wong *et al*., 2007). In 2003, the US Federal Highway Administration (FHWA) demonstrated that RCA in base and sub-base materials in roads could produce an acceptable level of performance, not only significantly reducing costs but also entailing significant environmental benefits (FHWA, 2003). Subsequently, in 2004, the California Department of Transportation (Cal-trans) ascertained that, while RCA collection startup costs may be high, the use of RCAs could significantly reduce overhead costs overall (Focus, 2004).

RCAs differ from virgin aggregates due to the amount of cement pastes remaining on their surface after going through the recycling process (Schutzbach, 1992; Paranavithana and Mohajerani, 2006). The presence of cement paste increases the porosity of the aggregates, reduces their particle density, and thus affects their quality and water absorption capacity. Utilizing RCA in hot mix asphalt mixtures thus affects the volumetric properties and performance of HMA mixtures (Topal *et al*., 2006). In this research, we investigate the feasibility of utilizing RCA in Dense-Graded and Gap-Graded hot mix asphalt mixtures, through some experimental tests.

1.2 Research problem statement

In recent years, the demand for natural aggregates has increased significantly due to rapid development and urbanization around the world. However, producing these aggregates from mines and natural resources can be very damaging to the environment (Surya *et al*., 2013). This depletion of quality primary aggregates, together with growing awareness of the need for environmental protection, have led to questioning, including at the international level, of the need for the continued wholesale extraction and use of aggregates from natural resources. Moreover, the availability of natural resources for future generations has also become an important issue (Poon *et al*., 2004).

Recycled Concrete Aggregate (RCA) is a kind of recycled material obtained from C & D wastes. There is increasing global demand to reuse RCA in new civil constructions due to its economic advantages, environmental benefits and energy saving (Moghadas Nejad *et al*., 2013). Reusing waste material is moreover one of the many ways of addressing the problem of excess solid waste materials in industrial and urban areas. Reducing the overuse of natural resources and saving them from exhaustion, reducing the environmental pollution from waste materials generated in urban and industrial areas, and contributing to savings in energy and money are some of the benefits of reusing waste materials in new engineering and industrial applications (Fontes *et al*., 2010).

In recent years, there have been some limited studies on the utilization of RCA in dense-graded hot mix asphalt mixtures. However, there has been no systematic study of the performance of RCA in gap-graded stone mastic asphalt. This research aims to fill that gap by evaluating the volumetric and mechanical properties of Gap-Graded Stone Mastic Asphalt (SMA) and Dense-Graded Hot Mix Asphalt (HMA) mixtures containing various percentages and sizes of Recycled Concrete Aggregates (RCA), based on experimental tests. The results are then tabulated, discussed and statistically analyzed.

1.3 Objectives of the study

The main objectives of this study are as follows:

1. To evaluate the engineering properties of the utilized materials in Dense-Graded and Gap-Graded hot mix asphalt mixtures.
2. To determine the Optimum Asphalt Content (OAC) of Dense-Graded and Gap-Graded hot mix asphalt mixtures containing RCA, based on the Marshall mix design method.
3. To evaluate the performance of Dense-Graded and Gap-Graded asphalt mixtures containing RCA and determine the optimum RCA content, based on experimental tests.

1.4 Hypothesis

- RCA materials have higher porosity, absorption, abrasion, impact and crushing values and a lower specific gravity than granite aggregates, all of which influences the performance of asphalt mixtures containing RCA.
- Regardless of the size of the RCA particles, as the RCA content increases in HMA and SMA mixtures, the optimum asphalt content (OAC) will increase as well.

- Due to the differing aggregate gradations of the HMA and SMA specimens, the HMA mixtures are more sensitive in fines and less in coarse aggregates. Therefore, any replacement of fine granites with F-RCA will impact significantly on the performance of the HMA specimens; while any replacement of course granites with C-RCA will impact significantly on the performance of the SMA specimens.
- While the replacement of granite aggregates with RCA will improve only the fatigue performance of the HMA and SMA specimens but will weaken other specifications such as Resilient Modulus, Rutting, Indirect Tensile Strength and Moisture Susceptibility, the right amount of RCA content will be able to satisfy comfortably the standard requirements for all these criteria.

1.5 Scope of the study

This research evaluates the feasibility of utilizing Recycled Concrete Aggregates (RCA) with different particle sizes in Dense-Graded (HMA) and Gap-Graded (SMA) hot mix asphalt mixtures. The aggregate gradations for the HMA and SMA mixtures were selected in accordance with ASTM D3515 and the Asphalt Institute (AI).

First of all, to verify the quality of the materials used and meet the first objective of the study, the engineering properties of the granite aggregates, RCA and 80-100 penetration grade binder were evaluated. The RCA materials were divided into three categories of fine (F-RCA), with an aggregate particle size of 2.36 mm and smaller; coarse (C-RCA), with an aggregate particle size larger than 2.36 mm; and a mixture of fine and coarse called mix (M-RCA). Five different percentages of RCA (0%, 20%, 40%, 60% and 80% by the weight of total mix) were mixed with HMA and SMA mixtures. The Marshall mix design method was then used to determine the Optimum Asphalt Content (OAC) for each percentage of RCA in order to achieve the second objective of the research.

The HMA and SMA slabs were fabricated based on the calculated OAC values, and compacted using a roller compactor. The required numbers of specimens with 100 mm or 200 mm diameters were cored out from the compacted slabs and subjected to Density, VTM, Stability, Flow, VMA, VFA, Resilient Modulus, Loaded Wheel Tracking (Rutting), Indirect Tensile (IDT) Strength, Moisture Susceptibility and Flexural Beam Fatigue tests to evaluate the performance of each specimen in order to fulfill the third and fourth objectives. All the performance tests were carried out on core specimens with a 100 mm diameter, except for the wheel tracking and flexural beam fatigue tests, for which 200 mm diameter cores and 380 mm × 63.5 mm × 50 mm beams were required and prepared from the compacted HMA and SMA slabs. Finally, the test results were explained, tabulated and statistically analyzed using ANOVA to show the significance between the data.

1.6 Outlines of the thesis

This thesis is organized into five chapters, as follows:

Chapter 1 contains an introduction to the research topic, including the background, the research problem statement, the main objectives of this research, the hypothesis, and the scope of the study.

Chapter 2 presents a literature review covering the history of different kinds of flexible pavements, aggregate gradations, mix design methods, Recycled Concrete Aggregates and their usage in new civil constructions such as concrete structures, and base and sub base layers of roads, as well as some new studies regarding the utilization of RCA materials in pavement top layers by a range of individuals and institutes from around the world.

Chapter 3 explains the methodologies used in this research, including the test procedures based on international standards.

Chapter 4 contains the test results and a discussion about the research findings. A statistical analysis of the test results is also provided in this chapter.

Chapter 5 presents the conclusions from this research, together with some recommendations for further research in the future.

CHAPTER II

2 LITERATURE REVIEW

2.1 Flexible pavements

Hot Mix Asphalt (HMA) is one of the oldest materials which human have been used to make the more durable and smoother roads since long time ago. The major role of pavement is to support a wheel load on the pavement surface, transfer and spread that load to the sub-grade without exceeding either the strength of the sub-grade or the internal strength of the pavement itself. Flexible pavements and asphalt paving mixtures consist of a well-graded, high quality aggregates and asphalt cement. Based on project requirements the aggregate gradation of asphalt mixtures should be changed by pavement designer engineers. Aggregates and binder should be mixed while hot to ensure a good coating of the aggregates and consistency of the mixture. The aggregates which are being used in the mixtures should follow the particular gradation to meet the requirements of local specifications. The basic ideas of road pavements are as follows:

- To prepare a suitable sub-grade or foundation.
- Provide the necessary drainage and construct high quality pavements which have enough thickness and internal strength to carry traffic loads.
- Be sufficiently impermeable to provide a penetration or internal accumulation of water and moistures.
- Have smooth and skid resistant surface which can resistant deterioration cause by weather and chemicals.

Typically the asphalt mixtures are heated to 121º C to 163º C (250º-325º F). Asphalt mixtures should be kept hot during transit to the site, where it is spread on the roadway and compacted by compactors to the proper density before the asphalt is cool. Most commonly hot mix asphalt is divided into three different types of dense-graded, open-graded, and gap-graded asphalt mixtures according to the gradation of the aggregate used in the mix (Asphalt Institute, 2007).

2.1.1 Dense-Graded asphalt

Dense-graded mixtures are the most common HMA mix type. The term dense-graded refers to the dense aggregate gradation used in these types of mixtures, which means that there is relatively little space between the aggregate particles in such mixtures. Historically, dense-graded mixtures were popular because they required relatively low asphalt binder contents, which kept their cost down. However, experience has shown that HMA with binder contents that are too low can be difficult to place and compact and may be prone to surface cracking and other durability problems. Dense-graded asphalt mixtures can be used in any layer of the pavement structure for any traffic level. Traffic level is a direct consideration in the design of dense-graded mixtures. Aggregate angularity, clay content, binder grade, compactive effort, and some volumetric properties vary with traffic levels in the dense-graded mixture design procedure.

Conventional HMA consists of mixes with a nominal maximum aggregate size in the range of 12.5 mm to 19 mm. Dense-graded hot mix asphalt mixture contains of high quality asphalt binder and aggregates which thoroughly compacted into a uniform and a dense mass. Different sizes of aggregates (from fine to coarse) are being used in each dense-graded mix to fulfill the qualification of the pavement. Dense-graded mixtures also provide the mixture designer with the greatest flexibility to tailor the mixture for the specific application. The dense-graded mixture design procedure provides the flexibility to increase the design VMA (Voids in Mineral Aggregates) requirements up to 1.0% to produce mixtures with improved fatigue resistance and durability. Increasing the VMA requirement increases the effective binder content of these mixtures over that for normal dense-graded mixtures. The use of higher effective binder content dense-graded mixtures should be considered for surface and base layers when the traffic level exceeds 10,000,000 ESALs. Some of the advantages of well designed dense-graded asphalt mixtures are; good interlock of aggregates, low permeability, good strength and cheaper price due to lower binder content (Pedersen *et al*. 2011).

2.1.2 Open-Graded Friction Course (OGFC)

An open-graded hot mix asphalt pavements have a high percentage of air voids to let the water drain down through the pavement layers. These types of pavements provide a skid resistant surface and as a porous base layer can be used for drainage under either HMA or Portland Cement Concrete Pavements (PCCP). Open-Graded Friction Courses (OGFC) provides an open mix with permeable voids that provide drainage on the surface of HMA pavements under wet conditions. The water drains vertically through the OGFC to an impermeable, underlying layer and then lateral to the day-lighted edge of the OGFC. In addition, OGFC minimizing hydroplaning and providing high friction resistance on wet pavements. Reducing splash and spray, reducing the potential for hydroplaning, enhance visibility of pavement markings, reducing night time surface glare in wet weather and reducing tire noises are some of the advantages of OGFC layer.

There are some limitations in using this type of pavement, such as; snow and ice-control procedures may need adjustment while using OGFC, raveling and shoving mostly in intersections, locations with heavy turning movements and airfield ramp, special patching and rehabilitation techniques are needed to maintain adequate drainage (Asphalt Institute, 2007). OGFC is mostly used to improve the frictional properties of roadways. These mix types were first developed in Oregon (United States) in the 1930's and evolved through experimentation with plant mix seal coats. OGFCs were identified as an alternative to improve skid resistance by the Federal Highway Administration

(FHWA) in the 1970's after initiating a program to improve the frictional characteristics of our nation's highways. In 1980, the FHWA published a formalized mix design method for OGFCs. During the 1980's, many state agencies placed OGFCs as wearing layers. However, a number of agencies noted that the OGFC layers were susceptible to sudden and catastrophic failures.

These failures were caused by material specification, mix design and construction problems. These problems were primarily related to mix temperature during construction. Gradations associated with OGFCs are much coarser than typical dense-graded HMA. Because of the open nature of OGFCs, there were problems with drain-down during transportation. To combat the drain-down problems, most owners would allow the lower production temperatures. Allowing the reduced production temperatures increased the stiffness of the asphalt binder, thus reducing the potential for drain-down, but also led to other issues that increased the potential of raveling and delamination (the primary distresses leading to failure in OGFCs).

First, when the production temperatures were reduced, sufficient heat was not developed to adequately dry the aggregates during production. This led to moisture remaining in the aggregates and the increased potential for stripping. Additionally, reducing the mix production temperature resulted in the OGFC arriving at the project site cooler than the desired compaction temperature. When this occurred, the OGFC did not always bond with the underlying layer through the tack coat and resulted in an increased potential for raveling and delamination. During the 1980's the catastrophic raveling and delamination problems were of such magnitude that a number of agencies placed a moratorium on the use of OGFC (Cooley, 2009).

2.1.3 Stone Mastic Asphalt (SMA)

Stone Mastic Asphalt (SMA) is a type of gap-graded hot mix asphalt which consists of a coarse aggregates skeleton and a high binder content mortar. This type of mixture has been used in Europe since 1960's to provide better rutting resistance and resist the abrasive nature of studded tires in snowy regions. Because of its success in Europe, the United States government started to use SMA mixture in cooperation with the Federal Highway Administration (FHWA) since 1991 (Bukowski, 1993).

SMA is a mixture, with crushed coarse and fine aggregates, mineral filler, bitumen and fiber. Fiber is used to prevent binder drain-down during transportation and construction procedures. The technical basis of SMA is a stone skeleton with stone-on-stone contact unlike traditional dense graded mixes where aggregates tend to float in the mix with little contact between the large aggregate particles. The coarse aggregates must be hard, durable, and roughly cubical in shape when crushed. The stone-on-stone contact within the high quality aggregate resists the shear forces created by applied loads creating a very rut resistant pavement. High percentages of mineral filler and binder create a glue (called mastic) to hold the stones together and fill in the spaces between the coarse aggregate's skeleton. This mastic filled skeleton prevents water intrusion and provides excellent durability. A typical Dense-Graded Asphalt, Open-Graded Friction Course and Stone Mastic Asphalt mixtures are shown in Figure 2.1.

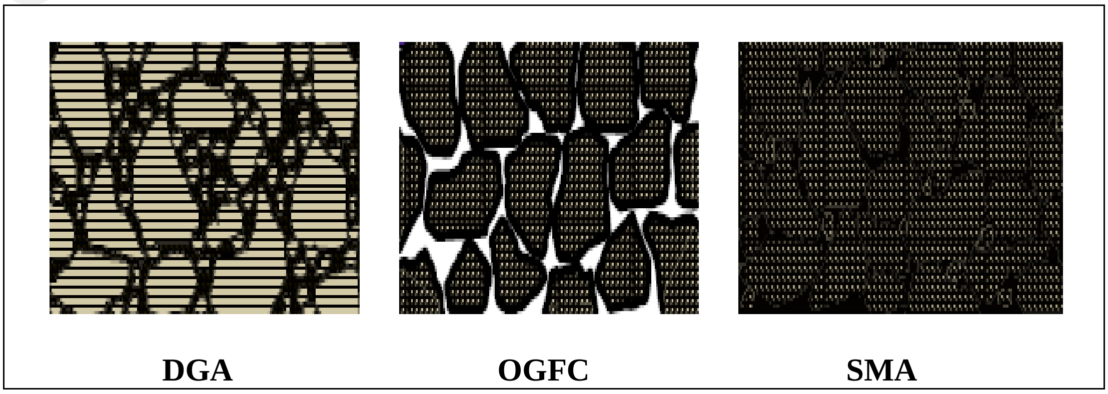

Figure 2.1: Dense Graded Asphalt (DGA), Open-Graded Friction Course and Stone Mastic Asphalt (SMA)

However, SMA has a higher level of binder content (6% or more) compared with other types of asphalt mixtures. This percentage of binder can increase the flexibility of pavement, but also can create some problems if comes to the surface during compaction such as flushing. On the other hand, insufficient binder in SMA will increase the air voids and allow water to permeate and affect the pavement performance by breaking the bond between stones and the bitumen, and allowing the bitumen to unravel. Figure 2.2 presents the aggregate gradation differences for different asphalt pavement surfacing.

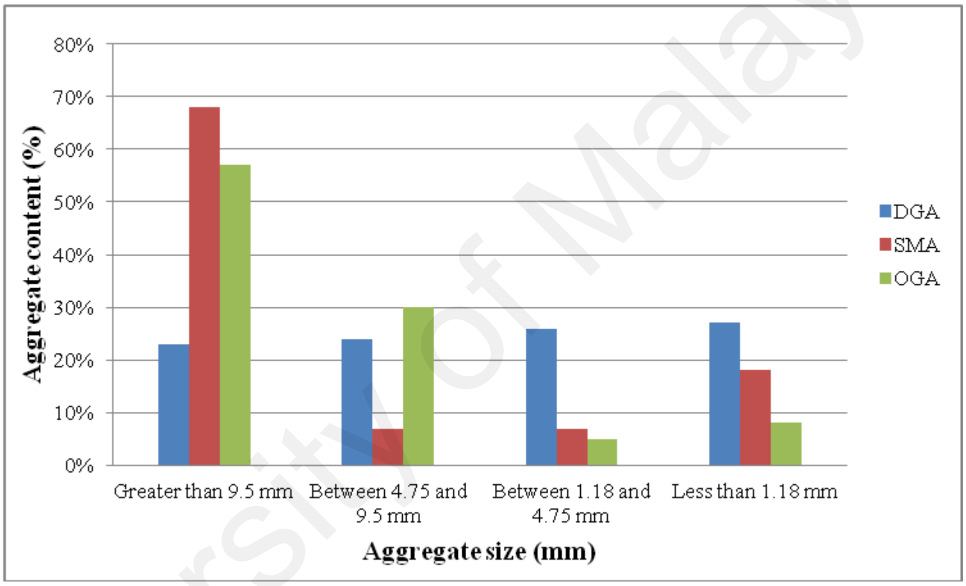

Figure 2.2: Aggregate Gradation for Different Types of Flexible Pavements

The dense-graded asphalt has about equal proportions of aggregate in each of the four sizes. Open graded asphalt (OGA) has a higher proportion of the larger stones (compared to DGA) and a smaller percentage of small stones and fines. SMA typically has a higher proportion of the larger stones and fine particles, but relatively few stones with the intermediate particle sizes (AAPA, 2000). The mix design procedure for SMA is the same with other types of asphalt mixtures. However, Superpave and Marshall mix design methods are more common and have shown better results (Asphalt Institute, 1969). Because of the coarse nature of SMA gradations, the voids in mineral aggregate (VMA) are generally specified to be 17 percent or higher. Therefore, to achieve the four percent air void content requirements in SMA mixtures, the volume of asphalt binder content has to be relatively high.

Because of the relatively high asphalt binder contents, one potential problem encountered with SMA that is not generally observed with dense-graded mixes is drain-down problem. Drain-down is a term that refers to an occurrence where the asphalt binder drains from the coarse aggregate structure during storage, transportation and/or lay-down. In essence, drain-down is a form of segregation; however, it is the asphalt binder and fines separating from the coarser particles. Drain-down can lead to flushed spots on the finished pavement surface which is undesirable (Brown and Cooley, 1998).

Two approaches are typically used to prevent drain-down. The first approach is, to use higher filler content (aggregate passing No. 200 sieve) which stiffens the asphalt binder and preventing the asphalt binder from draining off the asphalt mixtures. The second approach is to use the stabilizing additives such as fibers or modified binders. Both cellulose and mineral fibers have been used with success in SMA mixtures. Similar to the effect of the high fines content, utilization of asphalt binder modifiers and/or fibers tend to stiffen the asphalt binders and preventing drain-down.

2.2 Mix design methods

Pavement mix development is carried out to produce a cost- effective blend and gradation of aggregates and asphalt that yields a mix that has enough asphalt to ensure that the pavement is durable, the mix is adequately stable to satisfy the demands of traffic without distortion or displacement and there are enough voids in the total compacted mix to allow for a slight amount of additional compaction under traffic loading and a slight amount of asphalt expansion due to temperature increases without flushing, bleeding, and loss of stability.

The other objectives of asphalt mix design is to achieve a maximum void content to limit the permeability of harmful air and moisture into the mix and sufficient workability to permit efficient placement of the mix without segregation and without sacrificing stability and performance. Also, for surface mixes, proper aggregate texture and hardness to provide sufficient skid resistance in unfavorable weather conditions is an important parameter. The final goal of mix design is to select a uniquely designed asphalt content that will achieve a balance among all of the desired properties.

When the asphalt samples are prepared in laboratories, it can be analyzed to determine the mixture performance of the pavement. The main focus of this analysis is on density, Voids in Total Mix (VTM), Voids in Mineral Aggregates (VMA), Voids Filled with Asphalt (VFA) and Optimum Asphalt Content (OAC) defines the character of the mixtures and determines the mix performance and behavior. By analyzing the compacted asphalt mixture for the mentioned characteristics, some indication of its probable durability and in-service performance can be predicted. The first mix design procedure was developed by Clifford Richardson.

He established the concept that material selection was important, especially the attributes of fine aggregates and the presence of air voids and voids in mineral aggregates. His findings were published in "*The Modern Asphalt Pavement*" in 1905. The procedure that he developed was called the pat test, which comprised of compacting samples of sheet asphalt (a hot-sand asphalt mixture) against the brown Manila paper and visually evaluating the residual stains. A heavy stain indicated the high binder, a light stain showed the low amount of binder and medium stain showed the optimum asphalt content in the mixture.

Other researchers have continued to develop the mix design method since his procedure has been published. The most popular asphalt mix design method was developed by Hubbard-Field in the Second World War. In Hubbard-Field method, which was developed in the mid-1920s, the stability test was used to determine the maximum asphalt specimen load capacity. The specimen's dimension which was used for stability test in this method was 2 inches (50 mm) in diameter and 1 inch (25 mm) in height.

Study on flexible pavements and hot mix asphalt mixtures have been continued and developed to Hveem mix design, Marshall mix design and Superpave mix design methods. Superpave Mix Design was introduced between 1987 and 1993 by Strategic Highway Research Program (SHRP) and since today this method has been considered as a more developed procedure for asphalt mixture design. However, the most asphalt mixtures produced during the 50 years between the 1940s and 1990s used the Hveem and Marshall mix design methods (Khosla and Sadasivam, 2002).

2.2.1 Hveem mix design

The original Hveem mix design method was the brainchild of Francis Hveem when he was a Resident Engineer for the California Division of Highways in the late 1920s and 1930s. In the Hveem mix design method multiple initial specimens with different percentages of binder content must be prepared and tested to determine the optimum asphalt content value and a California Kneading Compactor (CKC) is used to compact the specimens. CKC is able to fabricate cylindrical specimen with approximately 64 mm (2.5 inches) height and 102 mm (4-inch) diameter. The Compaction pressure can be adjusted from 2.4 to 3.4 MPa (350 to 500 psi). CKC applies forces through a roughly triangular shaped foot that covers only a portion of the specimen face.

Compacted forces by tamps are applied uniformly on the free face of the specimen to achieve compaction. The CKC has a real advantage as being thought by most engineers to simulate the densification characteristics of pavement in the field (Khan *et al*., 1998; Masad *et al*., 1999). There are also some disadvantages of these types of compactors, such as: compaction devices are very expensive, bulky size and not portable. California kneading compacted specimens has shown differentiated density and air voids because of large variations in sizes and shapes. Also over the years, mix design methods have been developed, and new mix design methods require new equipment and methods of compactions. Therefore, new compactors should be developed to make a better simulation of field compaction in laboratories (Roberts *et al*., 1996; Asphalt Institute, 1997).

2.2.2 Marshall mix design

During World War II, the U.S. Army Corps of Engineers (USCOE) began evaluating various HMA mix design methods for use in airfield pavement design. The motivation for this search came from the ever-increasing wheel loads and tire pressures produced by larger and larger military aircraft. The most promising method eventually proved to be the Marshall stability method developed by Bruce G. Marshall at the Mississippi Highway Department in 1939. The Waterways Experiment Station (WES) took the original Marshall stability test and added a deformation measurement (flow meter) that was thought to assist in detecting excessively high asphalt contents. This appended test was eventually recommended for adoption by the U.S. army because it was designed to stress the entire sample (rather than just a portion of it) and the produced specimen's densities were close to field densities. Also, it was light and portable and facilitated rapid testing with minimal effort.

WES continued to refine the Marshall method through the 1950s with various tests on materials, traffic loading and weather variables. Today the Marshall method (despite its shortcomings) is probably the most widely used mix design methods in the world. Some of The Marshall impact compactor is capable of producing cylindrical specimens with 102 mm (4-inch) diameter and 64 mm (2.5 inches) height (corrections can be made for different sample heights). The tamper foot is flat and circular shape with a diameter of 98.4 mm (3.875 inches) corresponding to an area of 76 cm^2 (11.8 in^2). The compaction pressure is specified as a 457.2 mm (18 inches) free fall drop distance of a hammer assembly with a 4536 g (10 lb.) sliding weight. The numbers of blows are highly dependent on the anticipated traffic loading and can be adjusted to 35, 50 or 75 blows for each side of the sample.

The Marshall impact compactor is being used for SMA mixtures, but according to the NAPA, it is recommended to decrease the number of blows from 75 per each side (in HMA) to 50 blows in SMA to prevent aggregate breakage. However, recent studies have shown that, the expected density and air voids cannot be reached with 50 blows. Also, as the thickness of the specimens cannot be controlled while using the Marshall impact compactors, the density and air voids level are varied. Therefore, it is preferred not to use the Marshall compactor for fabrication of SMA specimens. Because, the result will be the same materials with variation in density and air voids due to different thicknesses of the specimens (NAPA, 1982).

2.2.3 Superpave mix design

Superpave is an acronym for Superior Performing Asphalt Pavements. It is the product of the Strategic Highway Research Program. Superpave includes a new mixture design and analysis system based on performance characteristics of the pavement. It is a multi-faceted system with a tiered approach to designing asphalt mixtures based on desired performance. Superpave includes some old rules of thumb and some new and mechanistic-based features. The Superpave mix design system is quickly becoming the standard system used in the United States (US). The US was looking for a new system to overcome pavement problems such as rutting and low temperature cracking that had become common with the use of design systems such as Marshall and Hveem.

The Superpave system offers solutions to these problems through a rational approach. The Superpave Gyratory Compactor (SGC) is not the perfect compactor for producing specimens that manifest all the properties of field-compacted pavement layers. However, it might be the best available compactor for conveniently producing laboratory scale specimens. It is convenient, versatile, and provides important information related to the engineering properties of asphalt mixture. Further, it is becoming the most widely accepted and used hot mix asphalt compaction device in the world. Many engineers believe that $N_{initial}$ (The initial number of gyrations) provides useful information regarding the compact ability of the asphalt mixtures (Asphalt Institute, 2007).

Excessive density at $N_{initial}$ indicates a potential tender mix and conversely, inadequate density indicates the contractor may have difficulty achieving the required density. It was concluded that the precision of the SGC was better than the mechanical Marshall hammer (Buchanan and Brown, 2001). The original Superpave N_{design} (N_{design} is used to vary the compactive effort of the design mixture and it is a function of climate and traffic level) compaction matrix, contained 28 levels (four temperatures seven traffic levels). Brown *et al.*, (1996) found that the recommended gyration levels may be excessive for lower levels of traffic. Brown and Buchanan (1999) recommended reducing the number of N_{design} compaction levels from 28 to four (50, 70, 100, and 130 gyrations) to address all traffic levels. They advised that the requirement for 11 percent air voids at N $_{initial}$ for low-volume roads was too stringent. They further recommended designing mixtures to N $_{design}$ gyrations and not N $_{Maximum}$ (maximum number of gyrations to achieve the laboratory density, which should never be exceeded in the field) and suggested that the slope of the compaction curve may not be a good indication of the strength of the HMA aggregate structure.

This compactor was produced to make comparable laboratory samples with tire load pressure of in-service compacted mixture after traffic compaction, but still it is not possible to achieve the field density with gyratory compactors in laboratory samples (Kumar and Goetz, 1997). SGC is capable of producing cylindrical specimens with 150 mm (6-inch) diameter and approximately 115 mm (4.5 inches) height (corrections can be made for different sample heights). The common compaction pressure is 600 kPa (87 psi) and number of gyrations are varies. The load is applied to the sample top and covers almost the entire sample top area.

The sample is inclined at 1.25° and rotates at 30 revolutions per minute as the load is continuously applied. This helps achieve a sample particle orientation that is somewhat like that achieved in the field after roller compaction. The gyratory testing machine is a combination of a kneading compactor and a shear testing machine. According to recent changes in the number and angle of gyration for SMA mixtures, Gyratory compactor specimens have shown better results in comparison with Marshall Impact Compactor specimens.

2.3 Aggregate in asphalt mixtures

Aggregate is the major structural skeleton of asphalt mixture to absorb and control different stresses on the pavement. The laboratory design of an asphalt mixture is essential to ensure optimal performance during the service life of the mix. In the laboratory phase, it is important to select the most suitable materials for the asphalt mixture. In order to prevent any failure in the pavement, one of the main design factors to be considered is aggregate and binder qualities which provide the mix with cohesion and also with the necessary tensile and shear strength to resist traffic loading and environmental damages (Bardesi, 2010). For this reason, the right selection of aggregate, bitumen, filler, and fines is crucial for optimal mix performance (Mo *et al*., 2009).

Another important factor in the prevention of cracking is the coarse aggregate used in the asphalt mixture. The gradation and shape of the coarse aggregates provide the internal friction and bearing capacity, which resists the stresses caused by traffic loads (Bardesi, 2010). Asphalt concrete is composed primarily of aggregate and asphalt binder. Aggregate typically makes up about 95% of asphalt mixture by weight, whereas asphalt binder makes up the remaining 5%. By volume, a typical hot mix asphalt mixture is about 85% aggregate, 10% asphalt binder, and 5% air voids. Small amounts of additives and admixtures are added to many asphalt mixtures to enhance their performance or workability (Peattie, 1979). Many studies indicated that physical characteristics and Chemical compositions of aggregate affect the workability and optimum bitumen content of the mixture, as well as the asphalt mixture properties (Topal and Sengoz, 2005; Topal and Sengoz, 2008).

The nature of the aggregate directly affects its adhesion to the bitumen and its resistance to fragmentation. In this sense, if the adhesion between aggregate and bitumen is poor, this produces many weak points where the cracking process will eventually develop and propagate throughout the asphalt mixture. Furthermore, if the resistance to fragmentation is not sufficiently high, the coarse aggregate could also crack, thus facilitating the cracking process (Petersen *et al*., 1982). Gradation, quality and shape (angularity and texture) of the aggregates play an important role in performance of asphalt mixtures.

The higher quantity of crushed and angular aggregates causes the better interlock between the materials and improve the performance of the asphalt mixtures (Abo-Qudais and Al-Shweily, 2007; Miller *et al*., 2011; Massad *et al*., 2005). Aggregates used in asphalt mixtures must be of good quality to ensure the resulting pavement will perform as expected. Aggregates used in HMA mixtures may be either crushed stone or crushed gravel. In either case, the material must be thoroughly crushed, and the resulting particles should be cubical rather than flat or elongated. Aggregates should be free of dust, dirt, clay, and other deleterious materials. Because aggregate particles carry most of the load in hot mix asphalt pavements, aggregates should be tough and abrasion resistant (Topal and Sengoz, 2008).

2.4 Bitumen in asphalt mixtures

Asphalt binders, sometimes referred to as asphalt cement binders or simply asphalt cement, are an essential component of asphalt concrete. They are the cement that holds the aggregate together. Asphalt binders are a co-product of refining crude petroleum to produce gasoline, diesel fuel, lubricating oils, and many other petroleum products. Asphalt binder is produced from the thick, heavy residue that remains after fuels and lubricants are removed from crude oil. This heavy residue can be further processed in various ways, such as steam reduction and oxidation, until it meets the desired set of specifications for asphalt binders. For demanding, high-performance applications, small amounts of polymers are sometimes blended into the asphalt binder, producing a polymer-modified binder (Pedersen *et al*., 2011).

Binder content is one of the most important characteristics of asphalt concrete. Use of the proper amount of binder is essential to good performance in asphalt concrete mixtures. Too little binder will result in a stiff mix that is difficult to place and compact and will be prone to fatigue cracking and other durability problems. Too much binder will be uneconomical, since binder is the most expensive component of the mixture and will make the mixture prone to rutting and shoving. Therefore, type, quality and characteristics of asphalt binder play the significant role on the mechanical response of asphalt mixtures (Kumar and Veeraragavan, 2011).

Typical asphalt binder contents range from 3.0% or less (for lean base course mixtures) to over 6.0% (for surface course mixtures and rich bottom layers), which are designed for exceptional durability and fatigue resistance (Asphalt Institute, 2007). Performance grading of asphalt binders was developed during SHRP. The main purpose of this way of classifying and selecting asphalt binders is to make certain that the binder has the correct properties for the given environment.

Performance grading was also meant to be based more soundly on basic engineering principles earlier methods of grading binders often used empirical tests, which were useful but did not provide any information on the fundamental engineering properties of the binder. Five penetration grades (PG) are specified for asphalt binders in ASTM D 946, 40-50, 60-70, 85-100, 120-150, and 200-300 (the lower the penetration, the harder the asphalt). Also six viscosity graded asphalt cements found in ASTM D3381 are: AC-2.5, AC-5, AC-10, AC-20, AC-30, and AC-40 (The lower the number of poises, the less viscous the asphalt cements). Properties of asphalt binders can be measured by penetration, softening point, viscosity, flash and fire, thin film oven, and specific gravity tests (Roberts *et al*., 1996).

2.5 Recycled Concrete Aggregate (RCA)

The Federal Highway Administration (FHWA) indicates that approximately 2 billion tons of natural aggregate are produced each year in the US. Also, aggregates production is expected to be increased to over 2.5 billion tons per year by 2020. This needed volume of aggregate has raised concerns about the availability of natural aggregates in the coming years (FHWA, 2004). Recycled Concrete Aggregate (RCA) is produced by crushing demolished concrete

structures such as buildings, bridges and dams. RCAs were initially used as filler materials and based on previous researches; it could be used as road sub-base materials and in nonstructural concrete applications such as curbs, canal lining, driveways and footpaths (Arm, 2001; Huang *et al*., 2002; McGrath, 2001; Mroueh and Wahlstram, 2002).

Waste materials to be used in pavement constructions can come from different sources, including demolition of civil engineering structures and industrial wastes. These materials are mostly classified based on their resources like industrial by-products (steel slag and coal fly ash), demolition by-products (concrete, tiles and bricks) and road by-products such as RAP (Recycled Asphalt Pavements) or RCP (Recycled Concrete Pavements) (Pihl and Milvang-Jensen, 2001). Concrete is the most basic construction material all around the world, which essentially consists of aggregates (sand, crushed stone or gravel), cement and water. Environmental and economic considerations have encouraged governments to find a ways to use recycled materials in new productions. When the concrete structure is demolished, repaired or renewed, recycling is an increasingly common method of re-using the rubble concretes. On the other hand, in recent years the knowledge of continued wholesale extraction and use of aggregates from natural resources has been questioned at the international level. This is the result of the depletion of quality primary aggregates and greater awareness on environmental protection. Moreover, the availability of natural resources for future generations has also been considered as an important issue (Poon *et al*., 2004). Waste material from demolished concrete structures is one of the largest wastes in the entire world. For example, this amount of waste in Europe is around 180 million tons per year or 480 kg per capita per year (Aggregates advisory, 1999). These ranges are from over 700 kg per person in a year in Germany and the Netherlands, 500 in UK to almost 200 in Greece, Sweden and Ireland. Therefore, concrete waste has become a global concern that requires a sustainable solution (CSIR, 2000).

Recent studies on RCAs have shown the acceptable potential to produce strong and durable materials for HMA pavements. However, the amount of fine RCA shouldn't exceed more than 30 percent of the fine aggregate portion of the pavement mixtures. This is because as the fine RCA increases, the density will be decreased due to higher mortar in fines which causes higher water absorption in the mixture (Wong *et al*., 2007). In 2003 the Federal Highway Administration (FHWA) proved the acceptable performance of RCA in base and sub-base materials of roads which not only significantly reduce the costs, but also have many environmental benefits (FHWA, 2003). In latter investigation, in 2004, California Department of Transportation (Cal-trans) discovered that even though the RCA collection startups costs are high, but in general overhead costs are significantly reduced (Focus, 2004).

Recycled concrete aggregates are different from virgin aggregates due to the amount of cement pastes remaining on the surface of the recycled aggregates after undergoing the recycling process (Schutzbach, 1992; Paranavithana and Mohajerani, 2006). The presence of cement paste increases the porosity of the aggregates, reduces the particle density, and thus affects the quality and water absorption capacity of the RCA. Therefore, utilizing RCA in Hot Mix Asphalt (HMA) mixtures affected the volumetric properties and performance of HMA mixtures (Topal *et al*., 2006).

2.5.1 Utilization of RCA in base and sub base layers

Many previous studies have shown that the engineering properties of recycled concrete aggregates from construction and demolition waste (C&D) make them suitable for use as granular material in embankments and sub-bases for paved roads (Roussat *et al*., 2008; Vegas *et al*., 2008; Perez and Pasandin, 2014). Petrarca (1984) investigated the use of RCA on some local projects in New York between 1977 and 1982. Concrete used for recycling in Petrarca's study was crushed from sidewalks, driveways, curbs, and pavements.

More than 100 tests were conducted and it was determined that crushed concrete, consistently met all requirements for excellent long term performance as dense-graded aggregate base or subbase. However, the quality of aggregates with sources used to produce RCA will depend on the original intended use of the PCC (NCHRP, 2001). Snyder and Bruinsma (1996) reported on five field studies and five laboratory studies to evaluate the use of RCA materials in unbound layers underneath pavements. Field studies included evaluations of existing pavement drainage systems for pavements utilizing RCA base materials and monitoring of various test sections containing RCA materials and natural aggregates. Based on the field studies, RCA materials within drainage base layers have the potential to precipitate calcium carbonate materials (called calcite).

The laboratory studies indicated that the amount of calcium carbonate precipitate was proportional to the amount of RCA materials passing the No. 4 (4.75mm) sieve.

However, washing RCA during processing practically eliminates the formation of the calcium carbonate precipitates. The test results reported by Poon and Chan (2006) indicated that the use of 100% recycled concrete aggregate increased the optimum moisture content and decreased the maximum dry density of the sub-base materials compared to those of natural sub-base materials.

The California bearing ratio (CBR) values (unsoaked and soaked) of the sub-base materials prepared with 100% recycled concrete aggregate were lower than those of natural sub-base materials. Nevertheless, the soaked CBR values for the recycled sub-base were greater than 30%, which is the minimum strength requirement in Hong Kong. Using the same methods, Khaled and Krizek (1996) found that RCA can be used as a base course in highway pavements if the recycled concrete aggregate is stabilized with as little as 4% cement and 4% fly ash by dry weight of the mix.

Unfortunately, using RCA for base and sub-base materials is associated with complications related to the high water solubility of RCA components, which can cause an increase of PH in nearby groundwater systems as well as possibly affecting the vegetation within the vicinity of the roads (Gilpin *et al*., 2004). Arulrajah *et al*., (2012a) investigated the recycled crushed brick when blended with recycled concrete aggregate and crushed rock for pavement sub-base applications. The research indicates that up to 25%, crushed brick could be safely added to recycled concrete aggregate and crushed rock blends in pavement sub-base applications. The repeated load triaxial test results on the blends indicate that the effects of crushed brick content on the mechanical properties in terms of permanent deformation and resilient modulus of both the recycled concrete aggregate and the crushed rock blends were marginal compared to the effects on dry density and moisture content. Arulrajah *et al*., (2012b) achieved a laboratory investigation into the geotechnical properties of recycled concrete aggregate (RCA). The Los Angeles abrasion loss tests indicated that the RCA is durable. CBR values were found to satisfy the local state road authority requirements for sub-base material. Repeated load triaxial tests established that the RCA would perform satisfactorily as a pavement sub-base material in the field. The results of the laboratory testing undertaken in this research indicated that RCA satisfied the criteria for use in pavement sub-base applications.

The possibility of using crushed concrete and demolition debris as sub-base coarse aggregate was investigated by Fabiana *et al*., (2011). CBR experiments were conducted, and the behavior of the recycled materials was compared with the behavior of limestone. The results showed that CBR of crushed concrete was similar to that of natural aggregate. Conversely, demolition debris presented a fairly decrease in its CBR. Perez *et al*., (2013), investigated the application of cement-treated granular material (CTGM) made by RCA, in the construction of actual road base in Spain. It was found that, the sections built utilizing CTGM showed similar performance compared to natural aggregates and the cement treated RCA is a real alternative in the construction of road bases and sub-bases.

2.5.2 Utilization of RCA in hot mix asphalt mixtures

Paranavithana and Mohajerani (2006) performed experiments on the effects of recycled concrete aggregates on the properties of HMA, in which 50% RCA by dry weight of total aggregates was used as coarse aggregate in the asphalt mixtures. The performance tests carried out on these mixes showed that, using RCA in HMA mixtures lowered the resilient modulus and creep resistance of the mix and increased the stripping potential of them. In addition, the mixes containing RCA showed large variations in strength under dry and wet conditions. Wong *et al*., (2007), studied on the utilization of RCA as a partial aggregate substitution in HMA. Three HMA mixes were included in the study by substituting granite filler/fines with 6% untreated, 45% untreated, and 45% heat-treated recycled concrete, respectively. All three mixes passed the wearing course criteria specified by the Singapore Land Transport Authority (SLTA), based on the Marshall mix design method. The performance tests on the mix with 6% RCA showed comparable resilient modulus and creep resistance to those of the traditional HMA mix. The mixes with the higher percentage of RCA showed higher resilient modulus and resistance to creep.

Another research was conducted by Topal *et al*., (2006), who studied on use of recycled concrete aggregates in hot-mix asphalt. They found that, RCA can substitute HMA aggregates and achieve the required Marshall Stability (MS) and Indirect Tensile Strength (IDT) of the mixtures. The test results indicated that, the Marshall Stability values increased with the increase of RCA in the mix. However, the voids in mineral aggregate (VMA) and the voids filled with asphalt (VFA) decreased with the increase in RCA content. This was believed to be due to crushing of RCA by the Marshall compactor during compaction. The tensile strength of the mix containing RCA was found to be higher than that of the control mix as the internal friction of RCA was higher than that of natural limestone aggregates. Eventually, RCA was not recommended to be used in the wearing course due to RCA's susceptibility to abrasion by vehicles.

Bhusal et al., (2011) investigated the volumetric properties of hot mix asphalt containing 5% recycled concrete aggregates. Test results revealed that the asphalt mixtures absorption increased by increasing the RCA content in the asphalt mixtures and based on the statistical analysis the influence of RCA in volumetric properties of hot mix asphalt was significant. Gul and Guler (2014) investigated the rutting performance of asphalt mixtures containing recycled concrete aggregates. They revised the Marshall mix design method to prepare the asphalt specimens to fulfill the minimum requirement in terms of uniaxial testing. The test results indicated that utilization of recycled concrete aggregate in asphalt mixtures improve the rutting performance of the asphalt mixtures.

Hassanied et al., (2016) assessed a case study on performance of recycled construction demolition wastes in asphalt mixtures. In this study various percentages of fine aggregates in hot mix asphalt mixtures were replaced by fine RCA. Test results indicated the feasibility of up to 30% fine RCA in hot mix asphalt mixtures in terms of Marshall stability and indirect tensile strength tests. Marques et al., (2014) investigated the comparative study between asphalt mixtures containing natural and recycled concrete aggregates. In this study, 25, 50 and 100% of virgin aggregates were replaced by recycled concrete aggregates. Test results showed that the values of air voids and voids filled with asphalt in mixtures containing 50% and 100% RCA did not meet the relevant standard requirement. Therefore, it was concluded that replacing the virgin aggregates with 25% of RCA not only have environmental and economic benefits, but also can satisfy the standard requirements for pavement surface.

Another research was carried out by Moghadas Nejad et al., (2013) on fatigue performance of hot mix asphalt mixtures containing recycled concrete aggregates. The indirect tensile fatigue test was used to measure the behavior of hot mix asphalt mixtures containing 0%, 35%, 70% and 100% RCA. It was found that, utilization of RCA in asphalt mixtures, reduce the production costs and prevent much fullness of the recycled materials in the environment. It was found that using up to 100% RCA instead of virgin limestone in the asphalt mixtures improved the fatigue performance of the asphalt specimens.

Beale and You (2010) investigated the feasibility of using RCA for a low-volume traffic road in Michigan, with 25%, 35%, 50%, and 75% of virgin aggregates by the weight of total aggregates substituted with RCA. It was found that, increasing the RCA's content decreased the VMA and VFA of the mixes. The laboratory test results indicated that all the 4 mixes containing RCA passed the minimum rutting specification of 0.32 inch rut depth. Dynamic modulus test results showed that the stiffness of the mixtures containing RCA was less than control mix, but using RCA in HMA mixtures reduced the energy needed for compaction. In terms of moisture susceptibility, all the mixes (except 75% RCA mix) passed the Tensile Strength Ratio (TSR) of 80%.

In a study conducted by Shen and Du (2004), the permanent deformation of Hot Mix Asphalt (HMA) mixtures containing Reclaimed Building Materials (RBM) has been investigated. The HMA specimens were produced by using four types of aggregates (100% river crushed stone, 100% RBM, the mixture of 50% crushed stone and 50% RBM and the mixture of coarse RBM and fine crushed stone) and two types of binders (AC-10 and AC-20). It was found that, regardless of the binder types, different types of aggregate mixtures had a significant effect on the permanent deformation of HMA specimens.

Lee *et al*., (2012) assessed the evaluation of pre-coated recycled concrete aggregates for hot mix asphalt. The RCA materials were pre-coated by coating thickness of 0.25, 0.45 and 0.65 mm slag cement before being used in the HMA mixtures. The rutting, moisture susceptibility and indirect tensile strength tests of the HMA mixtures containing pre-coated RCA (PCRCA) have shown satisfactory results based on the Transportation and Communications criteria of Taiwan.

Pasandin et al., (2015) investigated the influence of aging on binder extracted from asphalt mixtures containing recycled concrete aggregates. Virgin aggregates were replaced by 0% and 30% RCA in the asphalt mixtures and the extracted binder was later tested in terms of dynamic viscosity, dynamic shear rheometer, penetration and softening point tests. Test results indicated that, the aging caused by heat treatment increased the stiffness of the asphalt mixtures and RCA has a small influence. However, when there is no curing time for the asphalt mixtures, the RCA protects the binder in terms of aging.

Arabani and Azarnoosh (2012) evaluated the dynamic properties of hot mix asphalt mixtures containing recycled concrete aggregate and still slags. The Marshall mix design method was used for fabrication of six different HMA mixtures, containing three different types of aggregates (dacite, recycled concrete and steel slag) and tested in terms of fatigue, stability, indirect tensile resilient modulus and dynamic creep tests. Test results revealed that, the HMA specimens containing coarse steel slags and fine RCA could perform better than the other mixtures.

In the other experiment conducted by Arabani *et al*., (2012), the effect of recycled waste concrete in asphalt mixtures has been evaluated. The RCA materials were used as a partial or total replacement with dacite including replacement of coarse aggregate (CA), fine aggregate (FA) and fillers in the HMA mixtures. Based on the performance tests, the mixture containing coarse dacite and fine RCA was the optimal mixtures in terms of fatigue, rutting, resilient modulus and Marshall stability test results.

In another join experiment by Pasandin and Perez (2013), the feasibility of using construction and demolition wastes in HMA mixtures was evaluated. The Marshall mix design method was used for the fabrication of HMA mixtures containing 0%, 5%, 10%, 20% and 30% RCA. Based on their previous researches (Perez *et al.*, 2010a; Perez *et al.*, 2010b and Perez *et al.*, 2010c), it was found that, conditioning the asphalt mixtures for 4 hours in an oven (at the mixing temperature) before compaction could considerably improve the moisture susceptibility of the mixtures. It was believed that, during the conditioning, the surface of the RCA will be properly coated by the binder, which reduces the porosity of the RCA and results in lower moisture sensitivity. Moreover, resilient modulus, fatigue, moisture sensitivity, stiffness and rutting test results of the mixtures containing various percentages of RCA showed the acceptable results to that of the conventional mixtures.

The effect of demolition waste as recycled aggregate in HMA mixture was evaluated by Wu *et al.*, (2013). The demolished waste (DW) materials were divided into two groups called recycled coarse aggregate (RCA) and recycled fine aggregate (RFA). Three types of asphalt mixtures were produced containing RFA and coarse lime stones, RCA and fine limestone and the mixture of coarse and fine limestone as a control mix. The freeze and thaw (for moisture susceptibility), scan electron microscope, immersion Marshall and rutting at high temperature tests were carried out to evaluate the performance of the recycled materials in the specimens. Test results showed that, the specimens made by RCA and fine limestone performed better resistance to rutting and low temperature cracking compared to the other two mixtures while the moisture resistance of the RFA was higher than the RCA and control specimens. However, based on the performance test results, all the specimens could satisfy the China's technical asphalt pavement construction specifications.

The investigation on mechanical properties of HMA mixtures containing RCA was carried out by Mills-Beale and You (2010). The dynamic modulus (E^*), rutting, resilient modulus, Construction Energy Index (CEI) and tensile strength ratio (TSR) of the HMA mixtures containing various percentages of the RCA were determined to evaluate the performance of the HMA specimens. Test results revealed that, the dynamic stiffness of the hybrid mixtures were less than control mix. However, in terms of rutting, all the specimens could fulfill the minimum standard requirements and in terms of TSR (moisture susceptibility), all the specimens could meet the specification criterion except the mixtures containing 75% RCA. Moreover, it was found that, using RCA in HMA mixtures could save some amounts of compaction energy.

2.6 Performance tests of asphalt mixtures

There are some asphalt mixture performance tests to ensure pavement engineers about the reliable mixture performance over a wide range of materials, traffic and climatic conditions. These tests are divided to volumetric and mechanical tests. Measuring density, Voids in Total Mix (VTM), Voids in Mineral Aggregate (VMA) and Voids Filled with Asphalt (VFA) are some of the volumetric tests for asphalt specimens. Moreover, Marshall Stability, Flow and other advanced tests such as Resilient Modulus, Fatigue, Moisture Induced Damage, Loaded Wheel Tracking (rutting) and Indirect Tensile Strength are considered as mechanical performance tests.

2.6.1 Bulk density and air voids

Density is one of the most important parameters in future performance of pavement. Well designed and compacted asphalt mixtures may contain enough air voids to prevent rutting due to plastic flow. The percentage of air voids must be sufficient and low enough to prevent permeability of air and water to the body of pavement and high enough to prevent plastic flow after a few years of opening to traffic (Brown, 1990).

The percentage of air voids in asphalt mixtures are directly related to density, and a high level of density can be achieved by increasing the compaction, binder content and/or filler content. It is clear that with decreasing the air voids in asphalt mixture, the density will be increased, but reducing the air void level by adding extra amounts of binder or filler content to the mix does not necessarily have a positive effect on asphalt mixture performance (Roberts *et al*., 1996).

2.6.2 Marshall stability and flow

The purpose of the Marshall stability test is to measure the strength of the compacted asphalt mixtures. Brown and Mallick (1994) found that, the variability of Marshall stability results in Stone Mastic Asphalt (SMA) and dense-graded mixtures are significantly different and the results of dense-graded mixtures are considerably higher. The average of stability for the dense-graded mixtures is 2500 pounds, which is approximately 50 percent higher than the gap-grade mixtures (SMA). The stability test results are used as one of the most important factors in Marshall mix design procedure to measure the Optimum Asphalt Content (OAC) for asphalt mixtures with different percentages of binder content.

The highest temperature of pavement during the summer is 60ºC, so all the specimens must be kept and conditioned in 60ºC before testing. Viscosity of binder has a significant effect on stability of asphalt mixes and anything that increases the viscosity of the binder increases the Marshall stability. Also, using more crushed angular aggregates instead of rounded or sub-rounded aggregates in asphalt mixture are the other effective factor for increasing the stability. Flow is a vertical deformation of the asphalt specimen and is measured at the same time as the Marshall stability. The high flow value of an asphalt mix sample will result in permanent deformation in the pavement under traffic, and low flow value might result from insufficient binder or high voids, which will result premature cracks due to the brittleness of pavement during service life (Roberts *et al*., 1996).

2.6.3 Resilient modulus

The repeated load indirect tension test, or resilient modulus test (M_R), is used to measure the elastic properties of asphalt mixtures by calculating the stress-strain behavior of asphalt specimens (Baladi and Harichandran, 1989). The standard specimen dimension, used for the resilient modulus test is a 2.5 inch (62.5mm) by 4 inches (100mm) specimen, and for Hot Mix Asphalt (HMA) specimens, the applied load to stress level is between 5 to 20 percent of indirect tensile strength (Asphalt Institute, 2007). This test has become popular with many asphalt laboratories, due to simplicity and applicability to test field cores. According to Michael *et al*., (2002), there is no significant relation between M_R and rutting, but the results at low temperatures are somewhat related to cracking, as stiffer mixes (higher MR) at low temperatures tend to crack earlier than more flexible mixtures (lower MR).

The resilient modulus is highly dependent on temperature due to the softening point of the asphalt binder and as the temperature increases the resilient modulus of the asphalt mixture decreases. Also finding the relationship between resilient modulus and temperature can be used to prove the acceptability of asphalt concrete over the nominal range of the temperature that the pavement will be faced in the field and the susceptibility of compacted asphalt mixture to cracking (Gartner, 1987). Comparative study of dense-graded and open-graded asphalt mixtures show the value of resilient modulus in open-graded mixture is lower than dense-graded mixture at the same temperatures. The higher level of air voids in open-graded mixtures would result in a higher recovered strain and the measured resilient modulus would be higher and increasing density of aggregate results in a higher resilient modulus.

The resilient modulus test results provide a basic constitutive relationship between stiffness and stress state of pavement materials for use in pavement design procedures and the structural analysis of layered pavement systems. The resilient modulus test simulates the conditions in pavement due to application of moving wheel loadings. As a result, the test provides an excellent means for comparing the behavior of pavement construction materials under a variety of conditions and stress states (Witczak, 2004).

2.6.4 Permanent deformation (Rutting)

During the past several years, many states experienced problems with the amount and severity of permanent deformation in hot mix asphalt pavements. This problem with permanent deformation, or rutting, was attributed to an increase in truck tire pressures, axle loads, and volume of traffic (Brown and Cooley, 1999).

The risk of permanent deformation is considerably higher during summer that heavy vehicles are travelling on a pavement and a considerable distress is being imposed to the pavement structure. The repetition of heavier axle loads becomes more significant with higher traffic volume. The loads from the repeated traffic can create pronounced amounts of permanent deformation or rutting. The mentioned incident can occur even on straight road sections, bus stops or close to traffic lights due to the slow speed and heavy loads of the trucks and trailers (Tapkin and Keskin, 2013).

Rutting is the earliest accruing distress and sometimes appears after only a few months and might be due to some failures in asphalt layers or underlying layers such as the subgrade soil being overstressed or the required density was not achieved due to inadequate compaction (WAPA, 2011). Particle shape of aggregates is important for workability and performance of asphalt mixes. Angular particles, rather than flat, thin, and elongated particles are recommended for use in hot mix asphalt mixtures (Roberts *et al.*, 1996). Angular particles, a property found in most crushed stone, provide a better interlocking property than rounded particles and provide better performance and less rutting under repetitive traffic loads. On the other hand, characteristics of fine aggregates play an important role in pavement rut performance, as well (Chowdury *et al.*, 2001). Rutting also can be attributed to improper asphalt mix design such as high asphalt content, excessive filler and high amounts of rounded aggregates in mix design or insufficient asphalt layer thickness. Use of excessive asphalt cement in the mix causes the loss of internal friction between aggregate particles, which results in the loads being carried by the asphalt cement rather than the aggregate structure.

Mechanical deformation might be one of the mechanisms involved in rut development. Mechanical deformation can occur when an element under the pavement surface loses its integrity for one reason or another and is displaced under the load. A rut resulting from this type of action will generally be accompanied by a substantial pattern cracking, provided the distress is allowed to progress sufficiently (Kandhal, 1998). Several tests exist that allow designers to evaluate the rutting potential in a lab environment, but there is no direct correlation for the magnitude of lab rutting compared to magnitude of field rutting (Kandhal and Cooley, 2002). Figure 2.3 shows the schematic permanent deformation (rutting) in asphalt pavement under the wheel load.

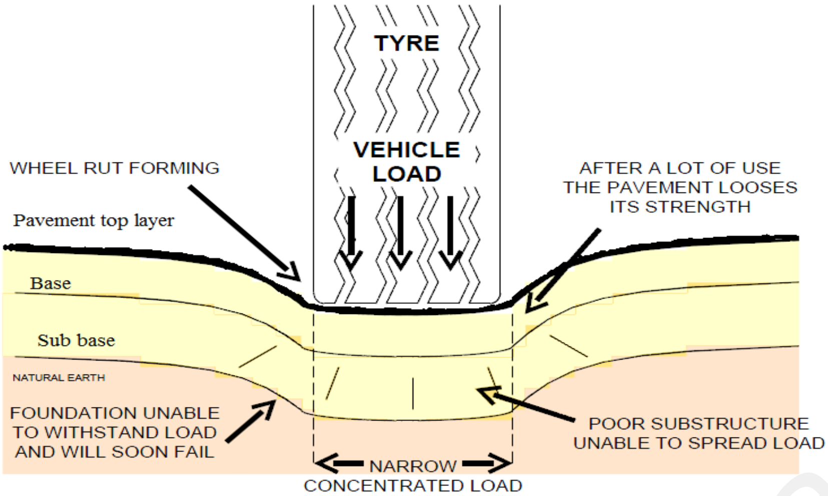

Figure 2.3: Schematic rutting in pavement layers under the vehicle wheel load.

With the purpose of simulating the effect of actual traffic loads on the rutting performance of pavements, Load Wheel Tracking machines or other types of equipments, such as the Georgia Loaded Wheel Tester (GLWT), Asphalt Pavement Analyzer (APA), Hamburg Wheel Tracking Device (HWTD) and LCPC (French) Wheel Tracker are being used to evaluate the level of rut resistance of the compacted asphalt mixtures in the laboratories.

2.6.5 Indirect Tensile (IDT) strength

The Indirect Tensile (IDT) Strength test is applied to measure the tensile properties of the asphalt specimens which can be used to predict the future performance of the flexible pavements. According to the experiments, the IDT strength test is a very good indicator of mixture adhesion and the higher tensile strength results in better resistance to rutting, fatigue and temperature cracking. However, to estimate the rutting potential of the flexible pavement, it is necessary to consider its adhesion, internal friction, volumetric properties, and IDT strength (Anderson *et al*., 2003; Christensen and Bonaquist, 2002).

Some parameters such as binder type, asphalt content, sand content, nominal maximum aggregate size, air voids content and gradation can highly affect the indirect tensile strength test results. Air voids and density play major roles in IDT, and dense asphalt materials have shown higher IDT results so far. Also, IDT is significantly affected by asphalt binder grade (stiffness), where the higher PG asphalt binder resulted in higher IDT strength (Christensen *et al*., 2004). The schematic section of the indirect tensile strength test is shown in Figure 2.4.

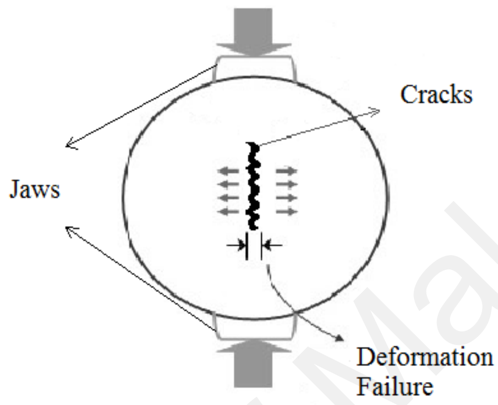

Figure 2.4: Schematic section of Indirect Tensile (IDT) strength (Moisture susceptibility)

In the late 1970s and early 1980s, a significant number of pavements in the United States began to experience distress and premature rutting, raveling and wear due to moisture sensitivity of asphalt mixtures. Regardless of these premature distresses, some methods were needed to identify the behavior of the asphalt pavement in the presence of water and moisture (Epps *et al*., 2000). Moisture susceptibility is an HMA mixture's tendency toward stripping. Stripping is the loss of bond between the asphalt and aggregate. To combat moisture susceptibility, proper mix design is essential. However, if a mix is properly designed, but not compacted correctly, it still may be susceptible to moisture damage. Therefore, an HMA design should be tested in a situation where moisture does infiltrate air voids of the mixture. For this reason many tests are performed at 7 percent air voids (Roberts *et al*., 1996). Many factors, such as aggregate characteristics, asphalt characteristics, environment, construction practices, drainage or traffic can contribute to stripping.

This test is not categorized as a performance-based test for asphalt mixes, but is for two main purposes. The first is to show the moisture susceptibility of asphalt binder and aggregate and the second is to measure the effectiveness of anti-stripping additives. According to the Superpave, this value must be 80 percent or higher to prevent stripping problems after construction (Asphalt Institute, 2007). Sufficient asphalt binder content to coat the aggregates and proper compaction to achieve the expected density can prevent damage due to the intrusion of water. However, in some cases the asphalt mixtures require an additive to improve the moisture resistance of the mix, such as hydrated lime and proprietary liquid anti-strip agents.

2.6.6 Fatigue cracking

Premature fatigue cracking seriously reduces the life of many in-service flexible pavements. Most mechanistic design procedures are to obtain the desired fatigue life for new pavements by considering the tensile stress (or strain) at the bottom of the bound asphaltic layers. These design procedures assume that fatigue cracks originate at the bottom of the bound layers and propagate vertically upwards towards the surface of the pavement under the influence of the stress field produced by the contact between the tire and pavement. At a normal contact pressure, the maximum horizontal tensile stress occurs at the bottom of the bound layers, and the maximum horizontal compressive stress occurs at the surface of the pavement. Fatigue cracking generally occurs with loads, which are too heavy for the pavement or repetitive unexpected passes with traffic or overweight trucks, and these problems become worse by inadequate pavement drainage or thickness due to poor quality control during the construction (Roberts, 1996). Fatigue testing of asphalt mixtures has been the focus of numerous studies that have utilized a variety of sample shapes, sizes, and testing apparatus (Matthews *et al*., 1993).

Using rolling wheel compaction for preparation of fatigue specimens is more recommended and for the most reliable prediction of field performance based on laboratory specimens, use of rolling wheel compaction has been shown to produce specimens with properties closer to actual field-cored samples. This method of sample preparation has been successfully employed as a performance prediction tool to evaluate the susceptibility of fatigue to both accelerated pavement testing and in-service pavements (Harvey *et al*., 1994). Although fatigue has been generally accepted as occurring more often in aged, brittle pavements, studies on aged samples indicate this may be a consequence of accumulated damage and not necessarily related to binder brittlement (Harvey and Tsai, 1997).

For thin pavements, fatigue cracking starts at the bottom of the HMA due to high tensile strains and migrated upward toward the surface; whereas for thick pavements, cracks start on the HMA surface due to tensile strains at the surface and migrated downward, and if not properly repaired in time, this distress allows moisture to infiltrate and leads to problems arising from moisture damage (Brown *et al*., 2001). Figure 2.5 illustrates a fatigue failure of a pavement in the actual field.

Figure 2.5: Fatigue cracks in asphalt pavement

There are two types of controlled loading that can be applied in fatigue test: controlled-stress (or force) and controlled-strain (or displacement). In the controlled-stress tests, the stress remains constant and the strain increases with the number of repetitions. On the other hand, in the controlled-strain tests, the strains are held constant and the stress decreases with the cyclic strain application (Huang, 2004).

The controlled-stress loading represented the behavior of thick pavements where the HMA layer was approximately more than six inches thick and the controlled-strain loading mode was applicable to thin pavements, which the HMA layers are less than two inches thick. According to Ghuzlan and Carpenter (2000), the fatigue life obtained using controlled stress testing was shorter than the fatigue life obtained from the controlled-strain testing.

Damage occurred faster in the controlled-stress testing than controlled-strain testing, because the same stress was used during the test, whereas it decreased during controlled-strain testing. increasing the voids content leads to a lower fatigue performance; changes in aggregate type or grading has a small effect on the fatigue response; and increasing the stiffness of the mix does not necessarily lead to poorer fatigue behavior, although sample heating and machine compliance may be affecting the results. Binder type can have the greatest affect and the rheology alone is insufficient to predict fatigue performance. Other than asphalt properties, aggregate type, grading, and mixture properties appear to affect the fatigue resistance of the asphalt mixes. Some studies have shown that the initial stiffness is very much affected by the angularity of the aggregate type, in which increased angularity increased the stiffness value up to about 25% (Carswell *et al*., 1997).

CHAPTER III

3 METHODOLOGY

3.1 Engineering properties of the utilized materials

Aggregate is primarily responsible for the load supporting capacity of pavements, so good aggregates must have the proper particle size and grading, acceptable toughness, angular shape and other important specifications to meet the required standards. Another key component is mastic, which consists of fines, fillers, binder and sometime fibers (in SMA mixtures) which provide strong binding between the asphalt mixture materials. The main challenge for pavement engineers is to make sure that the engineering properties of the utilized materials are within the acceptable ranges based on the relevant standards.

3.1.1 Los Angeles (LA) abrasion

The Los Angeles abrasion test determines the resistance of coarse aggregates to abrasion, impact and grinding in a rotating steel drum containing specific numbers of steel balls. The procedures for the LA abrasion test are fully illustrated in ASTM C 131. Based on the ASTM standard, the maximum allowable value of LA abrasion for pavement top layers is 30%.

Aggregates in asphalt pavement top layers near the pavement surface are subject to abrasion under traffic loads and require more toughness than aggregates in lower layers, where loads have dissipated or are not as concentrated. Relatively high resistance to wear, as indicated by a low percentage of abrasion loss, is therefore a desirable characteristic of aggregates to be used in asphalt pavement surface layers. However, an aggregate with a higher level of abrasion might be used in lower layers of road pavement, as vehicle loads have less impact on these.

3.1.2 Aggregate Impact Value (AIV)

This test is designed to determine the aggregate impact value of coarse aggregates in accordance with BS 812 Part 3. The aggregate impact value is a measure of the strength of an aggregate against impact loading. The initial aggregate sample should pass through a 12.5 mm sieve but be retained by a 9.5 mm one. Several attempts to develop an aggregate impact value (AIV) test have been made, but the most successful one is subjecting the aggregate sample, held in a steel mold, to 15 blows of a metal hammer weighing 14kg delivered from a height of 38cm. The aggregate sample is then removed from the mold and the percentages of aggregates passing through a 2.36 mm sieve show the aggregate impact value. Normally, an aggregate impact value of 15% or lower is considered as suitable for road surfacing.

3.1.3 Aggregate Crushing Value (ACV)

The aggregate crushing value test is required to ensure that road surfacing aggregates have a satisfactory resistance to crushing under a roller compactor during road construction, and adequate resistance to surface abrasion from traffic wheel loads. This test is designed to measure the resistance of an aggregate to crushing under a gradually applied compressive load. The lower the value of the ACV test, the better resistance of that particular aggregate to crushing.

We determined aggregate crushing value in accordance with BS 812: Part 3. A sample of 14mm size chippings of the aggregate to be tested was placed in a steel mold and a steel plunger was inserted into the mold on top of the chippings. The chippings were subjected to a force rising up to 400KN over a period of 10 minutes. Based on the BS, the aggregate crushing value should not exceed 30% to be suitable for pavement top layers.

3.1.5 Polished Stone Value (PSV)

The PSV of an aggregate is a measure of resistance to the polishing action of vehicle tires under conditions similar to those occurring on the surface of a road. The value is established by subjecting the aggregate to a standard polishing process, and then testing the aggregate with a Portable Skid Resistance Tester. The surface of the aggregates tends to get polished due to the traffic. The degree of polishing depends on traffic conditions, such as volume, weight, speed, acceleration, and braking, as well as the nature of the aggregates. The PSV test procedure is fully described in BS 812, Part 3.

The skid resistance of pavements is an important element in pavement engineering. The top surface layer of a pavement should be capable of providing adequate skid resistance with the given mix; and the mix in question should also be capable of providing sufficient stability to ensure the durability of the skid resistance. The value of PSV for surface layers should be at least 40 or above to fulfill the minimum requirements laid down in the relevant standards.

The polished stone value of aggregates can be calculated using Equation 3.1.

$$PSV = S + 52.5 - C \tag{3.1}$$

Where

S = Mean sample skid value

C = Mean control sample skid value

3.1.6 Soundness

The soundness test measures the resistance of aggregates to disintegration due to weathering. The aggregates are subjected to alternate cooling and heating cycles in the presence of abrasive agents (generally chemical solutions) such as sodium or magnesium sulfate. The abrasive agent penetrates fine cracks in the aggregates. Due to repetitive drying and wetting, salts get deposited in the cracks and the cracks grow in size, causing disintegration of aggregates along the weak shear plane (Kandhal *et al*., 1997). The soundness test was carried out in accordance with the British Standard (BS 812, Part 3). This test is an empirical screening test of weathering and is useful to evaluate new (unknown specifications) sources of aggregates. The sulfate soundness test has been an accepted method of aggregate testing for many years, but despite this acceptance, it has been widely criticized and several reports have shown its inability to accurately predict aggregate performance in the field (Roberts *et al*., 1996).

3.1.6 Flakiness and elongation index

Flaky aggregate has less strength than cubical aggregate, and does not create the dense matrix that well graded cubical aggregates are able to do, so it provides less texture when used in surface dressing. Flaky is the term applied to aggregate or chippings that are flat and thin in length or width. Aggregate particles are said to be flaky when their thickness is less than 0.6 of their mean size.

The flakiness index is found by expressing the weight of the flaky aggregate as a percentage of the aggregate tested. This can be done by grading the size fractions obtained from a normal grading aggregate in special sieves (test plates) to test flakiness. These sieves have elongated, rather than square, apertures and allow aggregate particles to pass that have a dimension less than the normal specified size (0.6 of the normal size). This grading process is normally performed by hand, because flaky chippings tend to lie on the sieve surface rather than fall through the apertures. The flakiness test is carried out in accordance with BS 812, part 3. According to the British Standard, the flakiness index must be below 20 percent to be acceptable for use in asphalt pavements. The elongation index of aggregates is the percentage by weight of particles whose longest dimension (length) is greater than 1.8 times the mean dimension. The elongation of the aggregates is measured in the same manner as flakiness, but using an elongation gauge.

3.1.7 Specific gravity and absorption of aggregates

Specific gravity is one of the characteristics used to measure the volume occupied by aggregate in various mixtures containing aggregates, such as asphalt mixtures. This characteristic is also used to estimate the pores and voids in aggregates. According to ASTM C 127 and ASTM C 128, the specific gravity of an aggregate is the ratio of the weight of a unit volume of material to the weight of the same volume of water at 73.4°F (23°C). These standards are used to measure specific gravity and the absorption of coarse and fine aggregates respectively. The specific gravity of the aggregates used in asphalt mixtures plays an important role in the longer-term performance of pavements. White *et al*., (2001) believed the specific gravity of fine aggregates to be more important than that of coarse aggregates. Kandhal *et al*., (1999) meanwhile used these tests to determine the amount of asphalt binder absorbed by aggregates and the percentage of voids in mineral aggregates (VMA). According to the ASTM standard, the specific gravity of granite aggregate (type of aggregate) must be between 2.60 to 2.65, and aggregates within this range are acceptable for use in asphalt mixtures. Specific gravity is critical information in designing asphalt pavements. It is used in calculating air voids, voids in mineral aggregate (VMA), and voids filled with asphalt (VFA). All of these characteristics are critical to a well performing and durable asphalt mix.

The absorption of aggregates is the ability of aggregate particles to take in a liquid. Water absorption is closely related to the porosity of aggregates, meaning the ratio of the volume of the pores to the total volume of the particle. Water absorption can also be an indicator of binder absorption in asphalt mixtures. A highly absorptive aggregate could lead to a low durability asphalt mix. The specific gravity test can be used to determine air voids as well. Bulk specific gravities are used to adjust the relative quantities of the aggregate components used in an asphalt mixture to take account of the differing specific gravities of various aggregates. There are three generally accepted types of specific gravities for aggregates, depending on the defined volume of the particles: apparent, bulk and effective specific gravity.

3.1.8 Angularity number

The shape of the particles forming aggregates can influence the workability and strength characteristics of asphalt mixtures. Angular particles, such as crushed stone and gravels and some natural gravels and sands, tend to interlock when compacted and resist displacement. The best interlocking tends to be obtained when sharp-cornered and cube-shaped aggregates are used in asphalt mixtures. It is therefore important to measure the angularity of aggregates before these are used in asphalt mixtures, to prevent future failures in the pavement. This test is fully described in BS 812, part 3. The angularity value should be between 6 to 9 to fulfill the minimum requirement for road surfacing layers laid down in the relevant standards.

The angularity number of aggregates can be measured using Equation 3.2.

$$\textit{Angularity Number (AN)} = 67 - 100\,[W/(CG_A)] \quad (3.2)$$

Where:

W = Weight (in grams) of aggregates in the cylinder.

C = Weight (in grams) of water required to fill the cylinder.

G_A = Specific gravity of aggregate

3.1.9 Aggregate particle size distribution (Gradation)

Aggregate particle size distribution is another concern for pavement engineers seeking to design a durable and high performance pavement. Permanent deformation and fatigue cracking (rutting) are the major types of distress modes experienced in the service life of pavements. The gradation of aggregates in hot asphalt mixtures is also an important aspect in pavement design which can affect fatigue and rutting (Golalipour *et al*., 2012; Sousa *et al*., 1998). Roberts *et al*., (1996) found that gradation affects almost every important property of asphalt mixtures, including stiffness, stability, durability, permeability, workability, fatigue resistance, frictional resistance and resistance to moisture damage.

To measure the gradation of aggregates, a sample of dry aggregates of known weight is separated through a series of sieves with progressively smaller openings. Once separated, the weight of particles retained on each sieve is measured and compared to the total sample weight. The resulting particle size distribution is a percentage of retained aggregates (by weight) on each sieve size. The results are usually expressed either in a table or as figures. A typical graph uses the percentage of aggregate by weight passing a certain sieve size on the y-axis, and a sieve size raised to the n^{th} power ($n = 0.45$) is typically used as the x-axis units. Power grading curves (0.45) are very helpful in assessing aggregate gradation characteristics and in making necessary adjustments in mix designs. This curve was developed in the 1960s by the Federal Highway Administration (FHWA) and for years has been the most widely accepted method for plotting gradations for comparison to the maximum density gradation. The 0.45 power is known as a maximum density curve, and is represented by a straight line from the lower left of the chart to the intersection of the desired maximum particle size, plus the 100% passing line at the upper right of the chart.

In this study, the gradation of dense-graded hot mix asphalt and gap-graded stone mastic asphalt specimens was designed in accordance with ASTM D3515 and the Asphalt Institute (AI) respectively. Figures 3.1 and 3.2 represent the selected aggregate gradations between the upper and lower boundaries used in this research for HMA and

SMA mixtures. Also, these aggregate gradations were used to calculate the Optimum Asphalt Content (OAC) of each mixture based on the Marshall mix design procedure.

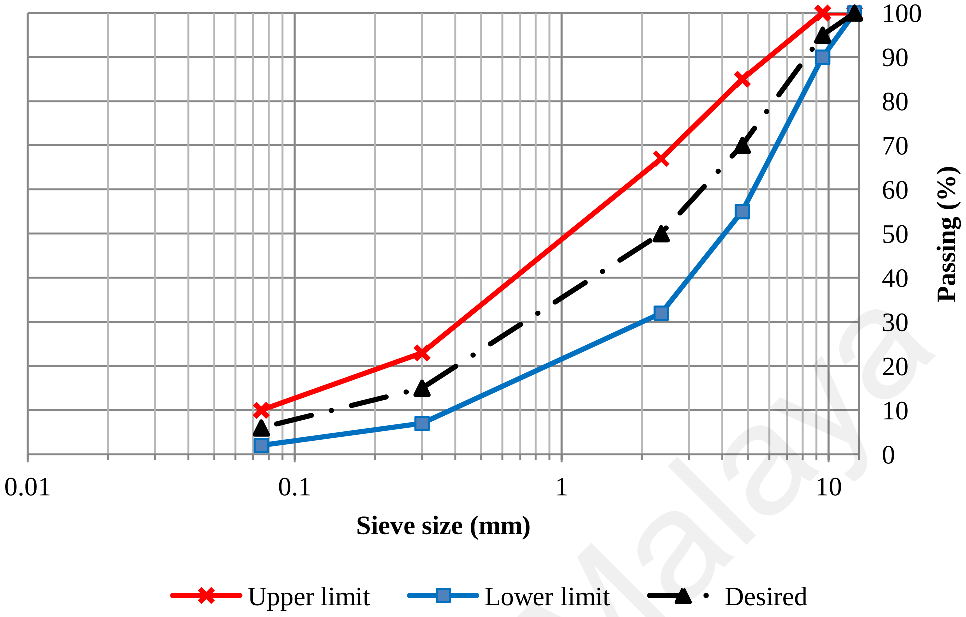

Figure 3.1: HMA aggregate gradation based on ASTM D3515

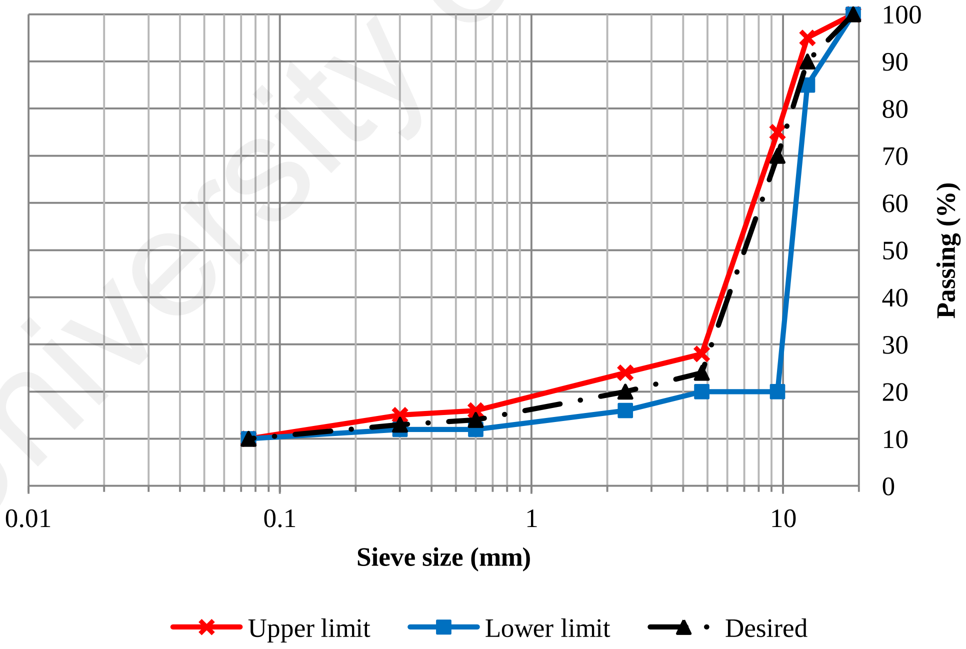

Figure 3.2: SMA aggregate gradation based on Asphalt Institute (2007)

3.2 Asphalt binder tests

Binders are thermoplastic materials that liquefy when heated and solidify when cooled. Asphalt binders are characterized by their consistency or ability to flow at different temperatures. It is therefore necessary either to define an equipment temperature or an equipment consistency when comparing the temperature consistency characteristics of one asphalt binder with another. The tests and specifications we used incorporated these characteristics.

The following are the consistency tests we performed on asphalt binders:

- Penetration: This is one of the oldest empirical tests used to measure the consistency of asphalt cement. The objective of penetration is to classify bitumen samples into different grades by determining the consistency of the bitumen. The penetration procedure is fully illustrated in ASTM D5. The test can be run at the standard temperature (25°C) or at other temperatures such as 0.4 and 46°C. A typical penetration test consists of three measurements made on the asphalt binder sample, and the results are averaged to provide the single test value. Penetration is measured in units of 0.1mm, so the penetration value of 80/100 bitumen would be between 8mm and 10mm.

- Softening point: The softening point of a bitumen sample is measured by the ring and ball (R & B) method in accordance with ASTM D36. The procedure is fully illustrated. The softening point of bitumen is defined as the temperature at which bitumen attains a particular degree of softening.

- Flash and Fire Point: Tar and bitumen, especially cutback bitumen, are flammable liquids at high temperatures, so could catch fire if care is not exercised during construction. It is therefore important to note the flash and fire point of the particular bitumen being used so as to control the temperature of the material during mixing and construction. The most common method to determine the flash point of an asphalt binder is the Cleveland Open Cup (COC) flash point test (ASTM D92). In this test, a small cup filled with bitumen is subjected to a rise in temperature at a specified rate. A small flame of 0.16 in diameter is applied to the surface of the cup containing molten bitumen at specified intervals until a flash first appears at any point on the surface. That particular temperature is considered as the flash point.

- Viscosity: The viscosity of a binder is a measure of its flow characteristics, and the performance of a bituminous mix is greatly affected by its viscosity. This test is in accordance with ASTM D4402. A Brookfield rotational Viscometer is used to measure the binder viscosity. The viscosity grading of asphalt cement is based on a viscosity measurement at 135°C (275°F). This temperature is selected because it is close to the asphalt compaction temperature. The viscosity of asphalt binders can also be measured at 60° C (140°F), as the highest actual pavement temperature in the summer, or 170°C (329°F), which is approximately the mixing and mixture laying down temperatures. The test results are sometimes plotted on a viscosity-temperature graph with a line connecting the two points. The slope of this line is an indication of the temperature susceptibility of the asphalt binder (the greater the slope of the line, the greater the temperature susceptibility of the asphalt binder).

3.3 Marshall mix design method and sample preparation

The Optimum Asphalt Content (OAC) of the HMA and SMA mixtures were measured based on the Marshall mix design method, in accordance with ASTM D 1559. The Marshall method is generally used for dense-graded Hot Mix Asphalts (HMA) using Performance Graded (PG) binders, and which contain a maximum aggregate size of one inch or less. However, it has also been successfully used for Stone Mastic Asphalt (SMA) mix designs with acceptable performance results. Due to its simplicity, the Marshal mix design method is still the most commonly used method for designing asphalt mixtures (Tia, 2005).

We obtained granite aggregates, 80/100 penetration grade bitumen, fillers, oil palm fibers and recycled concrete aggregates (RCA) for use in this research. The crushed granite aggregates were provided by the Kajang rock quarry (located near Kuala Lumpur). To obtain the RCA, (figure 3.3) concrete infrastructures were first demolished and crushed into large chunks. The reinforcing steel bars were subsequently removed and the concrete debris was transferred to a crusher machine to produce proper sized aggregates. The RCA was produced from the structural normal weight concrete beams from concrete laboratory of University of Malaya (UM). The concrete had a density of 2400 kg/cm^3 and compressive strength of 40 MPa. Also, 80/100 binder was obtained from the university materials suppliers. In order to produce better adhesion between the aggregates and bitumen during the mix procedure and remove excessive dust from the surface of the aggregates, the crushed concrete and granite aggregates were submerged, washed and then dried well before being used in the asphalt mixtures.

Figure 3.3: RCA production from concrete reinforced beams

Next, the required amounts of aggregate, fillers and RCA were weighed and placed in an oven at 200°C for 2 hours. The binder contents used in the asphalt mixtures varied from 5 to 8.5% by the weight of the aggregates. The required quantity of 80/100 binder was weighed and heated for a period of 1 hour at 150°C. Hot aggregates (including RCA) were mixed with the binder at 160 ± 5°C until all the aggregates were coated. However, to prevent binder drain down (in SMA mixtures), the loose form fibers (0.3 percent by the weight of total mix) were blended with the hot aggregates before the binder was introduced. Finally, the weighed amount of filler was added and mixed thoroughly. All the mixtures were conditioned for 4 hours at 150°C and then compacted. Filter paper was fitted at the bottom of the hot mold and the mixture was poured in three layers. The specimens were compacted with a Marshall compactor, delivering 75 and 50 blows on each side of the HMA and SMA specimens respectively. The maximum sizes of the aggregate in the HMA and SMA mixtures were 9.5mm and 12.5mm, in accordance with ASTM D3515 and Asphalt Institute (AI) standards.

Finally, five different percentages of RCA (0%, 20%, 40%, 60% and 80%) were blended with virgin granite aggregates (by the total weight of the aggregates in the mixture) to produce the HMA and SMA specimens. These percentages were divided into three categories: coarse RCA (C-RCA), fine RCA (F-RCA), and a mix of both the previous two (M-RCA) with the virgin aggregates (VA). In addition, a 0% RCA mixture (100% VA mix) was used as a control mix. The fine RCA (F-RCA) contained aggregate particle sizes of 2.36 mm and smaller; Coarse RCA (C-RCA) contained aggregate particle sizes larger than 2.36 mm; and the mixture of F-RCA and C-RCA together was called M-RCA.

3.3.1 Theoretical Maximum Density (TMD)

The theoretical maximum density (TMD) of the HMA and SMA mixtures was measured in accordance with ASTM D2041 and the Rice Method. Three compacted and one non-compacted (loose mixture) specimens were prepared from each set of Marshall with equal binder content. The compacted specimens were tested in terms of density, Marshall stability and flow tests, while the loose mixture was used for TMD measurement. The asphalt mixture prepared for the TMD test was spread and separated in a tray, weighed and vacuumed in a submerged condition for 25 minutes. Next, the weight of the loose specimen (submerged in water) was measured. The theoretical Maximum Density (TMD) was calculated using the following equations:

$$TMD = G_{mm} \times \rho_w \tag{3.3}$$

$$G_{mm} = \{1 / [((1 - P_b) / G_{se}) + P_b / G_b]\} \tag{3.4}$$

$$G_{mm} = \frac{A}{A - C} \tag{3.5}$$

Where:

TMD = Theoretical Maximum Density (g/cm^3)

G_{mm} = Maximum theoretical specific gravity

ρ_w = Density of water (1g/cm^3)

P_b = Asphalt content, percent by the weight of the mix

G_{se} = Effective specific gravity of the mix

G_b = Specific gravity of asphalt cement

A = Mass of dry specimen (g)

C = Mass of specimen in water (g)

3.3.2 Determination of Optimum Asphalt Content (OAC)

The Optimum Asphalt Content (OAC) of the HMA and SMA mixtures containing different sizes and percentages of RCA was measured based on the Marshall Stability (MS), density and air void values of the tested specimens. After all the data was collected, plots were developed to show the relationship between the various properties of Marshall Stability, Voids in Total Mix (VTM) and Density versus the binder content. In accordance with the Marshall mix design method, the OAC was determined from the percentage of asphalt content in the Stability, Density and VTM graphs. The stability and density curves peaked at two different percentages of binder content. In addition, 4% air voids from the VTM curve were also selected as a third percentage of binder. Finally, the average of these three values produced the OAC of the HMA and SMA mixtures respectively for each level and size of RCA content.

3.4 Hot Mix Asphalt (HMA) and Stone Mastic Asphalt (SMA) slab preparation

The estimated OAC values obtained above were used to produce the HMA and SMA slabs, and the required number of specimens were cored out and subjected to performance tests. The target thickness of 65 mm and 4% air voids were used to determine the amounts of required materials for each slab, using the same mixing procedures and material temperatures as explained in Section 3.2 above. Equation 3.6 below was used to measure the mass of bituminous mixtures for the HMA and SMA slab preparations. The asphalt mixtures were compacted with a target air void of 4%, except for the moisture susceptibility test, for which the air void level was 6%. Based on the aggregate gradations of the asphalt mixtures, the total amounts of coarse, fine and fillers were 30%, 64% and 6% in the HMA and 76%, 14% and 10% in the SMA mixtures respectively. For slab fabrication, 0%, 20%, 40%, 60% and 80% of virgin granite aggregates were replaced (by weight of aggregates) with three different grades of RCA (C-RCA, F-RCA and M-RCA) and mixture containing 100% virgin aggregates (0% RCA) were used as control specimens.

$$M = 10^{-6} \times L \times l \times h \times TMD \times \left(\frac{100 - v}{100}\right) \tag{3.6}$$

M = Mass of slab (kg)

L = Interior length of mold (mm)

h = Thickness of slab (mm)

TMD = Theoretical Maximum Density (kg/m^3)

v = Air voids (%)

3.5 Performance tests

To evaluate the volumetric and mechanical properties of the HMA and SMA mixtures containing RCA, the asphalt specimens were subjected to a series of performance tests, namely density and air void, Marshall stability and flow, voids in mineral aggregates (VMA) and voids filled with asphalt (VFA), resilient modulus (M_R), loaded wheel tracking, indirect tensile (IDT) strength, moisture susceptibility and flexural fatigue tests. For this purpose, a total of 78 and 156 core specimens of 100mm diameter with target air voids of 4% (containing mineral filler) and 156 core specimens of 100mm diameter with target air voids of 6% (containing hydrated lime stone powder as filler) and 156 core specimens of 200mm diameter and 78 beam cut specimens were taken out of the slabs and tested.

3.5.1 Bulk density and air void

The ASTM D2726 test method was used to determine the bulk specific gravity and density of the compacted bituminous mixtures. Specifically, the bulk density was measured by weighing in air and water using the following equations:

$$d = G_{mb} \times \rho_w \tag{3.7}$$

$$G_{mb} = \frac{W_D}{W_{SSD} - W_{SUB}} \tag{3.8}$$

Where:

d = Bulk density (g/cm^3)

G_{mb} = Bulk specific gravity of the mix

ρ_w = Density of water (1 g/cm^3)

W_D = Mass of specimen in air (g)

W_{SUB} = Mass of specimen in water (g)

W_{SSD} = Saturated surface dry mass (g)

Second, a void analysis was carried out in accordance with ASTM D3203. The voids of the specimens were measured using the following equations applying the value of the measured Theoretical Maximum Density (TMD).

$$VTM = [1- (\frac{d}{TMD})] \times 100 \tag{3.9}$$

Where:

d = Bulk Density (g/cm^3)

TMD = Theoretical Maximum Density (g/cm^3)

3.5.2 Marshall stability (MS) and flow

Marshal stability and flow tests were carried out in accordance with ASTM D 1559. The Marshall stability was calculated on the basis of the maximum load carried by the compacted SMA and HMA specimens at 60° C (140° F), with a loading rate of two inches per minute (50.8 mm/min). Meanwhile, the flow was determined from the vertical deformation of the asphalt specimen at the same time during the Marshall stability test (measured from the start of loading until the stability began to fall). The Marshall Stability of asphalt specimens with variations in thickness was corrected using the ASTM correlation ratio table shown in Appendix C. To measure the stability and flow of the HMA and SMA specimens, each specimen was immersed in a water bath for 30 minutes at 60°C. The specimen was then removed from the bath and placed between the jaws of the Marshal stability apparatus. The load was applied and the value of the stability and flow was read and recorded.

3.5.3 Voids in Mineral Aggregates (VMA) and Voids Filled with Asphalt (VFA)

Voids in Mineral Aggregates (VMA) and Voids Filled with Asphalt (VFA) were determined using the equations below:

$$VMA = 100 \times [1 - \frac{G_{mb}(1-P_b)}{G_{sb}}] \quad (3.10)$$

$$VFA = \frac{VMA - VTM}{VMA} \times 100 \quad (3.11)$$

Where:

P_b = Asphalt content, percent by the weight of the mix

VMA = Voids in Mineral Aggregates (%)

G_{mb} = Bulk specific gravity of the mix

P_b = Asphalt content, percent by the weight of the mix

G_{sb} = Bulk specific gravity of the aggregates

VFA = Voids Filled with Asphalt (%)

VTM = Air voids (%)

3.5.4 Resilient modulus (M_R)

The modulus of asphalt is an essential parameter for designing flexible pavements applying the elastic-layered system theory. Indeed, the Resilient Modulus (M_R) test has long been one of the most popular tests for asphalt mixtures used to measure the response of asphaltic pavements to actual wheel loads (Ahmadinia *et al.*, 2012). In this study, a Material Testing Apparatus (MATTA) was used to determine the resilient modulus of the SMA and HMA specimens. The standard specimen dimensions used for the resilient modulus test were 2.5 inches (62.5 mm) by 4 inches (100 mm), with an applied load to stress level of between 5% and 20% of the indirect tensile strength (Asphalt Institute, 2007). Figure 3.4 presents the resilient modulus test setup.

Figure 3.4: Resilient modulus test setup

The MATTA test was carried out in accordance with ASTM D4123, which is a standard test method for the indirect tension of the resilient modulus of asphalt mixtures. This test is non-destructive. The total number of 39 HMA and 39 SMA (36 specimens containing RCA and 3 specimens as control samples) core specimens with 100 mm diameter and target air voids of 4% were subjected to resilient modulus test at temperatures of 25°C and 40°C. Each specimen was kept in a MATTA machine for at least 2 hours at the relevant temperature (25°C or 40°C), during which indirect repeated axial pulses were applied to the asphalt specimens to measure the horizontal deformations of the curved surface of the specimens with two attached Linear Variable Displacement Transducers (LVDTs). The test results were recorded automatically using computer software. All parameters required in the computer software, including Poisson’s ratio, load, pulse period, conditioning pulse count and rise time were adjusted in accordance with the nominal standard. For each sample, the test was repeated twice, after a 90° rotation of the sample, to verify the recorded results. The resilient modulus values of the HMA and SMA specimens were measured using the following equation.

$$M_R = \frac{P}{Ht}\ (0.27 + \mu) \tag{3.12}$$

Where:

M_R = Resilient modulus (Psi)

P = Applied load (Pounds)

H = Total recoverable horizontal deformation (inches)

t = Sample thickness (inches)

μ = Poisson's ratio

3.5.5 Loaded Wheel Tracking (LWT)

Rutting resistance is one of the most important and critical performance requirements of asphalt mixtures, particularly in hot climates. There are several tests used to evaluate rutting in asphalt mixtures, such as the Marshall test, wheel track test, static and dynamic creep tests, and indirect tensile tests (Tayfur *et al*., 2007). The wheel tracking test is the most commonly recommended of these tests, as it produces a more authentic field simulation (Lu and Redelius, 2007). A Loaded Wheel Tracking (LWT) test was accordingly conducted in accordance with BS 598-110 to determine the wheel tracking rate and depth at 45°C for the moderate to heavily stressed sites. Table 3.1 shows the maximum allowable rut depth and rut rate values of the asphalt mixtures at 45°C and 60°C respectively. Also, the loaded wheel tracking test setup is presented in figure 3.5.

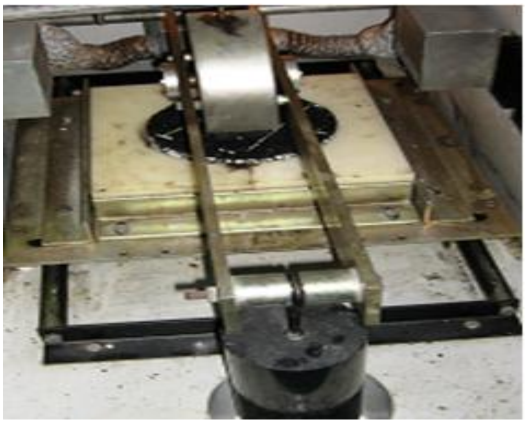

Figure 3.5: Loaded wheel tracking test setup

In the present study, 78 SMA and 78 HMA core specimens (72 specimens containing RCA and 6 control specimens made of virgin aggregates) of 200mm diameter were cored out from fabricated slabs. Each core specimen was pre-conditioned at 45°C for 6 hours before starting the actual test. The loading wheel was set in motion to turn over the specimen at the rate of 21 cycles per minute. A 520 $\pm$5 N load was applied to the surface of the specimen through a 50 mm wide moving wheel, and the rut depth value was recorded every 5 minutes (105 cycles). The test was continued for 45 minutes or until a 15mm deformation occurred in the specimen (whichever came first). The Tracking Rate (T_R) and Wheel Tracking Rate (W_{TR}) were defined using the equations below.

$$T_R = 3.6\,(r_n - r_{(n-3)}) + (r_{(n-1)} - r_{(n-2)}) \quad (3.13)$$

$$W_{TR} = 10.4 \times T_{RM} \times \frac{\omega}{L} \quad (3.14)$$

Where:

r_n = Depth measurement at n^{th} reading

W_{TR} = Wheel tracking rate

T_{RM} = Mean value of T_R

ω = Width of wheel contact area

L = Total load

Table 3.1: British Standard requirements for rutting test (BS 598-110)

Description	Test temperature (°C)	Max rut rate (mm/hr)	Max rut depth (mm)
Moderate to heavily stressed sites requiring high rut resistance	45	2	4
Very heavily stressed sites requiring very high rut resistance	60	5	7

3.5.5 Indirect Tensile (IDT) strength

The Indirect Tensile (IDT) Strength test measures the tensile properties of asphalt specimens so that these can be used to predict the future performance of flexible pavements (road surfaces). Previous experiments show that the IDT strength test is a very good indicator of mixture adhesion, with higher tensile strength resulting in better resistance to rutting, fatigue and temperature cracking (Anderson *et al*., 2003; Christensen *et al*., 2004; Christensen and Bonaquist, 2002). However, in order to estimate accurately the rutting potential of a flexible pavement, its adhesion, internal friction, volumetric properties and IDT strength all need to be taken into account. The ID test setup is shown in figure 3.6.

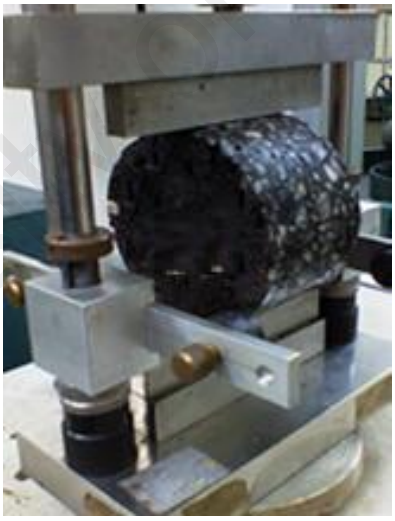

Figure 3.6: Indirect tensile strength test setup

In this study, the Indirect Tensile Strength (IDT) of the specimens was evaluated in accordance with ASTM D6931. The tensile characteristics of the SMA and HMA mixtures were measured by placing the specimen between the machine jaws (13 mm wide strip) and applying a compressive load at a constant strain rate of 50.8 mm/min (2 inch/min) at 25°C. The maximum vertical highest load (N) was recorded as a load to failure, and the Indirect Tensile (IDT) Strength of the asphalt specimens was then determined using the equation below.

$S = 2000P/\pi tD$ (3.15)

Where:

S = IDT strength (kPa)

P = Maximum vertical load (N)

t = Thickness of the test specimen (mm)

D = specimen diameter (mm).

3.5.6 Moisture susceptibility

Moisture induced damage is the loss of bonding and adhesive failure between asphalt mixture materials due to the presence of water in the structure of the pavement layers. Many factors, such as aggregate characteristics, asphalt characteristics, environment, construction practices, drainage or traffic can contribute to moisture damage and stripping. However, the moisture susceptibility of asphalt mixtures can be improved by using anti-stripping agents or specific kinds of fillers (Saad and Mohammad, 2005; Caro *et al.*, 2008).

The Indirect Tensile (IDT) Strength test is a common test to evaluate the moisture susceptibility of pavement layers, with or without anti-stripping additives, to water and moisture in accordance with AASHTO T283. Although conventional cored specimens actually used in road building tend to have air voids lower than 6%, there is a risk that air voids lower than 6% might not allow the specimens to become sufficiently damaged during the laboratory test. Therefore, in this research, a number of HMA and SMA slabs were fabricated with an air void target of 6% to serve as specimens for this test. The total numbers of 78 core specimens with 100 mm diameter and 6% air voids (containing mineral filler) and 78 core specimens with 100 mm diameter and 6% air voids (containing hydrated lime powder) were provided for each type of asphalt mixtures (HMA and SMA), including 72 specimens containing RCA and 6 specimens as control.

Previous research (Tomas *et al*., 2006; Sangsefidi *et al*., 2014; Xiao and Amirkhanian, 2009; Kim *et al*., 2012) further suggests that hydrated limestone can have a significant impact on the performance of asphalt mixtures in terms of moisture susceptibility. Accordingly, in this test two types of mineral filler and hydrated lime stone powder were used to produce the asphalt specimens, and the effect of hydrated limestone powder (as a total replacement for mineral fillers) on the moisture sensitivity of the HMA and SMA mixtures was also evaluated. As the thicknesses of the asphalt specimens varied due to different percentages of RCA content, all the asphalt specimens were trimmed (from top and bottom) into the desired uniform thickness of 55 mm.

Finally, the selected HMA and SMA core specimens need to have approximately the same average bulk density in each group. The specimens were divided into two groups: conditioned specimens and unconditioned specimens. The purpose of this division was to determine first the indirect tensile strength of the unconditioned specimens, and then compare this with the conditioned group to ascertain the effect of moisture susceptibility on the asphalt mixtures. The conditioned specimens were subjected to vacuum saturation for 5 minutes; placed in a water bath for 24 hours at 60°C; and then, before actual testing, all the specimens were submerged in the bath at 25°C for two hours. The unconditioned specimens were meanwhile kept at room temperature. Subsequently, the Tensile Strength Ratio (TSR) was measured for both the conditioned and dry specimens using the following equation.

$$TSR = 100 \times \frac{S_{Conditioned}}{S_{Unconditioned}} \tag{3.16}$$

The TSR value above represents the loss of strength caused by moisture conditioning, and hence shows the performance of the asphalt mixture in terms of moisture susceptibility. The TSR is usually expressed as a percentage, with a higher TSR value indicating better resistance to moisture damage. Based on the relevant standards and on previous experiments, the desired value for TSR should be higher than 80% in the surface layer of pavements (Kenedy and Anagnos, 1984; Aksoy *et al.*, 2005; Kok and Yilmaz, 2009; Khodaii *et al.*, 2012; Kim *et al.*, 2012; Moghadas Nejad *et al.*, 2012).

3.5.7 Flexural beam fatigue

A repeated flexure test was conducted to evaluate the fatigue properties of the asphalt mixtures and to estimate the likely pavement life of different types of asphalt mixture containing RCA. Repeated haversine loads were applied at the third points of a beam specimen. The load rate was variable, but generally around 1 to 2 cycles per second. This produces a constant bending movement over the center portions of the beam as it seeks to return to its original position and to maintain the zero position during the rest period. The deflection caused by the load is measured at the center of the beam.

In this study, the flexural fatigue beam test was carried out in accordance with AASHTO TP8. For this purpose the compacted HMA and SMA slabs containing various percentages of RCA were cut and trimmed into 380mm × 63.5mm × 50mm beam samples. The total numbers of 39 HMA and 39 SMA (36 of them containing RCA and 3 control specimens made of virgin granite aggregates) beams were cut out of the fabricated slabs. Based on the AASHTO standard, the strain testing range should be between 200 and 700 micro strains. Since fatigue is prominent within a temperature range of 10°C and 30°C, a mean temperature of 20°C is recommended for the test, and this is the test temperature currently found in the AASHTO TP 8 standard.

The computer attached to the machine in our test was capable of measuring stiffness, stress, dissipated energy and number of cycles (fatigue life). The beam specimens were placed in the jig and held in place by a clamping device. The machine was then set to induce an actuated cyclic constant strain of 500 micro strains. The higher end of the testing range was selected for critical beam testing. A frequency of 10Hz was used to provide cyclic intensity. The test temperature was set to 20°C. The software automatically captured the deflection of the beam and the changing stresses after each application of strain rate, and saved these for future retrieval. The specimens were strained to a maximum deflection of 500 micro strains. Some of the characteristics and equations used to determine the beam fatigue properties are shown below:

$$\sigma_t = (0.357)/ (bh^2) \tag{3.17}$$

where:

σ_t = Maximum Tensile Stress

P= load applied by actuator (N)

b= average specimen width (m)

h= average specimen height (m)

and:

$$\varepsilon_t = (12\delta h)/3L^2 - 4a^2) \tag{3.18}$$

where:

ε_t = Maximum Tensile Strain

δ = maximum deflection at center of beam (m)

a = Space between inside clamps, 0.357/3 (m) (0.119m)

L = length of beam between outside clamps, 0.357m

and:

$$S= \sigma_t / \varepsilon_t \tag{3.19}$$

where:

S= Flexure Stiffness

σ_t = Tensile Stress

ε_t = Tensile Strain

and:

$$\phi = 360fs \tag{3.20}$$

where:

ϕ = Phase Angle

f= load frequency

s= time lag between P_{max} and δ_{max} (seconds)

and:

$$D = \pi\sigma_t\,\varepsilon_t \sin(\phi) \tag{3.21}$$

D= Dissipated Energy (J/m^3)

Cumulative Dissipated Energy = ΣD_i

where:

D_i = D for the i^{th} load cycle

$$S = A\,e^{bn} \tag{3.22}$$

where:

S= Initial Stiffness

e = natural logarithm

A = constant

b = constant

n = load cycles

3.6 Analysis of variance (ANOVA)

The main objective of this research is to evaluate the feasibility of utilizing RCA in HMA and SMA mixtures. To achieve this objective and provide a deeper understanding of the research, the analysis of variance (ANOVA) technique was applied to different

SMA samples, and the results were statistically contrasted and compared. In addition, a single-factor and two-factor variance analysis (without replication) were also applied to assess the significance of each of the factors involved in determining the performance of the HMA and SMA specimens containing RCA.

ANOVA is not only a statistical method used to evaluate differences and relationships between the means of two or more data sets, but also a guide to assist researchers to determine the most likely differences to be expected from random variations in a given set of measurements. In other words, ANOVA helps us to determine which factors are more likely to have contributed to a given event. ANOVA is a robust and suitable means to determine whether differences are statistically significant.

In this study, ANOVA was applied using SPSS software and Microsoft Excel – the latter actually contains three different ANOVA functions, available through the Analysis ToolPak, applicable to basic variance analyses. These are detailed below:

- Single Factor carries out a simple analysis of variance between two data sets.
- Two Factors without Replication performs a variance analysis between two or more data sets. If there is only one sample from each data set, two factor without replication is recommended.
- Two Factors with Replication is employed for a variance analysis shared by two or more sets of data, in particular when the number of the samples is more than one from each data set.

The main problem with using one factor is that this factor may mask a second factor. This can be overcome by applying a single two-way ANOVA, which simultaneously tests the effects of the two factors. The F-ratio refers to the probability of the information generated by ANOVA: it compares the level of variation between groups with the variation within the same groups. Generally speaking, when the F-ratio is larger, the variation between the groups is more significant. The level of significance of data sets can be evaluated using the F-ratio and by comparing it with the value of the F-critical for each sample. When the F-ratio (F-statistic) is larger, the variation between the groups is statistically significant. If, on the other hand, the F-ratio is smaller, the differences between the scores may simply be the result of chance. The observed *P-value* indicates the probability of the F-ratio being observed when the results of the mean test are equal. When the P-value is smaller than the preferred significance level (α), the corresponding variant is more significant. The significance level (α) applied to this study is 0.05, representing a 5% probability of the hypothesis represented by the model.

CHAPTER IV

4 RESULTS AND DISCUSSION

4.1 Introduction

This chapter discusses the results of the tests detailed in Chapter 3. High quality asphalt mixtures need high quality materials, including acceptable ranges for aggregate durability, angularity and other criteria for aggregates. Binder also plays a significant role in asphalt mixtures. We therefore began the process by analyzing the test results of the asphalt mixture materials: granite aggregates, Recycled Concrete Aggregates (RCA) and asphalt binder. The results for all of these were compared with the minimum requirements laid down in the relevant standards, to gauge the validity of the selected materials. The Determination of Optimum Asphalt Content (OAC) was carried out in accordance with the Marshall mix design procedure, using the optimum amount of 0.3 percent fiber by weight of total mix in all the Marshall sets for the Stone Mastic Asphalt (SMA) preparation. The performance of the Marshall sets in terms of stability, density and air voids (VTM) was plotted against the percentage of the binder so as to determine the Optimum Asphalt Content.

This chapter also presents the performance test results of the SMA and HMA compacted specimens containing five different percentages of RCA (0%, 20%, 40%, 60% and 80%). Each percentage was further divided into three parts, called Fine-RCA (F-RCA), coarse-RCA (C-RCA) and a combination of fine and coarse RCA (M-RCA). Table 4.1 lists the abbreviations of the various HMA and SMA mixtures. All the specimens were subjected to density, stability, flow, resilient modulus, loaded wheel tracking, indirect tensile strength (IDT), moisture susceptibility and flexural fatigue tests, and the results were tabulated and compared.

Table 4.1: HMA/SMA Mixture Abbreviations

Mix Name	Abbreviation
Virgin Aggregate	VA
Coarse RCA + Fine VA	C-RCA+F-VA
Fine RCA + Coarse VA	F-RCA+C-VA
Coarse & Fine RCA + Coarse & Fine VA	M-RCA+M-VA

4.2 Aggregate test results and analysis

Aggregate quality is a key determinant of the performance of asphalt mixtures; and the performance of asphalt concrete mixtures is in turn greatly influenced by the properties of the aggregate blend. The aggregate properties that significantly influence the performance of asphalt mixtures are size, shape, strength and gradation, so these are the properties of coarse and fine aggregates used in asphalt mixtures that must be checked and tested.

4.2.1 Los Angeles abrasion

This test was carried out in accordance with the ASTM C131 standard, which states that the value of the aggregates should not exceed 30 percent. Table 4.2 shows, the measured values of Los Angeles abrasion for the granite aggregate and Recycled Concrete Aggregate (RCA) were 18.3% and 24.5% respectively – which are acceptable values based on ASTM C131 requirement.

Table 4.2: Los Angeles Abrasion Values of Granite and RCA

Aggregate size (mm)	Aggregate weight before test (g)	Aggregate weight after test (g)	Weight loss (g)	Wearing (%)
		Granite		
9.5-12.5	2500	2093.1	406.9	16.2
12.5-19.0	2500	1989.5	510.5	20.4
Total	5000	4082.6	917.4	18.3
		RCA		
9.5-12.5	2500	1872.5	627.5	25.1
12.5-19.0	2500	1902.1	597.9	23.9
Total	5000	3774.6	1225.4	24.5

4.2.2 Aggregate Impact Value

This test was carried out in accordance with the British Standard (BS 812: Part 3), according to which the aggregate Impact Value should not exceed 15 percent. The AIV test results of granite and RCA are presented in Table 4.3 below.

Table 4.3: Aggregate Impact Values of Granite and RCA

Sample No.	Aggregate Size (mm)	Aggregate weight before test (g)	Aggregate weight after test (g)	Weight passing 2.36 mm sieve (g)	Wearing (%)
			Granite		
1	10-14	620	583	37	5.97
2	10-14	620	580	40	6.45
Average	10-14	620	581.5	38.5	6.21
			RCA		
1	10-14	620	551	69	11.13
2	10-14	620	548.5	71..5	11.53
Average	10-14	620	549.75	70.25	11.33

As these results show, the impact value of the granite aggregates is considerably lower than that of the RCA. However, both the granite and RCA materials are within the 15% AIV threshold for use in asphalt mixtures.

4.2.3 Aggregate Crushing Value

The same standard was used for the Aggregate Crushing Value (ACV) test as for the AIV test. However, in this case the ACV must not exceed 30 percent. The test results are shown in Table 4.4 below. As was to be expected, the RCA showed lower resistance to crushing than the granite aggregates. But again, both types of materials were within the maximum acceptable range of 30% laid down in the British Standard.

Table 4.4: Aggregate Crushing Values of Granite and RCA

Sample No.	Aggregate size (mm)	Aggregate weight before test (g)	Aggregate weight after test (g)	Weight passing 2.36 mm sieve (g)	ACV (%)
			Granite		
1	10-14	1400	1143	257	18.36
2	10-14	1400	1074	326	23.28
Average	10-14	1400	1108.5	291.5	20.82
			RCA		
1	10-14	1400	1021	379	27.07
2	10-14	1400	986	414	29.57
Average	10-14	1400	1003.5	396.5	28.32

4.2.4 Polished Stone Value

This test was carried out in accordance with the British Standard, which sets a minimum allowable value of 40 for the PSV. Four aggregate samples were prepared for the PSV test, and the results are tabulated in Table 4.5. The PSV of the two control aggregate samples was also measured using Equation 4.1; the results for this are shown in Table 4.6.

Table 4.5: PSV values of Granite and RCA

Sample No.	PSV					Average
			Granite			
1	47	47	49	48	47	47.6
2	49	49	48	49	48	48.6
3	48	49	48	49	49	48.6
4	50	47	49	49	50	49
Average						48.45
			RCA			
1	49	47	48	48	49	48.2
2	49	48	48	48	49	48.4
3	50	49	49	49	50	49.4
4	50	48	49	48	48	48.8
Average						48.7

Table 4.6: PSV Control Samples of Granite and RCA

Sample No.	PSV					Average
			Granite			
1	50	50	51	50	51	50.4
2	49	50	49	51	51	50
Average						50.2
			RCA			
1	50	48	50	51	51	50
2	50	49	48	51	50	49.6
Average						49.8

$$PSV_{Granite} = S + 52.5 - C \tag{4.1}$$

Where:

S = Mean sample skid value

C = Mean control sample skid value

$PSV_{Granite} = 48.45 + 52.5 - 50.2$

$PSV_{Granite} = 50.75$

and;

$PSV_{RCA} = S + 52.5 – C$

$PSV_{RCA} = 48.70 +52.5 - 49.8$

$PSV_{RCA} = 51.4$

As can be seen, the Polished Stone Values of both the granite and RCA materials were well within the limits set by the BS standard. Hence, both types of aggregates are suitable for use in asphalt mixtures in terms of skid resistance and PSV values.

4.2.5 Soundness

According to the British Standard (BS 812: Part 3), the maximum allowable value of the soundness test is 12 percent. The percentage of loss was calculated from Equation 4.2 below. The soundness values of the granite and RCA were measured according to this equation, and the results are shown in Table 4.7.

Percentage of loss = {[(Aggregate weight before test) – (Aggregate weight after test)] / (Aggregate weight before test)} $\times$ 100 (4. 2)

Table 4.7: Soundness Test

Aggregate size (mm)	Aggregate weight before test (g)	Aggregate weight after test (g)	Percentage of loss (%)
Granite			
19-38	1500 .0	1483.9	1.07
9.5-19	1500.2	1472.4	1.85
4.75-9.5	1500.4	1465.5	2.33
Total Loss			5.25
RCA			
19-38	1500 .0	1479.7	1.35
9.5-19	1500.2	1463.9	2.42
4.75-9.5	1500.4	1459.2	2.75
Total Loss			6.52

As can be seen from the table, the soundness test for the granite and RCA materials produced values of 5.25% and 6.52% respectively, both of which are well below the maximum limit of 12% set by the relevant standard.

4.2.6 Flakiness and elongation index

This test was also carried out in accordance with BS 812: Part 3. The results for the flakiness and elongation of the granite and RCA materials are shown in Tables 4.8 and 4.9 below. Equation 4.3, also below, was used to measure the percentage of the flakiness index in the granite and RCA materials.

Table 4.8: Flakiness Index of Granite and RCA

Passing sieve (mm)	Retained sieve (mm)	Number of aggregates	Number of passing	Flakiness index (%)
		Granite		
28	20	194	8	4.12
20	14	433	37	8.54
14	10	521	39	7.48
10	6.3	359	41	11.42
Average				7.89
		RCA		
28	20	183	8	4.37
20	14	419	47	11.21
14	10	532	55	10.34
10	6.3	348	46	13.22
Average				9.79

Table 4.9: Elongation Index of Granite and RCA

Passing sieve (mm)	Retained sieve (mm)	Number of aggregates	Number of passing	Flakiness index (%)
		Granite		
28	20	194	14	7.22
20	14	433	22	5.08
14	10	521	37	7.10
10	6.3	359	47	13.09
Average				8.12
		RCA		
28	20	183	5	2.73
20	14	419	17	4.06
14	10	532	24	4.51
10	6.3	348	35	10.05
Average				5.35

Aggregate Flakiness Index (%) = [(Number of aggregate passing) / (Total number of aggregates)] $\times$ 100 (4.3)

According to the BS standard, the maximum allowable value for the flakiness of aggregate is 20 percent. The calculated values for both the granite and RCA materials met this standard.

4.2.7 Aggregate specific gravity and water absorption

The normal specific gravity of granite aggregates is between 2.6 and 2.65. However, as might be expected, the specific gravity of RCA is lower than that of virgin granite aggregates because of increased water absorption due to its more porous structure and the presence of some attached mortars on the surface of the RCA. In order to ascertain the actual specific gravity and water absorption of the RCA, the crushed concretes were submerged in water, washed well, and then dried before being tested. The results are shown in Table 4.10 below.

Table 4.10: Aggregate Specific Gravity

Specimen No.	Weight of sample in air (g)	Weight of sample in water (g)	Saturated weight (g)	Water Absorption	Specific gravity
			Coarse Granite		
1	1000	621.4	1004.6	0.46	2.609
2	1000	621.5	1004.2	0.42	2.613
Average				0.44	2.611
			Fine Granite		
1	1000	632.8	1009.7	0.97	2.653
2	1000	633.1	1012.5	1.15	2.636
Average				1.11	2.644
			Coarse RCA		
1	1000	569.2	1026.7	2.67	2.186
2	1000	569.5	1027.1	2.71	2.185
Average				2.69	2.185
			Fine RCA		
1	1000	630.5	1042.6	4.26	2.427
2	1000	629.8	1043	4.30	2.420
Average				4.28	2.423

Based on the laboratory experiments, the process of submerging the crushed concretes, washing and drying them has a significant positive effect on the performance of the RCA materials, considerably reducing their water absorption and increasing their specific gravity. Fine recycled concrete aggregates are the most absorptive materials with the absorption of almost 8%. Therefore the RCA materials were submerged, washed and dried before being used in the asphalt mixtures to removed the excessive cement and dust which was produced during crushing procedure an reduced the absorption of fine RCA to 4.28 %.

4.2.8 Angularity number

This test was carried out in accordance with the same British Standard as earlier (BS 812: Part 3). Equation 4.4 was used to measure the angularity number of the granite and RCA. The angularity number test results for the granite and RCA materials are presented in Table 4.11.

Table 4.11: Angularity Number of granite and RCA

Sieve size (mm)	**Weight of aggregates (g)**		
	A	**B**	**C**
		Granite	
5-6.3	409.5	408.5	411
6.3-9.5	791	799.5	793
9.5-14	1336.5	1334	1337.5
14-19	1786	1791	1788.5
Total	4323	4333	4330
		RCA	
5-6.3	439.5	439	438
6.3-9.5	762	765	763
9.5-14	1364	1366	1362.5
14-19	1721.5	1721	1724.5
Total	4287	4291	4288

Angularity Number (AN) = $67 - 100\,[W/(CG_A)]$ (4.4)

where:

W = Weight (in grams) of aggregates in the cylinder.

C = Weight (in grams) of water required to fill the cylinder.

G_A = Specific gravity of aggregate

$W_{Granite} = (4323 + 4333 + 4330) / 3$

$W_{Granite} = 4328.7$ g

C = 2733 g

$G_A = 2.610$

$AN_{Granite} = 67 - 100\,[4328.7 / (2733 \times 2.610)] = 6.31$

and:

$W_{RCA} = (4287 + 4291 + 4288) / 3$

$W_{RCA} = 4288.7$ g

$C = 2609$ g

$G_A = 2.18$

$AN_{RCA} = 67 - 100 [4288.7 / (2609 \times 2.18)] = 8.40$

Under the relevant British Standard, the angularity number of aggregates used in pavement construction should be between 6 and 9. As can be seen, the values calculated for both types of granite and recycled concrete aggregates met this standard.

4.3 Summary of aggregate test results

Table 4.12 contains a summary of the engineering properties of the virgin granite aggregates and recycled concrete aggregates.

Table 4.12: Summary of Engineering Properties of Granite and RCA

Test	Standard used	Granite	RCA	Standard requirements
LA	ASTM C131	18.3 %	24.5 %	Below 30 %
AIV	BS812: Part 3	6.21%	11.33%	Below 15 %
ACV	BS812: Part 3	20.82 %	28.32%	Below 30 %
PSV	BS812: Part 3	50.75	51.40	Above 40
Soundness	BS812: Part 3	5.25	6.52	Below 12 %
Flakiness Index	BS812: Part 3	7.89%	9.79%	Below 20 %
Elongation	BS812: Part 3	8.12%	5.35%	Below 20 %
Specific Gravity (Coarse)	ASTM C127-07	2.611	2.185	Between 2.60 and 2.65
Specific Gravity (Fine)	ASTM C128-07	2.644	2.423	-
Water Absorption (Coarse)	ASTM C127-07	0.44%	2.69%	-
Water Absorption (Fine)	ASTM C128-07	1.11%	4.28%	-
Angularity Number	BS812: Part 3	6.31	8.40	Between 6 and 9

Based on these test results, both types of aggregates satisfy the standard requirements and so are suitable for use in pavement construction.

4.4 Aggregate gradation

In this study, ASTM D3515 and Asphalt Institute (AI) aggregate gradations were used to design the HMA and SMA mixtures. Details of these aggregate gradations, including the percentages of materials meeting the desired gradation, the desired retain, and the upper and lower boundaries for HMA and SMA asphalt mixtures are given in Tables 4.13 and 4.14 respectively.

Table 4.13: HMA Aggregate Gradation Based on ASTM D3515

Sieve Size (mm)	Upper Limit (%)	Lower Limit (%)	Desired Passing (%)	Desired Retain (%)
12.5	100	……	100	0
9.5	90	100	95	5
4.75	55	85	70	25
2.36	32	67	50	20
0.3	7	23	15	35
0.075	2	10	6	9
Pan	0	0	0	6
Total				100%

Table 4.14: SMA Aggregate Gradation Based on Asphalt Institute (2007)

Sieve Size (mm)	Upper Limit (%)	Lower Limit (%)	Desired Passing (%)	Desired Retain (%)
19	100	100	100	0
12.5	95	85	90	10
9.5	75	20	70	20
4.75	28	20	24	46
2.36	24	16	20	4
0.6	16	12	14	6
0.3	15	12	13	1
0.075	10	10	10	3
Pan	0	0	0	10
Total				100%

An aggregate particle size of 2.36 mm or smaller is considered as fine, while an aggregate particle size larger than 2.36 mm is defined as coarse. Based on this, the total amounts of coarse, fine and fillers were 30%, 64% and 6% in the HMA and 76%, 14% and 10% in the SMA mixtures respectively.

4.5 Binder test results

80/100 penetration grade binder was used to produce the HMA and SMA specimens. This section sets out the quality controls carried out on the 80/100 asphalt binder to make sure it met the required specifications.

4.5.1 Penetration

The penetration test was carried out in accordance with ASTM D5. The test results are presented in Table 4.15 below.

Table 4.15: Penetration of binder

No. of samples	Penetration result
1	85
2	85
3	84
Average	84.66

The value of 84.66 is within the standard range for 80/100 penetration grade binders, so this binder is suitable in terms of the penetration test.

4.5.2 Softening point

This test was carried out in accordance with ASTM D 36. Table 4.16 below shows the results.

Table 4.16: Softening Point of binder

No. of samples	Softening Point (°C)
1	47.5
2	48
Average	47.75

Generally, binders with higher softening points will perform better in hot mix asphalt pavements. The value in this case of 47.25 is however acceptable for an 80/100 binder, and meets the requirements for the bitumen in question.

4.5.3 Flash and fire point

This test was carried out in accordance with ASTM D92, and the results are shown in Table 4.17 below.

Table 4.17: Flash and Fire Point of binder

Flash point (°C)	Fire point (°C)
289	303

The calculated values show that this binder can be heated up to 289° C without any risk of ignition.

4.5.4 Viscosity

The viscosity test was carried out in accordance with ASTM D 4402. The results are shown in Table 4.18 below.

Table 4.18: Asphalt Viscosity

No. of samples	Viscosity at 135°C (Pa.s)	Viscosity at 165°C (Pa.s)
1	0.247	0.106
2	0.260	0.093
Average	0.254	0.099

The average viscosity values of 0.254 at 135°C and 0.099 at 165°C are reasonable for an 80/100 binder as a viscoelastic material. It means that the material in question will produce a high stiffness modulus at the service temperature and also be capable of covering the aggregates with a thin film of asphalt binder.

4.6 Summary of asphalt test results

Table 4.19 below contains a summary of the asphalt binder test results. The values obtained from this test show that this type of binder can fulfill the standard requirements and so is suitable for use in pavement construction.

Table 4.19: Summary of Asphalt Test Results

Test	Standard used	Test results	Standard requirement
Penetration	ASTM D5	84.66	84 - 95
Softening point	ASTM D36	47.25	47 - 49
Flash point	ASTM D92	289	275 - 302
Fire point	ASTM D92	303	>302
Viscosity at 135°C	ASTM D4402	0.254	-
Viscosity at 165°C	ASTM D4402	0.099	-

4.7 OAC determination of HMA and SMA mixtures

The Marshall mix design method was used to determine the Optimum Asphalt Content (OAC) of the HMA and SMA mixtures. As the RCA content of the asphalt mixtures increases, their absorption capacity also increases. We therefore selected eight binders with different percentages of RCA content, from 5% to 8.5%. For each of these binders, three Marshall specimens were fabricated and tested in terms of density, Marshall stability and air voids, in order to determine the optimum level of binder content for each asphalt mixture. As described in Chapter three, an OAC measurement was carried out in accordance with the Marshall mix design method. In order to ascertain the optimum level of binder for each size and percentage of RCA, the maximums of the density and stability curves were measured, and these were then taken as two values for optimum binder content. In addition, a third value was measured from the 4% air void level curve. Finally, the mean of these measured values was calculated, to produce the Optimum Asphalt Content value. These tests and the results are described in more detail below.

4.7.1 OAC of HMA mixtures containing F-RCA

The purpose of the Marshall mix design method is to select the best performing gradation in terms of stability, density and 4% air voids. Figure 4.1 shows the density, Marshal stability and VTM values of the HMA mixtures containing F-RCA. Further details of the Marshall mix design, including tables, graphs and equations, are presented in Appendix A.

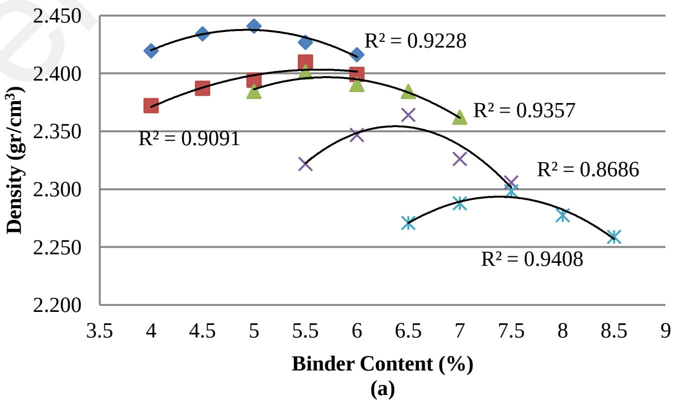

(a)

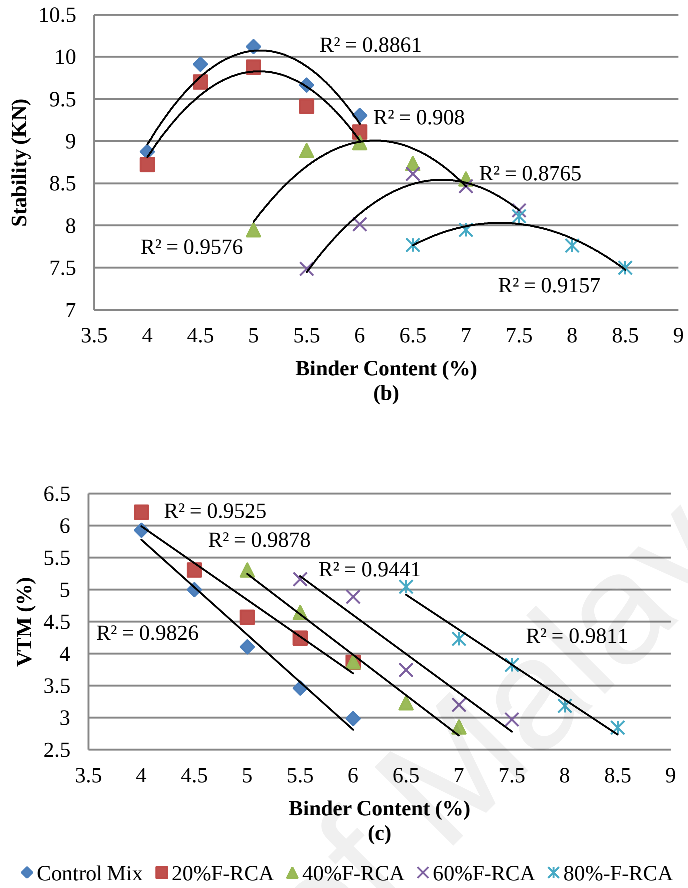

Figure 4.1: Density (a), Stability (b) and VTM (c) of the HMA mixtures containing F-RCA versus binder content

The OAC values of the HMA mixtures containing various percentages of F-RCA were measured. As Table 4.20 below shows, the OAC values ranged from 5.1% in the control mix (0% RCA) to 7.3 in the HMA mixtures containing 80% F-RCA. The latter result probably stems from the higher level of fines in the given HMA mixture. As presented earlier in Table 4.14 (concerning aggregate gradations), 64% of the HMA mixture consisted of aggregates with a particle size of 2.36 mm or smaller. As these fine granite aggregates are replaced by higher proportions of F-RCA, higher levels of binder content become necessary due to the higher absorption capacity of F-RCA than fine granite aggregates.

Table 4.20: OAC of HMA mixtures containing F-RCA

Mix Design	Optimum Asphalt Content (%)
Control Mix (0% RCA)	5.1
20% F-RCA	5.5
40% F-RCA	5.9
60% F-RCA	6.5
80% F-RCA	7.3

4.7.2 OAC of HMA mixtures containing C-RCA

Figure 4.2 below presents the Density, Marshall Stability and VTM results for the HMA mixtures containing C-RCA, while Table 4.21 shows the calculated optimum asphalt content for the various HMA mixtures containing C-RCA. Together, these suggest that the influence of coarse RCA on the optimum binder level of the asphalt mixtures is less than that of fines. This minor change is because the total amounts of coarse aggregates in the HMA mixtures was 30% which is less than half of the fines content in the mixtures.

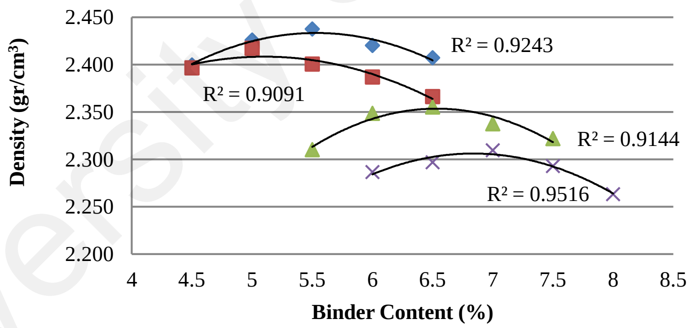

(a)

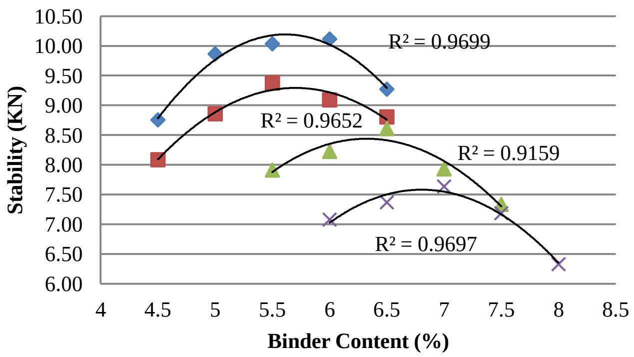

(b)

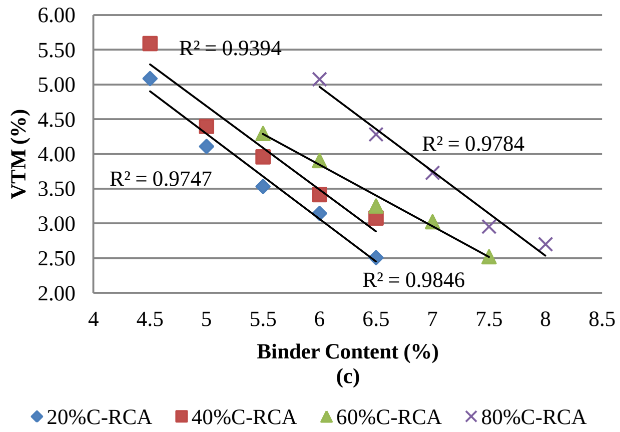

Figure 4.2: Density (a), Stability (b) and VTM (c) of the HMA mixtures containing C-RCA versus binder content

Table 4.21: OAC of HMA mixtures containing C-RCA

Mix Design	Optimum Asphalt Content (%)
Control Mix (0% RCA)	5.1
20% C-RCA	5.4
40% C-RCA	5.5
60% C-RCA	6.2
80% C-RCA	6.8

4.7.3 OAC of HMA mixtures containing M-RCA

Figure 4.3 displays the Marshall properties of the HMA mixtures containing M-RCA, while Table 4.22 sets out the OAC of these. As the latter shows, as the amount of M-RCA increased from 20% to 80%, the OAC level increased from 5.4% to 7%. The lower density and stability and higher VTM of the HMA mixtures containing RCA than the control mix reflects the higher porosity and lower density of RCA compared to those of granite aggregates.

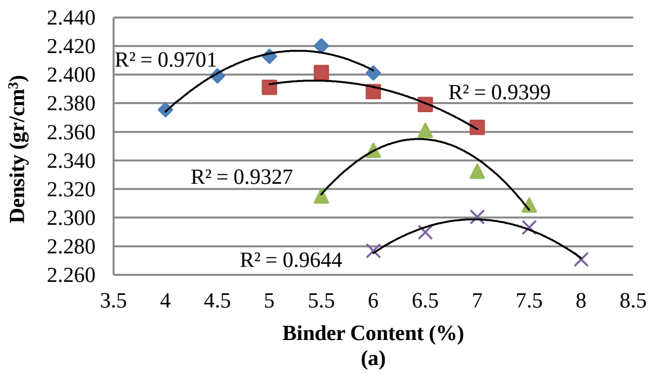

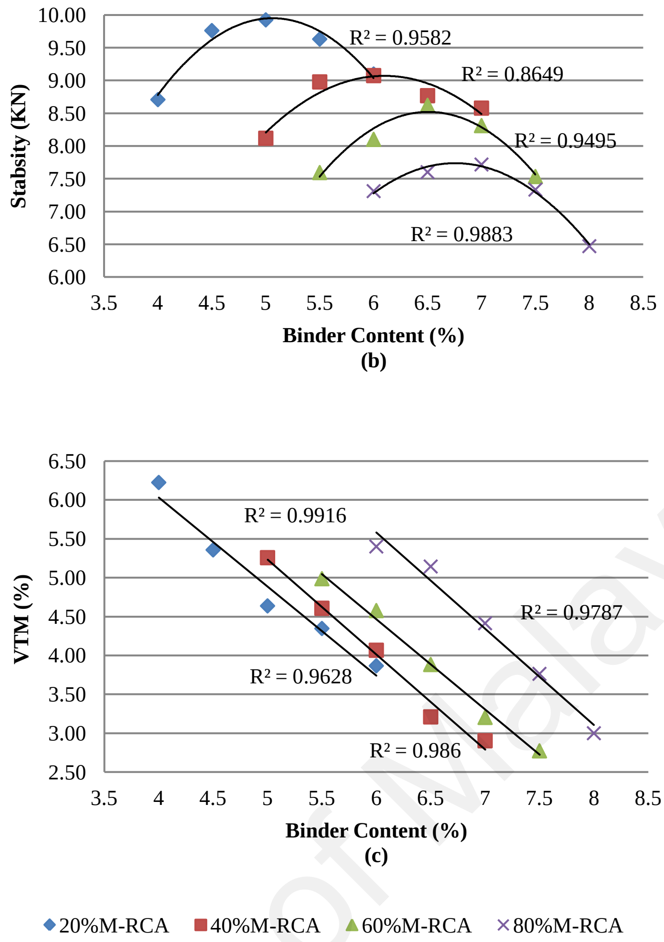

Figure 4.3: Density (a), Stability (b) and VTM (c) of the HMA mixtures containing M-RCA versus binder content

As demonstrated in Tables 4.12 and 4.13 earlier, RCA materials have a lower specific gravity and higher water absorption than granite aggregates. As a result, regardless of the size of the RCA particles, any replacement of virgin granite aggregates with RCA inevitably raises the need for binder content and hence the OAC level.

Table 4.22: OAC of HMA mixtures containing M-RCA

Mix Design	Optimum Asphalt Content (%)
Control Mix (0% RCA)	5.1
20% M-RCA	5.4
40% M-RCA	5.9
60% M-RCA	6.4
80% M-RCA	7.0

4.7.4 OAC of SMA mixtures containing F-RCA

Figure 4.4 shows the Marshall properties of the stone mastic asphalt mixtures containing F-RCA. Further details, including tables, figures and equations, are provided in Appendix B. As shown in the aggregate gradation of the various SMA mixtures in Table 4.14 earlier, the levels of coarse and fine contents were 76% and 14% respectively. It is reasonable to assume that any replacement of coarse aggregates with RCA should lead to major changes in the binder content of the SMA mixtures and in their performance.

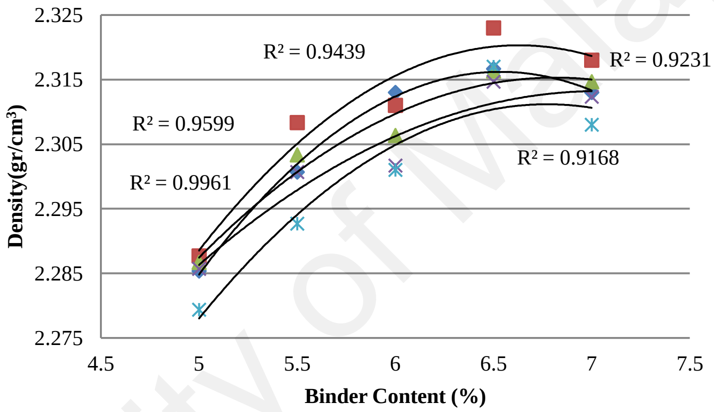

(a)

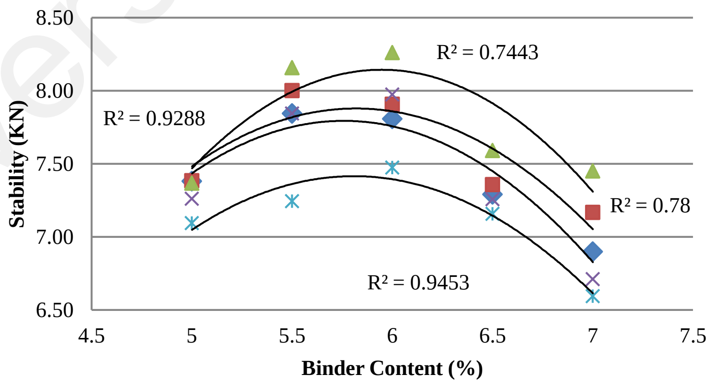

(b)

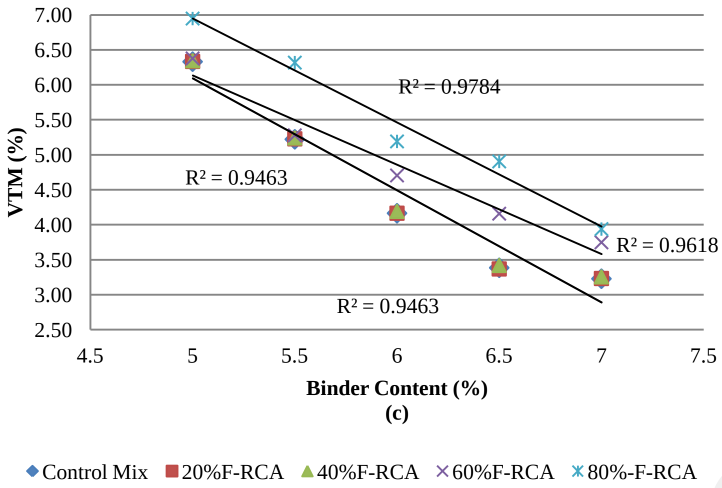

Figure 4.4: Density (a), Stability (b) and VTM (c) of the SMA mixtures containing F-RCA versus binder content

The OAC values of the SMA mixtures containing F-RCA are displayed in Table 4.23, based on plotted graphs. As mentioned earlier, the level of fines in this specific SMA mixture was only 14% of the total aggregates present. The fines therefore have less influence on the Marshall properties of the asphalt mixture. The OAC results reveal that there was no substantial change between the control samples and the samples containing 80% F-RCA: as the level of F-RCA increased from 0% (in the control mix) to 80%, the OAC value changed only from 6.2% to 6.5%.

Table 4.23: OAC of SMA mixtures containing F-RCA

Mix Design	Optimum Asphalt Content (%)
Control Mix (0% RCA)	6.2
20% F-RCA	6.2
40% F-RCA	6.3
60% F-RCA	6.5
80% F-RCA	6.5

4.7.5 OAC of SMA mixtures containing C-RCA

The Density, Marshall Stability and VTM values of the SMA mixtures containing various percentages of C-RCA were plotted against the binder content. Figure 4.5 shows the results. The OAC values, derived from the peak of the density and stability curves together with the 4% of VTM curves, are meanwhile set out in Table 4.24.

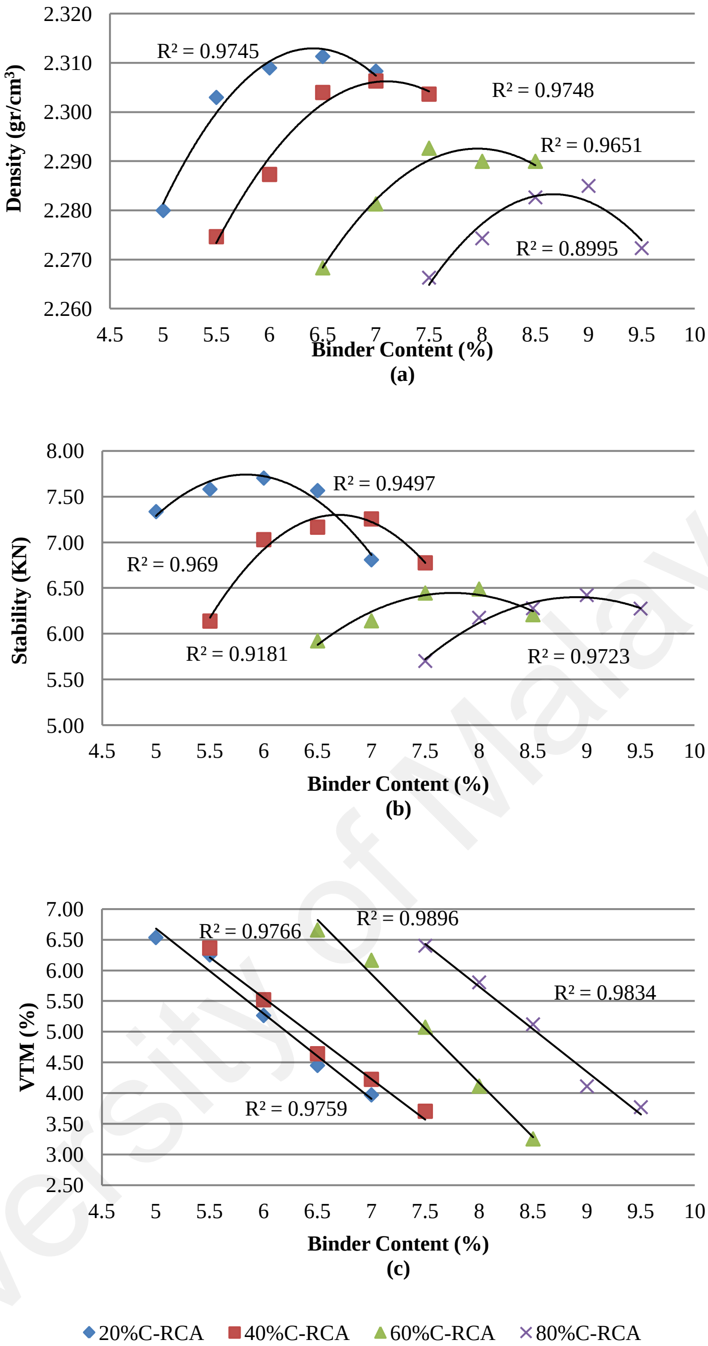

Figure 4.5: Density (a), Stability (b) and VTM (c) of the SMA mixtures containing C-RCA versus binder content

It is clear from the OAC values of the SMA mixtures containing C-RCA shown in Table 4.24 that the performance of the SMA mixtures was highly affected by the level of coarse aggregates. 76% of the SMA mixtures used in this research contained coarse aggregates. As the C-RCA content increased from 20% to 80%, the OAC values also increased markedly from 6.4% to 8.9%

Table 4.24: OAC of SMA mixtures containing C-RCA

Mix Design	Optimum Asphalt Content (%)
Control Mix (0% RCA)	6.2
20% C-RCA	6.4
40% C-RCA	7.0
60% C-RCA	7.9
80% C-RCA	8.9

4.7.6 OAC of SMA mixtures containing M-RCA

Figure 4.6 shows the Marshall properties of the SMA mixtures containing M-RCA. As can be seen from Table 4.25, as the mixture of coarse and fine granite aggregates in the SMA mixtures was replaced with M-RCA, higher levels of binder content were needed. This is probably due to the higher porosity of the recycled concrete aggregates than the virgin granite ones, which leads to higher absorption of the binder into the asphalt mixture. Replacing the granite aggregates with M-RCA up to the level of 40% did not produce any substantial change in the OAC values of the SMA mixtures; however, as the M-RCA content increased from 40% to 80%, the OAC values increased significantly from 6.6% to 7.8%.

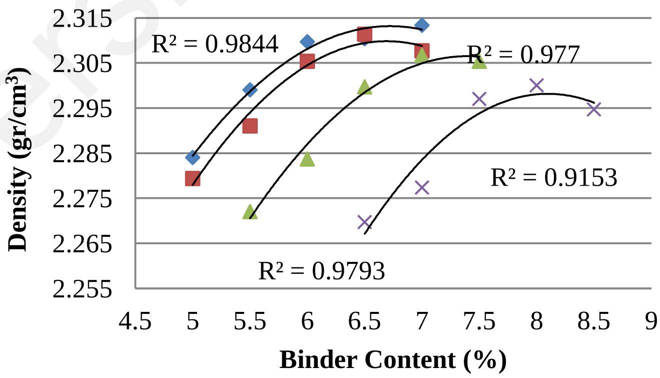

(a)

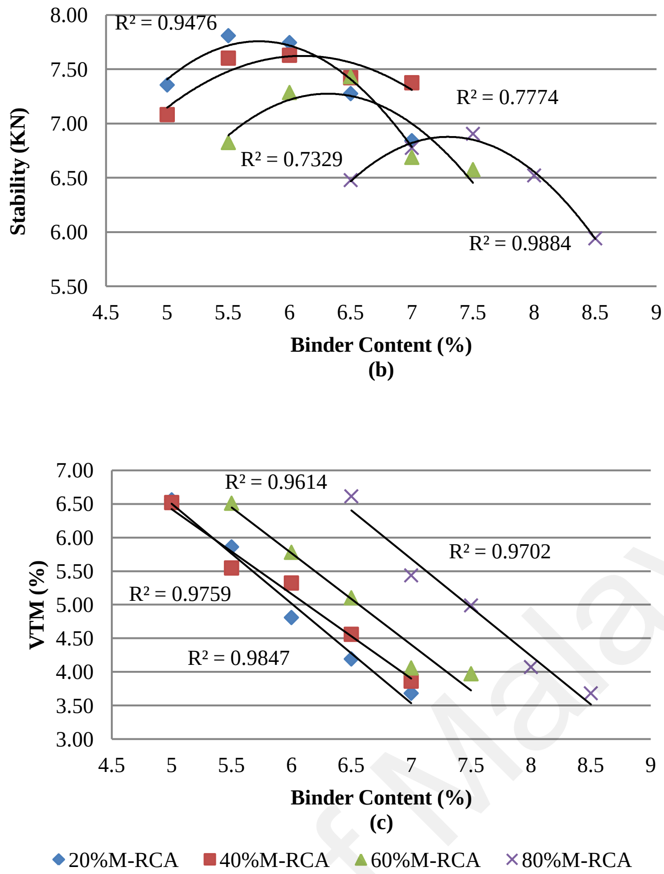

Figure 4.6: Density (a), Stability (b) and VTM (c) of the SMA mixtures containing M-RCA versus binder content

Table 4.25: OAC of SMA mixtures containing M-RCA

Mix Design	Optimum Asphalt Content (%)
Control Mix (0% RCA)	6.2
20% M-RCA	6.4
40% M-RCA	6.6
60% M-RCA	7.0
80% M-RCA	7.8

4.8 Performance test results

This section presents the performance tests results of the hot mix asphalt and stone mastic asphalt core samples. A total of 390 core specimens of a 100mm diameter, 156 core specimens of 200mm diameter and 78 beams with the specific dimensions of 380mm × 63.5mm × 50mm were cored and cut out of the HMA and SMA slabs. As mentioned earlier in Chapter 3, all the slabs were designed with an air void target level of 4%, except for those used for the moisture susceptibility test, for which the VTM design was 6%, in line with the requirements of the relevant standard. The required number of specimens were cored out of the HMA and SMA slabs and subjected to different performance tests to evaluate the feasibility of using these types of recycled concrete aggregates in dense-graded and gap-graded asphalt mixtures. The performance tests applied to the core specimens of a 100mm diameter and 4% air voids were Density, Air void, Marshall Stability, Flow, Resilient Modulus. The 100mm diameter specimens containing 6% air voids were subjected to Moisture Susceptibility and Indirect Tensile (IDT) Strength tests. The 200mm diameter core specimens were meanwhile subjected to a wheel tracking test to measure the rut depth and rut rate of the HMA and SMA mixtures containing RCA; while slab cut beam specimens were used for a Flexural Beam Fatigue test

4.8.1 Bulk density and air void

Density and VTM tests were carried out in accordance with ASTM D 2726. The bulk density of the core specimens of 100mm were measured by weighing them first dry, then submerged in water, and finally in saturated surface dry conditions. The density was then calculated from the relevant equations. The HMA and SMA core specimens containing different sizes and percentages of RCA were subjected to this test. The averages for bulk density and air void for the HMA and SMA specimens are shown in Figures 4.7 and 4.8 respectively.

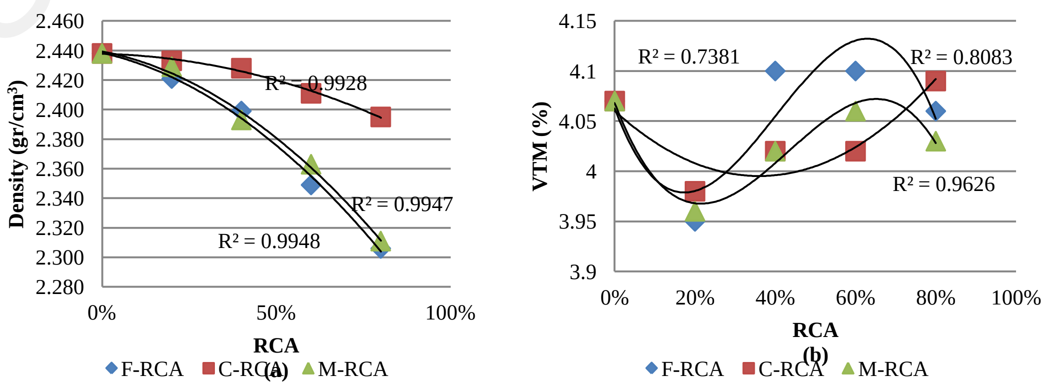

Figure 4.7: Average of Bulk Density (a) and VTM (b) of the HMA specimens containing RCA

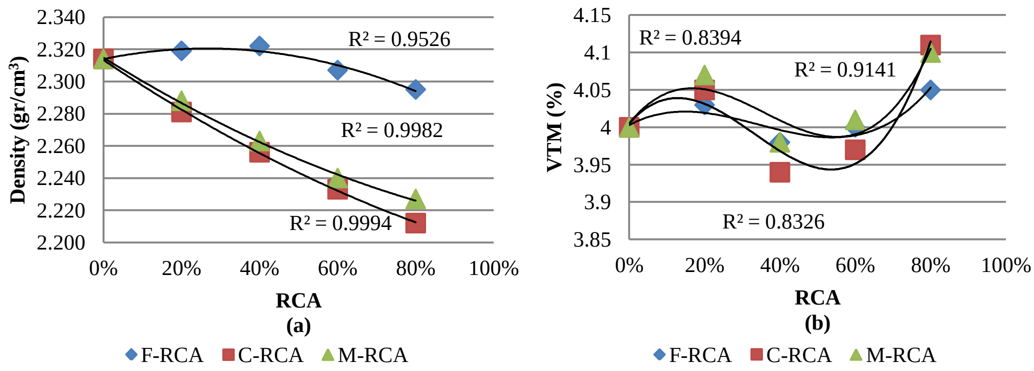

Figure 4.8: Average of Bulk Density (a) and VTM (b) of the SMA specimens containing RCA

To measure air voids, the HMA and SMA specimens were compacted with a target of 4% VTM content. The calculated VTM values indicate that, regardless of the RCA content in the HMA and SMA asphalt mixtures, the air void can be kept under control. The SMA specimens containing 80% C-RCA and 80% M-RCA had only slightly higher VTM values than the other asphalt specimens, perhaps due to the breaking of the C-RCA during compaction.

4.8.2 Marshall stability (MS) and flow

This test was carried out in accordance with ASTM D1559. The HMA and SMA core specimens of 100mm diameter were each conditioned for 40 minutes in a water bath at 60° C and then subjected to Marshall stability and Flow tests. The volumes of the core specimens were calculated, and the recorded stability values were adjusted using the ASTM stability correlation ratio shown in Appendix C. The average of the corrected stability and flow values of the HMA and SMA specimens were also plotted against their RCA content: the results of this are shown in Figures 4.9 and 4.10 respectively.

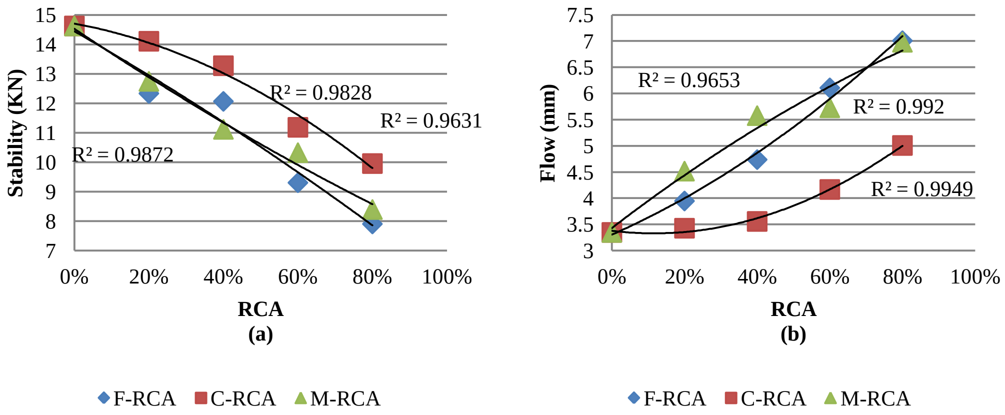

Figure 4.9: Average of Marshal Stability (a) and Flow (b) of the HMA specimens containing RCA

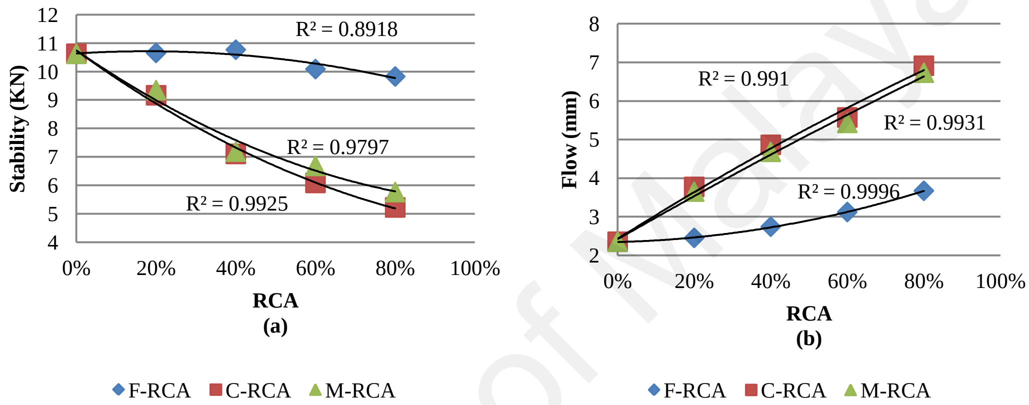

Figure 4.10: Average of Marshal Stability (a) and Flow (b) of the SMA specimens containing RCA

Regardless of the level of RCA content in the asphalt mixtures, the Marshall Stability values of the HMA specimens were found to be considerably higher than those of the SMA specimens, due to the dense gradation of the aggregates in the HMA. The calculated Marshall Stability (MS) values for the SMA and HMA mixtures containing 100% virgin aggregate (VA) were 10.63 and 14.63 KN. The test results indicate that 20% and 40% levels of F-RCA can increase the Marshall stability values of SMA mixtures to 10.66 and 10.77 KN respectively. The flow values of both types of asphalt mixture initially increased only gradually as the RCA content increased, but at 80% C-RCA and M-RCA in the SMA and 80% F-RCA and M-RCA in the HMA specimens, the flow values began to rise more significantly. According to the Asphalt Institute (AI), the minimum stability value of SMA and HMA should be 6.2 KN and 9 KN respectively. The F-RCA in the SMA and C-RCA in the HMA mixtures did not have much impact; however, as the level of C-RCA and M-RCA increased to 80% in the SMA mixtures, the stability values of these fell to 5.23 KN and 5.77 KN (both below the AI specifications). In the HMA mixtures, on the other hand, almost all the specimens produced acceptable stability values except for at 80% F-RCA and M-RCA levels, for which the stability decreased to 7.91 and 8.4 KN.

3.8.3 Voids in Mineral Aggregates (VMA) and Voids Filled with Asphalt (VFA)

In the asphalt mixtures containing 100% VA, the calculated values of Voids in Mineral Aggregates (VMA) and Voids Filled with Asphalt (VFA) were 15.55 and 73.91% in the SMA and 15.44 and 73.64% in the HMA mixtures. The tests show that, as the level of RCA increases in the asphalt mixtures, the VMA and VFA values increase as well. Figures 4.11 and 4.12 summarize the VMA and VFA values of the HMA and SMA mixtures containing RCA.

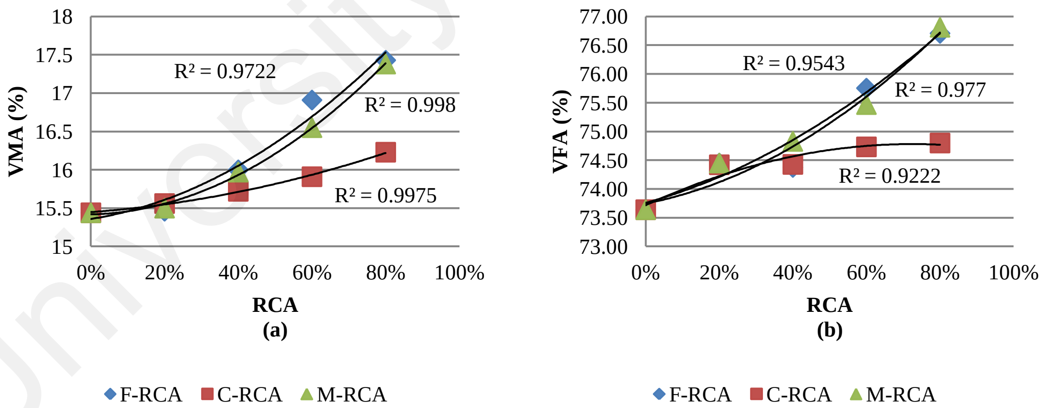

Figure 4.11: Average of VMA (a) and VFA (b) of the HMA specimens containing RCA

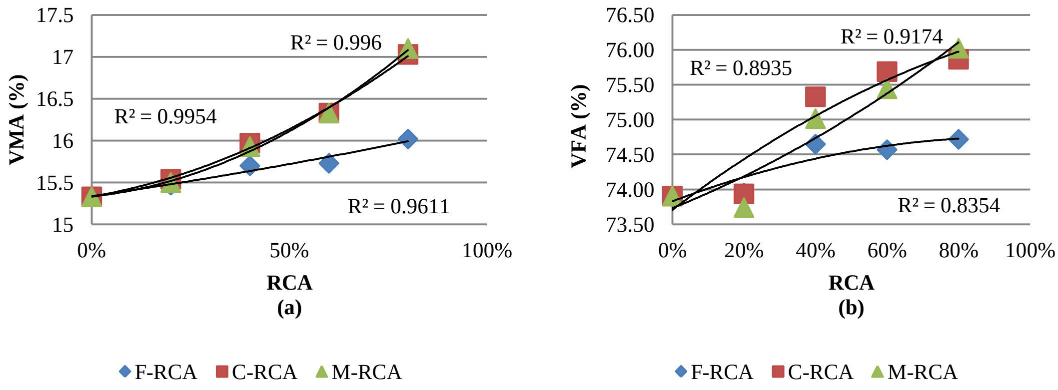

Figure 4.12: Average of VMA (a) and VFA (b) of the SMA specimens containing RCA

These higher OAC levels are probably a result of the higher porosity and absorption of the RCA than VA. According to the AI, the minimum acceptable value of VMA is dependent on the nominal maximum aggregate size of the mixture and the desired air void level, as shown in Table 4.26.

Table 4.26: Minimum VMA requirement Based on nominal maximum aggregate size (AI, 2007)

Nominal Maximum Aggregate Size (mm)	Void in mineral aggregates (VMA) Design air voids		
	3%	4%	5%
2.36	19	20	21
4.75	16	17	18
9.5	14	15	16
12.5	13	14	15
19	12	13	14
25	11	12	13
37.5	10	11	12

The nominal maximum aggregate sizes of the HMA and SMA mixtures are 9.5mm and 12.5mm respectively, and the desired air void level is 4% for both mixtures. The acceptable VFA values for the asphalt specimens should therefore be between 65% and 78% for medium traffic volumes and 70% and 80 % for heavy traffic volumes. The minimum VMA values for the HMA and SMA are meanwhile 15% and 14% respectively. In summary, the tests show that all the SMA and HMA specimens can meet the required VMA and VFA criteria.

4.8.4 Resilient modulus (M_R)

For this test, carried out in accordance with ASTM D4123, the HMA and SMA core specimens of 100mm diameter were conditioned at 25°C and 40°C for a minimum of two hours and then subjected to a resilient modulus test. Figures 4.13 and 4.14 show the average resulting Resilient Modulus (M_R) values for the HMA and SMA mixtures containing RCA at 25°C and 40°C respectively. These M_R values were lower than those of the VA control mixtures, and fell further as the RCA content increased. According to the Malaysian Road Transport Department (JKR), the minimum resilient modulus required for flexible pavement surfaces at 25°C is 2500 Mpa. However, the minimum resilient modulus value for typical mixtures in laboratory conditions is 2100 Mpa.

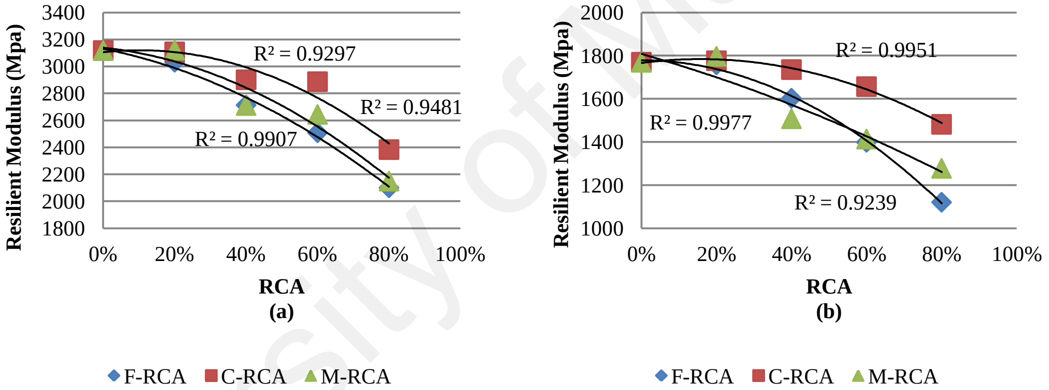

Figure 4.13: Average of Resilient Modulus at 25°C (a) and 40°C (b) for the HMA specimens containing RCA

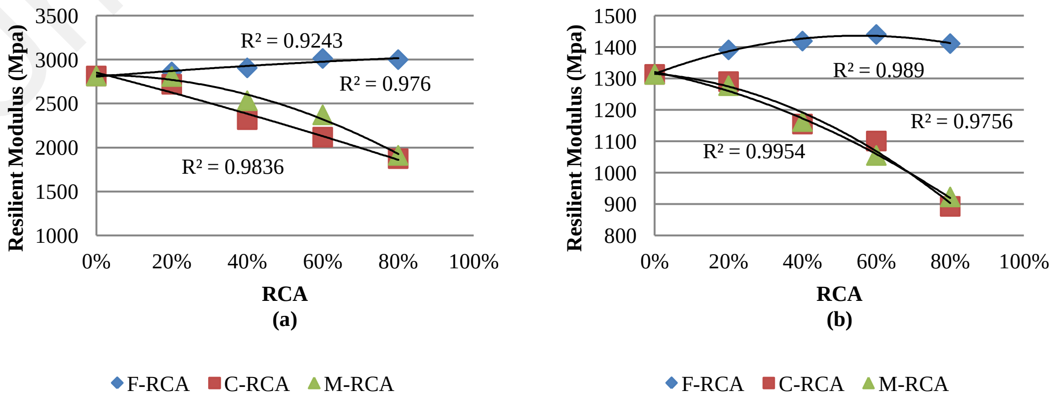

Figure 4.14: Average of Resilient Modulus at 25°C (a) and 40°C (b) for the SMA specimens containing RCA

The SMA specimens containing 20% and 40% F-RCA produced higher residual modulus values than the VA control specimens, and the M_R values increased slightly to 2860 and 2906 Mpa, while the M_R values of the VA-SMA and VA-HMA were 2814 and 3119 Mpa respectively. The reduction of resilient modulus value in the asphalt mixtures containing RCA are believed to be due to the higher percentage of binder contents in the asphalt mixtures. In sum, all the HMA and SMA specimens met the minimum requirements for residual modulus, except the SMA specimens containing 80% C-RCA and 80% M-RCA. The substantial fall in M_R values in the SMA mixtures when the coarse RCA content was increased was probably due to the higher levels of coarse aggregates in SMA than in the HMA mixtures.

4.8.5 Loaded Wheel Tracking (LWT)

A Loaded Wheel Tracking (LWT) test was carried out, in accordance with the British Standard (BS 598-110: 1998), to measure the susceptibility of the HMA and SMA asphalt mixtures to plastic deformation at high temperatures by simulating road tire pressure on the specimens. Stone Mastic Asphalt is a rut resistance asphalt mixture, so should generally have higher resistance to permanent deformation (rutting) than hot mix asphalt mixtures.

4.8.5.1 Wheel tracking depth

Figure 4.15 illustrates the loaded wheel tracking test results and the effect of C-RCA on the HMA and SMA specimens in terms of permanent deformation. The rut depth values for SMA mixtures with 0, 20, 40, 60 and 80% C-RCA content after 45 minutes were 1.65, 2.52, 3.63, 4.46 and 6.17mm respectively. The rut depth values for the HMA mixtures containing the same level of C-RCA content were meanwhile 2.90, 2.91, 3.00, 4.09 and 6.33 mm. Expressing this in percentage terms, as the C-RCA content increased from 0% (VA mix) to 20, 40, 60 and 80%, the rut depth values increased to 52.7%, 120%, 170.3%, 273.9% in the SMA and 0.34%, 3.45%, 41.03% and 118.27% in the HMA specimens. In other words, the impact of the C-RCA on the SMA specimens was considerably higher than on the HMA mixtures in terms of wheel tracking depth.

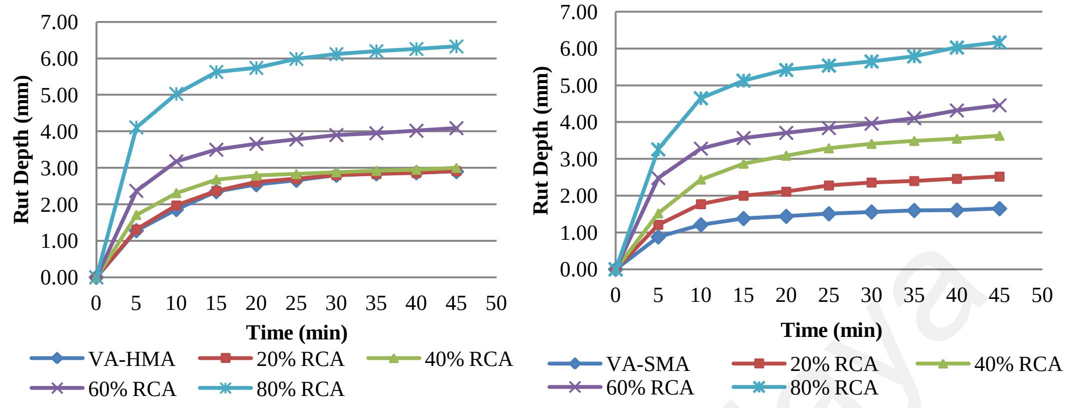

(a) *(b)*

Figure 4.15: Effect of C-RCA on rut depth of HMA (a) and SMA (b) specimens

Figure 4.16 illustrates the rut depth values of the HMA and SMA specimens containing F-RCA. SMA mixtures with 0%, 20%, 40%, 60% and 80% F-RCA showed 1.65, 1.60, 1.41, 2.97 and 3.28 mm and HMA specimens showed 2.90, 2.96, 3.31, 4.47 and 7.08 mm rut depths after 45 minutes. Again, in percentage terms this means that, as the F-RCA content rose from 0% to 80% in the HMA mixtures, the rut depth values increased to 2.07%, 14.14%, 54.14% and 144.14% respectively. However, the rut depth results for the SMA mixtures were rather different. With these, the rut depth in fact fell from 1.65mm in VA-SMA to 1.6 and 1.41mm in 20% and 40% F-RCA; but it then increased to 2.97 and 3.28mm at 60% and 80% F-RCA levels. In other words, up to the 40% level F-RCA had a positive effect on the rutting resistance of the SMA mixtures. This was probably due to the higher density and Marshall Stability values of the SMA specimens containing 20% and 40% F-RCA.

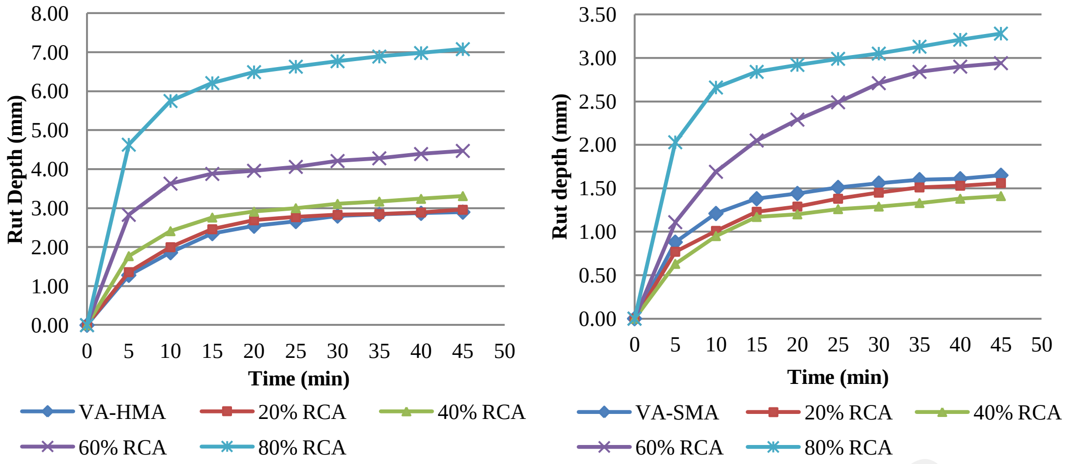

(a) *(b)*

Figure 4.16: Effect of F-RCA on rut depth of HMA (a) and SMA (b) specimens

The rut depth values of the HMA and SMA specimens containing M-RCA are shown in Figure 4.17. As can be seen, the rut depth values of the SMA and HMA specimens containing M-RCA were lower than the control mixes, and any increase in RCA content in the asphalt mixtures increased their rut depth resistance values.

The relevant British Standard lays down a maximum allowable rutting rate at 45°C of 4mm (Table 3.1). Although the majority of rut depth values increased when RCA was added in both the SMA and HMA mixtures, most of the specimens nevertheless met the standard requirements. The exceptions were the SMA mixtures with 60% and 80% C-RCA and M-RCA content, and the HMA mixtures with 80% C-RCA and M-RCA content and 60 and 80% F-RCA content respectively.

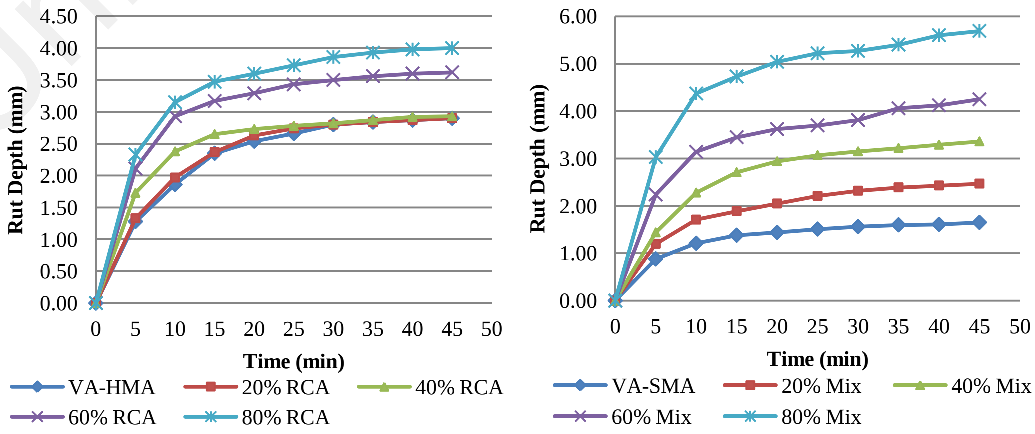

(a) *(b)*

Figure 4.17: Effect of M-RCA on rut depth of HMA (a) and SMA (b) specimens

4.8.5.2 Wheel tracking rate

The wheel tracking rate W_{TR} or rut rate is the second most important factor to be considered in rutting studies. The rut rates of the control mixtures (0% RCA) were 0.34 mm/hr for the SMA and 0.40 mm/hr for the HMA. The rut rate values of the SMA and HMA mixtures containing various levels of RCA are displayed in Figure 4.18. At all levels of RCA content, the rut rate values of the HMA mixtures were considerably higher than those of the SMA specimens. At the same time, the rut rate values of most of the specimens were within the 2mm/hr BS requirement – the exceptions being 60% and 80% C-RCA in the SMA specimens, whose rut rate values rose to 2.05 and 2.16 mm/hr respectively.

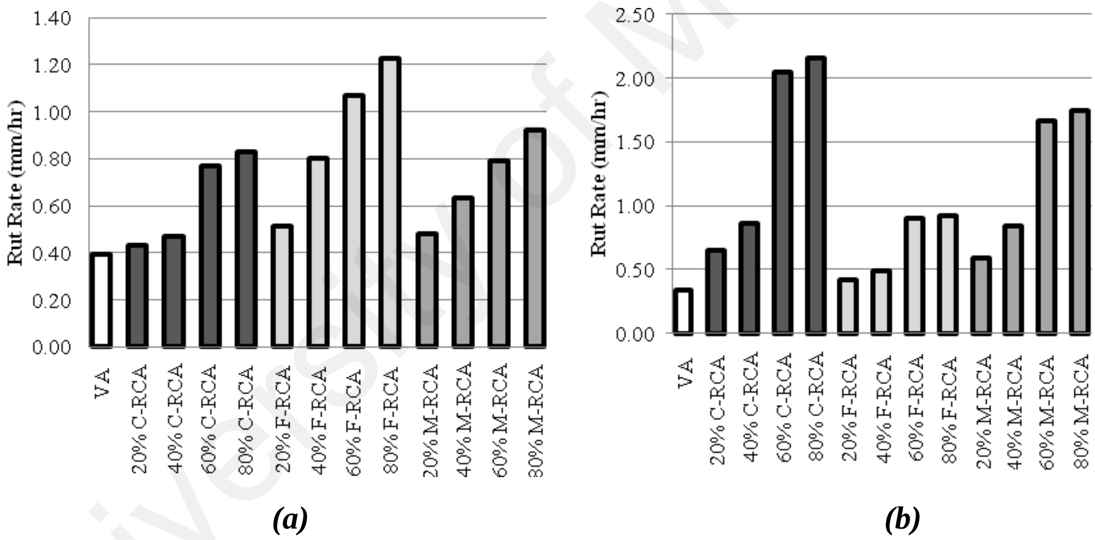

Figure 4.18: Rut rate values of HMA (a) and SMA (b) mixtures containing RCA

Overall, the mixtures containing higher levels of RCA showed higher rut rates. However, the differences between the rut rates for VA-SMA and 20% and 40% F-RCA or VA-HMA and 20% and 40% C-RCA respectively were relatively small; whereas, as the level of RCA increased beyond 40% to 60% and then 80%, the rut rates rose more significantly. This is probably caused by the high amount of fines and low amount of coarse aggregates in HMA, and the same phenomenon in reverse proportions in the SMA aggregate gradation.

4.8.6 Indirect Tensile (IDT) strength

The Indirect Tensile Strength (IDT) of the HMA and SMA specimens was evaluated in accordance with ASTM D6931. Two types of fillers were used to provide a better understanding of the impact of fillers on the IDT strength and moisture susceptibility of the asphalt specimens. The first type was a standard mineral filler (MF) prepared by sieving granite aggregates. The second was a hydrated limestone powder (HL) which, based on some tests (Chapter 3), this filler is able to improve the moisture susceptibility of the asphalt mixtures. The HMA and SMA specimens were tested as both conditioned (C) and un-conditioned (UC) samples. The test results are presented below.

4.8.6.1 Indirect tensile strength of HMA mixtures

Figure 4.19 shows the average IDT strength values of the HMA specimens containing F-RCA. These results show the HMA specimen containing 20% F-RCA and HL to be the optimal mixture, with a UC-IDT strength value of 1075.85 kPa. The average UC-IDT strengths of the control specimens (100% VA) were 1050.38 kPa and 1055.01 kPa for the HMA specimens containing MF and HL respectively, both slightly lower than the optimal value. The results further indicate that utilizing HL instead of MF as filler in the HMA specimens containing F-RCA does not have much impact on UC-IDT strength. However, the impact of HL compared with MF on C-IDT strength was more substantial.

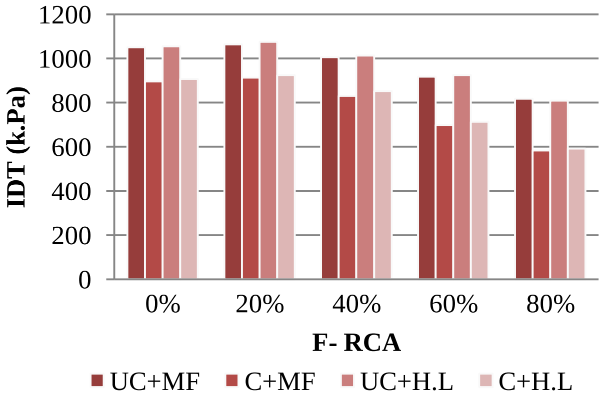

Figure 4.19: Indirect Tensile Strength of HMA Specimens containing F- RCA

The HMA specimens containing 80% F-RCA and MF produced the lowest C-IDT strength value of 582.51 kPa. The OAC results of these HMA specimens revealed that, as the levels of F-RCA increased from 0% (control mix) to 80%, so the required level of asphalt content increased from 5% to 7.1%. In addition, the bulk density test results of the F-RCA HMA generally fell as the level of F-RCA in the asphalt mixtures increased, except for the 20% F-RCA mixture. It is likely that the higher binder content and lower bulk density induced this reduction in IDT strength. In addition, the level of fine aggregates in the HMA mixture was 64% of the total aggregate content, so any replacement of fine granite aggregates with F-RCA could have a significant impact on the performance of the HMA mixtures.

The IDT strength of the HMA specimens containing C-RCA is presented in Figure 4.20 below. They show that replacing the virgin coarse granite aggregates with 20% C-RCA in the HMA mixtures improves the IDT strength of the asphalt mixture. However, as the amount of C-RCA increases beyond 20% to 40% and more, IDT strength falls significantly.

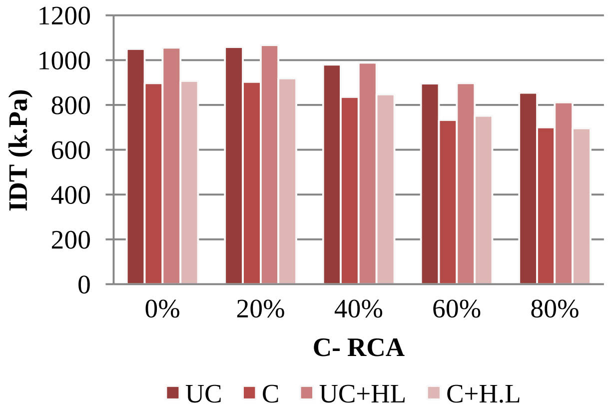

Figure 4.20: Indirect Tensile Strength of HMA Specimens containing C- RCA

The highest IDT strength value obtained in the test was 1066.59 kPa in the HMA specimens containing 20% C-RCA and HL as filler, while, the lowest value was 694.85 kPa in the conditioned HMA specimens containing 80% C-RCA and MF. Turning to the bulk density test, as the amounts of C-RCA increased from 0% (control mix) to 20% in the HMA mixtures, the average bulk density rose slightly from 2.435 g/cm^3 to 2.441 g/cm^3 (with little or no OAC change), producing a higher IDT strength value. As the amount of C-RCA increased from 20% to 80%, the bulk density fell significantly while the level of binder needed increased from 5.2 % to 6.6 % - thus resulting in a reduction in IDT strength.

The average IDT strength values of the HMA specimens containing M-RCA are displayed in Figure 4.21. These show that using HL as filler instead of MF has no significant effect on the IDT strength properties of the specimens, with the exception of the specimens containing 20% M-RCA. The average UC-IDT strength of the specimens containing 20% M-RCA and HL was 1080.49 kPa – higher than the UC-IDT strength of the HMA specimens containing 100% VA (and HL) or the HMA specimens containing 20% M-RCA (and MF), both which had an average value of 1055.01 kPa.

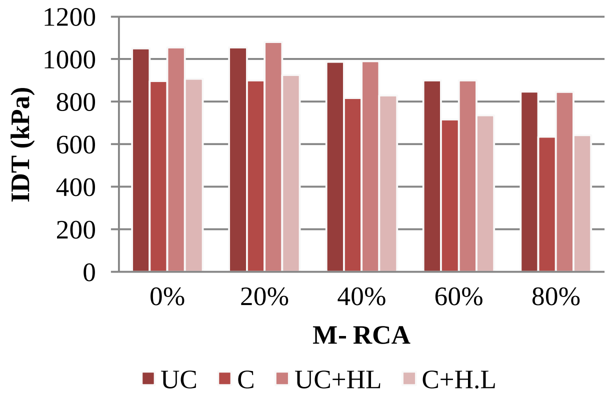

Figure 4.21: Indirect Tensile Strength of HMA Specimens containing M- RCA

Finally, the lowest average IDT strength of 634.63 kPa came from the C-IDT in the HMA specimens containing 80% M-RCA and MF. The IDT Strength of the HMA mixtures containing M-RCA may have stemmed from the bulk density and OAC values of the specimens. As the levels of M-RCA increased from 0% to 20% in the HMA specimens, the bulk density values increased, from 2.435 g/cm^3 to 2.441 g/cm^3, while the OAC showed only a small increase of 0.3%. However, as the levels of M-RCA content increased from 20% to 40%, 60% and 80%, the bulk density values fell to 2.391 g/cm^3, 2.360 g/cm^3 and 2.310 g/cm^3 respectively, and the optimum asphalt content increased to 5.7%, 6.2% and 6.8%.

4.8.6.2 Indirect tensile strength of SMA mixtures

Figure 4.22 below summarizes the results of the indirect tensile strength tests on the various SMA specimens. These include specimens containing different percentages of F-RCA; both conditioned and unconditioned specimens; and those containing mineral filler (MF) or hydrated limestone powder (HL) respectively.

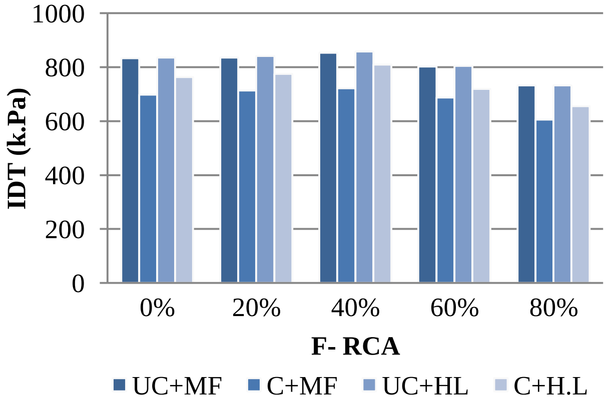

Figure 4.22: Indirect Tensile Strength of SMA Specimens containing F- RCA

The first thing to note is that, while using HL rather than MF filler had no significant effect on the indirect tensile strength of the unconditioned SMA specimens containing F-RCA, it did increase the IDT strength of the conditioned specimens. Second, the unconditioned SMA specimens containing 40% F-RCA had the highest indirect tensile strength for the mixtures containing both MF and HL. The lowest average IDT strength was 605.67 kPa for the conditioned specimens containing 80% F-RCA and MF as filler; while the highest average IDT strength was 858.14 kPa for the SMA specimens containing 40% F-RCA and HL as filler. In other words, replacing the granite fines with up to 40% F-RCA improved the IDT strength of the SMA mixtures.

Looking at bulk density, the average bulk density of the SMA specimens increased from 2.317 g/cm^3 in the control specimens (100% VA) to 2.328 g/cm^3 in the specimens containing 40% F-RCA. In contrast, the density of the specimens containing 80% C-RCA decreased to 2.288 g/cm^3. The higher density of the SMA specimens containing 40% F-RCA and lower density of the SMA specimens containing 80% F-RCA presumably caused their higher and lower IDT strength values. The average IDT strength values of the SMA specimens containing C-RCA are displayed in Figure 4.23 below.

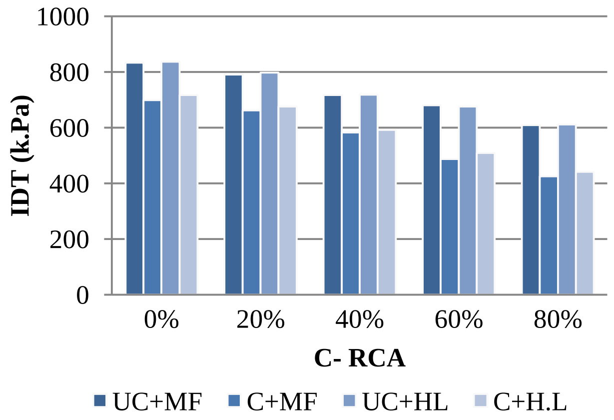

Figure 4.23: Indirect Tensile Strength of SMA Specimens containing C- RCA

The SMA specimens containing 100% VA (control mix) and HL as filler produced an unconditioned IDT strength value of 836.13 kPa, slightly higher than the control specimens containing MF with a value of 832.66 kPa. 836.13 kPa was therefore the optimum value in terms of IDT strength. However, as with the SMA specimens containing 80% F-RCA, the conditioned specimens containing 80% C-RCA produced a much lower value of 425.01 kPa – the lowest of all those obtained. The bulk density values of the SMA specimens containing C-RCA fell significantly as the amount of C-RCA increased in the SMA mixtures. However, the OAC values rose from 6.1% in the VA-SMA to 8.6% in the SMA specimens containing 80% C-RCA. The higher bitumen content and lower density may well have caused this. In addition, 76% of the total aggregates in the SMA specimens were coarse aggregates, and SMA mixtures are normally more sensitive to the quality of the coarse aggregates than fines or fillers. Moreover, the LA, AIV and ACV test results of the recycled concrete aggregates were considerably lower than those for the virgin granite aggregates. The higher C-RCA content in the SMA mixtures was presumably therefore one of the reasons for the greater changes in terms of indirect tensile strength values.

The average IDT strength values of the SMA specimens containing M-RCA are shown in Figure 4.24 below. These show that replacing VA with M-RCA resulted in lower IDT strength. The unconditioned SMA specimens containing 100% VA and HL as filler produced the highest value of 836.13 kPa, slightly higher than the SMA specimens containing 100% VA and MF with an IDT strength value of 823.66 kPa.

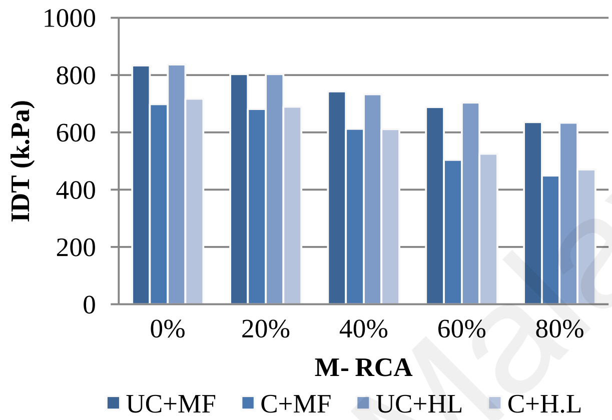

Figure 4.24: Indirect Tensile Strength of SMA Specimens containing M- RCA

In summary, regardless of the RCA particle size, the IDT strength of the asphalt mixtures generally fell as their RCA content increased – except for the 20% and 40% F-RCA mixtures, which showed increased IDT strength. In addition, the IDT strength values fell by much more in the SMA specimens containing C-RCA, due probably to the higher amounts of coarse aggregates in these SMA mixtures.

4.8.7 Moisture susceptibility

The Tensile Strength Ratio (TSR) of the asphalt specimens was measured as a ratio of the indirect tensile (IDT) strength of the conditioned to dry specimens. This section presents the TSR values of the SMA and HMA specimens containing RCA, which represent the reduction in IDT strength after the specimens were submerged in a 60°C water bath for 24 hours. This reduction in IDT strength is caused by the loss of adhesive bonds between the mixture materials due to the presence of water or moisture – otherwise known as moisture susceptibility or moisture induced damage.

4.8.7.1 Tensile Strength Ratio of SMA and HMA mixtures containing F-RCA

Figure 4.25 summarizes the TSR values of the SMA and HMA specimens containing F-RCA. The tests on the SMA specimens containing 0% RCA (control mix) showed that the TSR values increased from 84% to 91% when HL was used instead of MF in the asphalt mixtures. In other words, hydrated lime powder considerably improved the moisture damage resistance of the control SMA mixtures.

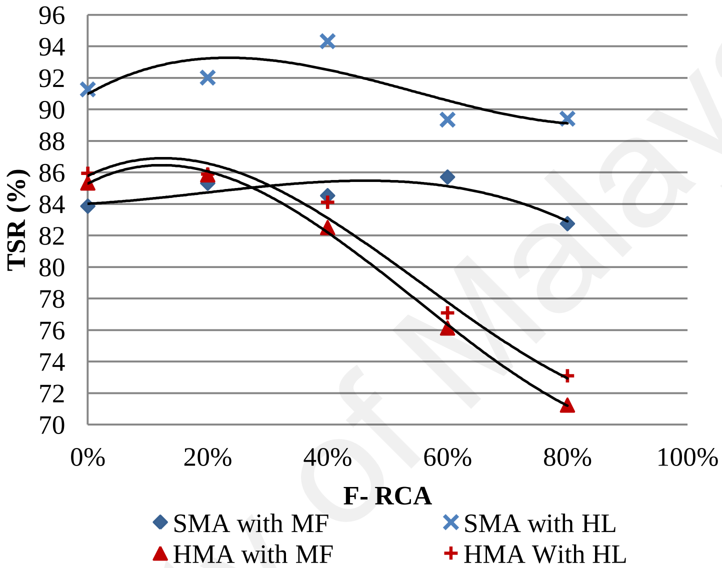

Figure 4.25: Tensile Strength Ratio of SMA and HMA Specimens containing F-RCA

Turning now to the SMA specimens containing F-RCA and MF, as the F-RCA content of these increased from 0% (control mix) to 60%. The TSR value also increased slightly, from 84% to 86%, with 60% F-RCA plus MF being the optimum mixture in terms of moisture resistance. The optimal mixture for the SMA specimens containing F-RCA and HL, on the other hand, was at 40% F-RCA content; and the TSR values of these increased from 91% in the control mix to 94% at 40% F-RCA.

In the HMA specimens containing F-RCA, the highest resistance to moisture susceptibility was achieved by mixtures containing 20% F-RCA, for both MF and HL fillers. As the F-RCA content increased from 0% to 20%, the TSR increased from 85%

to 86%, but as the F-RCA content increased from 20% to 80%, the TSR fell from 86% to 71% in the HMA specimens containing MF and 73% in the HMA specimens containing HL.

These results show that using HL instead of MF significantly improved the TSR values of both the SMA and HMA mixtures, although this improvement was more robust in the SMA than in the HMA mixtures. The levels of fine and filler aggregates were 64% and 6% (of the total aggregate content) in the HMA and 14% and 10% in the SMA mixtures. The above results for these specimens in terms of moisture susceptibility could be due to the aggregate gradations as well as improvements in IDT strength through utilizing hydrated lime powder as filler.

4.8.7.2 Tensile Strength Ratio of SMA and HMA mixtures containing C-RCA

The TSR values of the HMA and SMA specimens containing C-RCA are presented in Figure 4.26. First of all, in both the SMA and HMA mixtures containing 100% virgin granite aggregate (control mixes), the TSR values slightly increased when HL was used instead of MF.

Second, the moisture induced damage test results on the SMA mixtures containing C-RCA and MF produced little or no difference between the TSR values of VA-SMA and of SMA containing 20% C-RCA. In other words, replacing the coarse granite aggregates with up to 20% C-RCA in the SMA mixtures had no significant impact on the moisture susceptibility of the asphalt mixtures. However, as the C-RCA content increased from 20% to 40%, the TSR value fell to 81%, only slightly above the minimum AASHTO requirement. This suggests that the maximum acceptable C-RCA content in the SMA mixtures in terms of moisture resistance is 40%.

Finally, with the SMA specimens containing C-RCA and HL, as the more and more of the mineral filler content was replaced with HL, the moisture resistance of the mixtures increased. However, even although utilizing HL instead of MF was effective and increased the TSR values of the SMA mixtures containing C-RCA, C-RCA content should be limited to 40% to prevent moisture damage to the pavement.

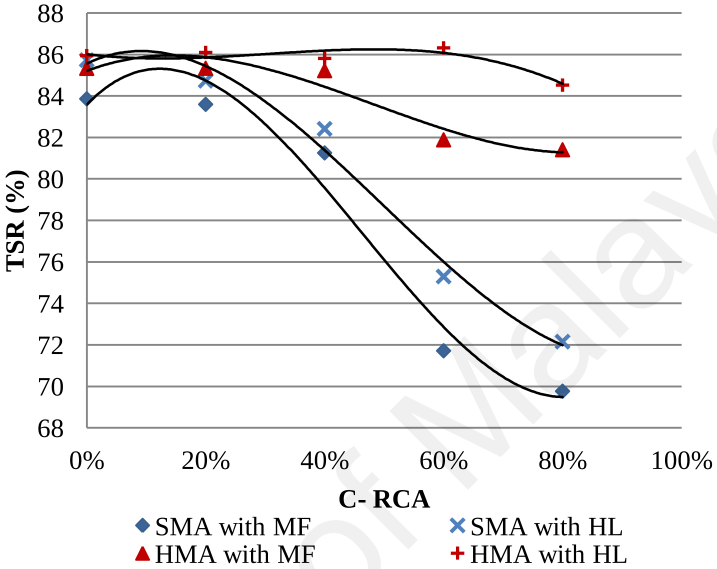

Figure 4.26: Tensile Strength Ratio of SMA and HMA Specimens containing C-RCA

From Figure 4.26 above, it is clear that the test HMA mixtures containing C-RCA produced better results than the SMA mixtures. As the C-RCA content increased from 0% in the control specimens to 40%, the TSR values remained the same, at 85% and 86% in the HMA mixtures containing MF and HL respectively. While using HL as filler resulted in slightly better TSR values for these specimens, even the HMA mixture containing 80% C-RCA and MF produced an acceptable value of 81% for moisture susceptibility. It is believed that, even though replacing 80% of the total amounts of the coarse granite aggregates with the C-RCA in the HMA mixture could affect the moisture performance of the HMA, but the obtained TSR values indicated that the TSR reduction trend was acceptable and all the measured values were within the standard requirement.

4.8.7.3 Tensile Strength Ratio of SMA and HMA mixtures containing M-RCA

The TSR values of the HMA and SMA mixtures containing different percentages of M-RCA are displayed in Figure 4.27. These show first of all that, regardless of the M-RCA content, using HL instead of MF significantly enhanced the moisture resistance of the asphalt mixtures. In the SMA mixtures containing M-RCA, the optimum value in terms of tensile strength ratio was 86% for both the control mix and the mixture containing 20% M-RCA and HL; and the TSR values of the SMA specimens containing MF also increased up to 20% M-RCA content. However, as the M-RCA content increased from 20% to 40%, the TSR values fell from 85% to 82% in the SMA mixtures containing MF and from 86% to 84% in the mixtures containing HL filler. Moreover, as the M-RCA content increased further from 40% to 60% and beyond, the TSR values fell even more. In sum, the M-RCA content should not exceed 40% in the SMA mixtures to optimize resistance to the moisture damage.

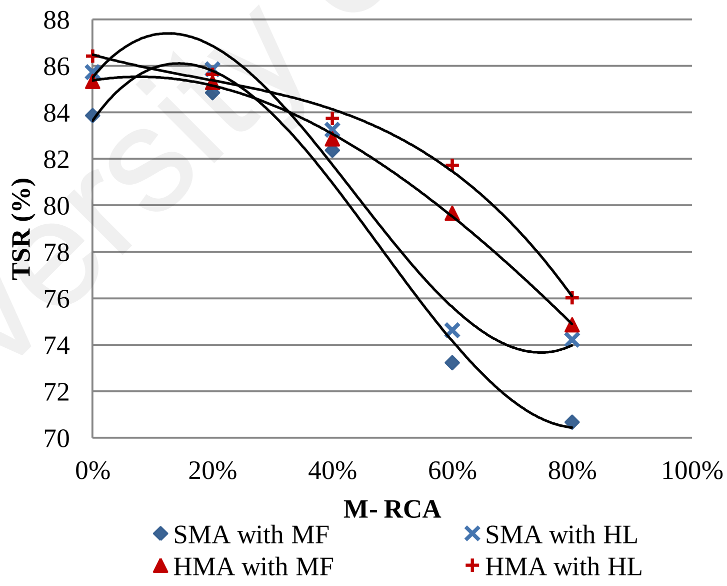

Figure 4.27: Tensile Strength Ratio of SMA and HMA Specimens containing M-RCA

As Figure 4.27 above shows, there were no significant differences in TSR values between the HMA control mixes and the mixtures containing 20% M-RCA, for both MF and HL fillers. Based on the AASHTO standard, flexible pavements should have a minimum TSR value of 80%. Replacing up to 60% of the fine and coarse granite aggregates with M-RCA in the HMA mixtures comfortably met this moisture susceptibility. The HMA mixtures containing 60% M-RCA had a TSR value of 80% in the mixtures using MF as filler and 82% in the mixtures using HL: thus it would be better to use HL than MF in such mixtures. Regardless of the RCA particle sizes or content levels, the HMA and SMA mixtures containing HL performed better than the mixtures containing MF in terms of moisture susceptibility, with lower losses in IDT strength after conditioning.

4.8.8 Flexural beam fatigue

The flexural beam fatigue test was carried out in accordance with the AASHTO TP-8 standard, which is the standard method for determining the fatigue life of compacted hot mix asphalt subjected to repeated flexural bending. Both types of asphalt specimens were tested at 20°C, 500 micro-strains and a frequency of 10Hz. Each test was repeated three times to verify its accuracy. Under the AASHTO standard, the fatigue specimens need to be cut and surface trimmed before being used in the test. For this purpose the HMA and SMA compacted slabs were cut into the specific dimensions of 380mm × 63.5mm × 50mm.

4.8.8.1 HMA flexural beam fatigue

Figure 4.28 below summarizes the flexural fatigue test results of the HMA specimens containing various percentages of RCA. Note that the figure shows only the average stiffness values of each set of specimens plotted against their RCA content levels. Fuller details and data on the results of these tests on the HMA specimens can be found in Appendix D. As the graphs show, regardless of the RCA particle size, increasing the RCA content improved the fatigue performances of the HMA mixtures.

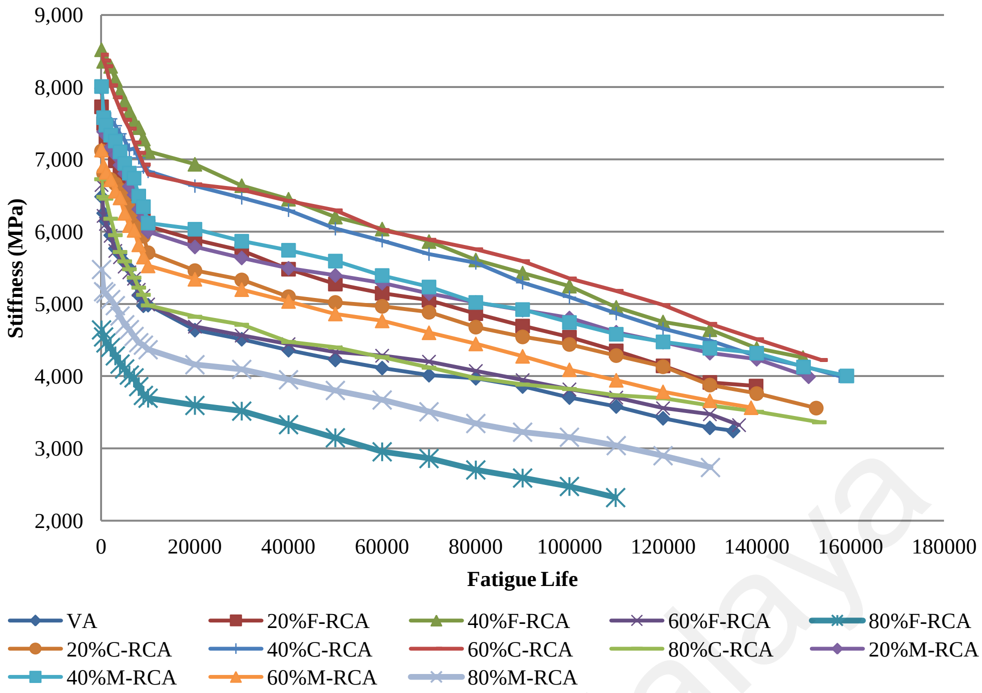

Figure 4.28: Average of flexural stiffness of HMA specimens containing RCA versus fatigue life

Generally, fatigue failure is defined as the number of load cycles a material can bear before falling to below 50% of its initial stiffness. While the fatigue life of a given mix does not in practice exactly correspond to the level of stiffness of the mix, measuring the number of load cycles needed to produce failure (a fall in stiffness of over 50%), does provide a reasonably correlation with actual fatigue life.

Based on our results, adding RCA generally enhanced the maximum tensile stresses of the HMA beam specimens, except for at the levels of 80% F-RCA and 80% M-RCA. As the strain values were constant in this test, a similar trend was observed in the stiffness values of the HMA beams. As mentioned earlier, RCA materials are much more absorptive than granite aggregates. Moreover, as RCA particle sizes get smaller, their level of absorption increases. As a result, higher binder content is needed to produce acceptable asphalt mixtures.

In the case of our tests, the improvement in fatigue performance of the HMA specimens could be related to the higher binder content in those containing RCA, which led to better flexibility and elasticity (phase angle) and hence better fatigue resistance. The phase angle represents the visco-elastic behavior of asphalt mixtures. Its value can be between 0° and 90°. Lower phase angle values indicate higher elasticity in asphalt mixtures, while higher values represent higher viscosity. To put it another way, 0° signifies highly elastic materials and 90° highly viscous materials. The elasticity of bituminous materials has a positive effect on the fatigue performance of asphalt mixtures. Against that, viscous asphalt mixtures are more resistant to rutting damage under wheel loads.

In our tests, as the number of pulses increased in the fatigue tests, the phase angle values slightly increased and reached their highest levels at the terminal stiffness or failure point (50% of initial stiffness). On the other hand, in most cases lower phase angle values produced higher fatigue life. Even although the initial stiffness of the HMA beam specimens containing 40% F-RCA was higher than that of those containing 60% C-RCA, 60% C-RCA emerged as the optimal value in terms of stiffness because it had a lower slope of stiffness curve as well as a slightly higher terminal stiffness value. As shown in the figure 4.28, the average stiffness value of the HMA containing 60% C-RCA dropped rapidly from the beginning of the test to 10000 cycles, but continued to resist fatigue beyond 10000 cycles, resulting in a flatter stiffness curve slope and higher terminal stiffness value. The average values of stiffness and fatigue life of the HMA control specimen (VA) increased by 30% and 14% respectively by utilizing 60% C-RCA. Generally, regardless of the RCA particle sizes, the fatigue performance of the HMA mixtures improved when the RCA content was increased, in terms of both stiffness values and number of cycles needed to reach terminal stiffness (failure). Only at the 80% M-RCA and 80% F-RCA levels did the HMA samples exhibit lower fatigue life than the control mix.

While, as just explained, using RCA improved the fatigue life of the HMA mixtures, RCA levels (of both particle sizes) of up to 40% produced only small differences in terminal stiffness, and there were no substantial differences in this respect between the HMA mixtures containing 40% C-RCA, 40% F-RCA and 40% M-RCA. This could be because, as the RCA content increased in the HMA mixtures, so the OAC levels increased as well.

The higher binder content increased the elasticity behavior of the asphalt mixtures and resulted in better fatigue resistance. At the same time, as the F-RCA content increased in the HMA specimens, the stiffness and fatigue life increased up to 40% content and then dropped considerably at the 60% and 80% levels. This could be due to the higher percentages of fines compared to coarse aggregates. According to the aggregate gradation of the HMA mixtures, 70% (by weight of total mix) of the HMA structure was made of aggregates with particle sizes of 2.36 mm or less. Given these different specifications and physical properties of RCA compared to virgin granite aggregates, as the fine granite aggregates were replaced by F-RCA, this had a more noticeable affect on the performance of the HMA specimens in this test.

4.8.8.2 SMA flexural beam fatigue

Fuller data on the flexural beam fatigue test on the SMA specimens containing various sizes and percentages of RCA are provided in Appendix E. Figure 4.29 below presents the average stiffness values of these SMA specimens against their fatigue life.

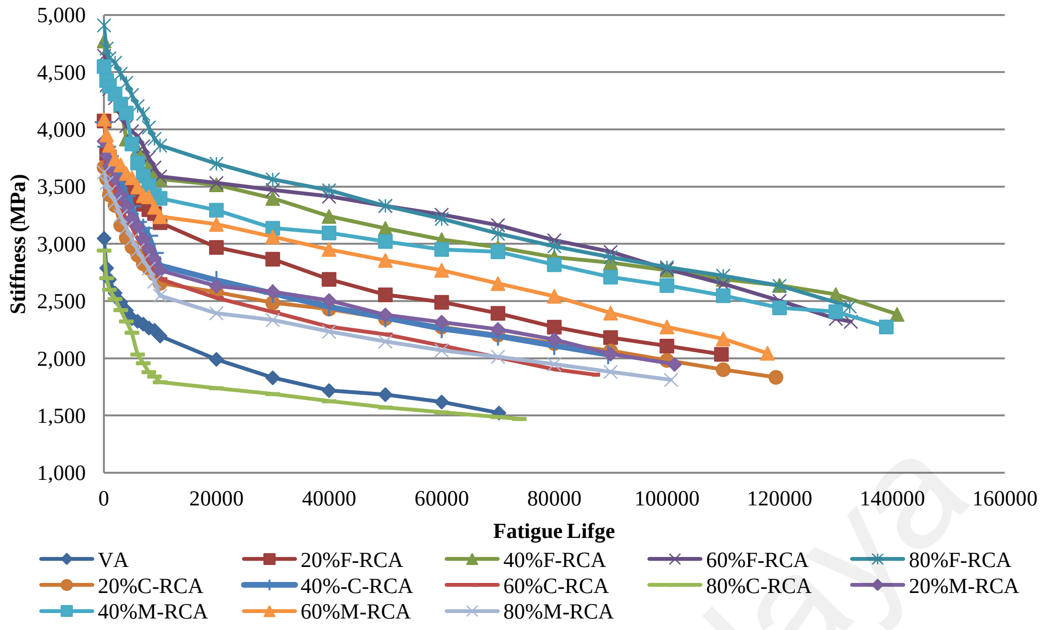

Figure 4.29: Average of flexural stiffness of SMA specimens containing RCA versus fatigue life

As can be seen, the SMA specimens showed generally lower fatigue resistance than the HMA mixtures. Indeed, the HMA specimens displayed almost twice the initial and even terminal stiffness of the SMA specimens. The likely reason for this is the denser aggregate gradation of the HMA mixtures, leading to higher density and stability values and hence better fatigue performance.

Notwithstanding these overall weaker results, and regardless of RCA particle size, adding RCA content did improve the fatigue performance of the SMA specimens as well. Again, this is probably due to the fact that, as the granite aggregates were replaced by RCA, higher binder content was needed, which in turn increased the elasticity of the asphalt mixtures and led to better fatigue performance. Almost all the specimens improved in terms of both initial and terminal stress, stiffness and modulus values, when compared to the control specimen, and these improvements could be directly related to their levels of RCA content. Only the SMA mixtures containing 80% C-RCA produced slightly lower results than the control specimens in terms of resistance to fatigue over 10000 cycles.

Although the initial and terminal stiffness values of the SMA specimens containing 20% C-RCA and 40% C-RCA were close to each other and followed very similar patterns, the specimen containing 20% C-RCA resisted almost 34% longer than the one containing 40% C-RCA in terms of fatigue life. The stiffness value of the SMA specimens containing 60% C-RCA was meanwhile slightly lower than that of those containing 20% C-RCA and 40% C-RCA, but the difference was minor. The SMA specimens containing 60% C-RCA also followed the same patterns as those with 20% C-RCA and 40% C-RCA up to 20000 cycles, but the slope of their curves steepened significantly after 20000 cycles, indicating lower resistance to fatigue and lower fatigue life. As the C-RCA content increased to 80%, the stiffness values dropped significantly. The lower impact and crushing values of coarse RCA than coarse granite aggregates were presumably the reason for this, leading to aggregate fracture under compaction and degradation and segregation in these SMA mixtures.

As Figure 4.29 also shows, as the fine granite aggregates were replaced with F-RCA, the fatigue performance of the specimens improved. Adding 20%, 40%, 60% and 80% F-RCA increased the fatigue life of the SMA mixtures by 56%, 100%, 89% and 89% respectively. As can be seen there was no considerable change between SMA specimens containing 60% F-RCA and 80% F-RCA in terms of fatigue life. While the initial stiffness of the mixture containing 80% F-RCA was higher than that of 60% F-RCA, the stiffness value of the latter started to drop rapidly after 100000 cycles, ending up lower than the 80% F-RCA.

Turning now to the SMA specimens containing M-RCA, those containing 40% M-RCA performed better than the other levels of M-RCA, improving the fatigue life of the VA-SMA by up to 98%. Meanwhile, although the average initial and terminal stiffness of the SMA specimens containing 80% M-RCA were lower than those of the specimens containing 20% M-RCA, both performed similarly in terms of the number of cycles needed to reach 50% of initial stiffness (fatigue life); and both of improved the fatigue life of the SMA mixtures overall by around 44%. In other words, fatigue life improved as M-RCA content increased from 0% (VA-SMA) up to 40%; but it fell again when the level of M-RCA increased to 60%, and reach its lowest point at 80% of M-RCA. The most likely reason for this is that, as the M-RCA content increased in the SMA mixtures, the percentage of coarse granite aggregates being replaced by C-RCA increased as well. As mentioned earlier, stone mastic asphalt consists of 76% coarse aggregates (by weight of total mix) and so is very sensitive to the specifications and quality of the coarse aggregates in it. SMA specimens are highly affected by coarse aggregates due to their lower specific gravity and higher abrasion, impact value and crushing value than virgin granite aggregates.

4.9 Summary of performance tests

Asphalt pavements (road surfaces) are excellent paving materials if properly designed, produced and laid. The performance of asphalt mixtures is complex, and depends on getting the right combination of aggregates, binders and additives. Rutting, moisture susceptibility and fatigue are the main causes of distress in asphalt pavements. Rutting is a longitude load deformation that develops in an asphalt pavement under the action of channelized loading caused by traffic. It is one of the most important causes of failure in asphalt pavements – which can be due to a failure of the base, sub-base or sub-grade, poor materials, poor compaction, poor drainage or weak mix design. Mix design weakness can be due to very high or very low air voids, low viscosity of the binder, low density, low stability or high asphalt content, all resulting in higher flow or stripping problems. Stripping is the breaking of the adhesive bond between the aggregates and the binder due to the presence of moisture or water. Fatigue cracking generally occurs with loads which are too heavy for the pavement or an unexpectedly high level of passes by traffic or overweight trucks, and can be aggravated by inadequate pavement drainage or thickness due to poor quality control during construction. Cracks in asphalt pavements can lead to greater exposure to moisture or water, thermal effects or spalling, which in turn may cause more damage over time. The moisture susceptibility and fatigue resistance of asphalt mixtures are therefore further vital specifications for pavement design.

The basic characteristics and effects of using RCA materials on the properties of HMA and SMA mixtures have been fully described in earlier sections. This section of the research focuses only on the allowable RCA content in terms of rutting, fatigue and moisture susceptibility (the main pavement distresses). Table 4.27 below presents the maximum allowable RCA content levels for the HMA and SMA mixtures, based on the standard requirements.

Table 4.27: Maximum allowable RCA content for HMA and SMA mixtures

	Test	Standard	Allowable RCA Content		
			C-RCA	F-RCA	M-RCA
SMA	Rutting	BS 598-110	40%	80%	50%
	Moisture Susceptibility	AASHTO T 283	40%	80%	40%
	Fatigue	AASHTO TP-8	70%	80%	80%
HMA	Rutting	BS 598-110	60%	50%	70%
	Moisture Susceptibility	AASHTO T 283	80%	50%	70%
	Fatigue	AASHTO TP-8	80%	70%	60%

To summarize, in order to ensure that SMA mixtures are appropriately resistant to the key distresses of rutting, moisture susceptibility and fatigue cracking, the RCA content should not exceed 40%, 80% and 40% in SMA mixtures containing C-RCA, F-RCA and M-RCA respectively. For the HMA mixtures, the maximum recommended levels are 60% C-RCA, 50% F-RCA and 60% M-RCA.

4.10 Analysis of variance (ANOVA)

The main objective of this research was to evaluate the volumetric and mechanical properties of Dense-Graded Hot Mix Asphalt (HMA) and Gap-Graded Stone Mastic Asphalt (SMA) mixtures containing recycled concrete aggregates. For this purpose, the performance of the HMA and SMA mixtures containing various percentages of RCA were evaluated through a range of tests. In order to compare the differences between the methods for the research variables, the outcomes of the tests were statistically analyzed and their significance within certain confidence limits was determined using a single-way and two-way analysis of variances without replication (ANOVA).

Prior to data analysis, all the data were first subjected to a normality test. The results showed that all the variables were distributed normally; moreover, the homogeneity test confirmed that the variances were homogenous. The significance level (α) used in this research was 0.05. Tables 4.28 and 4.29 below summarize the variance analysis (ANOVA) results for the HMA and SMA mixtures respectively. Fuller details of the ANOVA outputs are provided in Appendix F and Appendix G respectively.

Table 4.28: ANOVA outcomes for HMA test results

Test	*SS*	*MS*	*F*	*P-value*	*F critical*
OAC	7.1093	1.7773	124.0000	< 0.05	3.8379
Stability	63.9612	15.9903	50.6364	< 0.05	3.8379
Flow	16.3086	4.0772	14.3786	< 0.05	3.8379
Density	0.0204	0.0051	11.7916	< 0.05	3.8379
VTM	0.0229	0.0057	5.9756	< 0.05	3.8379
VMA	5.3502	1.3376	12.7780	< 0.05	3.8379
VFA	10.5456	2.6364	10.5257	< 0.05	3.8379
M_R @ 25°C	1.63E+06	4.07E+05	56.7577	< 0.05	3.8379
M_R @ 40°C	4.98E+05	1.24E+05	15.2400	< 0.05	3.8379
Dry IDT	6.9100	1.7275	134.8548	< 0.05	3.8379
Wet IDT	10.4383	2.6096	52.7686	< 0.05	3.8379
HL Dry IDT	7.4170	1.8543	93.1321	< 0.05	3.8379
HL Wet IDT	10.8499	2.7125	57.0068	< 0.05	3.8379
TSR	0.0187	0.0047	8.4306	< 0.05	3.8379
HL TSR	0.0174	0.0043	9.0349	< 0.05	3.8379
Rut Depth	18.6368	4.6592	10.4786	< 0.05	3.8379
Rut Rate	0.7740	0.1935	22.1516	< 0.05	3.8379
Fatigue (Stiffness)	2.29E+08	1.91E+07	15.8951	< 0.05	1.7830

Table 4.29: ANOVA outcomes for SMA test results

Test	*SS*	*MS*	*F*	*P-value*	*F critical*
OAC	4.7627	1.1907	4.8665	< 0.05	3.8379
Stability	27.3967	6.8492	6.0139	< 0.05	3.8379
Flow	20.5763	5.1441	10.7292	< 0.05	3.8379
Density	0.0092	0.0023	6.8039	< 0.05	3.8379
VTM	0.0279	0.0070	15.5539	< 0.05	3.8379
VMA	3.6083	0.9021	14.1228	< 0.05	3.8379
VFA	7.1387	1.7847	14.2487	< 0.05	3.8379
M_R @ 25°C	6.24E+05	1.56E+05	5.6394	< 0.05	3.8379
M_R @ 40°C	1.20E+05	2.99E+04	7.5139	< 0.05	3.8379
Dry IDT	4.3102	1.0775	16.4854	< 0.05	3.8379
Wet IDT	6.6878	1.6720	9.9955	< 0.05	3.8379
HL Dry IDT	4.4433	1.1108	17.0746	< 0.05	3.8379
HL Wet IDT	6.4186	1.6046	9.8412	< 0.05	3.8379
TSR	0.0250	0.0062	4.5030	< 0.05	3.8379
HL TSR	0.0190	0.0048	3.9276	< 0.05	3.8379
Rut Depth	22.2777	5.5694	15.3416	< 0.05	3.8379
Rut Rate	4.0726	1.0182	12.4756	< 0.05	3.8379
Fatigue (Stiffness)	6.23E+07	5.19E+06	13.7935	< 0.05	1.7878

As the tables show, the measured *P-values* for both types of asphalt mixtures were below the significance level of 0.05 (alpha) in terms of volumetric, mechanical and experimental test results. Moreover, the F ratio values were larger than $F_{Critical}$, again for both types of mixture. This confirms that the impact of the RCA materials on the performance of the HMA and SMA mixtures was significant, at a confidence level of 95%, and that the effects of the various different sizes and percentages of RCA in the HMA and SMA mixtures were significantly different.

CHAPTER V

5 CONCLUSIONS AND RECOMMENDATIONS

5.1 Conclusions

This study presents the results of experiments designed to ascertain the influence of adding various sizes and percentages of Recycled Concrete Aggregate (RCA) on the performance of Hot Mix Asphalt (HMA) and Stone Mastic Asphalt (SMA). To that end, it looked into three main objectives. The first objective was to evaluate the engineering properties of the materials used, namely granite aggregate, RCA and 80-100 binder. The second objective was to determine the optimum asphalt content of HMA and SMA mixtures containing RCA, based on the Marshall mix design method. The third objective was the most important: to evaluate the performance of the fabricated HMA and SMA specimens. Finally, the test results were analyzed and verified using the analysis of variance (ANOVA) method. This section summarizes the overall conclusions achieved through this research. The key findings are below.

1- The Marshall specimens had a higher air void content than the expected level (4%), and that this level increased in both the HMA and SMA mixtures, regardless of the size of the RCA particles, as the RCA content increased. This was probably because of the aggregates and RCA breaking down during compaction by the Marshall hammer. The reduction of the number of Marshall compactor blows from 75 to 50 in the SMA mixtures could be another reason for the higher air void levels in these. The excess cements attached to the surface of the RCA could increase the bitumen absorption in the asphalt mixtures and thus reduce adhesion between the RCA and the binder.

2- During the tests we found that submerging and washing the RCA materials before using them in the asphalt mixture considerably increased the performance of the HMA and SMA mixtures. We therefore ensured that the recycled concrete aggregates were soaked, washed and dried well before being used.

3- RCA has a porous structure, with a lower specific gravity than virgin aggregates. Since the levels of coarse aggregates are considerably higher in SMA mixtures, any replacement of VA coarse aggregates with C-RCA could significantly affect the performance of the mixture due to lower density and C-RCA fracture under pressure. Conversely, since HMA has a higher level of fines than coarse aggregates, any replacement of VA fines with F-RCA can place higher demands on the asphalt content and thereby reduce the density values of the mixtures, affecting their performance.

4- Turning to the question of optimum asphalt content (OAC), RCAs are much more absorptive materials than granite aggregates. As a result, and regardless of the RCA particle size, as the RCA content increased in the asphalt mixtures, the OAC went up as well. On the other hand, we found that utilizing hydrated lime powder instead of mineral fillers in both the HMA and SMA mixtures had no significant effect on the OAC values.

5- Regardless of the RCA particle size, the increase rate in rut depth and rut rate values in the asphalt mixtures containing 20% and 40% RCA was considerably lower than 60% and 80% respectively; moreover, as the level of RCA increased towards 60% and 80%, the level of rut resistance reduction became more significant.

6- Adding RCA to the HMA and SMA mixtures produced notably different results in the IDT strength and moisture susceptibility tests – probably due to the aggregate gradations of the mixtures. Coarse and fine aggregates accounted for 76% and 14% respectively of the SMA mixtures, but 30% and 64% of the HMA mixtures. The SMA mixtures were therefore much more dependent on the specifications of the coarse aggregates (i.e. LA abrasion, aggregate impact value and aggregate crushing value) than a conventional asphalt mixture. Any replacement of virgin aggregates with RCA would therefore have a particularly significant effect on the engineering properties of the SMA. In line with this, replacing the coarse-VA with C-RCA in the SMA and fine-VA with F-RCA in the HMA mixtures each had the most impact on the performance of the relevant asphalt specimens.

7- C-RCA and M-RCA had no positive effect on the IDT strength of the SMA mixtures, but replacing up to 20% VA with RCA did improve the IDT strength of the HMA specimens. Moreover, using up to 40% F-RCA increased the IDT strength of the SMA mixtures by increasing their bulk density. Meanwhile, utilizing up to 60% F-RCA increased the tensile strength and hence the moisture resistance of the SMA mixtures. Last but not least, while 80% F-RCA content led to reduced TSR values in the SMA specimens, those containing up to 40% C-RCA, 40% M-RCA and 80% F-RCA were still able to meet the minimum AASHTO requirements.

8- Utilizing 20% F-RCA in the HMA mixture containing Mineral Filler (MF) improved the TSR value of the mixture. Moreover, the HMA specimens containing up to 40% C-RCA did not show any changes in terms of moisture induced damage. This suggests that HMA mixtures with up to 80% C-RCA, 60% M-RCA and 40% F-RCA can easily meet the standard requirements in terms of moisture susceptibility. Using hydrated limestone (HL) powder as filler had no substantial effect on the IDT strength of the dry specimens, but did significantly improve the IDT strength of the conditioned HMA and SMA mixtures, both of which produced higher TSR values and moisture resistance.

9- The flexural beam fatigue test results showed substantial improvements in both types of asphalt mixtures. Generally, the initial stiffness of the asphaltic samples increased as the RCA content increased in the HMA and SMA mixtures. Since the strain values remained almost constant (strain controlled test), similar trend were observed from the relevant tensile stress values as well. We found that, due to the denser structure of the HMA mixtures and their higher stability values, their measured initial stiffness was almost twice as high as that of the SMA specimens. At the same time, almost all of the HMA and SMA specimens showed higher fatigue resistance than the asphalt mixtures containing virgin granite aggregates (control mix) except for 80% M-RCA and 80% F-RCA in HMA, and 80% C-RCA in SMA mixtures, which produced slightly lower results than the SMA control mix.

10- While our experiments showed that adding RCA to asphalt mixtures does affect their volumetric and mechanical properties, SMA mixtures with up to 40% coarse, 80% fine and 40% mixed RCA content, and HMA mixtures with up to 60% coarse, 50% fine and 60% mixed RCA content, can nevertheless comfortably satisfy the standard requirements, depending of course on the demands of the particular project and on traffic volume. These findings could help to promote the re-use and recycling of waste materials, especially RCA, in road construction, thereby helping to conserve natural resources for future generations as well as generating economic and environmental benefits.

5.2 Recommendations

Finally, based on the experience gained from this research, we have a number of recommendations for future research and future researchers.

1- We advise against the use of the Marshall impact compactor for asphalt mixtures containing RCA, particularly for SMA mixtures containing large amounts of coarse aggregates. This is because such impact compactors can cause the RCA and the coarse aggregates on the surface to break, such that the desired density and air voids may not be achieved. The Super-pave gyratory compactor may be better able to compact asphalt mixtures containing RCA with less breakage and segregation.
2- It is recommended to submerge and wash the RCA materials before using them in the asphalt mixtures to reduce the excessive attached cements on the surface of the crushed aggregates and improve the adhesion between RCA and other materials in asphalt mixtures.
3- The measured load to failure in the IDT tests was lower than we had expected for both the HMA and SMA mixtures – largely, we suspect, because we used unmodified 80/100 (penetration graded) binder to produce the HMA and SMA specimens. High viscosity or modified binders should improve the performance of asphalt mixtures containing RCA in this respect, and we therefore recommend the use of such binders instead of conventional ones.
4- Future studies might try to use recycled concrete aggregates in Open-Graded Friction Course (OGFC) and porous asphalts in order to evaluate the performance of these types of mixtures, in addition to the ones we tested.

References

AAPA (2000). Stone Mastic Asphalt: Design and Application Guide, Australian Asphalt Pavement Association, Bitumen Contractors Association, Implementation Guide No 4, Australia.

AASHTO T-283 (1986). Resistance of compacted bituminous mixture to moisture induced damage. American Association of State Highway and Transportation Officials, AASHTO Provisional Standards, USA.

AASHTO TP8 (2002). A Test Standard for Determining the Fatigue Life of Compacted Hot-Mix Asphalt Subjected to Repeated Flexural Bending. American Association of State Highway and Transportation Officials, AASHTO Provisional Standards, USA.

Abo-Qudais, S., & Al-Shweily, H. (2007). Effect of Aggregate Properties on Asphalt Mixtures Stripping and Creep Behavior. Journal of Construction and Building Materials, 21 (9):1886-1898.

Aggregates advisory service-UK. (1999). Construction and demolition waste management practices and their economic impacts. Study for DGXI- European commission. Digest No. 016.

Ahmadinia, E., Zargar, M., Karim, M. R., & Abdelaziz, M. (2012). Performance evaluation of utilization of waste polyethylene terephthalate (PET) in stone mastic asphalt. Journal of Construction and Building Materials, 36:984-989.

Aksoy, K., Samlioglu, K., Tayfur, S., & Ozen, H. (2005). Effects of various additives on the moisture damage sensitivity of asphalt mixtures. Journal of Construction and Building Materials, 19 (1): 11- 18.

Anderson, R. M., Christensen, D. W., & Bonaquist, R. (2003). Estimating the rutting potential of asphalt mixtures using superpave gyratory compaction properties and indirect tensile strength. Journal of the Association of Asphalt Paving Technologists, 72: 1-26.

Anjam Kumar, A., & Veeraragavan, A. (2011). Dynamic mechanical characterization of asphalt concrete mixes with modified asphalt binders. Journal of Materials Science and Engineering A, 528(21): 6445-6454.

Arabani, M., & Azarnoosh, A. R. (2012). The effect of recycled concrete aggregate and steel slag on the dynamic properties of asphalt mixtures. Journal of Construction and Building Materials, 35 (1): 1-7.

Arabani, M., Moghadas Nejad, F., & Azarnoosh, A. R. (2013). Laboratory evaluation of recycled waste concrete into asphalt mixtures. International Journal of Pavement Engineering, 14(6): 531-539.

Arm, M. C. (2001). Self-cementing properties of crushed demolished concrete in unbound layers: results from triaxial tests and field tests. Journal of Waste Management, 21(3): 235-239.

Arulrajah, A., Piratheepan, J., Bo, M. W., & Ali, M. (2012b). Geotechnical properties of recycled concrete aggregate in pavement sub-base applications. ASTM Geotechnical Testing Journal, 35(5):1-9.

Arulrajah, A., Piratheepan, J., Bo, M. W., & Sivakugan, N. (2012a). Geotechnical characteristics of recycled crushed brick blends for pavement sub-base applications. Canadian Geotechnical Journal, 49(7):796-811.

Asphalt Institute, (1969). Surface treatment and asphalt penetration macadam, manual series (MS-13). Asphalt Institute (AI), College Park, Maryland, USA.

Asphalt Institute, (2007). The asphalt handbook, manual series No. 4 (MS-4) 7th Edition, Asphalt Institute (AI), College Park, Maryland, USA.

Asphalt Institute, (1997). Mix Design Methods for Asphalt concrete Manual Series (MS02), Asphalt Institute (AI), College Park, Maryland, USA.

ASTM C127, (2007). Standard Test Method for Specific Gravity and Absorption of Coarse Aggregate. Philadelphia, PA, American Society for Testing and Materials.

ASTM C128, (2007). Standard Test Method for Density, Relative Density (Specific Gravity), and Absorption of Fine Aggregate. Philadelphia, PA, American Society for Testing and Materials.

ASTM C131, (2006). Standard Test Method for Resistance to Degradation of Small-Size Coarse Aggregate by Abrasion and Impact in the Los Angeles Machine. Philadelphia, PA, American Society for Testing and Materials.

ASTM D1559, (1989). Test Method for Resistance of Plastic Flow of Bituminous Mixtures Using Marshall Apparatus. American Society for Testing and Material, West Conshohocken, PA, USA.

ASTM D2041, (2003). Standard Test Method for Theoretical Maximum Specific Gravity and Density of Bituminous Paving Mixtures, American Society for Testing and Material, West Conshohocken, PA, USA.

ASTM D2726, (2000). Standard Test Method for Bulk Specific Gravity and Density of Non-Absorptive Compacted Bituminous Mixtures, American Society for Testing and Material, West Conshohocken, PA, USA.

ASTM D3203, (2005). Standard Test Method for Percent Air Voids in Compacted Dense and Open Bituminous Paving Mixtures, American Society for Testing and Material, West Conshohocken, PA, USA.

ASTM D3381, (2009). Standard Specification for Viscosity-Graded Asphalt Cement for Use in Pavement Construction, Volume 04.03, American Society for Testing and Material, West Conshohocken, PA, USA.

ASTM D3515, (2001). Standard Specification for Hot-Mixed, Hot-Laid Bituminous Paving Mixtures, American Society for Testing and Material, West Conshohocken, PA, USA.

ASTM D36, (1986). Test Method for Softening Point of Bituminous Material, Volume 04.03, Annual Book of ASTM Standards, American Society for Testing and Material, Philadelphia, USA.

ASTM D4123, (1995). Standard Test Method for Indirect Tension Test for Resilient Modulus of Bituminous Mixtures (Withdrawn 2003), ASTM International, West Conshohocken, PA, USA.

ASTM D4402, (1987). Test Method for Viscosity Determinations of Unfilled Asphalts Using the Brookfield Thermo sell Apparatus, Volume 04.03, Annual Book of ASTM Standards, American Society for Testing and Material, Philadelphia, USA.

ASTM D5, (1986). Test Method for penetration of Bituminous Material, Volume 04.03, Annual Book of ASTM Standards, American Society for Testing and Material (ASTM), Philadelphia, USA.

ASTM D6931, (2007). Standard Test Method for Indirect Tensile (IDT) Strength of Bituminous Mixtures, American Society for Testing and Material, West Conshohocken, PA, USA.

ASTM D92, (1986). Test Method for Flash and Fire Point of Bituminous Material, Volume 04.03, Annual Book of ASTM Standards, American Society for Testing and Material, Philadelphia, USA.

ASTM D946, (1999). Standard Specification for Penetration-Graded Asphalt Cement for Use in Pavement Construction, Volume 04.03, Annual Book of ASTM Standards, American Society for Testing and Material, Philadelphia, USA.

Baladi, G.Y., & Harichandran, R. S. (1989). Asphalt mix design and indirect test: a new horizon, ASTM Special Technical Publication, No 1041, USA.

Bardesi, A. (2010). Introducción a las mezclas bituminosas. Curso de Mezclas Bituminosas: dosificación, fabricación, puesta en obra y control de calidad, Intevia, Barcelona, Spain.

Beale, M. J., and You Z. (2010). The mechanical properties of asphalt mixtures with recycled concrete aggregates. Journal of Construction and Building Materials, 24 (3): 230-235.

Bhusal, S., Li, X., & Wen, H. (2011). Evaluation of effects of recycled concrete aggregate on volumetrics of hot-mix asphalt. Transportation Research Record: Journal of the Transportation Research Board, (2205), 36-39.

British Standards Institution, (1998). Methods of test for the determination of wheel-tracking rate and depth. BS 598-110, UK.

Brown, E. R. (1990). Density of asphalt concrete-how much is needed? NCAT Research Report 90-3, Annual Meeting of the Transportation Research Board, Washington, DC, USA.

Brown, E. R., & Buchanan, M. S. (1999) NCHRP Research Results Digest 237: Superpave Gyratory Compaction Guidelines, Transportation Research Board, TRB, National Research Council, Washington, D.C, USA.

Brown, E.R., & L.A. Cooley. (1999). Designing stone matrix asphalt mixtures for rut resistant pavement. NCHRP Report 425, Transportation Research Board, Washington, D.C. USA.

Brown, E.R., & Mallick, R.B. (1994), Stone Matrix Asphalt properties Related to Mixture Design, NCAT Research Report No. 94-02). Alabama: NCAT Auburn University, USA.

Brown, E.R., Hanson, D. I., & Mallick, R. B. (1996). Evaluation of superpave gyratory compaction of HMA. Transportation Research Record 1543, Transportation Research Board, Washington, D.C. USA.

Brown, E.R., Kandhal, P.S., & Zhang, J. (2001), Performance testing for hot mix asphalt, NCAT Research Report No.01-05, Alabama: NCAT Auburn University, USA.

Buchanan, M. S., & Brown, E. R. (2001), Effect of superpave gyratorycompactor type on compacted hot mix asphalt density. Transportation Research Board, National Research Council, Washington DC, USA.

Bukowski, J. R. (1993). The Future of SMA in America. Asphalt Institute, Lexington, Ky. USA.

Caro, S., Masad, E., Bhasin, A., & Little, D. N. (2008). Moisture susceptibility of asphalt mixtures, Part 1: mechanisms. International Journal of Pavement Engineering, 9 (2): 81-88.

Carswell, J., Cornelius, P & Planque, L. (1997). The effects of mixture variables on the fatigue performance of bituminous materials. AAPA International Flexible Pavements Conference, 10th, Perth, Western Australia. Paper 13.

Chowdury A., Button J.W., Kohale V., & Jahn, D. W. (2001), Evaluation of superpave fine aggregate angularity specification, Report No. 404011-1, International Center for Aggregate Research, Austin, TX, USA.

Christensen, D. W., & Bonaquist, R. (2002). Use of strength tests for evaluating the rut resistance of asphalt concrete. Journal of the Association of Asphalt Paving Technologists, 71: 692- 711.

Christensen, D. W., Bonaquist, R., Anderson, D. A., & Gokhale, S. (2004). Indirect tensile strength as a simple performance test. Transportation Research Circular: New Simple Performance Tests for Asphalt Mixes. Transportation Research Board (TRB), E- C 068: 44-57.

Cooley, L. A., Brumfield, J. W., Hicks, G., Mallick, R. B., Mogawer, W. S., Partl, M., & Poulikakos, L. (2009). NCHRP Report 640: Construction and Maintenance Practices for Permeable Friction Courses, TRB, National Research Council, Washington, DC, USA.

CSIR. (2000). Reusing construction and demolition waste. Building and Construction Technology, Techno Brief.

Epps, J. A., Sebaaly, P. E., Penaranda, J., Maher, M. R., McCann, M. B. & Hand, A. J. (2000). Compatibility of a test for moisture-induced damage with superpave volumetric mix design, NCHRP Report No. 444, University of Nevada, USA.

Fabiana, D. A., Conceic, O. L., & Liedi, B. (2011). Laboratory evaluation of recycled construction and demolition waste for pavements. Journal of Construction and Building Materials, 25:2972-2979.

FHWA, (2003). Summary of California recycled concrete aggregate review. California department of transportation (Cal-trans). U.S. Department of Transportation. Federal Highway Administration.

FHWA, (2004). Transportation applications of recycled concrete aggregates: FHWA state of the practice national review. IF-05-013. U.S. Department of Transportation. Federal Highway Administration.

Focus. (2004). Recycled concrete study identifies current uses best practices. U.S. department of transportation, Federal Highway Administration. Publication No: FHWA- HRT- 04- 024. U.S. Department of Transportation. Federal Highway Administration.

Fontes, L. P. T. L., Triches, G., Pais, J. C., & Pereira, P. A. A. (2010). Evaluating permanent deformation in asphalt rubber mixtures. Journal of Construction and Building Materials, 24 (7): 1193-1200.

Gartner, W. (1987). Asphalt concrete mix design: Development of more rational approaches. ASTM Committee D-4 on Road and Paving Material, Bal Harbor (Florida), USA.

Ghuzlan, K. A., & Carpenter, S. H. (2000), Energy-derived, damage-based failure criterion for fatigue testing, Transportation Research Record. TRB, 1723, 141-149. National Research Council, Washington D.C, USA.

Gilpin, R., Robinson, J. R., Menzie, W. D., & Hyun, H. (2004). Recycling of construction debris as aggregate in the mid- Atlantic region, USA, Journal of Resources, Conservation and Recycling, 42(3): 275–294.

Golalipour, A., Jamshidi, E., Niazi, Y., Afsharikia, Z., & Khadem, M. (2012). Effect of aggregate gradation on rutting of asphalt pavements. Procedia-Social and Behavioral Sciences. 53(3): 440-449.

Gul, W. A., & Guler, M. (2014). Rutting susceptibility of asphalt concrete with recycled concrete aggregate using revised Marshall Procedure. Construction and Building Materials, 55, 341-349.

Harvey, J., & Tsai, B. (1997). Long-term oven aging effects on fatigue and initial stiffness of asphalt concrete, Transportation Research Record 1590.

Harvey, J., Lee, T., Sousa, J., Pak, J., & Monismith, C. L. (1994). Evaluation of fatigue and permanent deformation properties of several asphalt-aggregate fields mixes using strategic highway research program, Transportation Research Record 1454, 123.

Hassanieh, D. Z. A., Chehab, G. R., Srour, I., & Kassem, H. A. (2016). Recycling cementitious constituents of construction demolition waste in asphalt mixes: the case of Lebanon. International Journal of Sustainable Society, 8(2), 109-125.

Huang, W. L., Lin, D. H., Chang, N. B., & Lin, K. S. (2002). Recycling of construction and demolition waste via a mechanical sorting process. Journal of Resources Conservation and Recycling, 37(1): 23-37.

Huang, Y. H. (2004). Pavement Analysis and Design, Pearson Prentice Hall, Second Edition, New Jersey, USA.

Kandhal, P. S. (1998), Intersection rutting rectified, Roads and Bridges, Transportation Research Board. Des Plaines, IL. 33(5): 20-28.

Kandhal, P. S., & Cooley, L. A. (2002). Evaluation of Permanent Deformation of Asphalt Mixtures using Loaded Wheel Tester, National Center for Asphalt Technology. Report 02-08.

Kandhal, P. S., Mallick, R. B & Huner, M. (1999). Development of a new test method for measuring bulk specific gravity of fine aggregates. Research Report (NCAT Report No 99-07), Auburn University, USA.

Kenedy, T. W., & Anagnos, J. N. (1984). Wet-dry indirect tensile test for evaluating moisture susceptibility of asphalt mixtures. Research report 253-8, Center for Transportation Research, University Of Texas, Texas, USA.

Khaled, R. J., & Krizek, F. (1996). Fiber-reinforced recycled crushed concrete as a stabilized base course for highway pavements, Northwestern University, Evanston, IL.

Khan, Z. A., Wahab, H. I., Asi, I., & Ramadhan, R. (1998). Comparative study of asphalt concrete laboratory compaction methods to simulate field compaction, Journal of Construction and Building Materials, 12:373-384.

Khodaii, A., Kazemi Tehrani, H., & Haghshenas, H. F. (2012). Hydrated lime effect on moisture susceptibility of warm mix asphalt. Journal of Construction and Building Materials, 36(1):165-170.

Khosla, N. P., & Sadasivam, S. (2002). Evaluation of the effects of mixture properties and compaction methods on the predicted performance of superpave mixtures. Final Report FHWA/NC/2002-030, North Carolina State University, USA.

Kim, Y. R., Pinto, I., & Park, S. W. (2012). Experimental evaluation of anti-stripping additives in bituminous mixtures through multiple scale laboratory test results. Journal of Construction and Building Materials, 29(1): 386-393.

Kim, Y., Lim, J., Lee, M., Kown, S., Huang, S., & Wei, L. (2013). Comprehensive evaluation of polymer-modified SMA mixture produced with new polyethylene wax-based WMA additive with adhesion promoter. Characteristics of non-asphalt components of asphalt paving mixtures (AFK 30). Annual Meeting of the Transportation Research Board (TRB).

Kok, B. V., & Yilmaz, M. (2009). The effects of using lime and styrene–butadiene–styrene on moisture sensitivity resistance of hot mix asphalt. Journal of Construction and Building Materials, 23(1):1999-2006.

Kumar, A., & Goetz, W. H. (1997). The gyratory testing machines a design tool and an instrument for bituminous mixture evaluation, Asphalt Paving Technology, 43:350-371.

Lee, C. H., Du, J. C., & Shen, D. H. (2012). Evaluation of pre-coated recycled concrete aggregate for hot mix asphalt. Journal of Construction and Building Materials, 28(1):66-71.

Lu, X., & Redelius, P. (2007). Effect of bitumen wax on asphalt mixture performance. Journal of Construction and Building Materials, 21(11):1961-1970.

Marques, V. D. C., de Queiroz, B. O., de Lacerda, D. M., Gouveia, A. M. D. A., & de Melo, R. A. (2014). Mechanical Performance of Asphalt Mixtures with Natural Aggregates and Recycled Aggregates for Surface Course. In Key Engineering Materials (Vol. 600, pp. 657-666). Trans Tech Publications.

Masad, E., Muhunthan, B., Naga, S., & Thomas, H. (1999). Quantifying laboratory compaction effects on the internal structure of asphalt concrete, Transportation Research Record.168: 179-185.

Massad, E., Al-Rousan, T., Button, J. W., Little, D. N., & Tutumluer, E. (2005). Test methods for characterizing aggregate shape, texture and angularity. Technical Report NCHRP 4-30A, National Cooperative Highway Research Program, National Research Council.

Matthews, J. M., Monismith, C. L., & Craus, J. (1993). Investigation of laboratory fatigue testing procedures for asphalt aggregate mixtures. Journal of Transportation Engineering, 119(4):634-654.

McGrath, C. (2001). Waste minimization in practice. Journal of Resources Conservation and Recycling, 32 (3-4): 227-238.

Michael, S., Bruce, A. C., & Andrew, D. (2002), Investigation of recycled martial asphalt pavement (RAP) mixtures, Center for Transportation Studies, Report No. MN/RC-2002-15, Minnesota Department of Transportation, USA.

Miller. C., Vasconcelos, K., Little, D. N., & Bhasin, A. (2011). Investigating aspects of aggregate properties that influence asphalt mixtures performance. Research Report for DTFH61-06-C-00021, Texas A & M University at College Station and the University of Texas at Austin, Texas, USA.

Mo, L., Huurman, M., Wu, S., & Molenaar, A. A. A. (2009). Raveling investigation of porous asphalt concrete based on fatigue characteristics of bitumen-stone adhesion and mortar. Journal of Material and design, 30:170-179.

Moghadas Nejad, F., Azarhoosh, A. R., Hamedi, GH. H., & Azarhoosh, M. J. (2012). Influence of using nonmaterial to reduce the moisture susceptibility of hot mix asphalt. Journal of Construction and Building Materials, 31(1):384- 388.

Moghadas Nejad, F., Azarhoosh, A. R., & Hamedi, G. H. (2013). The effects of using recycled concrete on fatigue behavior of hot mix asphalt. Journal of Civil Engineering and Management, 19(sup1), S61-S68.

Mroueh, U., & Wahlstram, M. (2002). By-products and recycled materials in earth construction in Finland. An assessment of applicability. Journal of Resources Conservation and Recycling, 35(1-2):117-129.

NAPA (1982), Development of Marshall Procedures for Designing Asphalt Paving Mixtures, Information Series 84, National Asphalt Pavement Association (NAPA), Lanham, MD.

NCHRP (2001). Appropriate use of waste and recycled materials in the transportation industry-an information database. Project 4-21, Transportation Research Board, NRC, CRP-CD-5.

Paranavithana, S., & Mohajerani, A. (2006). Effects of recycled concrete aggregate on properties of asphalt concrete, Journal of Resource Conservation and Recycling, 48(1):1-12.

Pasandín, A. R., & Perez, I. (2013). Laboratory evaluation of hot-mix asphalt containing construction and demolition waste. Journal of Construction and Building Materials, 43 (1): 497-505.

Pasandín, A. R., & Pérez, I. (2014). Effect of ageing time on properties of hot-mix asphalt containing recycled concrete aggregates. Journal of Construction and Building Materials, 52: 284-293.

Pasandín, A. R., & Pérez, I. (2014). Mechanical properties of hot-mix asphalt made with recycled concrete aggregates coated with bitumen emulsion. Construction and Building Materials, 55, 350-358.

Pasandín, A. R., Pérez, I., Oliveira, J. R., Silva, H. M., & Pereira, P. A. (2015). Influence of ageing on the properties of bitumen from asphalt mixtures with recycled concrete aggregates. Journal of Cleaner Production, 101, 165-173.

Peattie, K. R. (1979). The analytical design of flexible pavements, Lecture Notes, Department of Civil Engineering Symposium, University of Glasgow.

Pedersen, (2011). NCHRP report 673. A manual for design of hot mix asphalt with commentary. National cooperative highway research program. Transportation Research Board (TRB). Washington, D.C, USA.

Perez, I., Pasandín, A. R., & Gallego, J. (2010a). Impact of construction and demolition waste aggregates on stripping in hot-mix asphalt. In: Presented at 89th annual meeting of the transportation research board, Washington, D. C, USA.

Perez, I., Pasandín, A. R., & Gallego, J. (2012b). Stripping in hot mix asphalt produced by aggregates from construction and demolition waste. Journal of Waste Management & Research, 30(1):3-11.

Perez, I., Pasandín, A. R., & Medina, L. (2012c). Hot mix asphalt using C&D waste as coarse aggregates. Journal of Materials & Design, 36(1):840-846.

Perez, P., Agrela, F., Herrador, R., & Ordonez, J. (2013). Application of cement-treated recycled materials in the construction of a section of road in Malaga, Spain. Journal of Construction and Building Materials, 44(1):593-599.

Petersen, J. C., Plancher, H., Ensley, E. K., Venable, R. L., & Miyake, G. (1982). Chemistry of asphalt-aggregate interaction: relationship with pavement moisture-damage prediction test. Transportation Research Record. Transportation Research Board (TRB), National Research Council, Washington, DC, 843:95-104.

Petit, C., Al-Qadi, I. l., & Millien, A. (2004). Cracking in pavements. Mitigation, risk assessment and prevention. Proceeding of the fifth international RILEM conference, Limoges, France.

Petrarca, R. W., & Galdiero, V. A. (1984). Summary of Testing of Recycled Crushed Concrete, Transportation Research Record. Transportation Research Board (TRB). National Research Council, Washington, DC, 989:19-26.

Pihl, K.A., & Milvang-Jensen, O. (2001). The motivation factors in the development and sustainment of a well-functioning recycling industry for road and non-road byproducts in Denmark. In proceedings of the specialty conference on beneficial use of recycled materials in transportation applications, Arlington, Virginia. 13-15th November 2001. University of New Hampshire, Durham, USA, 19-27.

Poon, C. S., & Chan, D. (2006). Feasible use of recycled concrete aggregates and crushed clay brick as unbound road sub-base, Journal of Construction and Building Materials, 20(8):578-585.

Poon, S. C., Shui, Z. H., Lam, L., Fok, H., & Kou, S. C. (2004). Influence of moisture states of natural and recycled aggregates on the slump and compressive strength of hardened concrete. Journal of Cement and Concrete, 34(1):31-36.

Roberts, F. L., Kandhal, P. S., Brown, E. R., Lee, D. Y., & Kennedy, T.W. (1996). Hot mix asphalt materials, mixture, design, and construction (2nd edition), Lanham, Maryland: NAPA Education Foundation.

Roussat, N., Me´hu, J., Abdelghafour, M., & Brula, P. (2008). Leaching behaviour of hazardous demolition waste. Journal of Waste Management, 28:2032-2040.

Saad, A. Q., & Mohammad, W. M. (2005). New chemical anti-stripping additives for bituminous mixtures. Journal of ASTM International, 2(8):1-11.

Sangsefidi, E., Ziari, H., & Mansourkhaki, A. (2014). The effect of aggregate gradation on creep and moisture susceptibility performance of warm mix asphalt. International Journal of Pavement Engineering, 15 (2): 133-142.

Satish, C., & Rajan, C. (2013). Performance Characteristics of bituminous concrete with industrial wastes as filler. Journal of Materials in Civil Engineering, ASCE, 139(5): 467-475.

Schutzbach, A. M. (1992). Case study of a full-depth asphalt concrete inlay. Flexible pavement construction, performance and recycling. Transportation Research Record. Transportation Research Board (TRB). National research council, Washington, D.C, USA, 1337:42-50.

Shen, D. H., & Du, J. C. (2004). Evaluation of building materials recycling on HMA permanent deformation. Journal of Construction and Building Materials, 18(1):391-397.

Snyder, M. B., & Bruinsma, J. E. (1996). Review of Studies Concerning Effects of Unbound Crushed Concrete Bases on PCC Pavement Drainage, Transportation Research Record. Transportation Research Board. National Research Council, Washington, DC, 1519:51-58.

Sousa, J. B., Pais, J. C., Prates, M., Barros, R., Langlois, P., & Leclerc, A. M. (1998). Effect of Aggregate Gradation on Fatigue Life of Asphalt Concrete Mixes. Transportation Research Record. Journal of the Transportation Research Board. Volume 1630. Pages 62-68.

Surya, M., Kanta Rao, V. V. L., & Lakshmy, P. (2013). Recycled aggregate concrete for Transportation Infrastructure. 2nd Conference of Transportation Research Group of India (2nd CTRG). Procedia - Social and Behavioral Sciences, 104:1158-1167.

Tapkin, S. (2008). Mechanical evaluation of asphalt-aggregate mixtures prepared with fly ash as a filler replacement. Canadian Journal of Civil Engineering, 35(1), 27-40.

Tapkın, S., & Keskin, M. (2013). Rutting Analysis of 100 mm Diameter Polypropylene Modified Asphalt Specimens Using Gyratory and Marshall Compactors. Journal of Materials Research, 16(2):546-564.

Tayfur, S., Ozen, H., & Aksoy, A. (2007). Investigation of rutting performance of asphalt mixtures containing polymer modifiers. Journal of Construction and Building Materials, 21(2):328-337.

Thomas, K. P., McKay, J. F., & Branthaver, J. F. (2006). Surfactants in Aged Asphalt and Impact μ on Moisture Susceptibility of Laboratory-prepared Mixes. Journal of Road Materials and Pavement Design, 7(4):477-490.

Tia. M., (2005). Fundamentals and practice of asphalt mixture design procedures to assure adequate performance, 13th Conference on Pavement Engineering, Hsin Chu, Taiwan.

Topal, A., & Sengoz, B. (2005). Determination of fine aggregate angularity in relation with the resistance to rutting of hot-mix asphalt, Journal of Construction and Building Materials, 19(2):155-163.

Topal, A., & Sengoz, B. (2008). Evaluations of compacted aggregate resistant test compared with the fine aggregate angularity standards, Journal of Construction and Building Materials, 22(5):993-998.

Topal, A., Ozturk, A.U., and Baradan, B. (2006). Use of recycled concrete aggregates in hot-mix asphalt. In Proceeding of Eight CANMET/ACI International Conference on Recent Advances in Concrete Technology, SP- 235-20. American Concrete Institute. 31st May- 3rd June 2006. Montreal, Quebec, Canada, pp 282-295.

Vegas, I., Ibañez, J. A., San José, J. T., & Urzelai, A. (2008). Construction demolition wastes, waelz slag and MSWI bottom ash: a comparative technical analysis as material for road construction. Journal of Waste Management, 28(3):565-574.

WAPA, (2011). Washington Asphalt Pavement Association. Surface Distresses, Asphalt Pavement Guide, Retrieved on June 24, 2011, from http://www.asphaltwa.com/wapa_web/modules/11_guidance/11_surface_distress.htm.

White, T. D., Johnson, S. R., & Yzenas, J. J. (2001). Aggregate contribution to hot mix asphalt (HMA) performance, American Society for Testing and Materials (ASTM) STP 1412, West Conshohocken, PA.

Witczak, M. W. (2004). NCHRP Project No. 1-28 A, Resilient Modulus for Flexible Pavement Design, University of Maryland-College Park, Arizona State University, Tempe, Arizona, USA.

Wong, Y. D., Sun, D. D., & Lai, D. (2007). Value-added utilization of recycled concrete in hot-mix asphalt. Journal of Waste Management, 27(2):294-301.

Wu, S., Zhong, J., Zhu, J., & Wang, D. (2013). Influence of demolition waste used as recycled aggregate on performance of asphalt mixture. Journal of Road Materials and Pavement Design, 14(3):679-688.

Xiao, F., & Amirkhanian, S. N. (2009). Laboratory investigation of moisture damage in rubberised asphalt mixtures containing reclaimed asphalt pavement. International Journal of Pavement Engineering, 10(5): 19-328.

Xue, Y., Hou, H., Zhu, S., & Zha, J. (2009). Utilization of municipal solid waste incineration ash in stone mastic asphalt mixture: pavement performance and environmental impact. Journal of Construction and Building Materials, 23(2):989-996.

List of Publications:

- **Pourtahmasb, M. S**., Karim, M. R. (2014). Performance evaluation of stone mastic asphalt and hot mix asphalt mixtures containing recycled concrete aggregate. Journal of Advances in Materials Science and Engineering. DOI: http://dx.doi.org/10.1155/2014/863148. (ISI- Cited Publication)

- **Pourtahmasb, M. S**., Karim, M. R. (2014). Utilization of recycled concrete aggregates in stone mastic asphalt mixtures. Journal of Advances in Materials Science and Engineering. DOI: http://dx.doi.org/10.1155/2014/902307. (ISI- Cited Publication)

- **Pourtahmasb, M. S**., Karim, M. R., Shamshirband, S. (2015). Resilient modulus prediction of asphalt mixtures containing recycled concrete aggregate using an adaptive neuro-fuzzy methodology. Journal of Construction and building materials. 82: 257-263. DOI: 10.1016/j.conbuildmat.2015.02.030. (ISI- Cited Publication)

- **Pourtahmasb, M. S**., Karim, M. R. (2011). Typical types of Hot Mix Asphalt (HMA) pavements deterioration (distress) and maintenance methods. Transport Research Conference (TRC), University Science Malaysia (USM), Pinang, Malaysia.

- **Pourtahmasb, M. S**., Zargar, M., Ahmadinia, E and Karim, M. R. (2012). Specifications of aggregates used in stone mastic asphalt and the minimum standard requirement. International Technical Conference (ITC), Kuala Lumpur, Malaysia.

- Zargar, M., **Pourtahmasb, M. S**., Ahmadinia, E and Karim, M. R. (2012). Utilization of Celolose oil palm fibers in Stone Mastic Asphalt (SMA) mixtures. International Technical Conference (ITC), Kuala Lumpur, Malaysia.

- **Pourtahmasb, M. S**., Karim, M. R., Almasi, M. H and Mirzapour Munes, S. (2013). Evaluation of permanent deformation on wearing course of flexible pavements using, Loaded Wheel Tracking (LWT) Test. Malaysian Universities Transportation Research Forum and Conference (MUTRFC), University Kebangsaan Malaysia (UKM), Malaysia.

- Almasi, M. H., Karim, M. R., Mirzapour Munes, S and **Pourtahmasb, M. S**. (2013). Feeder bus network design problems. Malaysian Universities Transportation Research Forum and Conference (MUTRFC), University Kebangsaan Malaysia (UKM), Malaysia.

Appendices

APPENDIX A

Optimum Asphalt Content (OAC) of HMA mixtures containing RCA

- **0% RCA (HMA)**

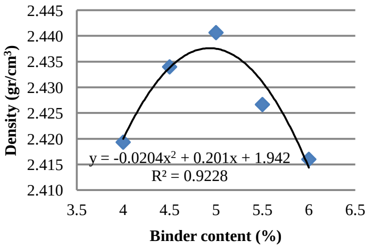

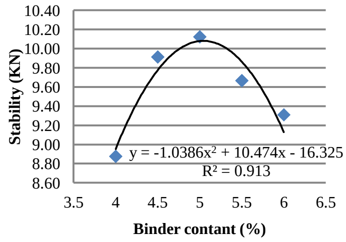

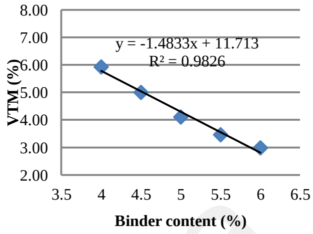

Density: $\Longrightarrow$ $y = -0.0204\, x^2 + 0.201\, x + 1.942$

$$\frac{dy}{dx} = 0 \Longrightarrow \boldsymbol{x = 4.926}$$

Stability: $\Longrightarrow$ $y = -1.0386\, x^2 + 10.474\, x - 16.325$

$$\frac{dy}{dx} = 0 \Longrightarrow \boldsymbol{x = 5.042}$$

VTM: $\Longrightarrow$ $y = -1.4833x + 11.713$

$Y = 4 \Longrightarrow y = -1.4833x + 11.713 = 4 \Longrightarrow$ $\boldsymbol{x = 5.20}$

OAC of the HMA Mixture containing 0% RCA

Property	**Selected binder content (%)**
Peak of density curve	**4.926**
Peak of stability curve	**5.042**
4% air voids, from VTM curve	**5.200**
OAC	**5.1**

- **20% Fine RCA (HMA)**

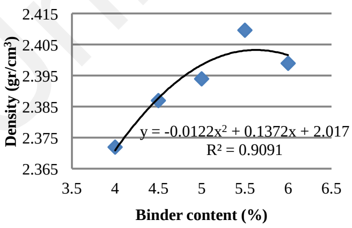

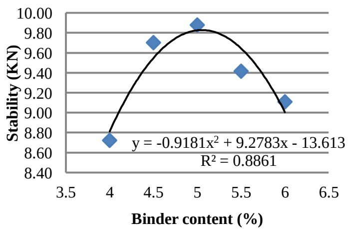

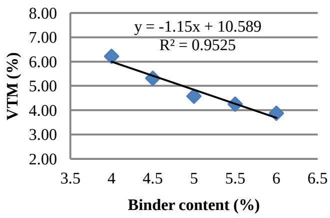

Density: $\Longrightarrow$ $y = -0.0122\, x^2 + 0.1372\, x + 2.017$

$$\frac{dy}{dx} = 0 \Longrightarrow \boldsymbol{x = 5.623}$$

Stability: $\Longrightarrow$ $y = -0.9181\, x^2 + 9.2783\, x - 13.613$

$$\frac{dy}{dx} = 0 \Longrightarrow \boldsymbol{x = 5.053}$$

VTM: $\Longrightarrow$ $y = -1.15\,x + 10.589$

$Y = 4 \Longrightarrow y = -1.15\,x + 10.589 = 4 \Longrightarrow \boldsymbol{x = 5.730}$

OAC of the HMA Mixture containing 20% F-RCA

Property	**Selected binder content (%)**
Peak of density curve	**5.623**
Peak of stability curve	**5.053**
4% air voids, from VTM curve	**5.730**
OAC	**5.5**

- **40% Fine RCA (HMA)**

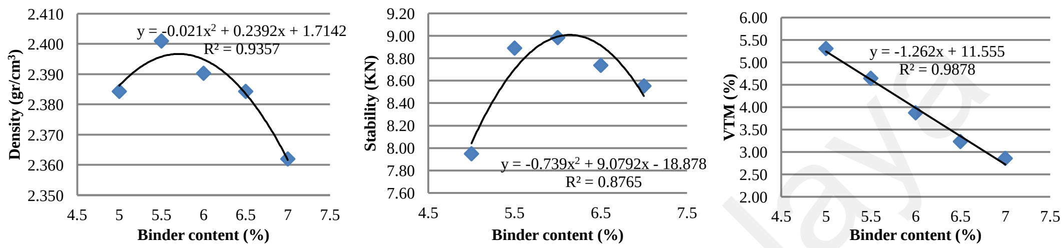

Density: $\Longrightarrow$ $y = -0.021\,x^2 + 0.2392\,x + 1.7142$

$\frac{dy}{dx} = 0 \Longrightarrow \boldsymbol{x = 5.69}$

Stability: $\Longrightarrow$ $y = -0.739\,x^2 + 9.0792\,x - 18.878$

$\frac{dy}{dx} = 0 \Longrightarrow \boldsymbol{x = 6.14}$

VTM: $\Longrightarrow$ $y = -1.262\,x + 11.555$

$Y = 4 \Longrightarrow y = -1.262\,x + 11.555 = 4 \Longrightarrow \boldsymbol{x = 5.98}$

OAC of the HMA Mixture containing 40% F-RCA

Property	**Selected binder content (%)**
Peak of density curve	**5.69**
Peak of stability curve	**6.14**
4% air voids, from VTM curve	**5.98**
OAC	**5.9**

- **60% Fine RCA (HMA)**

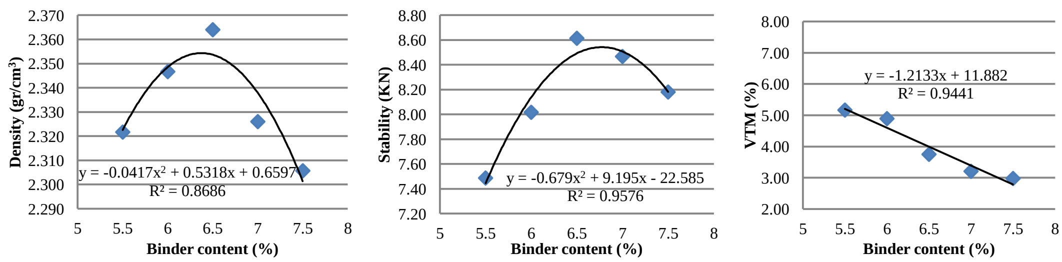

Density: $\Longrightarrow$ $y = -0.0417x^2 + 0.5318x + 0.6597$

$\frac{dy}{dx} = 0 \Longrightarrow \boldsymbol{x = 6.370}$

Stability: $\Longrightarrow$ $y = -0.679\,x^2 + 9.195\,x - 22.585$

$$\frac{dy}{dx} = 0 \Longrightarrow \boldsymbol{x = 6.771}$$

VTM: $\Longrightarrow$ $y = -1.2133x + 11.882$

$Y = 4 \Longrightarrow -1.2133x + 11.882 = 4 \Longrightarrow \boldsymbol{x = 6.497}$

OAC of the HMA Mixture containing 60% F-RCA

Property	**Selected binder content (%)**
Peak of density curve	**6.370**
Peak of stability curve	**6.771**
4% air voids, from VTM curve	**6.497**
OAC	**6.5**

- **80% Fine RCA (HMA)**

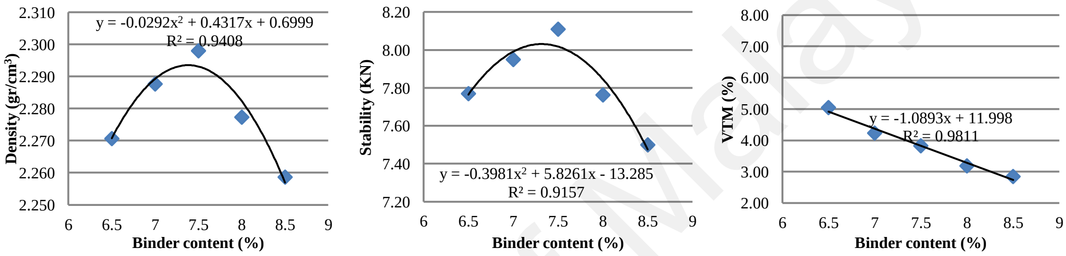

Density: $\Longrightarrow$ $y = -0.0292\,x^2 + 0.4317\,x + 0.6999$

$$\frac{dy}{dx} = 0 \Longrightarrow \boldsymbol{x = 7.390}$$

Stability: $\Longrightarrow$ $y = -0.3981\,x^2 + 5.8261\,x - 13.285$

$$\frac{dy}{dx} = 0 \Longrightarrow \boldsymbol{x = 7.317}$$

VTM: $\Longrightarrow$ $y = -1.0893\,x + 11.998$

$Y = 4 \Longrightarrow -1.0893\,x + 11.998 = 4 \Longrightarrow \boldsymbol{x = 7.341}$

OAC of the HMA Mixture containing 80% F-RCA

Property	**Selected binder content (%)**
Peak of density curve	**7.390**
Peak of stability curve	**7.317**
4% air voids, from VTM curve	**7.341**
OAC	**7.3**

- **20% Coarse RCA (HMA)**

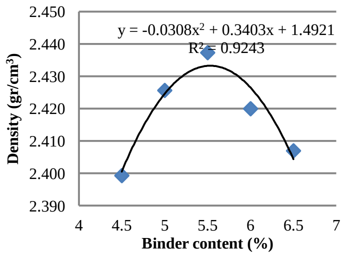

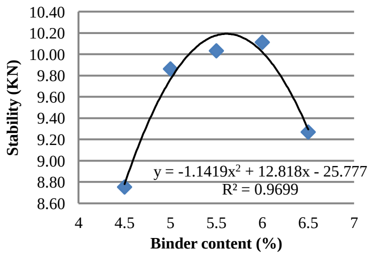

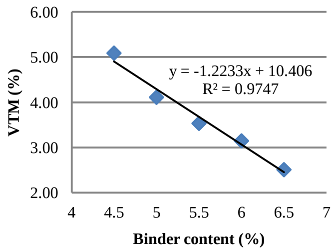

Density: $\Longrightarrow$ $y = -0.0308\,x^2 + 0.3403\,x + 1.4921$

$$\frac{dy}{dx} = 0 \Longrightarrow \boldsymbol{x = 5.52}$$

Stability: $\Longrightarrow$ $y = -1.1419\,x^2 + 12.818\,x - 25.777$

$$\frac{dy}{dx} = 0 \Longrightarrow \boldsymbol{x = 5.61}$$

VTM: $\Longrightarrow$ $y = -1.2233\,x + 10.406$

$Y = 4 \Longrightarrow y = -1.2233\,x + 10.406 = 4 \Longrightarrow \boldsymbol{x = 5.23}$

OAC of the HMA Mixture containing 20% C-RCA

Property	**Selected binder content (%)**
Peak of density curve	**5.52**
Peak of stability curve	**5.61**
4% air voids, from VTM curve	**5.23**
OAC	**5.4**

- **40% Coarse RCA (HMA)**

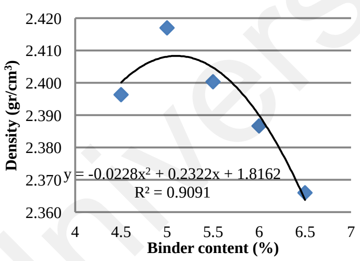

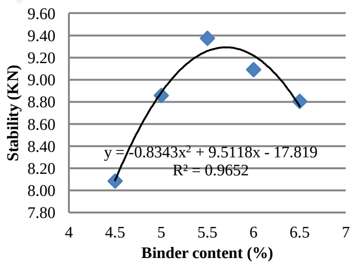

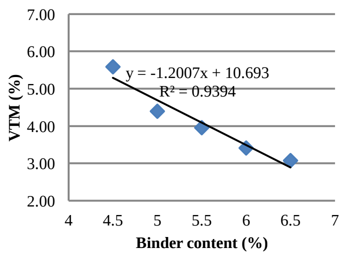

Density: $\Longrightarrow$ $y = -0.0228\,x^2 + 0.2322\,x + 1.8162$

$$\frac{dy}{dx} = 0 \Longrightarrow \boldsymbol{x = 5.092}$$

Stability: $\Longrightarrow$ $y = -0.8343\,x^2 + 9.5118\,x - 17.819$

$$\frac{dy}{dx} = 0 \Longrightarrow \boldsymbol{x = 5.701}$$

VTM: $\Longrightarrow$ $y = -1.2007x + 10.693$

$Y = 4 \Longrightarrow -1.2007x + 10.693 = 4 \Longrightarrow \boldsymbol{x = 5.575}$

OAC of the HMA Mixture containing 40% C-RCA

Property	**Selected binder content (%)**
Peak of density curve	**5.092**
Peak of stability curve	**5.701**
4% air voids, from VTM curve	**5.575**
OAC	**5.5**

- **60% Coarse RCA (HMA)**

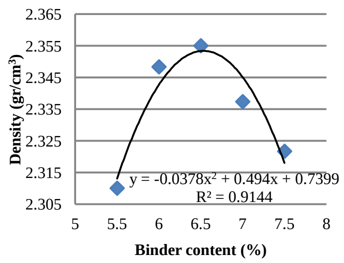

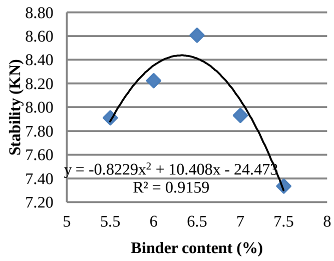

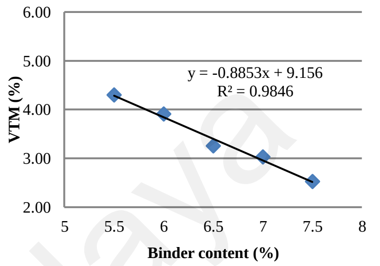

Density: $\Longrightarrow$ $y = -0.0378\,x^2 + 0.494\,x + 0.7399$

$$\frac{dy}{dx} = 0 \Longrightarrow \boldsymbol{x = 6.53}$$

Stability: $\Longrightarrow$ $y = -0.8229\,x^2 + 10.408\,x - 24.473$

$$\frac{dy}{dx} = 0 \Longrightarrow \boldsymbol{x = 6.32}$$

VTM: $\Longrightarrow$ $y = -0.8853\,x + 9.156$

$Y = 4 \Longrightarrow y = -0.8853\,x + 9.156 = 4 \Longrightarrow \boldsymbol{x = 5.82}$

OAC of the HMA Mixture containing 60% C-RCA

Property	**Selected binder content (%)**
Peak of density curve	**6.53**
Peak of stability curve	**6.32**
4% air voids, from VTM curve	**5.82**
OAC	**6.2**

- **80% Coarse RCA (HMA)**

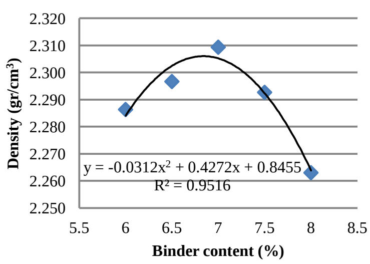

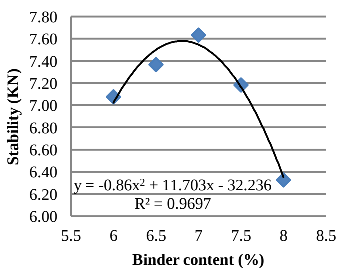

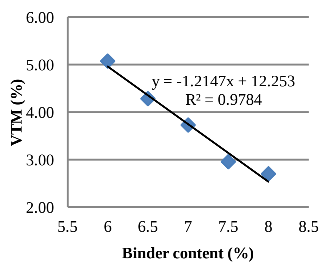

Density: $\Longrightarrow$ $y = -0.0312\,x^2 + 0.4272\,x + 0.8455$

$$\frac{dy}{dx} = 0 \Longrightarrow \boldsymbol{x = 6.85}$$

Stability: $\Longrightarrow$ $y = -0.86\,x^2 + 11.703\,x - 32.236$

$$\frac{dy}{dx} = 0 \Longrightarrow \boldsymbol{x = 6.80}$$

VTM: $\Longrightarrow$ $y = -1.2147x + 12.253$

$Y = 4 \Longrightarrow y = -1.2147x + 12.253 = 4 \Longrightarrow \boldsymbol{x = 6.79}$

OAC of the HMA Mixture containing 80% C-RCA

Property	**Selected binder content (%)**
Peak of density curve	**6.85**
Peak of stability curve	**6.80**
4% air voids, from VTM curve	**6.79**
OAC	**6.8**

➢ **20% Mix RCA (HMA)**

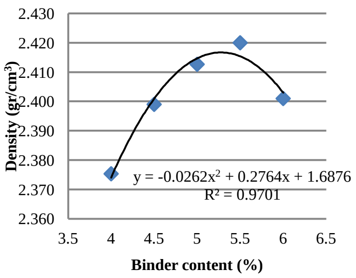

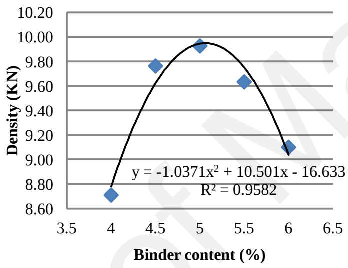

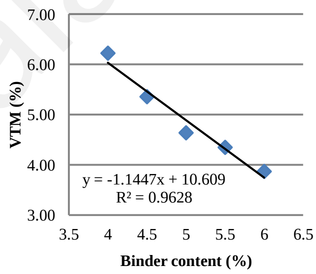

Density: $\Longrightarrow$ $y = -0.0262x^2 + 0.2764x + 1.6876$

$$\frac{dy}{dx} = 0 \Longrightarrow \boldsymbol{x = 5.275}$$

Stability: $\Longrightarrow$ $y = -1.0371\,x^2 + 10.501\,x - 16.633$

$$\frac{dy}{dx} = 0 \Longrightarrow \boldsymbol{x = 5.063}$$

VTM: $\Longrightarrow$ $y = -1.1447\,x + 10.609$

$Y = 4 \Longrightarrow -1.1447\,x + 10.609 = 4 \Longrightarrow \boldsymbol{x = 5.77}$

OAC of the HMA Mixture containing 20% M-RCA

Property	**Selected binder content (%)**
Peak of density curve	**5.275**
Peak of stability curve	**5.063**
4% air voids, from VTM curve	**5.77**
OAC	**5.4**

➢ **40% Mix RCA (HMA)**

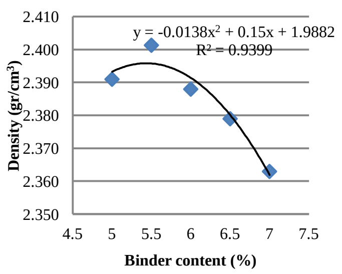

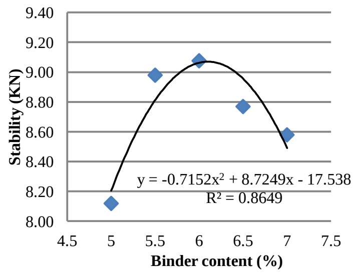

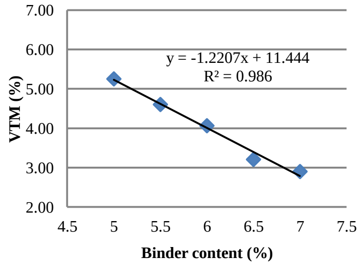

Density: $\Longrightarrow$ $y = -0.0138\,x^2 + 0.15\,x + 1.9882$

$\frac{dy}{dx} = 0 \Longrightarrow \boldsymbol{x = 5.43}$

Stability: $\Longrightarrow$ $y = -0.7152\,x^2 + 8.7249\,x - 17.538$

$\frac{dy}{dx} = 0 \Longrightarrow \boldsymbol{x = 6.10}$

VTM: $\Longrightarrow$ $y = -1.2207\,x + 11.444$

$Y = 4 \Longrightarrow -1.2207\,x + 11.444 = 4 \Longrightarrow \boldsymbol{x = 6.10}$

OAC of the HMA Mixture containing 40% M-RCA

Property	**Selected binder content (%)**
Peak of density curve	**5.43**
Peak of stability curve	**6.10**
4% air voids, from VTM curve	**6.10**
OAC	**5.9**

➢ **60% Mix RCA (HMA)**

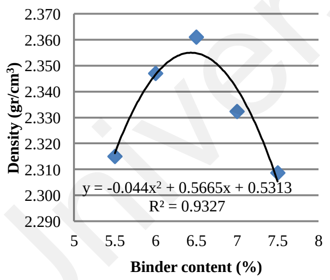

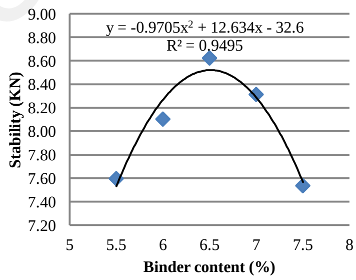

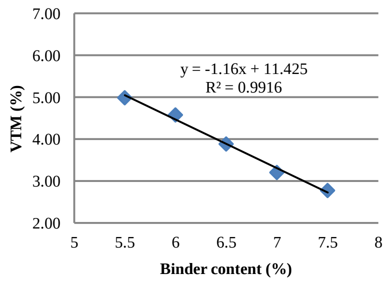

Density: $\Longrightarrow$ $y = -0.044\,x^2 + 0.5665\,x + 0.5313$

$\frac{dy}{dx} = 0 \Longrightarrow \boldsymbol{x = 6.437}$

Stability: $\Longrightarrow$ $y = -0.9705\,x^2 + 12.634\,x - 32.6$

$\frac{dy}{dx} = 0 \Longrightarrow \boldsymbol{x = 6.509}$

VTM: $\Longrightarrow$ $y = -1.16\,x + 11.425$

$Y = 4 \Longrightarrow -1.16\,x + 11.425 = 4 \Longrightarrow \boldsymbol{x = 6.401}$

Table 11: OAC of the HMA Mixture with 60% M-RCA

Property	Selected binder content (%)
Peak of density curve	**6.437**
Peak of stability curve	**6.509**
4% air voids, from VTM curve	**6.401**
OAC	**6.4**

- **80% Mix RCA (HMA)**

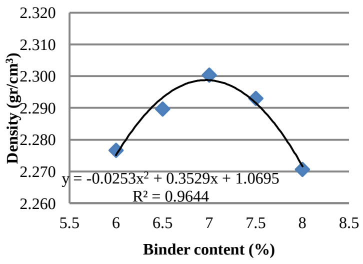

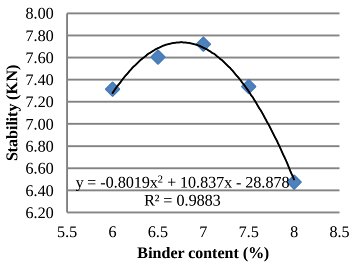

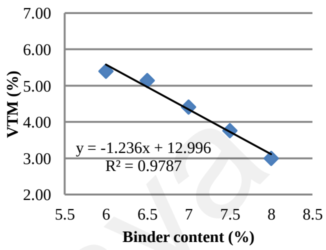

Density: $\Longrightarrow \quad y = -0.0253\, x^2 + 0.3529\, x + 1.0695$

$$\frac{dy}{dx} = 0 \Longrightarrow \boldsymbol{x = 6.974}$$

Stability: $\Longrightarrow \; y = -0.8019\, x^2 + 10.837\, x - 28.878$

$$\frac{dy}{dx} = 0 \Longrightarrow \boldsymbol{x = 6.757}$$

VTM: $\Longrightarrow \quad y = -1.236\, x + 12.996$

$Y = 4 \Longrightarrow -1.236\, x + 12.996 = 4 \Longrightarrow \boldsymbol{x = 7.278}$

OAC of the HMA Mixture containing 80% M-RCA

Property	Selected binder content (%)
Peak of density curve	6.974
Peak of stability curve	6.757
4% air voids, from VTM curve	7.278
OAC	7.0

APPENDIX B

Optimum Asphalt Content (OAC) of SMA mixtures containing RCA

➢ **0% RCA (SMA)**

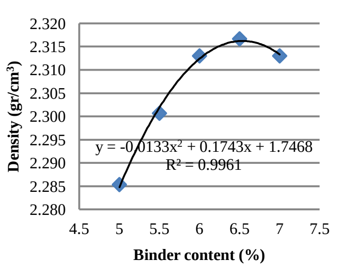

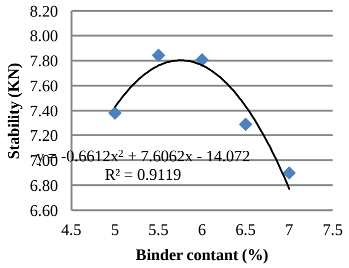

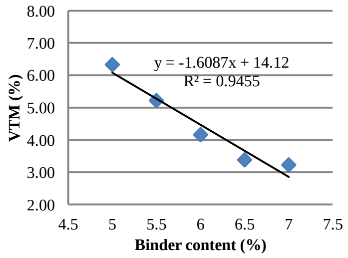

Density: $\Longrightarrow$ $y = -0.0133\,x^2 + 0.1743\,x + 1.7468$

$$\frac{dy}{dx} = 0 \Longrightarrow \boldsymbol{x = 6.553}$$

Stability: $\Longrightarrow$ $y = -0.6612\,x^2 + 7.6062\,x - 14.072$

$$\frac{dy}{dx} = 0 \Longrightarrow \boldsymbol{x = 5.752}$$

VTM: $\Longrightarrow$ $y = -1.6087x + 14.12$

$Y = 4 \Longrightarrow y = -1.6087x + 14.12 = 4 \Longrightarrow \boldsymbol{x = 6.291}$

Flow: $\Longrightarrow$ $y = 0.2657\,x^2 - 2.4252\,x + 8.1729$

OAC of the SMA Mixture containing 0% RCA

Property	Selected binder content (%)
Peak of density curve	6.553
Peak of stability curve	5.752
4% air voids, from VTM curve	6.291
OAC	6.2

➢ **20% Fine RCA (SMA)**

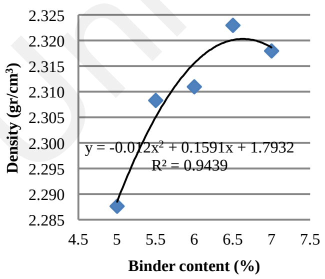

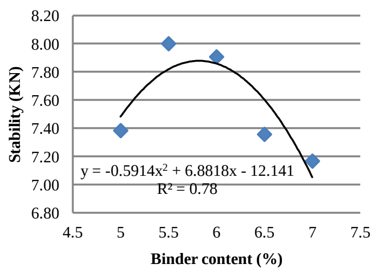

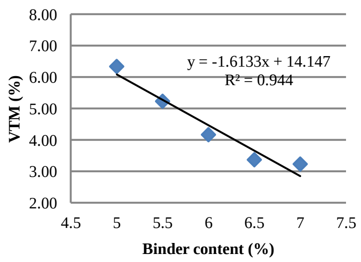

Density: $\Longrightarrow$ $y = -0.012\,x^2 + 0.1591\,x + 1.7932$

$$\frac{dy}{dx} = 0 \Longrightarrow \boldsymbol{x = 6.629}$$

Stability: $\Longrightarrow$ $y = -0.5914\,x^2 + 6.8818\,x - 12.141$

$$\frac{dy}{dx} = 0 \Longrightarrow \boldsymbol{x = 5.818}$$

VTM: $\Longrightarrow$ $y = -1.6133\,x + 14.147$

$Y = 4 \Longrightarrow y = -1.6133\,x + 14.147 = 4 \Longrightarrow \boldsymbol{x = 6.290}$

Flow: $\Longrightarrow$ $y = 0.2914x^2 - 2.6958x + 8.865$

OAC of the SMA Mixture containing 20% F-RCA

Property	**Selected binder content (%)**
Peak of density curve	**6.629**
Peak of stability curve	**5.818**
4% air voids, from VTM curve	**6.290**
OAC	**6.2**

- **40% Fine RCA (SMA)**

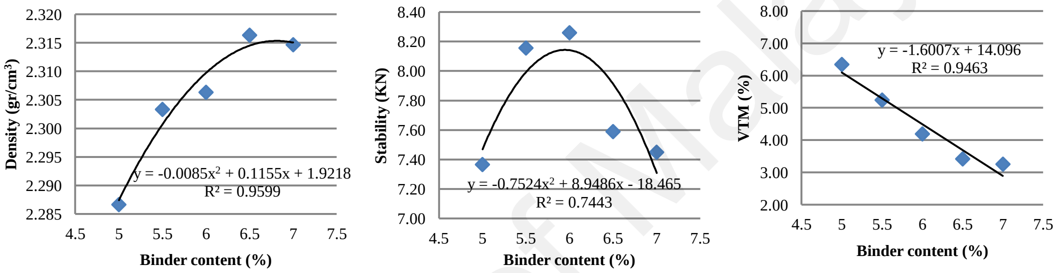

Density: $\Longrightarrow$ $y = -0.0085\,x^2 + 0.1155\,x + 1.9218$

$$\frac{dy}{dx} = 0 \Longrightarrow \boldsymbol{x = 6.794}$$

Stability: $\Longrightarrow$ $y = -0.7524\,x^2 + 8.9486\,x - 18.465$

$$\frac{dy}{dx} = 0 \Longrightarrow \boldsymbol{x = 5.947}$$

VTM: $\Longrightarrow$ $y = -1.6007\,x + 14.096$

$Y = 4 \Longrightarrow y = -1.6007x + 14.096 = 4 \Longrightarrow \boldsymbol{x = 6.307}$

Flow: $\Longrightarrow$ $y = 0.2933\,x^2 - 2.7253\,x + 9.0493$

OAC of the SMA Mixture containing 40% F-RCA

Property	**Selected binder content (%)**
Peak of density curve	**6.794**
Peak of stability curve	**5.947**
4% air voids, from VTM curve	**6.307**
OAC	**6.3**

- **60% Fine RCA (SMA)**

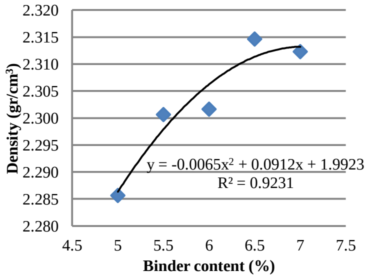

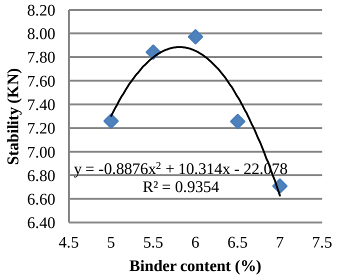

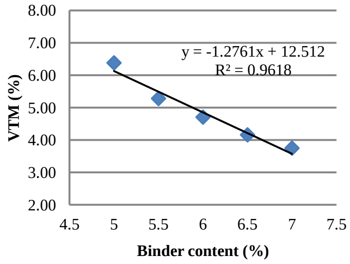

Density: $\Longrightarrow$ $y = -0.0065x^2 + 0.0912x + 1.9923$

$$\frac{dy}{dx} = 0 \Longrightarrow \boldsymbol{x = 7.015}$$

Stability: $\Longrightarrow$ $y = -0.8876\,x^2 + 10.314\,x - 22.078$

$$\frac{dy}{dx} = 0 \Longrightarrow \boldsymbol{x = 5.81}$$

VTM: $\Longrightarrow$ $y = -1.2761\,x + 12.512$

$Y= 4 \Longrightarrow -1.2761\,x + 12.512 = 4 \Longrightarrow \boldsymbol{x = 6.67}$

Flow: $\Longrightarrow$ $y = 0.3467\,x^2 - 3.396\,x + 11.172$

OAC of the SMA Mixture containing 60% F-RCA

Property	**Selected binder content (%)**
Peak of density curve	**7.015**
Peak of stability curve	**5.810**
4% air voids, from VTM curve	**6.670**
OAC	**6.5**

- **80% Fine RCA (SMA)**

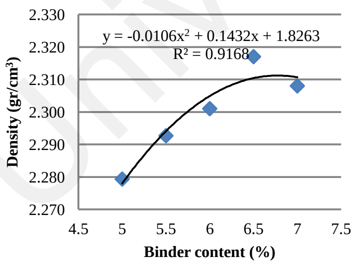

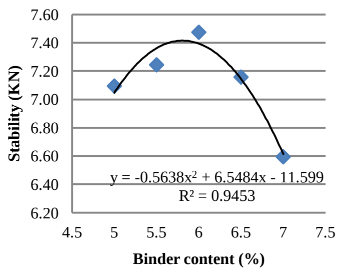

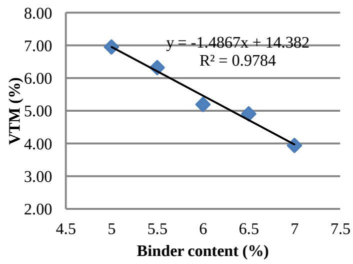

Density: $\Longrightarrow$ $y = -0.0106\,x^2 + 0.1432\,x + 1.8263$

$$\frac{dy}{dx} = 0 \Longrightarrow \boldsymbol{x = 6.755}$$

Stability: $\Longrightarrow$ $y = -0.5638\,x^2 + 6.5484\,x - 11.599$

$$\frac{dy}{dx} = 0 \Longrightarrow \boldsymbol{x = 5.807}$$

VTM: $\Longrightarrow$ $y = -1.4867\ x + 14.382$

$Y = 4 \Longrightarrow -1.4867\ x + 14.382 = 4 \Longrightarrow \boldsymbol{x = 6.972}$

Flow: $\Longrightarrow$ $y = 0.4057\ x^2 - 4.1139\ x + 13.634$

OAC of the SMA Mixture containing 80% F-RCA

Property	Selected binder content (%)
Peak of density curve	**6.755**
Peak of stability curve	**5.807**
4% air voids, from VTM curve	**6.972**
OAC	**6.5**

- **20% Coarse RCA (SMA)**

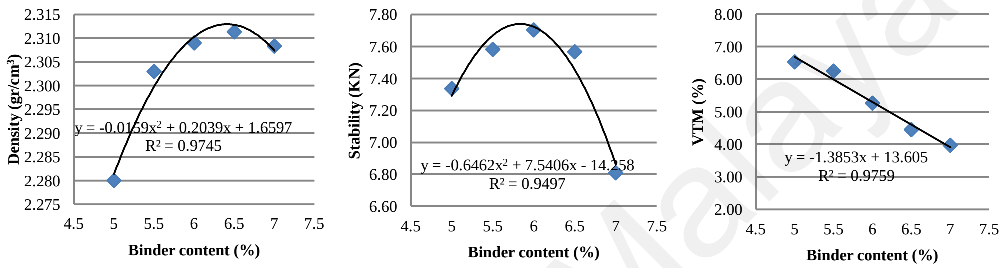

Density: $\Longrightarrow$ $y = -0.0159\ x^2 + 0.2039\ x + 1.6597$

$$\frac{dy}{dx} = 0 \Longrightarrow \boldsymbol{x = 6.412}$$

Stability: $\Longrightarrow$ $y = -0.6462\ x^2 + 7.5406\ x - 14.258$

$$\frac{dy}{dx} = 0 \Longrightarrow \boldsymbol{x = 5.835}$$

VTM: $\Longrightarrow$ $y = -1.3853\ x + 13.605$

$Y = 4 \Longrightarrow y = -1.3853\ x + 13.605 = 4 \Longrightarrow \boldsymbol{x = 6.933}$

Flow: $\Longrightarrow$ $y = 0.2781\ x^2 - 2.4265\ x + 8.0177$

OAC of the SMA Mixture containing 20% C-RCA

Property	Selected binder content (%)
Peak of density curve	**6.412**
Peak of stability curve	**5.835**
4% air voids, from VTM curve	**6.933**
OAC	**6.4**

- **40% Coarse RCA (SMA)**

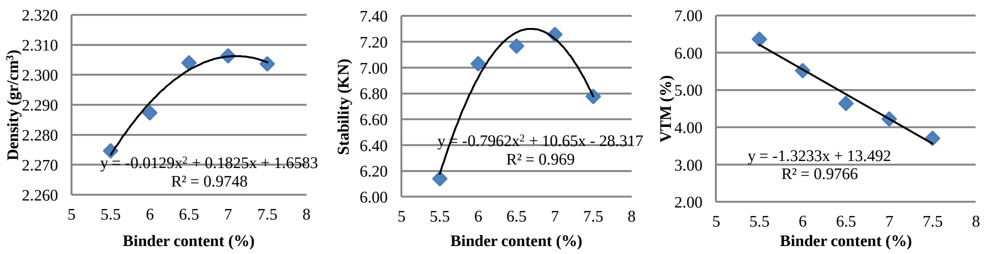

Density: $\Longrightarrow$ $y = -0.0129\,x^2 + 0.1825\,x + 1.6583$

$$\frac{dy}{dx} = 0 \Longrightarrow \boldsymbol{x = 7.073}$$

Stability: $\Longrightarrow$ $y = -0.7962\,x^2 + 10.65\,x - 28.317$

$$\frac{dy}{dx} = 0 \Longrightarrow \boldsymbol{x = 6.690}$$

VTM: $\Longrightarrow$ $y = -1.3233\,x + 13.492$

$Y = 4 \Longrightarrow -1.3233\,x + 13.492 = 4 \Longrightarrow \boldsymbol{x = 7.173}$

Flow: $\Longrightarrow$ $y = 0.379\,x^2 - 3.9863\,x + 13.463$

OAC of the SMA Mixture containing 40% C-RCA

Property	**Selected binder content (%)**
Peak of density curve	**7.073**
Peak of stability curve	**6.690**
4% air voids, from VTM curve	**7.173**
OAC	**7**

- **60% Coarse RCA (SMA)**

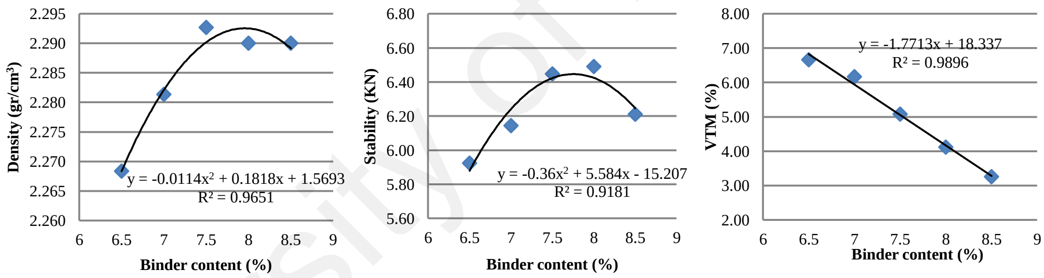

Density: $\Longrightarrow$ $y = -0.0114\,x^2 + 0.1818\,x + 1.5693$

$$\frac{dy}{dx} = 0 \Longrightarrow \boldsymbol{x = 7.974}$$

Stability: $\Longrightarrow$ $y = -0.36\,x^2 + 5.584\,x - 15.207$

$$\frac{dy}{dx} = 0 \Longrightarrow \boldsymbol{x = 7.760}$$

VTM: $\Longrightarrow$ $y = -1.7713\,x + 18.337$

$Y = 4 \Longrightarrow y = -1.7713\,x + 18.337 = 4 \Longrightarrow \boldsymbol{x = 8.090}$

Flow: $\Longrightarrow$ $y = 0.219\,x^2 - 2.2404\,x + 9.1779$

OAC of the SMA Mixture containing 60% C-RCA

Property	**Selected binder content (%)**
Peak of density curve	**7.974**
Peak of stability curve	**7.760**
4% air voids, from VTM curve	**8.090**
OAC	**7.9**

- **80% Coarse RCA (SMA)**

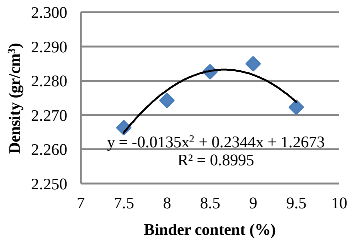

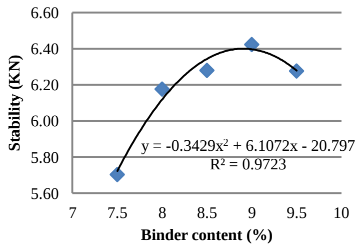

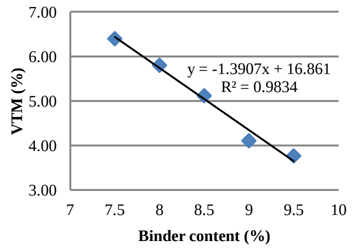

Density: $\Longrightarrow$ $y = -0.0135\ x^2 + 0.2344\ x + 1.2673$

$$\frac{dy}{dx} = 0 \Longrightarrow \boldsymbol{x = 8.681}$$

Stability: $\Longrightarrow$ $y = -0.3429\ x^2 + 6.1072\ x - 20.797$

$$\frac{dy}{dx} = 0 \Longrightarrow \boldsymbol{x = 8.905}$$

VTM: $\Longrightarrow$ $y = -1.3907x + 16.861$

$Y = 4 \Longrightarrow y = -1.3907x + 16.861 = 4 \Longrightarrow \boldsymbol{x = 9.248}$

Flow: $\Longrightarrow$ $y = 0.1933\ x^2 - 2.1367\ x + 9.8667$

OAC of the SMA Mixture containing 80% C-RCA

Property	Selected binder content (%)
Peak of density curve	**8.681**
Peak of stability curve	**8.905**
4% air voids, from VTM curve	**9.248**
OAC	**8.9**

- **20% Mix RCA (SMA)**

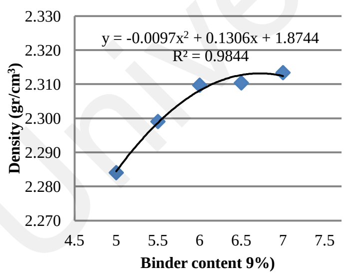

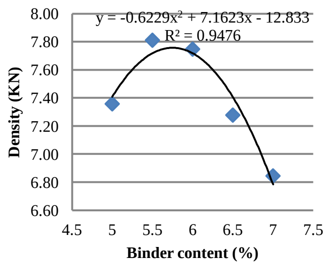

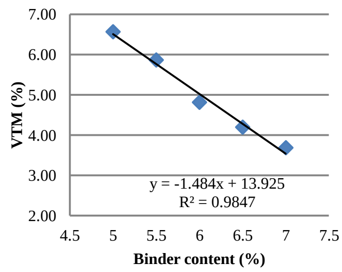

Density: $\Longrightarrow$ $y = -0.0097x^2 + 0.1306x + 1.8744$

$$\frac{dy}{dx} = 0 \Longrightarrow \boldsymbol{x = 6.732}$$

Stability: $\Longrightarrow$ $y = -0.6229\ x^2 + 7.1623\ x - 12.833$

$$\frac{dy}{dx} = 0 \Longrightarrow \boldsymbol{x = 5.692}$$

VTM: $\Longrightarrow$ $y = -1.484\ x + 13.925$

$Y = 4 \Longrightarrow -1.484\,x + 13.925 = 4 \Longrightarrow \boldsymbol{x = 6.688}$

Flow: $\Longrightarrow \quad y = 0.2886\,x^2 - 2.5435\,x + 8.287$

OAC of the SMA Mixture containing 20% M-RCA

Property	Selected binder content (%)
Peak of density curve	**6.732**
Peak of stability curve	**5.692**
4% air voids, from VTM curve	**6.688**
OAC	**6.4**

- **40% Mix RCA (SMA)**

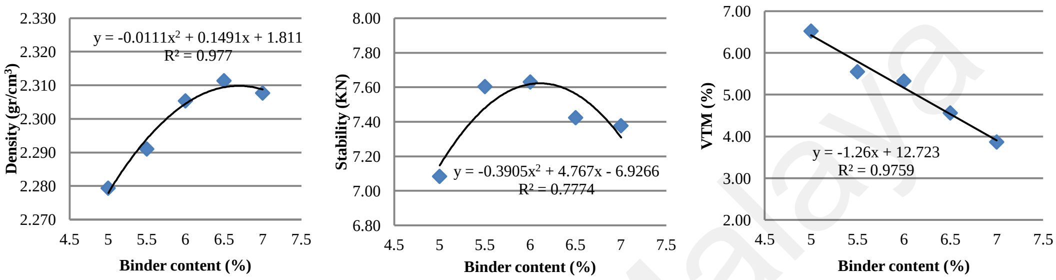

Density: $\Longrightarrow \quad y = -0.0111\,x^2 + 0.1491\,x + 1.811$

$$\frac{dy}{dx} = 0 \Longrightarrow \boldsymbol{x = 6.716}$$

Stability: $\Longrightarrow \quad y = -0.3905\,x^2 + 4.767\,x - 6.9266$

$$\frac{dy}{dx} = 0 \Longrightarrow \boldsymbol{x = 6.104}$$

VTM: $\Longrightarrow \quad y = -1.26\,x + 12.723$

$Y = 4 \Longrightarrow -1.26\,x + 12.723 = 4 \Longrightarrow \boldsymbol{x = 6.923}$

Flow: $\Longrightarrow \quad y = 0.3295\,x^2 - 2.9836\,x + 9.5668$

OAC of the SMA Mixture containing 40% M-RCA

Property	Selected binder content (%)
Peak of density curve	**6.716**
Peak of stability curve	**6.104**
4% air voids, from VTM curve	**6.923**
OAC	**6.6**

- **60% Mix RCA (SMA)**

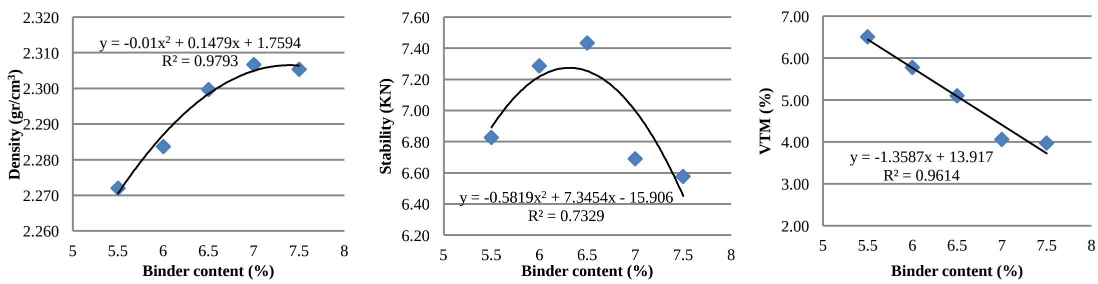

Density: $\Longrightarrow$ $y = -0.01\,x^2 + 0.1479\,x + 1.7594$

$$\frac{dy}{dx} = 0 \Longrightarrow \boldsymbol{x = 7.395}$$

Stability: $\Longrightarrow$ $y = -0.5819\,x^2 + 7.3454\,x - 15.906$

$$\frac{dy}{dx} = 0 \Longrightarrow \boldsymbol{x = 6.312}$$

VTM: $\Longrightarrow$ $y = -1.3587\,x + 13.917$

$Y = 4 \Longrightarrow -1.3587\,x + 13.917 = 4 \Longrightarrow \boldsymbol{x = 7.299}$

Flow: $\Longrightarrow$ $y = 0.3714\,x^2 - 3.7646\,x + 13.122$

OAC of the SMA Mixture containing 60% M-RCA

Property	**Selected binder content (%)**
Peak of density curve	**7.395**
Peak of stability curve	**6.312**
4% air voids, from VTM curve	**7.299**
OAC	**7**

- **80% Mix RCA (SMA)**

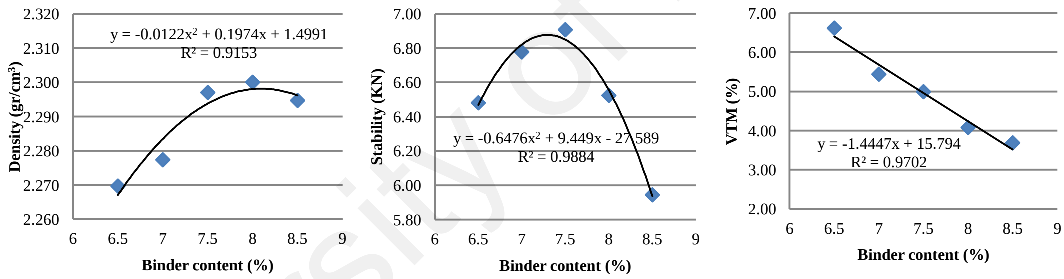

Density: $\Longrightarrow$ $y = -0.0122\,x^2 + 0.1974\,x + 1.4991$

$$\frac{dy}{dx} = 0 \Longrightarrow \boldsymbol{x = 8.09}$$

Stability: $\Longrightarrow$ $y = -0.6476\,x^2 + 9.449\,x - 27.589$

$$\frac{dy}{dx} = 0 \Longrightarrow \boldsymbol{x = 7.295}$$

VTM: $\Longrightarrow$ $y = -1.4447\,x + 15.794$

$Y = 4 \Longrightarrow -1.4447\,x + 15.794 = 4 \Longrightarrow \boldsymbol{x = 8.164}$

Flow: $\Longrightarrow$ $y = 0.0752\,x^2 + 0.0868\,x + 0.5915$

OAC of the SMA Mixture with 80% M-RCA

Property	**Selected binder content (%)**
Peak of density curve	8.090
Peak of stability curve	7.295
4% air voids, from VTM curve	8.164
OAC	7.8

APPENDIX C

Marshall Stability correlation ratio (ASTM D1559-82)

Volume of sample (cm^3)	Approximate thickness of sample (mm)	Correction ratio
200-213	25.4	5.56
214-225	27.0	5.00
226-237	28.6	4.55
238-250	30.2	4.17
251-264	31.8	3.85
265-276	33.3	3.57
277-289	34.9	3.33
290-301	36.5	3.03
302-316	38.1	2.78
317-328	39.07	2.50
329-340	41.3	2.27
341-353	42.9	2.08
354-367	44.04	1.92
368-379	46.0	1.79
380-392	47.6	1.67
393-405	49.2	1.56
406-420	50.8	1.47
420-431	52.4	1.39
432-443	54.0	1.32
444-456	55.6	1.25
457-470	57.2	1.19
471-482	58.7	1.14
483-495	60.3	1.09
496-508	61.9	1.04
509-522	63.5	1.00
523-535	65.1	0.96
536-546	66.7	0.93
547-559	68.3	0.89
560-573	69.8	0.86
574-585	71.4	0.83
586-598	73.0	0.81
599-610	74.6	0.79
611-625	76.2	0.76

APPENDIX D

Flexural beam fatigue test of HMA specimens

VA

Cycles	Stress (kPa)	Micro Strain	Stiffness (MPa)	Modulus (MPa)	Phase Angle (Deg)	Energy (kPa)
50	3.31E+03	5.11E+02	6.49E+03	5.38E+03	3.24E+01	1.09E+00
500	3.17E+03	5.06E+02	6.26E+03	5.11E+03	3.68E+01	1.07E+00
1000	3.06E+03	4.98E+02	6.15E+03	5.00E+03	3.65E+01	1.07E+00
2000	2.98E+03	5.00E+02	5.95E+03	4.82E+03	3.47E+01	1.05E+00
3000	2.90E+03	5.03E+02	5.77E+03	4.71E+03	3.47E+01	1.04E+00
4000	2.86E+03	5.02E+02	5.69E+03	4.69E+03	3.47E+01	1.03E+00
5000	2.79E+03	5.00E+02	5.58E+03	4.51E+03	3.47E+01	1.03E+00
6000	2.72E+03	4.95E+02	5.49E+03	4.40E+03	3.48E+01	1.01E+00
7000	2.66E+03	4.99E+02	5.32E+03	4.37E+03	3.48E+01	1.01E+00
8000	2.57E+03	5.02E+02	5.12E+03	4.30E+03	3.49E+01	1.01E+00
9000	2.50E+03	5.03E+02	4.98E+03	4.20E+03	3.48E+01	1.00E+00
10000	2.46E+03	4.93E+02	4.98E+03	4.13E+03	3.69E+01	9.90E-01
20000	2.33E+03	5.03E+02	4.64E+03	4.08E+03	3.50E+01	9.70E-01
30000	2.27E+03	5.02E+02	4.51E+03	4.01E+03	3.50E+01	9.70E-01
40000	2.19E+03	5.02E+02	4.36E+03	3.97E+03	3.50E+01	9.50E-01
50000	2.12E+03	5.02E+02	4.23E+03	3.90E+03	3.51E+01	9.50E-01
60000	2.07E+03	5.03E+02	4.11E+03	3.86E+03	3.50E+01	9.30E-01
70000	2.01E+03	5.01E+02	4.01E+03	3.81E+03	3.50E+01	9.30E-01
80000	1.97E+03	4.97E+02	3.97E+03	3.76E+03	3.51E+01	9.10E-01
90000	1.92E+03	4.98E+02	3.86E+03	3.72E+03	3.51E+01	9.10E-01
100000	1.85E+03	4.98E+02	3.70E+03	3.68E+03	3.51E+01	9.00E-01
110000	1.79E+03	4.99E+02	3.58E+03	3.61E+03	3.52E+01	9.00E-01
120000	1.71E+03	5.00E+02	3.42E+03	3.55E+03	3.52E+01	8.80E-01
130000	1.64E+03	5.00E+02	3.29E+03	3.50E+03	3.51E+01	8.60E-01
134985	1.62E+03	4.99E+02	3.24E+03	3.47E+03	3.52E+01	8.50E-01

20% F-RCA

Cycles	Stress (kPa)	Micro Strain	Stiffness (MPa)	Modulus (MPa)	Phase Angle (Deg)	Energy (kPa)
50	3.91E+03	5.06E+02	7.73E+03	5.71E+03	2.88E+01	6.80E-01
500	3.79E+03	5.05E+02	7.50E+03	5.60E+03	3.37E+01	6.60E-01
1000	3.65E+03	5.00E+02	7.31E+03	5.49E+03	3.36E+01	6.50E-01
2000	3.57E+03	4.98E+02	7.17E+03	5.41E+03	3.21E+01	6.40E-01
3000	3.49E+03	5.00E+02	6.98E+03	5.33E+03	3.14E+01	6.40E-01
4000	3.42E+03	5.00E+02	6.84E+03	5.25E+03	3.14E+01	6.30E-01
5000	3.33E+03	5.01E+02	6.65E+03	5.13E+03	3.15E+01	6.20E-01
6000	3.25E+03	5.00E+02	6.49E+03	5.07E+03	3.15E+01	6.00E-01
7000	3.17E+03	5.03E+02	6.29E+03	4.99E+03	3.16E+01	5.80E-01
8000	3.11E+03	5.07E+02	6.14E+03	4.90E+03	3.17E+01	5.60E-01
9000	3.07E+03	4.99E+02	6.16E+03	4.86E+03	3.17E+01	5.60E-01
10000	3.01E+03	4.95E+02	6.07E+03	4.73E+03	3.17E+01	5.50E-01
20000	2.93E+03	4.98E+02	5.89E+03	4.68E+03	3.18E+01	5.30E-01
30000	2.86E+03	4.98E+02	5.74E+03	4.53E+03	3.18E+01	5.30E-01
40000	2.74E+03	5.00E+02	5.48E+03	4.44E+03	3.18E+01	5.30E-01
50000	2.65E+03	5.03E+02	5.28E+03	4.31E+03	3.18E+01	5.20E-01
60000	2.58E+03	5.01E+02	5.15E+03	4.29E+03	3.19E+01	5.10E-01
70000	2.52E+03	4.99E+02	5.05E+03	4.23E+03	3.19E+01	5.00E-01
80000	2.44E+03	5.02E+02	4.87E+03	4.17E+03	3.19E+01	4.80E-01
90000	2.34E+03	4.98E+02	4.69E+03	4.08E+03	3.20E+01	4.80E-01
100000	2.28E+03	5.01E+02	4.54E+03	3.99E+03	3.19E+01	4.50E-01
110000	2.18E+03	5.01E+02	4.35E+03	3.89E+03	3.20E+01	4.30E-01
120000	2.07E+03	5.00E+02	4.14E+03	3.81E+03	3.21E+01	4.20E-01
130000	1.97E+03	5.02E+02	3.91E+03	3.72E+03	3.21E+01	4.00E-01
139871	1.94E+03	5.03E+02	3.86E+03	3.64E+03	3.21E+01	3.80E-01

40% F-RCA

Cycles	Stress (kPa)	Micro Strain	Stiffness (MPa)	Modulus (MPa)	Phase Angle (Deg)	Energy (kPa)
50	4.30E+03	5.05E+02	8.52E+03	5.94E+03	2.72E+01	1.63E+00
500	4.22E+03	5.05E+02	8.36E+03	5.86E+03	3.16E+01	1.58E+00
1000	4.19E+03	5.00E+02	8.37E+03	5.80E+03	3.20E+01	1.58E+00
2000	4.13E+03	4.98E+02	8.29E+03	5.79E+03	3.12E+01	1.57E+00
3000	4.04E+03	4.99E+02	8.11E+03	5.72E+03	3.00E+01	1.55E+00
4000	3.98E+03	5.01E+02	7.94E+03	5.64E+03	3.00E+01	1.55E+00
5000	3.89E+03	4.99E+02	7.80E+03	5.40E+03	3.01E+01	1.52E+00
6000	3.85E+03	5.02E+02	7.67E+03	5.35E+03	3.00E+01	1.52E+00
7000	3.77E+03	5.01E+02	7.53E+03	5.28E+03	2.99E+01	1.50E+00
8000	3.70E+03	4.97E+02	7.44E+03	5.21E+03	2.98E+01	1.49E+00
9000	3.63E+03	4.98E+02	7.28E+03	5.17E+03	2.99E+01	1.47E+00
10000	3.56E+03	5.00E+02	7.11E+03	5.11E+03	2.98E+01	1.46E+00
20000	3.45E+03	4.98E+02	6.93E+03	5.05E+03	2.99E+01	1.45E+00
30000	3.34E+03	5.03E+02	6.64E+03	4.92E+03	2.97E+01	1.42E+00
40000	3.24E+03	5.03E+02	6.45E+03	4.80E+03	2.97E+01	1.42E+00
50000	3.12E+03	5.03E+02	6.20E+03	4.73E+03	2.97E+01	1.39E+00
60000	3.04E+03	5.03E+02	6.04E+03	4.59E+03	2.98E+01	1.37E+00
70000	2.93E+03	5.00E+02	5.87E+03	4.46E+03	2.98E+01	1.35E+00
80000	2.79E+03	4.98E+02	5.61E+03	4.37E+03	3.00E+01	1.32E+00
90000	2.71E+03	4.99E+02	5.43E+03	4.31E+03	3.00E+01	1.30E+00
100000	2.62E+03	4.99E+02	5.25E+03	4.25E+03	3.02E+01	1.27E+00
110000	2.47E+03	4.99E+02	4.95E+03	4.18E+03	3.03E+01	1.26E+00
120000	2.39E+03	5.03E+02	4.75E+03	4.04E+03	3.02E+01	1.24E+00
130000	2.33E+03	5.02E+02	4.64E+03	3.96E+03	3.03E+01	1.21E+00
140000	2.21E+03	5.03E+02	4.38E+03	3.83E+03	3.03E+01	1.19E+00
149898	2.14E+03	5.02E+02	4.26E+03	3.77E+03	3.04E+01	1.18E+00

60% F-RCA

Cycles	Stress (kPa)	Micro Strain	Stiffness (MPa)	Modulus (MPa)	Phase Angle (Deg)	Energy (kPa)
50	3.36E+03	5.05E+02	6.65E+03	5.28E+03	3.05E+01	1.18E+00
500	3.15E+03	5.06E+02	6.22E+03	5.04E+03	3.44E+01	1.15E+00
1000	3.07E+03	5.03E+02	6.11E+03	4.99E+03	3.46E+01	1.13E+00
2000	2.97E+03	4.99E+02	5.94E+03	4.90E+03	3.27E+01	1.13E+00
3000	2.88E+03	5.02E+02	5.74E+03	4.86E+03	3.27E+01	1.11E+00
4000	2.84E+03	5.02E+02	5.65E+03	4.74E+03	3.29E+01	1.10E+00
5000	2.77E+03	5.02E+02	5.52E+03	4.63E+03	3.28E+01	1.09E+00
6000	2.72E+03	5.00E+02	5.44E+03	4.50E+03	3.29E+01	1.08E+00
7000	2.66E+03	4.97E+02	5.35E+03	4.40E+03	3.29E+01	1.06E+00
8000	2.59E+03	4.98E+02	5.20E+03	4.35E+03	3.29E+01	1.05E+00
9000	2.54E+03	4.97E+02	5.11E+03	4.20E+03	3.30E+01	1.05E+00
10000	2.50E+03	5.00E+02	4.99E+03	4.07E+03	3.29E+01	1.04E+00
20000	2.34E+03	5.00E+02	4.69E+03	3.95E+03	3.30E+01	1.03E+00
30000	2.29E+03	5.01E+02	4.56E+03	3.88E+03	3.30E+01	1.01E+00
40000	2.22E+03	5.00E+02	4.44E+03	3.80E+03	3.30E+01	9.90E-01
50000	2.18E+03	5.03E+02	4.33E+03	3.72E+03	3.31E+01	9.70E-01
60000	2.14E+03	5.00E+02	4.28E+03	3.66E+03	3.31E+01	9.60E-01
70000	2.08E+03	4.96E+02	4.20E+03	3.63E+03	3.32E+01	9.50E-01
80000	2.02E+03	4.97E+02	4.07E+03	3.58E+03	3.32E+01	9.10E-01
90000	1.97E+03	4.98E+02	3.95E+03	3.50E+03	3.32E+01	8.90E-01
100000	1.91E+03	5.00E+02	3.82E+03	3.49E+03	3.32E+01	8.80E-01
110000	1.86E+03	5.01E+02	3.70E+03	3.45E+03	3.32E+01	8.60E-01
120000	1.79E+03	5.03E+02	3.56E+03	3.41E+03	3.33E+01	8.50E-01
130000	1.74E+03	5.00E+02	3.47E+03	3.38E+03	3.33E+01	8.20E-01
136234	1.67E+03	5.03E+02	3.32E+03	3.29E+03	3.33E+01	8.30E-01

80% F-RCA

Cycles	Stress (kPa)	Micro Strain	Stiffness (MPa)	Modulus (MPa)	Phase Angle (Deg)	Energy (kPa)
50	2.36E+03	5.09E+02	4.64E+03	4.16E+03	3.34E+01	5.10E-01
500	2.31E+03	5.08E+02	4.54E+03	3.99E+03	3.75E+01	4.90E-01
1000	2.25E+03	5.05E+02	4.46E+03	3.90E+03	3.74E+01	4.80E-01
2000	2.20E+03	4.99E+02	4.40E+03	3.87E+03	3.62E+01	4.60E-01
3000	2.15E+03	5.03E+02	4.28E+03	3.79E+03	3.57E+01	4.60E-01
4000	2.10E+03	5.04E+02	4.17E+03	3.69E+03	3.57E+01	4.40E-01
5000	2.07E+03	5.04E+02	4.10E+03	3.63E+03	3.57E+01	4.30E-01
6000	2.02E+03	5.03E+02	4.02E+03	3.55E+03	3.58E+01	4.20E-01
7000	1.99E+03	5.00E+02	3.98E+03	3.48E+03	3.59E+01	4.00E-01
8000	1.94E+03	5.03E+02	3.86E+03	3.41E+03	3.58E+01	3.90E-01
9000	1.88E+03	5.02E+02	3.74E+03	3.37E+03	3.59E+01	3.70E-01
10000	1.84E+03	4.97E+02	3.70E+03	3.34E+03	3.59E+01	3.70E-01
20000	1.80E+03	5.00E+02	3.60E+03	3.26E+03	3.60E+01	3.50E-01
30000	1.74E+03	4.95E+02	3.52E+03	3.18E+03	3.60E+01	3.30E-01
40000	1.66E+03	4.97E+02	3.33E+03	3.12E+03	3.62E+01	3.20E-01
50000	1.57E+03	4.99E+02	3.15E+03	3.05E+03	3.62E+01	3.00E-01
60000	1.49E+03	5.03E+02	2.95E+03	2.93E+03	3.62E+01	2.70E-01
70000	1.44E+03	5.03E+02	2.86E+03	2.90E+03	3.63E+01	2.60E-01
80000	1.36E+03	5.02E+02	2.70E+03	2.85E+03	3.63E+01	2.50E-01
90000	1.30E+03	5.01E+02	2.59E+03	2.81E+03	3.64E+01	2.40E-01
100000	1.24E+03	5.02E+02	2.47E+03	2.78E+03	3.63E+01	2.20E-01
109873	1.17E+03	5.03E+02	2.32E+03	2.74E+03	3.63E+01	2.00E-01

20% C-RCA

Cycles	Stress (kPa)	Micro Strain	Stiffness (MPa)	Modulus (MPa)	Phase Angle (Deg)	Energy (kPa)
50	3.62E+03	5.09E+02	7.12E+03	5.56E+03	2.59E+01	7.60E-01
500	3.46E+03	5.08E+02	6.81E+03	5.44E+03	2.85E+01	7.40E-01
1000	3.40E+03	5.05E+02	6.74E+03	5.35E+03	2.91E+01	7.40E-01
2000	3.37E+03	5.01E+02	6.72E+03	5.24E+03	2.82E+01	7.20E-01
3000	3.33E+03	5.00E+02	6.66E+03	5.16E+03	2.76E+01	7.10E-01
4000	3.29E+03	5.00E+02	6.58E+03	4.90E+03	2.76E+01	7.00E-01
5000	3.25E+03	5.01E+02	6.50E+03	4.84E+03	2.74E+01	6.90E-01
6000	3.18E+03	5.02E+02	6.33E+03	4.76E+03	2.74E+01	6.70E-01
7000	3.09E+03	4.97E+02	6.22E+03	4.69E+03	2.75E+01	6.60E-01
8000	3.01E+03	4.96E+02	6.07E+03	4.61E+03	2.75E+01	6.40E-01
9000	2.96E+03	4.99E+02	5.94E+03	4.57E+03	2.75E+01	6.20E-01
10000	2.86E+03	5.00E+02	5.71E+03	4.41E+03	2.76E+01	6.00E-01
20000	2.74E+03	5.02E+02	5.46E+03	4.35E+03	2.76E+01	6.00E-01
30000	2.66E+03	4.98E+02	5.33E+03	4.26E+03	2.78E+01	5.80E-01
40000	2.57E+03	5.04E+02	5.10E+03	4.15E+03	2.77E+01	5.70E-01
50000	2.52E+03	5.02E+02	5.02E+03	4.07E+03	2.78E+01	5.50E-01
60000	2.47E+03	4.98E+02	4.97E+03	3.99E+03	2.77E+01	5.30E-01
70000	2.44E+03	4.99E+02	4.89E+03	3.90E+03	2.77E+01	5.20E-01
80000	2.35E+03	5.03E+02	4.68E+03	3.82E+03	2.78E+01	5.10E-01
90000	2.29E+03	5.03E+02	4.54E+03	3.76E+03	2.78E+01	4.80E-01
100000	2.23E+03	5.02E+02	4.44E+03	3.67E+03	2.80E+01	4.50E-01
110000	2.16E+03	5.03E+02	4.29E+03	3.60E+03	2.78E+01	4.40E-01
120000	2.07E+03	5.00E+02	4.13E+03	3.49E+03	2.79E+01	4.30E-01
130000	1.94E+03	5.01E+02	3.88E+03	3.40E+03	2.80E+01	4.10E-01
140000	1.88E+03	5.00E+02	3.76E+03	3.32E+03	2.80E+01	3.80E-01
152723	1.78E+03	4.99E+02	3.56E+03	3.23E+03	2.82E+01	3.50E-01

40% C-RCA

Cycles	Stress (kPa)	Micro Strain	Stiffness (MPa)	Modulus (MPa)	Phase Angle (Deg)	Energy (kPa)
50	4.03E+03	5.04E+02	8.00E+03	5.79E+03	2.44E+01	1.56E+00
500	3.87E+03	5.06E+02	7.66E+03	5.66E+03	2.72E+01	1.52E+00
1000	3.81E+03	5.05E+02	7.55E+03	5.51E+03	2.75E+01	1.52E+00
2000	3.78E+03	5.00E+02	7.56E+03	5.46E+03	2.53E+01	1.52E+00
3000	3.73E+03	4.99E+02	7.47E+03	5.36E+03	2.50E+01	1.50E+00
4000	3.67E+03	4.99E+02	7.36E+03	5.22E+03	2.52E+01	1.50E+00
5000	3.64E+03	5.00E+02	7.27E+03	5.17E+03	2.52E+01	1.48E+00
6000	3.59E+03	5.03E+02	7.13E+03	5.03E+03	2.53E+01	1.46E+00
7000	3.55E+03	4.96E+02	7.15E+03	4.97E+03	2.54E+01	1.45E+00
8000	3.51E+03	4.99E+02	7.02E+03	4.90E+03	2.53E+01	1.45E+00
9000	3.46E+03	5.02E+02	6.90E+03	4.76E+03	2.55E+01	1.43E+00
10000	3.41E+03	4.99E+02	6.84E+03	4.69E+03	2.55E+01	1.41E+00
20000	3.30E+03	4.98E+02	6.63E+03	4.60E+03	2.55E+01	1.40E+00
30000	3.25E+03	5.03E+02	6.47E+03	4.55E+03	2.57E+01	1.37E+00
40000	3.16E+03	5.01E+02	6.30E+03	4.47E+03	2.58E+01	1.35E+00
50000	3.03E+03	5.01E+02	6.04E+03	4.35E+03	2.57E+01	1.34E+00
60000	2.94E+03	5.01E+02	5.88E+03	4.26E+03	2.57E+01	1.33E+00
70000	2.85E+03	5.01E+02	5.69E+03	4.12E+03	2.58E+01	1.30E+00
80000	2.77E+03	4.98E+02	5.57E+03	4.08E+03	2.59E+01	1.27E+00
90000	2.64E+03	4.99E+02	5.29E+03	3.99E+03	2.58E+01	1.25E+00
100000	2.54E+03	4.99E+02	5.09E+03	3.93E+03	2.60E+01	1.22E+00
110000	2.43E+03	4.99E+02	4.87E+03	3.86E+03	2.59E+01	1.20E+00
120000	2.33E+03	5.01E+02	4.66E+03	3.81E+03	2.60E+01	1.19E+00
130000	2.25E+03	5.01E+02	4.49E+03	3.68E+03	2.60E+01	1.18E+00
140000	2.14E+03	5.00E+02	4.27E+03	3.59E+03	2.60E+01	1.16E+00
150000	2.07E+03	5.01E+02	4.14E+03	3.51E+03	2.61E+01	1.14E+00
157621	2.01E+03	5.02E+02	4.00E+03	3.42E+03	2.61E+01	1.13E+00

60% C-RCA

Cycles	Stress (kPa)	Micro Strain	Stiffness (MPa)	Modulus (MPa)	Phase Angle (Deg)	Energy (kPa)
50	4.29E+03	5.08E+02	8.45E+03	5.89E+03	2.50E+01	1.47E+00
500	4.23E+03	5.05E+02	8.37E+03	5.81E+03	2.78E+01	1.43E+00
1000	4.15E+03	5.00E+02	8.29E+03	5.77E+03	2.80E+01	1.41E+00
2000	4.01E+03	5.00E+02	8.03E+03	5.64E+03	2.65E+01	1.40E+00
3000	3.92E+03	4.99E+02	7.86E+03	5.54E+03	2.64E+01	1.40E+00
4000	3.83E+03	4.98E+02	7.70E+03	5.45E+03	2.65E+01	1.38E+00
5000	3.74E+03	4.96E+02	7.55E+03	5.38E+03	2.65E+01	1.38E+00
6000	3.71E+03	5.00E+02	7.43E+03	5.26E+03	2.67E+01	1.36E+00
7000	3.62E+03	5.00E+02	7.24E+03	5.13E+03	2.66E+01	1.35E+00
8000	3.53E+03	4.98E+02	7.09E+03	5.07E+03	2.67E+01	1.34E+00
9000	3.49E+03	5.03E+02	6.93E+03	5.00E+03	2.67E+01	1.34E+00
10000	3.41E+03	5.02E+02	6.79E+03	4.93E+03	2.69E+01	1.31E+00
20000	3.36E+03	5.05E+02	6.66E+03	4.88E+03	2.69E+01	1.31E+00
30000	3.28E+03	4.98E+02	6.58E+03	4.83E+03	2.67E+01	1.28E+00
40000	3.21E+03	5.00E+02	6.43E+03	4.79E+03	2.69E+01	1.27E+00
50000	3.14E+03	4.99E+02	6.30E+03	4.69E+03	2.69E+01	1.25E+00
60000	3.02E+03	5.01E+02	6.02E+03	4.51E+03	2.68E+01	1.23E+00
70000	2.95E+03	5.01E+02	5.89E+03	4.46E+03	2.68E+01	1.20E+00
80000	2.88E+03	5.01E+02	5.76E+03	4.36E+03	2.69E+01	1.18E+00
90000	2.80E+03	5.01E+02	5.59E+03	4.24E+03	2.70E+01	1.18E+00
100000	2.68E+03	5.01E+02	5.35E+03	4.18E+03	2.70E+01	1.17E+00
110000	2.58E+03	4.97E+02	5.18E+03	4.10E+03	2.72E+01	1.15E+00
120000	2.49E+03	4.99E+02	4.98E+03	4.01E+03	2.71E+01	1.13E+00
130000	2.35E+03	4.98E+02	4.72E+03	3.93E+03	2.72E+01	1.10E+00
140000	2.25E+03	4.98E+02	4.51E+03	3.80E+03	2.73E+01	1.09E+00
153629	2.12E+03	5.02E+02	4.23E+03	3.70E+03	2.73E+01	1.06E+00

80% C-RCA

Cycles	Stress (kPa)	Micro Strain	Stiffness (MPa)	Modulus (MPa)	Phase Angle (Deg)	Energy (kPa)
50	3.42E+03	5.09E+02	6.73E+03	5.29E+03	2.53E+01	9.80E-01
500	3.29E+03	5.08E+02	6.48E+03	5.17E+03	2.75E+01	9.50E-01
1000	3.26E+03	5.05E+02	6.46E+03	5.03E+03	2.80E+01	9.40E-01
2000	3.11E+03	5.03E+02	6.18E+03	4.92E+03	2.71E+01	9.30E-01
3000	2.97E+03	4.99E+02	5.95E+03	4.84E+03	2.70E+01	9.30E-01
4000	2.88E+03	5.03E+02	5.72E+03	4.69E+03	2.70E+01	9.20E-01
5000	2.81E+03	5.02E+02	5.59E+03	4.51E+03	2.71E+01	9.00E-01
6000	2.75E+03	5.02E+02	5.48E+03	4.44E+03	2.71E+01	8.80E-01
7000	2.70E+03	5.03E+02	5.36E+03	4.35E+03	2.71E+01	8.70E-01
8000	2.60E+03	4.97E+02	5.23E+03	4.26E+03	2.72E+01	8.60E-01
9000	2.54E+03	4.96E+02	5.13E+03	4.13E+03	2.73E+01	8.50E-01
10000	2.49E+03	4.99E+02	4.98E+03	4.07E+03	2.73E+01	8.40E-01
20000	2.43E+03	5.03E+02	4.82E+03	4.00E+03	2.73E+01	8.20E-01
30000	2.35E+03	4.99E+02	4.71E+03	3.94E+03	2.72E+01	8.00E-01
40000	2.25E+03	5.02E+02	4.47E+03	3.89E+03	2.73E+01	7.80E-01
50000	2.20E+03	5.00E+02	4.40E+03	3.83E+03	2.75E+01	7.60E-01
60000	2.13E+03	5.00E+02	4.26E+03	3.80E+03	2.75E+01	7.40E-01
70000	2.06E+03	5.01E+02	4.12E+03	3.75E+03	2.75E+01	7.20E-01
80000	1.99E+03	5.02E+02	3.97E+03	3.70E+03	2.76E+01	7.00E-01
90000	1.95E+03	5.03E+02	3.88E+03	3.69E+03	2.76E+01	6.90E-01
100000	1.92E+03	5.03E+02	3.82E+03	3.62E+03	2.77E+01	6.80E-01
110000	1.88E+03	5.03E+02	3.74E+03	3.57E+03	2.77E+01	6.60E-01
120000	1.84E+03	4.98E+02	3.69E+03	3.50E+03	2.78E+01	6.30E-01
130000	1.80E+03	5.00E+02	3.59E+03	3.47E+03	2.78E+01	6.20E-01
140000	1.75E+03	5.00E+02	3.51E+03	3.42E+03	2.78E+01	5.90E-01
153376	1.69E+03	5.01E+02	3.36E+03	3.37E+03	2.79E+01	5.60E-01

20% M-RCA

Cycles	Stress (kPa)	Micro Strain	Stiffness (MPa)	Modulus (MPa)	Phase Angle (Deg)	Energy (kPa)
50	4.03E+03	5.05E+02	7.99E+03	5.80E+03	2.68E+01	1.29E+00
500	3.73E+03	5.05E+02	7.38E+03	5.68E+03	2.98E+01	1.26E+00
1000	3.69E+03	5.03E+02	7.33E+03	5.49E+03	3.00E+01	1.26E+00
2000	3.59E+03	5.01E+02	7.17E+03	5.40E+03	2.84E+01	1.25E+00
3000	3.53E+03	4.99E+02	7.07E+03	5.35E+03	2.82E+01	1.24E+00
4000	3.45E+03	4.99E+02	6.92E+03	5.25E+03	2.84E+01	1.23E+00
5000	3.39E+03	4.98E+02	6.81E+03	5.15E+03	2.85E+01	1.23E+00
6000	3.31E+03	4.99E+02	6.63E+03	5.07E+03	2.85E+01	1.20E+00
7000	3.23E+03	4.96E+02	6.51E+03	4.96E+03	2.85E+01	1.18E+00
8000	3.16E+03	5.00E+02	6.31E+03	4.82E+03	2.86E+01	1.17E+00
9000	3.10E+03	5.00E+02	6.20E+03	4.79E+03	2.84E+01	1.17E+00
10000	3.02E+03	5.03E+02	6.00E+03	4.72E+03	2.85E+01	1.16E+00
20000	2.88E+03	4.98E+02	5.79E+03	4.67E+03	2.84E+01	1.15E+00
30000	2.81E+03	4.99E+02	5.64E+03	4.60E+03	2.86E+01	1.13E+00
40000	2.74E+03	4.99E+02	5.49E+03	4.53E+03	2.86E+01	1.13E+00
50000	2.69E+03	4.99E+02	5.40E+03	4.46E+03	2.88E+01	1.10E+00
60000	2.64E+03	4.99E+02	5.29E+03	4.38E+03	2.87E+01	1.08E+00
70000	2.58E+03	5.02E+02	5.15E+03	4.23E+03	2.88E+01	1.08E+00
80000	2.52E+03	5.01E+02	5.02E+03	4.14E+03	2.88E+01	1.06E+00
90000	2.47E+03	5.03E+02	4.92E+03	4.10E+03	2.88E+01	1.05E+00
100000	2.39E+03	4.98E+02	4.81E+03	3.99E+03	2.89E+01	1.05E+00
110000	2.31E+03	5.00E+02	4.61E+03	3.90E+03	2.89E+01	1.02E+00
120000	2.24E+03	5.00E+02	4.47E+03	3.86E+03	2.91E+01	9.80E-01
130000	2.17E+03	5.02E+02	4.32E+03	3.79E+03	2.90E+01	9.60E-01
140000	2.13E+03	5.03E+02	4.24E+03	3.70E+03	2.91E+01	9.50E-01
151096	2.00E+03	5.00E+02	3.99E+03	3.63E+03	2.92E+01	9.30E-01

40% M-RCA

Cycles	Stress (kPa)	Micro Strain	Stiffness (MPa)	Modulus (MPa)	Phase Angle (Deg)	Energy (kPa)
50	4.06E+03	5.07E+02	8.01E+03	5.78E+03	2.33E+01	1.01E+00
500	3.82E+03	5.04E+02	7.58E+03	5.62E+03	2.58E+01	9.60E-01
1000	3.77E+03	5.04E+02	7.48E+03	5.50E+03	2.65E+01	9.50E-01
2000	3.69E+03	5.03E+02	7.34E+03	5.41E+03	2.52E+01	9.30E-01
3000	3.63E+03	5.00E+02	7.26E+03	5.38E+03	2.52E+01	9.30E-01
4000	3.55E+03	5.00E+02	7.11E+03	5.26E+03	2.51E+01	9.10E-01
5000	3.46E+03	4.98E+02	6.95E+03	5.16E+03	2.52E+01	9.00E-01
6000	3.41E+03	5.00E+02	6.81E+03	5.07E+03	2.50E+01	8.80E-01
7000	3.34E+03	4.96E+02	6.74E+03	4.93E+03	2.50E+01	8.70E-01
8000	3.25E+03	5.01E+02	6.49E+03	4.88E+03	2.52E+01	8.50E-01
9000	3.17E+03	5.00E+02	6.35E+03	4.76E+03	2.51E+01	8.50E-01
10000	3.07E+03	5.02E+02	6.12E+03	4.70E+03	2.51E+01	8.30E-01
20000	3.02E+03	5.00E+02	6.04E+03	4.60E+03	2.50E+01	8.10E-01
30000	2.93E+03	4.99E+02	5.87E+03	4.56E+03	2.52E+01	8.00E-01
40000	2.87E+03	4.99E+02	5.74E+03	4.46E+03	2.52E+01	7.80E-01
50000	2.79E+03	4.99E+02	5.59E+03	4.37E+03	2.54E+01	7.70E-01
60000	2.68E+03	4.97E+02	5.39E+03	4.29E+03	2.53E+01	7.60E-01
70000	2.61E+03	4.98E+02	5.24E+03	4.15E+03	2.52E+01	7.30E-01
80000	2.51E+03	5.00E+02	5.02E+03	4.04E+03	2.53E+01	7.10E-01
90000	2.47E+03	5.01E+02	4.92E+03	3.91E+03	2.53E+01	6.90E-01
100000	2.39E+03	5.03E+02	4.74E+03	3.89E+03	2.54E+01	6.80E-01
110000	2.30E+03	5.02E+02	4.58E+03	3.79E+03	2.54E+01	6.70E-01
120000	2.24E+03	5.00E+02	4.48E+03	3.71E+03	2.54E+01	6.40E-01
130000	2.18E+03	4.97E+02	4.39E+03	3.68E+03	2.55E+01	6.10E-01
140000	2.14E+03	4.96E+02	4.32E+03	3.59E+03	2.56E+01	6.00E-01
150000	2.06E+03	4.99E+02	4.13E+03	3.50E+03	2.56E+01	5.90E-01
159260	2.00E+03	5.00E+02	4.00E+03	3.49E+03	2.57E+01	5.70E-01

60% M-RCA

Cycles	Stress (kPa)	Micro Strain	Stiffness (MPa)	Modulus (MPa)	Phase Angle (Deg)	Energy (kPa)
50	3.64E+03	5.11E+02	7.13E+03	5.60E+03	3.00E+01	1.16E+00
500	3.51E+03	5.08E+02	6.91E+03	5.49E+03	3.42E+01	1.13E+00
1000	3.43E+03	5.03E+02	6.82E+03	5.37E+03	3.43E+01	1.13E+00
2000	3.36E+03	5.00E+02	6.72E+03	5.26E+03	3.24E+01	1.11E+00
3000	3.27E+03	4.99E+02	6.56E+03	5.13E+03	3.15E+01	1.10E+00
4000	3.22E+03	4.97E+02	6.47E+03	5.08E+03	3.15E+01	1.09E+00
5000	3.13E+03	5.00E+02	6.26E+03	4.99E+03	3.14E+01	1.08E+00
6000	3.06E+03	5.02E+02	6.09E+03	4.91E+03	3.15E+01	1.06E+00
7000	3.00E+03	4.98E+02	6.02E+03	4.85E+03	3.15E+01	1.06E+00
8000	2.90E+03	4.99E+02	5.82E+03	4.76E+03	3.15E+01	1.04E+00
9000	2.84E+03	5.02E+02	5.65E+03	4.64E+03	3.16E+01	1.04E+00
10000	2.76E+03	5.00E+02	5.53E+03	4.54E+03	3.16E+01	1.02E+00
20000	2.68E+03	5.01E+02	5.34E+03	4.45E+03	3.16E+01	1.01E+00
30000	2.60E+03	5.00E+02	5.20E+03	4.36E+03	3.17E+01	9.98E-01
40000	2.52E+03	5.01E+02	5.04E+03	4.27E+03	3.18E+01	9.89E-01
50000	2.45E+03	5.03E+02	4.86E+03	4.18E+03	3.19E+01	9.80E-01
60000	2.37E+03	4.97E+02	4.77E+03	4.08E+03	3.18E+01	9.70E-01
70000	2.29E+03	4.98E+02	4.60E+03	3.99E+03	3.18E+01	9.60E-01
80000	2.21E+03	4.98E+02	4.45E+03	3.90E+03	3.19E+01	9.40E-01
90000	2.14E+03	5.00E+02	4.28E+03	3.81E+03	3.19E+01	9.20E-01
100000	2.06E+03	5.04E+02	4.09E+03	3.72E+03	3.19E+01	9.00E-01
110000	1.98E+03	5.03E+02	3.94E+03	3.62E+03	3.20E+01	8.80E-01
120000	1.91E+03	5.04E+02	3.78E+03	3.53E+03	3.20E+01	8.50E-01
130000	1.83E+03	5.00E+02	3.66E+03	3.44E+03	3.22E+01	8.30E-01
138798	1.77E+03	4.97E+02	3.56E+03	3.35E+03	3.21E+01	8.20E-01

80% M-RCA

Cycles	Stress (kPa)	Micro Strain	Stiffness (MPa)	Modulus (MPa)	Phase Angle (Deg)	Energy (kPa)
50	2.79E+03	5.09E+02	5.48E+03	4.21E+03	3.31E+01	6.30E-01
500	2.61E+03	5.05E+02	5.17E+03	4.09E+03	3.71E+01	6.10E-01
1000	2.57E+03	5.00E+02	5.15E+03	3.94E+03	3.74E+01	6.00E-01
2000	2.52E+03	4.98E+02	5.06E+03	3.87E+03	3.40E+01	5.80E-01
3000	2.47E+03	4.96E+02	4.98E+03	3.74E+03	3.40E+01	5.70E-01
4000	2.42E+03	5.00E+02	4.83E+03	3.68E+03	3.40E+01	5.50E-01
5000	2.37E+03	5.02E+02	4.71E+03	3.60E+03	3.42E+01	5.40E-01
6000	2.32E+03	5.00E+02	4.65E+03	3.50E+03	3.40E+01	5.20E-01
7000	2.29E+03	5.03E+02	4.55E+03	3.42E+03	3.41E+01	5.10E-01
8000	2.24E+03	5.02E+02	4.46E+03	3.33E+03	3.41E+01	5.00E-01
9000	2.20E+03	4.97E+02	4.43E+03	3.28E+03	3.42E+01	4.90E-01
10000	2.18E+03	4.98E+02	4.37E+03	3.23E+03	3.43E+01	4.90E-01
20000	2.08E+03	5.00E+02	4.16E+03	3.18E+03	3.43E+01	4.80E-01
30000	2.04E+03	4.98E+02	4.09E+03	3.12E+03	3.45E+01	4.70E-01
40000	1.98E+03	5.00E+02	3.95E+03	3.07E+03	3.44E+01	4.60E-01
50000	1.90E+03	4.99E+02	3.80E+03	3.02E+03	3.44E+01	4.40E-01
60000	1.83E+03	4.99E+02	3.67E+03	2.97E+03	3.45E+01	4.30E-01
70000	1.75E+03	5.00E+02	3.51E+03	2.92E+03	3.47E+01	4.20E-01
80000	1.67E+03	5.00E+02	3.35E+03	2.87E+03	3.47E+01	4.00E-01
90000	1.62E+03	5.01E+02	3.23E+03	2.82E+03	3.47E+01	3.70E-01
100000	1.58E+03	5.01E+02	3.16E+03	2.77E+03	3.48E+01	3.50E-01
110000	1.53E+03	5.02E+02	3.04E+03	2.71E+03	3.48E+01	3.20E-01
120000	1.45E+03	5.01E+02	2.90E+03	2.66E+03	3.49E+01	3.10E-01
130131	1.37E+03	5.02E+02	2.74E+03	2.61E+03	3.49E+01	2.80E-01

APPENDIX E

Flexural beam fatigue test of SMA specimens

VA

Cycles	Stress (kPa)	Micro Strain	Stiffness (MPa)	Modulus (MPa)	Phase Angle (Deg)	Energy (kPa)
50	1.57E+03	5.15E+02	3.05E+03	3.00E+03	4.03E+01	5.80E-01
500	1.40E+03	5.03E+02	2.79E+03	2.86E+03	4.53E+01	5.30E-01
1000	1.35E+03	5.01E+02	2.69E+03	2.80E+03	4.54E+01	5.20E-01
2000	1.28E+03	4.99E+02	2.57E+03	2.77E+03	4.31E+01	5.10E-01
3000	1.24E+03	4.99E+02	2.49E+03	2.71E+03	4.51E+01	5.00E-01
4000	1.21E+03	4.99E+02	2.42E+03	2.63E+03	4.46E+01	4.90E-01
5000	1.18E+03	5.01E+02	2.35E+03	2.60E+03	4.52E+01	4.90E-01
6000	1.17E+03	5.02E+02	2.32E+03	2.55E+03	4.45E+01	4.80E-01
7000	1.15E+03	5.00E+02	2.30E+03	2.51E+03	4.50E+01	4.80E-01
8000	1.13E+03	5.00E+02	2.27E+03	2.47E+03	4.47E+01	4.70E-01
9000	1.12E+03	5.00E+02	2.25E+03	2.42E+03	4.44E+01	4.70E-01
10000	1.10E+03	5.01E+02	2.20E+03	2.30E+03	4.54E+01	4.70E-01
20000	1.00E+03	5.02E+02	1.99E+03	2.27E+03	4.44E+01	4.40E-01
30000	9.19E+02	5.02E+02	1.83E+03	2.16E+03	4.38E+01	4.30E-01
40000	8.63E+02	5.02E+02	1.72E+03	2.06E+03	4.26E+01	4.10E-01
50000	8.47E+02	5.03E+02	1.68E+03	1.96E+03	4.26E+01	4.10E-01
60000	8.08E+02	4.99E+02	1.62E+03	1.90E+03	4.33E+01	4.00E-01
70169	7.66E+02	5.03E+02	1.52E+03	1.87E+03	4.37E+01	3.90E-01

20% F-RCA

Cycles	Stress (kPa)	Micro Strain	Stiffness (MPa)	Modulus (MPa)	Phase Angle (Deg)	Energy (kPa)
50	2.07E+03	5.08E+02	4.07E+03	3.67E+03	3.45E+01	8.60E-01
500	1.91E+03	5.04E+02	3.79E+03	3.35E+03	3.74E+01	8.20E-01
1000	1.88E+03	5.00E+02	3.76E+03	3.26E+03	3.79E+01	8.00E-01
2000	1.81E+03	5.00E+02	3.62E+03	3.12E+03	3.72E+01	7.40E-01
3000	1.77E+03	4.99E+02	3.55E+03	3.01E+03	3.74E+01	7.10E-01
4000	1.75E+03	5.00E+02	3.50E+03	2.97E+03	3.74E+01	7.00E-01
5000	1.73E+03	4.97E+02	3.48E+03	2.90E+03	3.74E+01	7.00E-01
6000	1.71E+03	5.03E+02	3.40E+03	2.85E+03	3.74E+01	6.70E-01
7000	1.68E+03	5.02E+02	3.35E+03	2.82E+03	3.77E+01	6.60E-01
8000	1.65E+03	5.00E+02	3.30E+03	2.62E+03	3.76E+01	6.60E-01
9000	1.63E+03	4.99E+02	3.27E+03	2.53E+03	3.76E+01	6.50E-01
10000	1.59E+03	4.99E+02	3.19E+03	2.43E+03	3.78E+01	6.50E-01
20000	1.48E+03	4.99E+02	2.97E+03	2.34E+03	3.78E+01	6.40E-01
30000	1.43E+03	4.97E+02	2.87E+03	2.24E+03	3.77E+01	6.40E-01
40000	1.34E+03	4.98E+02	2.69E+03	2.14E+03	3.79E+01	6.30E-01
50000	1.28E+03	5.00E+02	2.56E+03	2.05E+03	3.79E+01	6.30E-01
60000	1.25E+03	5.03E+02	2.49E+03	1.95E+03	3.80E+01	6.30E-01
70000	1.20E+03	5.00E+02	2.39E+03	1.91E+03	3.82E+01	6.10E-01
80000	1.14E+03	5.02E+02	2.27E+03	1.89E+03	3.82E+01	5.90E-01
90000	1.10E+03	5.02E+02	2.18E+03	1.84E+03	3.81E+01	5.90E-01
100000	1.05E+03	4.98E+02	2.11E+03	1.80E+03	3.82E+01	5.90E-01
109677	1.01E+03	4.95E+02	2.04E+03	1.73E+03	3.83E+01	5.70E-01

40% F-RCA

Cycles	Stress (kPa)	Micro Strain	Stiffness (MPa)	Modulus (MPa)	Phase Angle (Deg)	Energy (kPa)
50	2.42E+03	5.07E+02	4.77E+03	3.91E+03	2.58E+01	1.09E+00
500	2.27E+03	5.05E+02	4.50E+03	3.49E+03	2.94E+01	1.06E+00
1000	2.23E+03	5.00E+02	4.46E+03	3.37E+03	2.94E+01	1.05E+00
2000	2.15E+03	4.98E+02	4.32E+03	3.29E+03	2.86E+01	1.04E+00
3000	2.10E+03	4.99E+02	4.21E+03	3.21E+03	2.85E+01	1.04E+00
4000	1.97E+03	5.02E+02	3.92E+03	3.17E+03	2.85E+01	1.03E+00
5000	1.95E+03	5.02E+02	3.88E+03	3.10E+03	2.86E+01	1.03E+00
6000	1.92E+03	5.02E+02	3.82E+03	2.94E+03	2.85E+01	1.02E+00
7000	1.88E+03	5.00E+02	3.76E+03	2.88E+03	2.85E+01	1.00E+00
8000	1.84E+03	5.01E+02	3.67E+03	2.75E+03	2.86E+01	1.00E+00
9000	1.81E+03	5.00E+02	3.62E+03	2.70E+03	2.87E+01	9.90E-01
10000	1.78E+03	4.99E+02	3.57E+03	2.68E+03	2.87E+01	9.80E-01
20000	1.76E+03	4.99E+02	3.52E+03	2.62E+03	2.87E+01	9.80E-01
30000	1.69E+03	4.98E+02	3.40E+03	2.57E+03	2.88E+01	9.70E-01
40000	1.63E+03	5.03E+02	3.24E+03	2.52E+03	2.87E+01	9.60E-01
50000	1.57E+03	5.01E+02	3.14E+03	2.47E+03	2.89E+01	9.60E-01
60000	1.51E+03	4.97E+02	3.04E+03	2.39E+03	2.90E+01	9.40E-01
70000	1.49E+03	5.00E+02	2.97E+03	2.32E+03	2.89E+01	9.40E-01
80000	1.44E+03	5.00E+02	2.88E+03	2.26E+03	2.89E+01	9.20E-01
90000	1.42E+03	4.99E+02	2.84E+03	2.20E+03	2.90E+01	9.20E-01
100000	1.38E+03	4.99E+02	2.77E+03	2.13E+03	2.90E+01	9.00E-01
110000	1.35E+03	5.02E+02	2.69E+03	2.10E+03	2.91E+01	9.00E-01
120000	1.31E+03	4.97E+02	2.64E+03	2.04E+03	2.90E+01	8.80E-01
130000	1.28E+03	4.98E+02	2.56E+03	1.98E+03	2.91E+01	8.80E-01
140876	1.20E+03	5.04E+02	2.39E+03	1.93E+03	2.92E+01	8.60E-01

60% F-RCA

Cycles	Stress (kPa)	Micro Strain	Stiffness (MPa)	Modulus (MPa)	Phase Angle (Deg)	Energy (kPa)
50	2.35E+03	5.05E+02	4.64E+03	3.55E+03	2.99E+01	9.40E-01
500	2.21E+03	5.04E+02	4.39E+03	3.40E+03	3.26E+01	9.00E-01
1000	2.18E+03	5.00E+02	4.35E+03	3.38E+03	3.27E+01	8.80E-01
2000	2.14E+03	5.00E+02	4.27E+03	3.33E+03	3.24E+01	8.30E-01
3000	2.06E+03	5.01E+02	4.12E+03	3.27E+03	3.17E+01	8.00E-01
4000	2.01E+03	4.99E+02	4.03E+03	3.18E+03	3.17E+01	8.10E-01
5000	1.98E+03	4.98E+02	3.98E+03	3.12E+03	3.17E+01	8.00E-01
6000	1.96E+03	4.97E+02	3.94E+03	3.06E+03	3.18E+01	7.60E-01
7000	1.92E+03	4.98E+02	3.85E+03	3.02E+03	3.18E+01	7.80E-01
8000	1.87E+03	4.98E+02	3.76E+03	2.94E+03	3.17E+01	7.60E-01
9000	1.84E+03	5.01E+02	3.67E+03	2.87E+03	3.18E+01	7.70E-01
10000	1.80E+03	5.01E+02	3.59E+03	2.76E+03	3.19E+01	7.60E-01
20000	1.77E+03	5.00E+02	3.53E+03	2.64E+03	3.19E+01	7.30E-01
30000	1.74E+03	5.01E+02	3.47E+03	2.51E+03	3.19E+01	7.40E-01
40000	1.71E+03	5.00E+02	3.41E+03	2.48E+03	3.19E+01	7.20E-01
50000	1.68E+03	5.03E+02	3.33E+03	2.43E+03	3.20E+01	7.00E-01
60000	1.62E+03	4.98E+02	3.26E+03	2.35E+03	3.19E+01	6.90E-01
70000	1.58E+03	4.99E+02	3.16E+03	2.25E+03	3.20E+01	6.90E-01
80000	1.52E+03	5.02E+02	3.03E+03	2.16E+03	3.21E+01	6.80E-01
90000	1.47E+03	5.01E+02	2.93E+03	2.07E+03	3.21E+01	6.70E-01
100000	1.40E+03	5.03E+02	2.78E+03	1.99E+03	3.20E+01	6.60E-01
110000	1.32E+03	4.97E+02	2.65E+03	1.91E+03	3.21E+01	6.50E-01
120000	1.26E+03	5.02E+02	2.50E+03	1.82E+03	3.22E+01	6.50E-01
130000	1.18E+03	5.02E+02	2.35E+03	1.74E+03	3.23E+01	6.40E-01
132675	1.16E+03	5.00E+02	2.32E+03	1.58E+03	3.23E+01	6.10E-01

80% F-RCA

Cycles	Stress (kPa)	Micro Strain	Stiffness (MPa)	Modulus (MPa)	Phase Angle (Deg)	Energy (kPa)
50	2.49E+03	5.07E+02	4.91E+03	3.90E+03	2.99E+01	9.50E-01
500	2.36E+03	5.02E+02	4.71E+03	3.81E+03	3.32E+01	9.40E-01
1000	2.31E+03	5.00E+02	4.62E+03	3.73E+03	3.33E+01	9.20E-01
2000	2.28E+03	4.97E+02	4.58E+03	3.65E+03	3.24E+01	9.20E-01
3000	2.23E+03	4.97E+02	4.49E+03	3.59E+03	3.19E+01	9.10E-01
4000	2.20E+03	4.98E+02	4.41E+03	3.52E+03	3.19E+01	9.10E-01
5000	2.14E+03	4.98E+02	4.30E+03	3.46E+03	3.19E+01	9.10E-01
6000	2.10E+03	5.00E+02	4.20E+03	3.39E+03	3.20E+01	8.90E-01
7000	2.07E+03	5.00E+02	4.14E+03	3.31E+03	3.20E+01	8.90E-01
8000	2.02E+03	5.02E+02	4.02E+03	3.04E+03	3.20E+01	8.80E-01
9000	1.98E+03	5.04E+02	3.92E+03	2.95E+03	3.21E+01	8.80E-01
10000	1.93E+03	4.99E+02	3.86E+03	2.87E+03	3.21E+01	8.70E-01
20000	1.85E+03	5.01E+02	3.70E+03	2.78E+03	3.21E+01	8.70E-01
30000	1.79E+03	5.02E+02	3.56E+03	2.69E+03	3.21E+01	8.50E-01
40000	1.73E+03	4.99E+02	3.47E+03	2.60E+03	3.23E+01	8.40E-01
50000	1.66E+03	4.99E+02	3.33E+03	2.51E+03	3.22E+01	8.40E-01
60000	1.60E+03	4.98E+02	3.22E+03	2.43E+03	3.23E+01	8.20E-01
70000	1.55E+03	5.03E+02	3.09E+03	2.34E+03	3.23E+01	8.20E-01
80000	1.49E+03	5.00E+02	2.98E+03	2.25E+03	3.24E+01	8.00E-01
90000	1.44E+03	5.00E+02	2.88E+03	2.16E+03	3.23E+01	8.00E-01
100000	1.40E+03	5.01E+02	2.80E+03	2.07E+03	3.24E+01	7.80E-01
110000	1.36E+03	5.01E+02	2.72E+03	1.99E+03	3.24E+01	7.80E-01
120000	1.32E+03	5.02E+02	2.63E+03	1.90E+03	3.25E+01	7.60E-01
132467	1.23E+03	5.03E+02	2.45E+03	1.81E+03	3.25E+01	7.60E-01

20% C-RCA

Cycles	Stress (kPa)	Micro Strain	Stiffness (MPa)	Modulus (MPa)	Phase Angle (Deg)	Energy (kPa)
50	1.87E+03	5.09E+02	3.67E+03	3.41E+03	3.18E+01	9.00E-01
500	1.80E+03	5.03E+02	3.57E+03	3.38E+03	3.46E+01	9.00E-01
1000	1.71E+03	4.99E+02	3.43E+03	3.30E+03	3.46E+01	8.80E-01
2000	1.67E+03	4.99E+02	3.34E+03	3.22E+03	3.34E+01	8.60E-01
3000	1.58E+03	4.99E+02	3.16E+03	3.16E+03	3.34E+01	8.60E-01
4000	1.52E+03	4.98E+02	3.05E+03	3.05E+03	3.35E+01	8.60E-01
5000	1.49E+03	5.00E+02	2.97E+03	2.97E+03	3.35E+01	8.40E-01
6000	1.45E+03	4.98E+02	2.90E+03	2.83E+03	3.35E+01	8.40E-01
7000	1.41E+03	4.99E+02	2.83E+03	2.76E+03	3.35E+01	8.20E-01
8000	1.40E+03	5.01E+02	2.79E+03	2.66E+03	3.36E+01	8.00E-01
9000	1.37E+03	5.00E+02	2.74E+03	2.57E+03	3.38E+01	7.90E-01
10000	1.33E+03	5.01E+02	2.66E+03	2.44E+03	3.37E+01	7.60E-01
20000	1.30E+03	5.04E+02	2.58E+03	2.34E+03	3.38E+01	7.60E-01
30000	1.25E+03	5.02E+02	2.49E+03	2.29E+03	3.39E+01	7.40E-01
40000	1.21E+03	4.98E+02	2.43E+03	2.23E+03	3.39E+01	7.40E-01
50000	1.17E+03	5.00E+02	2.35E+03	2.18E+03	3.38E+01	7.40E-01
60000	1.14E+03	5.00E+02	2.27E+03	2.12E+03	3.39E+01	7.20E-01
70000	1.10E+03	4.99E+02	2.20E+03	2.07E+03	3.40E+01	7.10E-01
80000	1.06E+03	4.99E+02	2.13E+03	2.03E+03	3.40E+01	6.90E-01
90000	1.03E+03	4.97E+02	2.07E+03	1.97E+03	3.41E+01	6.90E-01
100000	9.90E+02	4.99E+02	1.98E+03	1.92E+03	3.42E+01	6.90E-01
110000	9.53E+02	5.01E+02	1.90E+03	1.86E+03	3.42E+01	6.70E-01
119368	9.19E+02	5.01E+02	1.83E+03	1.83E+03	3.43E+01	6.70E-01

40% C-RCA

Cycles	Stress (kPa)	Micro Strain	Stiffness (MPa)	Modulus (MPa)	Phase Angle (Deg)	Energy (kPa)
50	2.06E+03	5.06E+02	4.07E+03	3.67E+03	3.92E+01	7.10E-01
500	1.93E+03	5.02E+02	3.85E+03	3.50E+03	4.37E+01	6.90E-01
1000	1.88E+03	4.99E+02	3.77E+03	3.47E+03	4.38E+01	6.80E-01
2000	1.83E+03	4.98E+02	3.67E+03	3.34E+03	4.34E+01	6.20E-01
3000	1.79E+03	5.00E+02	3.58E+03	3.25E+03	4.31E+01	5.90E-01
4000	1.71E+03	5.00E+02	3.42E+03	3.16E+03	4.30E+01	6.00E-01
5000	1.67E+03	5.00E+02	3.33E+03	3.09E+03	4.26E+01	5.90E-01
6000	1.61E+03	5.03E+02	3.19E+03	3.01E+03	4.28E+01	5.60E-01
7000	1.58E+03	5.03E+02	3.14E+03	2.96E+03	4.25E+01	5.60E-01
8000	1.53E+03	4.97E+02	3.07E+03	2.85E+03	4.25E+01	5.60E-01
9000	1.46E+03	4.98E+02	2.92E+03	2.75E+03	4.22E+01	5.50E-01
10000	1.40E+03	4.97E+02	2.81E+03	2.68E+03	4.22E+01	5.50E-01
20000	1.34E+03	5.00E+02	2.68E+03	2.54E+03	4.23E+01	5.20E-01
30000	1.29E+03	5.01E+02	2.57E+03	2.41E+03	4.25E+01	5.30E-01
40000	1.23E+03	5.02E+02	2.45E+03	2.37E+03	4.25E+01	5.20E-01
50000	1.17E+03	4.99E+02	2.35E+03	2.24E+03	4.27E+01	5.10E-01
60000	1.13E+03	5.02E+02	2.26E+03	2.14E+03	4.26E+01	5.10E-01
70000	1.10E+03	5.00E+02	2.19E+03	2.08E+03	4.27E+01	4.90E-01
80000	1.06E+03	5.00E+02	2.11E+03	2.03E+03	4.28E+01	4.80E-01
89564	1.02E+03	5.03E+02	2.03E+03	1.91E+03	4.28E+01	4.70E-01

60% C-RCA

Cycles	Stress (kPa)	Micro Strain	Stiffness (MPa)	Modulus (MPa)	Phase Angle (Deg)	Energy (kPa)
50	1.89E+03	5.08E+02	3.72E+03	3.20E+03	4.05E+01	6.40E-01
500	1.82E+03	5.01E+02	3.63E+03	3.09E+03	4.36E+01	6.20E-01
1000	1.78E+03	5.04E+02	3.52E+03	3.04E+03	4.38E+01	6.20E-01
2000	1.74E+03	5.02E+02	3.46E+03	2.97E+03	4.40E+01	6.00E-01
3000	1.67E+03	4.98E+02	3.35E+03	2.92E+03	4.26E+01	6.00E-01
4000	1.60E+03	5.00E+02	3.20E+03	2.88E+03	4.28E+01	6.00E-01
5000	1.57E+03	5.00E+02	3.15E+03	2.83E+03	4.25E+01	5.90E-01
6000	1.53E+03	5.03E+02	3.05E+03	2.79E+03	4.25E+01	5.70E-01
7000	1.48E+03	4.99E+02	2.97E+03	2.75E+03	4.24E+01	5.50E-01
8000	1.41E+03	4.99E+02	2.83E+03	2.69E+03	4.25E+01	5.50E-01
9000	1.38E+03	4.99E+02	2.76E+03	2.62E+03	4.27E+01	5.20E-01
10000	1.34E+03	4.98E+02	2.69E+03	2.57E+03	4.27E+01	5.20E-01
20000	1.26E+03	5.00E+02	2.53E+03	2.49E+03	4.26E+01	5.00E-01
30000	1.20E+03	4.98E+02	2.41E+03	2.41E+03	4.26E+01	4.70E-01
40000	1.14E+03	4.99E+02	2.28E+03	2.36E+03	4.27E+01	4.60E-01
50000	1.11E+03	5.01E+02	2.21E+03	2.26E+03	4.27E+01	4.60E-01
60000	1.06E+03	5.00E+02	2.11E+03	2.18E+03	4.29E+01	4.40E-01
70000	1.00E+03	5.00E+02	2.01E+03	2.07E+03	4.29E+01	4.30E-01
80000	9.52E+02	5.00E+02	1.90E+03	1.98E+03	4.30E+01	4.20E-01
86850	9.25E+02	4.98E+02	1.86E+03	1.86E+03	4.30E+01	4.10E-01

80% C-RCA

Cycles	Stress (kPa)	Micro Strain	Stiffness (MPa)	Modulus (MPa)	Phase Angle (Deg)	Energy (kPa)
50	1.49E+03	5.06E+02	2.94E+03	2.86E+03	4.26E+01	4.40E-01
500	1.36E+03	5.02E+02	2.70E+03	2.69E+03	4.48E+01	4.00E-01
1000	1.30E+03	5.01E+02	2.60E+03	2.63E+03	4.63E+01	3.80E-01
2000	1.26E+03	5.01E+02	2.52E+03	2.57E+03	4.56E+01	3.80E-01
3000	1.21E+03	5.00E+02	2.42E+03	2.49E+03	4.56E+01	3.80E-01
4000	1.16E+03	4.98E+02	2.32E+03	2.43E+03	4.51E+01	3.60E-01
5000	1.11E+03	4.98E+02	2.22E+03	2.38E+03	4.51E+01	3.50E-01
6000	1.01E+03	4.97E+02	2.03E+03	2.30E+03	4.47E+01	3.30E-01
7000	9.75E+02	4.98E+02	1.96E+03	2.27E+03	4.47E+01	3.30E-01
8000	9.42E+02	5.01E+02	1.88E+03	2.15E+03	4.43E+01	3.20E-01
9000	9.19E+02	4.99E+02	1.84E+03	2.09E+03	4.45E+01	3.10E-01
10000	8.96E+02	5.00E+02	1.79E+03	2.04E+03	4.46E+01	3.10E-01
20000	8.70E+02	5.00E+02	1.74E+03	1.90E+03	4.45E+01	3.00E-01
30000	8.46E+02	5.01E+02	1.69E+03	1.82E+03	4.45E+01	3.00E-01
40000	8.13E+02	5.00E+02	1.63E+03	1.77E+03	4.42E+01	2.70E-01
50000	7.84E+02	4.99E+02	1.57E+03	1.69E+03	4.44E+01	2.70E-01
60000	7.63E+02	4.99E+02	1.53E+03	1.63E+03	4.44E+01	2.50E-01
70000	7.44E+02	5.00E+02	1.49E+03	1.55E+03	4.46E+01	2.50E-01
73782	7.38E+02	5.02E+02	1.47E+03	1.50E+03	4.49E+01	2.30E-01

20% M-RCA

Cycles	Stress (kPa)	Micro Strain	Stiffness (MPa)	Modulus (MPa)	Phase Angle (Deg)	Energy (kPa)
50	1.98E+03	5.07E+02	3.90E+03	3.42E+03	3.63E+01	7.90E-01
500	1.90E+03	5.03E+02	3.78E+03	3.29E+03	3.94E+01	7.70E-01
1000	1.84E+03	5.00E+02	3.68E+03	3.24E+03	3.98E+01	7.60E-01
2000	1.79E+03	5.00E+02	3.57E+03	3.15E+03	4.04E+01	7.60E-01
3000	1.72E+03	5.02E+02	3.42E+03	3.11E+03	4.04E+01	7.40E-01
4000	1.67E+03	5.01E+02	3.33E+03	3.07E+03	4.02E+01	7.40E-01
5000	1.61E+03	5.00E+02	3.22E+03	2.99E+03	3.96E+01	7.30E-01
6000	1.58E+03	5.00E+02	3.15E+03	2.93E+03	3.96E+01	7.10E-01
7000	1.53E+03	5.01E+02	3.04E+03	2.88E+03	3.97E+01	6.90E-01
8000	1.48E+03	5.00E+02	2.95E+03	2.81E+03	3.96E+01	6.90E-01
9000	1.43E+03	4.98E+02	2.87E+03	2.79E+03	3.99E+01	6.90E-01
10000	1.38E+03	4.99E+02	2.77E+03	2.72E+03	3.98E+01	6.70E-01
20000	1.32E+03	5.01E+02	2.63E+03	2.66E+03	3.98E+01	6.50E-01
30000	1.29E+03	5.00E+02	2.58E+03	2.59E+03	3.99E+01	6.50E-01
40000	1.25E+03	4.98E+02	2.51E+03	2.50E+03	4.00E+01	6.50E-01
50000	1.20E+03	5.03E+02	2.38E+03	2.43E+03	4.00E+01	6.40E-01
60000	1.16E+03	5.02E+02	2.32E+03	2.38E+03	3.99E+01	6.40E-01
70000	1.13E+03	5.01E+02	2.25E+03	2.32E+03	4.00E+01	6.30E-01
80000	1.08E+03	5.01E+02	2.16E+03	2.26E+03	4.02E+01	6.30E-01
90000	1.02E+03	5.00E+02	2.04E+03	2.22E+03	4.03E+01	6.10E-01
101364	9.68E+02	4.97E+02	1.95E+03	2.17E+03	4.03E+01	6.00E-01

40% M-RCA

Cycles	Stress (kPa)	Micro Strain	Stiffness (MPa)	Modulus (MPa)	Phase Angle (Deg)	Energy (kPa)
50	2.30E+03	5.05E+02	4.55E+03	3.49E+03	2.78E+01	9.80E-01
500	2.23E+03	5.03E+02	4.43E+03	3.18E+03	3.18E+01	9.50E-01
1000	2.19E+03	4.99E+02	4.38E+03	3.06E+03	3.19E+01	9.30E-01
2000	2.15E+03	4.98E+02	4.31E+03	2.91E+03	3.12E+01	9.20E-01
3000	2.11E+03	4.99E+02	4.22E+03	2.79E+03	3.06E+01	9.20E-01
4000	2.07E+03	4.99E+02	4.14E+03	2.71E+03	3.06E+01	9.00E-01
5000	1.94E+03	5.00E+02	3.87E+03	2.67E+03	3.05E+01	9.00E-01
6000	1.87E+03	5.03E+02	3.71E+03	2.54E+03	3.06E+01	8.90E-01
7000	1.81E+03	5.04E+02	3.59E+03	2.48E+03	3.07E+01	8.70E-01
8000	1.76E+03	5.00E+02	3.51E+03	2.39E+03	3.06E+01	8.70E-01
9000	1.70E+03	4.97E+02	3.43E+03	2.32E+03	3.07E+01	8.70E-01
10000	1.69E+03	4.97E+02	3.40E+03	2.27E+03	3.07E+01	8.50E-01
20000	1.64E+03	4.98E+02	3.30E+03	2.19E+03	3.07E+01	8.30E-01
30000	1.58E+03	5.03E+02	3.14E+03	2.11E+03	3.08E+01	8.30E-01
40000	1.54E+03	4.98E+02	3.10E+03	2.02E+03	3.07E+01	8.30E-01
50000	1.51E+03	5.00E+02	3.02E+03	1.94E+03	3.08E+01	8.00E-01
60000	1.48E+03	5.01E+02	2.95E+03	1.87E+03	3.08E+01	7.80E-01
70000	1.46E+03	4.99E+02	2.93E+03	1.79E+03	3.08E+01	7.50E-01
80000	1.40E+03	4.97E+02	2.82E+03	1.71E+03	3.09E+01	7.50E-01
90000	1.36E+03	5.02E+02	2.71E+03	1.63E+03	3.09E+01	7.10E-01
100000	1.32E+03	5.01E+02	2.64E+03	1.55E+03	3.10E+01	7.10E-01
110000	1.27E+03	5.00E+02	2.55E+03	1.53E+03	3.09E+01	6.90E-01
120000	1.23E+03	5.02E+02	2.44E+03	1.41E+03	3.09E+01	6.80E-01
130000	1.20E+03	4.97E+02	2.41E+03	1.34E+03	3.10E+01	6.80E-01
138971	1.14E+03	5.00E+02	2.28E+03	1.26E+03	3.11E+01	6.40E-01

60% M-RCA

Cycles	Stress (kPa)	Micro Strain	Stiffness (MPa)	Modulus (MPa)	Phase Angle (Deg)	Energy (kPa)
50	2.07E+03	5.05E+02	4.09E+03	3.71E+03	3.19E+01	8.80E-01
500	1.98E+03	5.00E+02	3.95E+03	3.57E+03	3.46E+01	8.50E-01
1000	1.93E+03	5.00E+02	3.86E+03	3.49E+03	3.53E+01	8.30E-01
2000	1.86E+03	4.98E+02	3.74E+03	3.40E+03	3.44E+01	8.00E-01
3000	1.84E+03	4.99E+02	3.69E+03	3.25E+03	3.41E+01	8.00E-01
4000	1.80E+03	4.99E+02	3.62E+03	3.19E+03	3.42E+01	7.80E-01
5000	1.79E+03	5.00E+02	3.58E+03	3.12E+03	3.42E+01	7.80E-01
6000	1.75E+03	5.01E+02	3.50E+03	3.06E+03	3.43E+01	7.50E-01
7000	1.72E+03	5.03E+02	3.42E+03	2.96E+03	3.43E+01	7.40E-01
8000	1.70E+03	4.98E+02	3.41E+03	2.85E+03	3.43E+01	7.40E-01
9000	1.66E+03	4.99E+02	3.32E+03	2.77E+03	3.46E+01	7.30E-01
10000	1.62E+03	5.00E+02	3.24E+03	2.68E+03	3.45E+01	6.80E-01
20000	1.58E+03	4.97E+02	3.17E+03	2.59E+03	3.46E+01	6.80E-01
30000	1.52E+03	4.97E+02	3.06E+03	2.50E+03	3.47E+01	6.60E-01
40000	1.47E+03	4.98E+02	2.95E+03	2.42E+03	3.47E+01	6.40E-01
50000	1.43E+03	5.01E+02	2.86E+03	2.33E+03	3.47E+01	6.40E-01
60000	1.39E+03	5.00E+02	2.77E+03	2.24E+03	3.49E+01	6.40E-01
70000	1.33E+03	5.00E+02	2.65E+03	2.15E+03	3.48E+01	6.20E-01
80000	1.27E+03	4.99E+02	2.54E+03	2.06E+03	3.49E+01	6.10E-01
90000	1.20E+03	5.00E+02	2.40E+03	1.98E+03	3.49E+01	6.10E-01
100000	1.14E+03	5.02E+02	2.27E+03	1.89E+03	3.51E+01	6.10E-01
110000	1.09E+03	5.01E+02	2.17E+03	1.80E+03	3.52E+01	5.90E-01
117869	1.02E+03	5.00E+02	2.05E+03	1.71E+03	3.52E+01	5.80E-01

80% M-RCA

Cycles	Stress (kPa)	Micro Strain	Stiffness (MPa)	Modulus (MPa)	Phase Angle (Deg)	Energy (kPa)
50	1.85E+03	5.09E+02	3.63E+03	3.31E+03	3.82E+01	7.80E-01
500	1.78E+03	5.03E+02	3.53E+03	3.18E+03	4.38E+01	7.50E-01
1000	1.73E+03	5.01E+02	3.46E+03	3.12E+03	4.38E+01	7.30E-01
2000	1.68E+03	5.00E+02	3.37E+03	3.07E+03	4.26E+01	7.10E-01
3000	1.62E+03	4.99E+02	3.24E+03	3.03E+03	4.24E+01	6.90E-01
4000	1.57E+03	4.99E+02	3.14E+03	2.97E+03	4.24E+01	6.90E-01
5000	1.52E+03	5.00E+02	3.04E+03	2.90E+03	4.25E+01	6.80E-01
6000	1.48E+03	5.01E+02	2.95E+03	2.88E+03	4.25E+01	6.60E-01
7000	1.43E+03	5.01E+02	2.86E+03	2.83E+03	4.24E+01	6.60E-01
8000	1.38E+03	4.97E+02	2.78E+03	2.76E+03	4.23E+01	6.40E-01
9000	1.33E+03	4.99E+02	2.67E+03	2.69E+03	4.24E+01	6.30E-01
10000	1.27E+03	4.98E+02	2.55E+03	2.63E+03	4.25E+01	6.30E-01
20000	1.20E+03	5.02E+02	2.39E+03	2.55E+03	4.26E+01	6.30E-01
30000	1.16E+03	4.98E+02	2.34E+03	2.45E+03	4.26E+01	6.10E-01
40000	1.12E+03	5.01E+02	2.23E+03	2.36E+03	4.28E+01	6.00E-01
50000	1.07E+03	4.99E+02	2.15E+03	2.28E+03	4.27E+01	5.90E-01
60000	1.04E+03	5.00E+02	2.07E+03	2.14E+03	4.26E+01	5.80E-01
70000	1.01E+03	5.01E+02	2.01E+03	2.10E+03	4.26E+01	5.80E-01
80000	9.74E+02	5.00E+02	1.95E+03	2.02E+03	4.27E+01	5.60E-01
90000	9.43E+02	5.01E+02	1.88E+03	1.93E+03	4.28E+01	5.50E-01
100749	9.06E+02	5.00E+02	1.81E+03	1.85E+03	4.28E+01	5.40E-01

APPENDIX F

Statistical analysis and NOVA outputs of HMA Specimens

ANOVA: Two-Factor Without Replication (OAC)

SUMMARY	*Count*	*Sum*	*Average*	*Variance*
FINE	5	30.3	6.06	0.748
COARSE	5	29	5.8	0.475
MIX	5	29.8	5.96	0.583
0	3	15.3	5.1	0
0.2	3	16.3	5.433333333	0.0033333
0.4	3	17.3	5.766666667	0.0533333
0.6	3	19.1	6.366666667	0.0233333
0.8	3	21.1	7.033333333	0.0633333

ANOVA

Source of Variation	*SS*	*df*	*MS*	*F*	*P-value*	*F crit*
Rows	0.172	2	0.086	6	0.0256	4.45897
Columns	7.109333333	4	1.777333333	124	3.13E-07	3.837853
Error	0.114666667	8	0.014333333			
Total	7.396	14				

ANOVA: Two-Factor Without Replication (STABILITY)

SUMMARY	*Count*	*Sum*	*Average*	*Variance*
FINE	5	56.26	11.252	7.05102
COARSE	5	63.17	12.634	3.95383
MIX	5	57.23	11.446	5.61703
0	3	43.89	14.63	0
0.2	3	39.2	13.0666667	0.858433
0.4	3	36.47	12.1566667	1.172033
0.6	3	30.83	10.2766667	0.885733
0.8	3	26.27	8.75666667	1.146033

ANOVA

Source of Variation	*SS*	*df*	*MS*	*F*	*P-value*	*F crit*
Rows	5.598173333	2	2.79908667	8.863853	0.009349	4.45897
Columns	63.96122667	4	15.9903067	50.63642	1.01E-05	.837853
Error	2.526293333	8	0.31578667			
Total	72.08569333	14				

ANOVA : Two-Factor Without Replication (FLOW)

SUMMARY	*Count*	*Sum*	*Average*	*Variance*
FINE	5	25.16	5.032	2.28992
COARSE	5	19.52	3.904	0.48598
MIX	5	26.16	5.232	1.86837
0	3	10.05	3.35	0
0.2	3	11.9	3.966667	0.297233
0.4	3	13.88	4.626667	1.029733
0.6	3	16.01	5.336667	1.056933
0.8	3	19	6.333333	1.313633

ANOVA

Source of Variation	*SS*	*df*	*MS*	*F*	*P-value*	*F crit*
Rows	5.126613	2	2.563307	9.039839	0.008854	4.45897
Columns	16.30863	4	4.077157	14.37863	0.001003	3.837853
Error	2.268453	8	0.283557			
Total	23.70369	14				

ANOVA: Two-Factor Without Replication (DENSITY)

SUMMARY	*Count*	*Sum*	*Average*	*Variance*
FINE	5	11.913	2.3826	0.002952
COARSE	5	12.105	2.421	0.000315
MIX	5	11.934	2.3868	0.002688
0	3	7.314	2.438	0
0.2	3	7.283	2.427667	3.73E-05
0.4	3	7.22	2.406667	0.00035
0.6	3	7.123	2.374333	0.001057

0.8	3	7.012	2.337333	0.0025		
ANOVA						
Source of Variation	*SS*	*df*	*MS*	*F*	*P-value*	*F crit*
Rows	0.004436	2	0.002218	5.137299	0.036726	4.45897
Columns	0.020366	4	0.005091	11.79164	0.001955	3.837853
Error	0.003454	8	0.000432			
Total	0.028256	14				

ANOVA: Two-Factor Without Replication (VTM)

SUMMARY	*Count*	*Sum*	*Average*	*Variance*		
FINE	5	20.28	4.056	0.00383		
COARSE	5	20.18	4.036	0.00193		
MIX	5	20.14	4.028	0.00187		
0	3	12.21	4.07	0		
0.2	3	11.89	3.963333	0.000233		
0.4	3	12.14	4.046667	0.002133		
0.6	3	12.18	4.06	0.0016		
0.8	3	12.18	4.06	0.0009		
ANOVA						
Source of Variation	*SS*	*df*	*MS*	*F*	*P-value*	*F crit*
Rows	0.00208	2	0.00104	1.087108	0.382258	4.45897
Columns	0.022867	4	0.005717	5.97561	0.015805	3.837853
Error	0.007653	8	0.000957			
Total	0.0326	14				

ANOVA: Two-Factor Without Replication (VMA)

SUMMARY	*Count*	*Sum*	*Average*	*Variance*		
FINE	5	81.24	16.248	0.79267		
COARSE	5	78.86	15.772	0.09667		
MIX	5	80.84	16.168	0.65757		
0	3	46.32	15.44	0		
0.2	3	46.52	15.50667	0.002533		
0.4	3	47.69	15.89667	0.023633		
0.6	3	49.37	16.45667	0.256533		
0.8	3	51.04	17.01333	0.460833		
ANOVA						
Source of Variation	*SS*	*df*	*MS*	*F*	*P-value*	*F crit*
Rows	0.649653	2	0.324827	3.103143	0.100563	4.45897
Columns	5.350227	4	1.337557	12.77798	0.001496	3.837853
Error	0.837413	8	0.104677			
Total	6.837293	14				

ANOVA: Two-Factor Without Replication (VFA)

SUMMARY	*Count*	*Sum*	*Average*	*Variance*		
FINE	5	374.92591	74.98518	1.505865		
COARSE	5	372.0216	74.40432	0.212373		
MIX	5	375.20002	75.04	1.41911		
0	3	220.91969	73.6399	0		
0.2	3	223.3234	74.44113	0.000287		
0.4	3	223.63028	74.54343	0.06134		
0.6	3	225.95514	75.31838	0.277523		
0.8	3	228.31901	76.10634	1.283157		
ANOVA						
Source of Variation	*SS*	*df*	*MS*	*F*	*P-value*	*F crit*
Rows	1.240835	2	0.620417	2.476989	0.145461	4.45897
Columns	10.54561	4	2.636403	10.52572	0.002835	3.837853
Error	2.003779	8	0.250472			
Total	13.79023	14				

ANOVA: Two-Factor Without Replication (M_R @ 25^{O} C)

SUMMARY	*Count*	*Sum*	*Average*	*Variance*
FINE	5	13475	2695	170284.5
COARSE	5	14402	2880.4	89031.3
MIX	5	13747	2749.4	161772.3

0	3	9357	3119	0
0.2	3	9263	3087.667	2366.333
0.4	3	8327	2775.667	11972.33
0.6	3	8042	2680.667	36864.33
0.8	3	6635	2211.667	22874.33

ANOVA

Source of Variation	*SS*	*df*	*MS*	*F*	*P-value*	*F crit*
Rows	90822.53	2	45411.27	6.336588	0.022425	4.45897
Columns	1627020	4	406755.1	56.75771	6.53E-06	3.837853
Error	57332.13	8	7166.517			
Total	1775175	14				

ANOVA: Two-Factor Without Replication (M_R @ 40^O C)

SUMMARY	*Count*	*Sum*	*Average*	*Variance*
FINE	5	7651	1530.2	74838.7
COARSE	5	8422	1684.4	15070.3
MIX	5	7767	1553.4	50898.8
0	3	5310	1770	0
0.2	3	5332	1777.333	380.3333
0.4	3	4847	1615.667	13116.33
0.6	3	4470	1490	20973
0.8	3	3881	1293.667	32764.33

ANOVA

Source of Variation	*SS*	*df*	*MS*	*F*	*P-value*	*F crit*
Rows	69128.13	2	34564.07	4.231912	0.055749	4.45897
Columns	497891.3	4	124472.8	15.24005	0.000822	3.837853
Error	65339.87	8	8167.483			
Total	632359.3	14				

ANOVA: Two-Factor Without Replication (DRY IDT)

SUMMARY	*Count*	*Sum*	*Average*	*Variance*
FINE	5	41.6	8.32	0.68465
COARSE	5	41.47	8.294	0.52493
MIX	5	41.52	8.304	0.54353
0	3	27.21	9.07	0
0.2	3	26.54	8.846667	0.000133
0.4	3	25.67	8.556667	0.014233
0.6	3	23.42	7.806667	0.010033
0.8	3	21.75	7.25	0.0277

ANOVA

Source of Variation	*SS*	*df*	*MS*	*F*	*P-value*	*F crit*
Rows	0.00172	2	0.00086	0.067135	0.93559	4.45897
Columns	6.90996	4	1.72749	134.8548	2.25E-07	3.837853
Error	0.10248	8	0.01281			
Total	7.01416	14				

ANOVA: Two-Factor Without Replication (WET IDT)

SUMMARY	*Count*	*Sum*	*Average*	*Variance*
FINE	5	33.46	6.692	1.29102
COARSE	5	34.8	6.96	0.539
MIX	5	33.94	6.788	0.87847
0	3	23.22	7.74	1.18E-30
0.2	3	22.43	7.476667	0.000133
0.4	3	21.44	7.146667	0.006033
0.6	3	18.55	6.183333	0.022533
0.8	3	16.56	5.52	0.2613

ANOVA

Source of Variation	*SS*	*df*	*MS*	*F*	*P-value*	*F crit*
Rows	0.184373	2	0.092187	1.864114	0.216486	4.45897
Columns	10.43833	4	2.609583	52.7686	8.63E-06	3.837853
Error	0.395627	8	0.049453			
Total	11.01833	14				

ANOVA: Two-Factor Without Replication (HL DRY IDT)						
SUMMARY	*Count*	*Sum*	*Average*	*Variance*		
FINE	5	41.7	8.34	0.7441		
COARSE	5	41.73	8.346	0.55513		
MIX	5	41.65	8.33	0.59485		
0	3	27.33	9.11	0		
0.2	3	26.72	8.906667	0.001733		
0.4	3	25.83	8.61	0.0148		
0.6	3	23.51	7.836667	0.017733		
0.8	3	21.69	7.23	0.0457		
ANOVA						
Source of Variation	*SS*	*df*	*MS*	*F*	*P-value*	*F crit*
Rows	0.000653	2	0.000327	0.016407	0.98376	4.45897
Columns	7.41704	4	1.85426	93.13209	9.6E-07	3.837853
Error	0.15928	8	0.01991			
Total	7.576973	14				

ANOVA: Two-Factor Without Replication (HL WET IDT)						
SUMMARY	*Count*	*Sum*	*Average*	*Variance*		
FINE	5	34.07	6.814	1.32383		
COARSE	5	35.48	7.096	0.58258		
MIX	5	34.53	6.906	0.90123		
0	3	23.49	7.83	1.18E-30		
0.2	3	22.98	7.66	0.0039		
0.4	3	21.84	7.28	0.0112		
0.6	3	19	6.333333	0.027433		
0.8	3	16.77	5.59	0.2512		
ANOVA						
Source of Variation	*SS*	*df*	*MS*	*F*	*P-value*	*F crit*
Rows	0.206813	2	0.103407	2.173246	0.176273	4.45897
Columns	10.84991	4	2.712477	57.00676	6.42E-06	3.837853
Error	0.380653	8	0.047582			
Total	11.43737	14				

ANOVA: Two-Factor Without Replication (TSR)						
SUMMARY	*Count*	*Sum*	*Average*	*Variance*		
FINE	5	3.99765	0.79953	0.003672		
COARSE	5	4.190414	0.838083	0.000287		
MIX	5	4.072312	0.814462	0.001825		
0	3	2.560088	0.853363	1.85E-32		
0.2	3	2.535418	0.845139	4.08E-08		
0.4	3	2.505971	0.835324	0.000218		
0.6	3	2.376905	0.792302	0.000841		
0.8	3	2.281994	0.760665	0.003048		
ANOVA						
Source of Variation	*SS*	*df*	*MS*	*F*	*P-value*	*F crit*
Rows	0.003779	2	0.001889	3.40742	0.08503	4.45897
Columns	0.018699	4	0.004675	8.43062	0.005722	3.837853
Error	0.004436	8	0.000554			
Total	0.026913	14				

ANOVA: Two-Factor Without Replication (HL TSR)						
SUMMARY	*Count*	*Sum*	*Average*	*Variance*		
FINE	5	4.061562	0.812312	0.003386		
COARSE	5	4.245391	0.849078	0.000279		
MIX	5	4.130944	0.826189	0.001645		
0	3	2.578485	0.859495	1.85E-32		
0.2	3	2.580072	0.860024	1.75E-05		
0.4	3	2.536717	0.845572	0.000122		
0.6	3	2.425629	0.808543	0.001161		
0.8	3	2.316994	0.772331	0.002348		
ANOVA						
Source of Variation	*SS*	*df*	*MS*	*F*	*P-value*	*F crit*

Rows	0.003447	2	0.001723	3.581685	0.077478	4.45897
Columns	0.01739	4	0.004348	9.034854	0.004613	3.837853
Error	0.00385	8	0.000481			
Total	0.024687	14				

ANOVA: Two-Factor Without Replication (RUT DEPTH)

SUMMARY	*Count*	*Sum*	*Average*	*Variance*
FINE	5	20.72	4.144	3.09283
COARSE	5	19.23	3.846	2.17913
MIX	5	16.52	3.304	0.27653
0	3	8.7	2.9	0
0.2	3	8.79	2.93	0.0007
0.4	3	9.29	3.096667	0.034233
0.6	3	12.23	4.076667	0.160133
0.8	3	17.46	5.82	2.4903

ANOVA

Source of Variation	*SS*	*df*	*MS*	*F*	*P-value*	*F crit*
Rows	1.813613	2	0.906807	2.039418	0.192424	4.45897
Columns	18.63684	4	4.65921	10.47861	0.002876	3.837853
Error	3.55712	8	0.44464			
Total	24.00757	14				

ANOVA: Two-Factor Without Replication (RUT RATE)

SUMMARY	*Count*	*Sum*	*Average*	*Variance*
FINE	5	4.013734	0.802747	0.123218
COARSE	5	2.897198	0.57944	0.04098
MIX	5	3.233359	0.646672	0.046761
0	3	1.2	0.4	4.62E-33
0.2	3	1.428685	0.476228	0.001778
0.4	3	1.908916	0.636305	0.028251
0.6	3	2.629261	0.87642	0.027819
0.8	3	2.977428	0.992476	0.042713

ANOVA

Source of Variation	*SS*	*df*	*MS*	*F*	*P-value*	*F crit*
Rows	0.131243	2	0.065621	7.512651	0.014573	4.45897
Columns	0.773956	4	0.193489	22.15157	0.00022	3.837853
Error	0.069878	8	0.008735			
Total	0.975077	14				

ANOVA: Single Factor (STIFFNESS VALUE, FATIGUE)

Groups	*Count*	*Sum*	*Average*	*Variance*
VA-HMA	25	118699.2423	4747.969694	996005.3288
20%F-RCA-HMA	25	144290.8724	5771.634897	1340370.764
40%F-RCA-HMA	26	171828.5401	6608.790003	1896080.859
60%F-RCA-HMA	25	120318.1017	4812.724068	896134.3158
80%F-RCA-HMA	21	77055.71994	3669.319997	452203.168
20%C-RCA-HMA	26	141455.7409	5440.60542	1164895.463
40%C-RCA-HMA	27	167299.9154	6196.293163	1517538.141
60%C-RCA-HMA	26	169923.8	6535.53077	1556408.722
80%C-RCA-HMA	25	122301.4437	4892.05775	995020.0703
20% M-RCA-HMA	26	151441.4736	5824.672063	1258351.577
40%M-RCA-HMA	27	158687.3935	5877.310871	1443579.054
60%M-RCA-HMA	25	133542.7798	5341.711193	1241896.01
80%M-RCA-HMA	24	99433.47229	4143.061346	643993.6987

ANOVA

Source of Variation	*SS*	*df*	*MS*	*F*	*P-value*	*F crit*
Between Groups	229497052.1	12	19124754.34	15.89505075	2.944E-26	1.78298419
Within Groups	379004616.7	315	1203189.259			
Total	608501668.8	327				

APPENDIX G

Statistical analysis and NOVA outputs of SMA Specimens

ANOVA: Two-Factor Without Replication (OAC)

SUMMARY	Count	Sum	Average	Variance		
FINE	5	31.7	6.34	0.023		
COARSE	5	36.4	7.28	1.257		
MIX	5	34	6.8	0.4		
0	3	18.6	6.2	0		
0.2	3	19	6.333333333	0.0133333		
0.4	3	19.9	6.633333333	0.1233333		
0.6	3	21.4	7.133333333	0.5033333		
0.8	3	23.2	7.733333333	1.4433333		
ANOVA						
Source of Variation	*SS*	*df*	*MS*	*F*	*P-value*	*F crit*
Rows	2.209333333	2	1.104666667	4.5149864	0.048697	4.45897
Columns	4.762666667	4	1.190666667	4.866485	0.027602	3.837853
Error	1.957333333	8	0.244666667			
Total	8.929333333	14				

ANOVA: Two-Factor Without Replication (STABILITY)

SUMMARY	Count	Sum	Average	Variance		
FINE	5	51.98	10.396	0.16958		
COARSE	5	38.23	7.646	4.94308		
MIX	5	39.63	7.926	4.01428		
0	3	31.89	10.63	0		
0.2	3	29.18	9.72666667	0.661433		
0.4	3	25.07	8.35666667	4.369733		
0.6	3	22.87	7.62333333	4.653333		
0.8	3	20.83	6.94333333	6.322533		
ANOVA						
Source of Variation	*SS*	*df*	*MS*	*F*	*P-value*	*F crit*
Rows	22.903	2	11.4515	10.05502	0.00656	4.45897
Columns	27.39669333	4	6.84917333	6.013938	0.015523	3.837853
Error	9.111066667	8	1.13888333			
Total	59.41076	14				

ANOVA: Two-Factor Without Replication (FLOW)

SUMMARY	Count	Sum	Average	Variance		
FINE	5	14.33	2.866	0.29153		
COARSE	5	23.46	4.692	3.01342		
MIX	5	22.84	4.568	2.79802		
0	3	7.05	2.35	0		
0.2	3	9.87	3.29	0.5328		
0.4	3	12.28	4.093333	1.381733		
0.6	3	14.12	4.706667	1.893033		
0.8	3	17.31	5.77	3.3156		
ANOVA						
Source of Variation	*SS*	*df*	*MS*	*F*	*P-value*	*F crit*
Rows	10.41076	2	5.20538	10.85706	0.005254	4.45897
Columns	20.57631	4	5.144077	10.72919	0.002664	3.837853
Error	3.835573	8	0.479447			
Total	34.82264	14				

ANOVA: Two-Factor Without Replication (DENSITY)						
SUMMARY	*Count*	*Sum*	*Average*	*Variance*		
FINE	5	11.557	2.3114	0.000116		
COARSE	5	11.296	2.2592	0.001601		
MIX	5	11.332	2.2664	0.001248		
0	3	6.942	2.314	0		
0.2	3	6.888	2.296	0.000409		
0.4	3	6.841	2.280333	0.001314		
0.6	3	6.78	2.26	0.001669		
0.8	3	6.734	2.244667	0.001956		
ANOVA						
Source of Variation	*SS*	*df*	*MS*	*F*	*P-value*	*F crit*
Rows	0.008003	2	0.004001	11.88005	0.004026	4.45897
Columns	0.009167	4	0.002292	6.803899	0.010896	3.837853
Error	0.002695	8	0.000337			
Total	0.019864	14				

ANOVA: Two-Factor Without Replication (VTM)						
SUMMARY	*Count*	*Sum*	*Average*	*Variance*		
FINE	5	20.06	4.012	0.00077		
COARSE	5	20.07	4.014	0.00453		
MIX	5	20.16	4.032	0.00257		
0	3	12	4	0		
0.2	3	12.15	4.05	0.0004		
0.4	3	11.9	3.966667	0.000533		
0.6	3	11.98	3.993333	0.000433		
0.8	3	12.26	4.086667	0.001033		
ANOVA						
Source of Variation	*SS*	*df*	*MS*	*F*	*P-value*	*F crit*
Rows	0.001213	2	0.000607	1.35316	0.311745	4.45897
Columns	0.027893	4	0.006973	15.5539	0.000766	3.837853
Error	0.003587	8	0.000448			
Total	0.032693	14				

ANOVA: Two-Factor Without Replication (VMA)						
SUMMARY	*Count*	*Sum*	*Average*	*Variance*		
FINE	5	78.25	15.65	0.07015		
COARSE	5	80.2	16.04	0.4558		
MIX	5	80.19	16.038	0.50387		
0	3	45.99	15.33	0		
0.2	3	46.51	15.50333	0.001233		
0.4	3	47.6	15.86667	0.021233		
0.6	3	48.39	16.13	0.12		
0.8	3	50.15	16.71667	0.365233		
ANOVA						
Source of Variation	*SS*	*df*	*MS*	*F*	*P-value*	*F crit*
Rows	0.504413	2	0.252207	3.948544	0.064134	4.45897
Columns	3.608293	4	0.902073	14.12285	0.001066	3.837853
Error	0.510987	8	0.063873			
Total	4.623693	14				

ANOVA: Two-Factor Without Replication (VFA)				
SUMMARY	*Count*	*Sum*	*Average*	*Variance*
FINE	5	371.79662	74.35932	0.157664
COARSE	5	374.72937	74.94587	0.909849
MIX	5	374.13236	74.82647	0.967672
0	3	221.72211	73.90737	0
0.2	3	221.62974	73.87658	0.013629
0.4	3	224.99412	74.99804	0.115514
0.6	3	225.70377	75.23459	0.345379
0.8	3	226.60861	75.5362	0.506926

ANOVA						
Source of Variation	*SS*	*df*	*MS*	*F*	*P-value*	*F crit*
Rows	0.960878	2	0.480439	3.835764	0.067907	4.45897
Columns	7.138722	4	1.78468	14.24867	0.001035	3.837853
Error	1.00202	8	0.125252			
Total	9.101619	14				

ANOVA: Two-Factor Without Replication (M_R @ 25^0 C)

SUMMARY	*Count*	*Sum*	*Average*	*Variance*
FINE	5	14593	2918.6	7517.8
COARSE	5	11846	2369.2	157590.7
MIX	5	12439	2487.8	138983.2
0	3	8442	2814	0
0.2	3	8388	2796	5008
0.4	3	7757	2585.667	88516.33
0.6	3	7504	2501.333	212354.3
0.8	3	6787	2262.333	408456.3

ANOVA						
Source of Variation	*SS*	*df*	*MS*	*F*	*P-value*	*F crit*
Rows	835824.9	2	417912.5	5.639416	0.029651	4.45897
Columns	623521.7	4	155880.4	2.10349	0.017213	3.837853
Error	592845.1	8	74105.63			
Total	2052192	14				

ANOVA: Two-Factor Without Replication M_R @ 40^0 C)

SUMMARY	*Count*	*Sum*	*Average*	*Variance*
FINE	5	6974	1394.8	2399.2
COARSE	5	5752	1150.4	28660.8
MIX	5	5731	1146.2	25837.2
0	3	3939	1313	0
0.2	3	3958	1319.333	3894.333
0.4	3	3737	1245.667	22549.33
0.6	3	3596	1198.667	44210.33
0.8	3	3227	1075.667	84561.33

ANOVA						
Source of Variation	*SS*	*df*	*MS*	*F*	*P-value*	*F crit*
Rows	202584.9	2	101292.5	7.513878	0.014566	4.45897
Columns	119743.1	4	29935.77	2.220636	0.015653	3.837853
Error	107845.7	8	13480.72			
Total	430173.7	14				

ANOVA: Two-Factor Without Replication (DRY IDT)

SUMMARY	*Count*	*Sum*	*Average*	*Variance*
FINE	5	34.73	6.946	0.13553
COARSE	5	31.34	6.268	0.58662
MIX	5	31.96	6.392	0.48612
0	3	21.57	7.19	0
0.2	3	20.98	6.993333	0.041033
0.4	3	19.67	6.556667	0.209733
0.6	3	18.74	6.246667	0.351433
0.8	3	17.07	5.69	0.3109

ANOVA						
Source of Variation	*SS*	*df*	*MS*	*F*	*P-value*	*F crit*
Rows	1.303293	2	0.651647	9.969606	0.006722	4.45897
Columns	4.310173	4	1.077543	16.48544	0.000626	3.837853
Error	0.522907	8	0.065363			
Total	6.136373	14				

ANOVA: Two-Factor Without Replication (WET IDT)

SUMMARY	Count	Sum	Average	Variance
FINE	5	29.34	5.868	0.13407
COARSE	5	24.65	4.93	0.9836
MIX	5	25.42	5.084	0.88883
0	3	18.09	6.03	0
0.2	3	17.75	5.916667	0.051633
0.4	3	16.29	5.43	0.2425
0.6	3	14.5	4.833333	0.923433
0.8	3	12.78	4.26	0.7167

ANOVA

Source of Variation	SS	df	MS	F	P-value	F crit
Rows	2.53036	2	1.26518	7.563624	0.014317	4.45897
Columns	6.687827	4	1.671957	9.995456	0.003348	3.837853
Error	1.338173	8	0.167272			
Total	10.55636	14				

ANOVA: Two-Factor Without Replication (HL DRY IDT)

SUMMARY	Count	Sum	Average	Variance
FINE	5	34.87	6.974	0.14483
COARSE	5	31.41	6.282	0.61312
MIX	5	32.02	6.404	0.48298
0	3	21.66	7.22	0
0.2	3	21.08	7.026667	0.045033
0.4	3	19.63	6.543333	0.236633
0.6	3	18.85	6.283333	0.347733
0.8	3	17.08	5.693333	0.313033

ANOVA

Source of Variation	SS	df	MS	F	P-value	F crit
Rows	1.364413	2	0.682207	10.48635	0.005813	4.45897
Columns	4.443267	4	1.110817	17.0746	0.000554	3.837853
Error	0.520453	8	0.065057			
Total	6.328133	14				

ANOVA: Two-Factor Without Replication (HL WET IDT)

SUMMARY	Count	Sum	Average	Variance
FINE	5	30.19	6.038	0.13587
COARSE	5	25.33	5.066	0.97088
MIX	5	26	5.2	0.824
0	3	18.57	6.19	0
0.2	3	18.07	6.023333	0.056933
0.4	3	16.6	5.533333	0.360033
0.6	3	15.02	5.006667	0.901433
0.8	3	13.26	4.42	0.7213

ANOVA

Source of Variation	SS	df	MS	F	P-value	F crit
Rows	2.774973	2	1.387487	8.509404	0.010454	4.45897
Columns	6.418573	4	1.604643	9.841218	0.003519	3.837853
Error	1.304427	8	0.163053			
Total	10.49797	14				

ANOVA: Two-Factor Without Replication (TSR)

SUMMARY	Count	Sum	Average	Variance
FINE	5	4.222352	0.84447	0.00014
COARSE	5	3.902208	0.780442	0.004589
MIX	5	3.949925	0.789985	0.004296
0	3	2.515994	0.838665	0
0.2	3	2.537688	0.845896	7.87E-05
0.4	3	2.482141	0.82738	0.000286
0.6	3	2.306672	0.768891	0.005898
0.8	3	2.23199	0.743997	0.005254

ANOVA						
Source of Variation	*SS*	*df*	*MS*	*F*	*P-value*	*F crit*
Rows	0.011932	2	0.005966	4.299191	0.053963	4.45897
Columns	0.024996	4	0.006249	4.502968	0.033728	3.837853
Error	0.011102	8	0.001388			
Total	0.04803	14				

ANOVA: Two-Factor Without Replication (HL TSR)

SUMMARY	*Count*	*Sum*	*Average*	*Variance*
FINE	5	4.327795	0.865559	0.000131
COARSE	5	4.003511	0.800702	0.003618
MIX	5	4.036994	0.807399	0.003432
0	3	2.572022	0.857341	0
0.2	3	2.571169	0.857056	8.11E-05
0.4	3	2.532793	0.844264	0.000775
0.6	3	2.376993	0.792331	0.005477
0.8	3	2.315322	0.771774	0.004874

ANOVA						
Source of Variation	*SS*	*df*	*MS*	*F*	*P-value*	*F crit*
Rows	0.012723	2	0.006362	5.251358	0.034948	4.45897
Columns	0.019032	4	0.004758	3.927595	0.047309	3.837853
Error	0.009691	8	0.001211			
Total	0.041446	14				

ANOVA: Two-Factor Without Replication (RUT DEPTH)

SUMMARY	*Count*	*Sum*	*Average*	*Variance*
FINE	5	10.91	2.182	0.76107
COARSE	5	18.43	3.686	3.06933
MIX	5	17.42	3.484	2.46508
0	3	4.95	1.65	7.4E-32
0.2	3	6.59	2.196667	0.267633
0.4	3	8.4	2.8	1.4673
0.6	3	11.68	3.893333	0.650433
0.8	3	15.14	5.046667	2.398433

ANOVA						
Source of Variation	*SS*	*df*	*MS*	*F*	*P-value*	*F crit*
Rows	6.663373	2	3.331687	9.177484	0.00849	4.45897
Columns	22.27769	4	5.569423	15.34157	0.000803	3.837853
Error	2.904227	8	0.363028			
Total	31.84529	14				

ANOVA: Two-Factor Without Replication (RUT RATE)

SUMMARY	*Count*	*Sum*	*Average*	*Variance*
FINE	5	3.07	0.614	0.07588
COARSE	5	6.06	1.212	0.70027
MIX	5	5.18	1.036	0.40523
0	3	1.02	0.34	0
0.2	3	1.66	0.553333	0.014233
0.4	3	2.19	0.73	0.0433
0.6	3	4.61	1.536667	0.342033
0.8	3	4.83	1.61	0.3991

ANOVA						
Source of Variation	*SS*	*df*	*MS*	*F*	*P-value*	*F crit*
Rows	0.94444	2	0.47222	5.786183	0.027912	4.45897
Columns	4.072627	4	1.018157	12.47563	0.001621	3.837853
Error	0.652893	8	0.081612			
Total	5.66996	14				

ANOVA: Single Factor (STIFFNESS VALUE, FATIGUE)						
Groups	*Count*	*Sum*	*Average*	*Variance*		
VA-SMA	18	40056.83475	2225.379708	181888.8247		
20%F-RCA-SMA	22	66840.25825	3038.193557	372561.9872		
40%F-RCA-SMA	25	86557.73013	3462.309205	450011.4984		
60%F-RCA-SMA	25	87326.04202	3493.041681	435341.0038		
80%F-RCA-SMA	24	88999.99221	3708.333009	550716.3524		
20%C-RCA-SMA	23	61351.80865	2667.469941	291177.2242		
40%C-RCA-SMA	20	59470.67412	2973.533706	396985.2166		
60%C-RCA-SMA	20	55625.91753	2781.295877	358835.1713		
80%C-RCA-SMA	19	38353.67459	2018.614452	204160.8905		
20% M-RCA-SMA	21	60501.41819	2881.019914	351396.1148		
40%M-RCA-SMA	25	83820.58384	3352.823354	488981.7118		
60%M-RCA-SMA	23	72311.87904	3143.994741	353742.6938		
80%M-RCA-SMA	21	56055.80931	2669.324253	345840.6739		
ANOVA						
Source of Variation	*SS*	*df*	*MS*	*F*	*P-value*	*F crit*
Between Groups	62288739.43	12	5190728.286	13.79345564	2.87642E-22	1.787750706
Within Groups	102734866.4	273	376318.1918			